

INFORMATION TO USERS

This manuscript has been reproduced from the microfilm master. UMI films the text directly from the original or copy submitted. Thus, some thesis and dissertation copies are in typewriter face, while others may be from any type of computer printer.

The quality of this reproduction is dependent upon the quality of the copy submitted. Broken or indistinct print, colored or poor quality illustrations and photographs, print bleedthrough, substandard margins, and improper alignment can adversely affect reproduction.

In the unlikely event that the author did not send UMI a complete manuscript and there are missing pages, these will be noted. Also, if unauthorized copyright material had to be removed, a note will indicate the deletion.

Oversize materials (e.g., maps, drawings, charts) are reproduced by sectioning the original, beginning at the upper left-hand corner and continuing from left to right in equal sections with small overlaps.

Photographs included in the original manuscript have been reproduced xerographically in this copy. Higher quality 6" x 9" black and white photographic prints are available for any photographs or illustrations appearing in this copy for an additional charge. Contact UMI directly to order.

ProQuest Information and Learning
300 North Zeeb Road, Ann Arbor, MI 48106-1346 USA
800-521-0600

UMI[®]

University of Alberta

**A stratigraphic and geochemical investigation of Upper Devonian shale and
marl aquitards, west-central Alberta, Canada.**

by

Catherine Cheryl Skilliter



**A thesis submitted to the Faculty of Graduate Studies and Research in partial
fulfillment of the requirements for the degree of Master of Science.**

Department of Earth and Atmospheric Sciences

Edmonton, Alberta

Spring, 2000



**National Library
of Canada**

**Acquisitions and
Bibliographic Services**

**395 Wellington Street
Ottawa ON K1A 0N4
Canada**

**Bibliothèque nationale
du Canada**

**Acquisitions et
services bibliographiques**

**395, rue Wellington
Ottawa ON K1A 0N4
Canada**

Your file Votre référence

Our file Notre référence

The author has granted a non-exclusive licence allowing the National Library of Canada to reproduce, loan, distribute or sell copies of this thesis in microform, paper or electronic formats.

The author retains ownership of the copyright in this thesis. Neither the thesis nor substantial extracts from it may be printed or otherwise reproduced without the author's permission.

L'auteur a accordé une licence non exclusive permettant à la Bibliothèque nationale du Canada de reproduire, prêter, distribuer ou vendre des copies de cette thèse sous la forme de microfiche/film, de reproduction sur papier ou sur format électronique.

L'auteur conserve la propriété du droit d'auteur qui protège cette thèse. Ni la thèse ni des extraits substantiels de celle-ci ne doivent être imprimés ou autrement reproduits sans son autorisation.

0-612-60178-1

Canada

University of Alberta

Library Release Form

Name of Author: **Catherine Cheryl Skilliter**

Title of Thesis: **A stratigraphic and geochemical investigation of Upper Devonian shale and marl aquitards, west-central Alberta, Canada.**

Degree: **Master of Science**

Year this Degree Granted: **2000**

Permission is hereby granted to the University of Alberta to reproduce single copies of this thesis and to lend or sell such copies for private, scholarly, or scientific research purposes only.

The author reserves all other publication and other rights in association with the copyright in the thesis, and except as hereinbefore provided, neither the thesis nor any substantial portion thereof may be printed or otherwise reproduced in any material form whatever without the author's prior written permission.

Catherine Skilliter

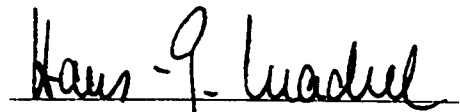
Catherine Skilliter
13 Hillsdale Crescent
Lower Sackville, Nova Scotia
Canada
B4E 2G8

December 17, 1999

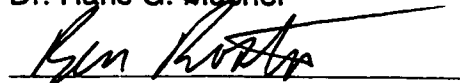
University of Alberta

Faculty of Graduate Studies and Research

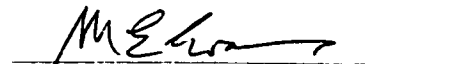
The undersigned certify that they have read, and recommend to the Faculty of Graduate Studies and Research for acceptance, a thesis entitled ***A stratigraphic and geochemical investigation of Upper Devonian shale and marl aquitards, west-central Alberta, Canada*** submitted by ***Catherine Cheryl Skilliter*** in partial fulfillment of the requirements for the degree of Master of Science.



Dr. Hans G. Machel



Dr. Benjamin J. Rostron



Dr. Michael E. Evans

Date: December 8, 1999

Abstract

A regional investigation of Devonian aquitards in west-central Alberta has identified the aquitards as effective barriers to (paleo-)fluids since the Late Devonian/Early Carboniferous. Aquitards thin progressively towards the disturbed belt, and in areas such as the Obed and Simonette fields, aquitards are absent, permitting interconnection between the four major Devonian carbonate aquifers (i.e., D-1 through D-4).

Aquitard lithofacies vary in depositional environments from basin, via slope (or ramp), to near-reef. Paragenetic sequences have been established for both near-reef and near-basinal lithofacies.

Stable isotopic analyses ($\delta^{18}\text{O}$ and $\delta^{13}\text{C}$) reveal that aquitards have been relatively impermeable to aqueous formation fluids since the Late Devonian/Early Carboniferous. Mercury injection data show that the aquitards are relatively effective seals to hydrocarbons. The near-marine $^{87}\text{Sr}/^{86}\text{Sr}$ ratios of the carbonate fractions within the aquitards differ significantly from highly radiogenic (^{87}Sr enriched), late-stage, carbonate cements within adjacent carbonate aquifers. This finding suggests the latter were precipitated from fluids containing an extrabasinal fluid component. Extrabasinal fluids likely entered the Devonian system through tectonic expulsion during the Laramide orogeny. These fluids are confined to Devonian carbonate aquifers and have probably moved in a predominantly northeast direction. In the vicinity of the disturbed belt region, cross formational fluid flow is likely, due to the absence of aquitards or in areas where the D-1 to the D-4 is hydrologically connected.

Acknowledgements

I would first like to acknowledge and thank Hans for his guidance and support throughout supervision of this thesis. Several others at UofA made this project possible, including: Don Resultay and Mark Labbe for thin section preparation; Diane Caird for XRD analyses; Ted Evans for help with magnetic susceptibility; Olga Levner, Stacey Hagan, Karlis Muehlenbachs, and Rob Creaser for help with stable and radiogenic isotope analyses; Arndt Buhlmann for computer software support; and Ben Rostron for discussions on fluid flow mechanisms.

In Calgary, thanks is extended to: Adam Hedinger, Jack Wendte, Mark Mallamo, Ken Watson, and Ross McLean for discussions regarding Devonian stratigraphy and structure; to the crew at the EUB, especially Lori, for assistance in core logging and sampling; to the AGS in Edmonton for use of the microfiche and copying services; to Regina Shedd and Jon Greggs at UofC for assistance in rounding up some valuable cross sections; to Soumini Reddy, Jerry Shaw, and Bernie Schulmeister at the Petroleum Recovery Institute (PRI) for their in-kind support in completing mercury injection tests. Accommodation in Calgary was most kindly provided by Kim Manzano, Chez Elizabeth and Marianne.

A special mention to Mare, Betsy, Astrid, Rajeev, Karen, Andrea, Nancy, Steph, Leslie, Devon, Darlene, George, and Ted for their friendship, guidance, and plenty of helpful discussions along the way. I am indebted to present and past "Gang" members including Maja, Matt, Karsten, Kim, Marianne, Lisa, and Jeff; it's been a pleasure working with you and I wish you success in all of your future endeavors! I offer a warm thank-you to my family for their support and to Simon for his constant love, commitment, and guidance.

An extra special thanks is extended to: Pat Cavell for her endearing support, never-ending discussions, and guidance throughout the entire project; and to Caroline Nixon, who was a great help in the initial stages of the project cleaning, crushing, and drilling samples, and completing magnetic susceptibility tests, and also near the end during some serious editing of the rough drafts of chapters. Your perseverance, persuasiveness, and encouragement moved me.

Table of Contents

1. Chapter 1 - Introduction.....	1
1.1. Introduction and Previous Studies.....	1
1.2. Objectives of the Research Project	5
1.3. Study Area and Core Control.....	6
2. Chapter 2 - Regional Geological Setting and Depositional History	8
2.1. Western Canada Sedimentary Basin	8
2.2. Devonian Stratigraphy	8
2.3. The Alberta Basin	10
2.3.1. West Shale Basin	10
2.4. WCSB Structures Influencing Devonian Stratigraphy.....	10
2.5. Woodbend Group	13
2.5.1. Stratigraphy and Depositional history	13
2.6. Winterburn Group.....	16
2.6.1. Stratigraphy and Depositional History	16
• Lower Winterburn Group	17
• Upper Winterburn Group	17
2.7. Basin Fill Units.....	19
2.8. Hydrostratigraphic Units of the WCSB	21
2.9. Identification of Aquitards	23
2.10. Shale and Marl Aquitards	23
2.10.1. Winterburn Group Aquitards	23
2.10.2. Woodbend/Winterburn Aquitard	23
2.10.3. Woodbend Group Aquitard	24
2.10.4. Majeau Lake Formation Aquitard.....	24
2.10.5. Beaverhill Lake Group Aquitards	24
2.10.6. Watt Mountain Formation Aquitard	24
2.11. Carbonate Aquifers.....	24
3. Chapter 3 - Stratigraphic and Structural Investigation of Middle to Upper Devonian Aquitards.....	25
3.1. Introduction and Objectives	25
3.2. Cross Section Methods	27

3.3. Hydrocarbon Production in Wells	28
3.4. Stratigraphic Cross Section Methods	28
3.5. Structural Cross Section Methods	29
3.6. Synopsis of Stratigraphic and Structural Investigations.....	29
3.6.1. Summary of Cross Sections A-A'	29
3.6.2. Summary of Cross Sections B-B'	32
3.6.3. Summary of Cross Sections C-C'	32
3.6.4. Summary of Cross Sections D-D'	37
3.6.5. Summary of Cross Sections E-E'	37
3.6.6. Summary of Cross Section F-F'	42

4. Chapter 4 - Lithofacies and Mineralogical Facies of Regional

Aquitards.....	45
4.1. Introduction.....	45
4.2. Lithological Facies	46
4.2.1. Introduction	46
4.2.2. Lithofacies A	49
4.2.3. Lithofacies B	53
4.2.4. Lithofacies AD.....	53
4.2.5. Lithofacies AE.....	58
4.2.6. Lithofacies C	61
4.2.7. Lithofacies G.....	64
4.2.8. Lithofacies GE	67
4.2.9. "Lithofacies F"	70
4.3. Mineralogical Facies	70
4.3.1. Introduction	70
4.3.2. Mineralogical Facies QCp.....	77
4.3.3. Mineralogical Facies CQp.....	77
4.3.4. "Mineralogical Facies Cq"	79
4.3.5. Mineralogical Facies Qdp	79
4.4. Correlations of Lithological and Mineralogical Facies.....	80
4.4.1. Introduction	80
4.4.2. Majeau Lake Formation	80
4.4.3. Duvernay Formation	83
4.4.4. Woodbend Group	87
4.4.5. Ireton Formation	91
4.4.6. Woodbend/Winterburn Group.....	91
4.4.7. Winterburn Group	95

4.5. Synopsis and Significance.....	100
4.5.1. Lithofacies Summary	100
4.5.2. Stratigraphic Correlations	102
• Majeau Lake and Duvernay Formations	102
• Woodbend Group	102
• Ireton Formation	103
• Woodbend/Winterburn Group.....	103
• Winterburn Group	103
4.5.3. Geographic Correlations	104
4.5.4. Mineralogical Facies Summary	104
4.5.5. Carbonate content	105
5. Chapter 5 - Diagenetic History of the Aquitards	106
5.1. Introduction and Objectives	106
5.2. Mineralogy	106
5.2.1. Introduction	106
5.2.2. Mineralogical Analyses from Core and Thin Sections.....	106
• Carbonate Phases	106
* Calcite	107
* Ankerite and Dolomite	107
• Quartz and Feldspars	112
• Clay and Sheet Silicate Minerals	117
• Sulfides	117
* Pyrite	117
• Sulfates.....	118
* Celestite	118
* Anhydrite	121
• Structures	122
• Coated Grains	122
• Pinch and Swell Structures.....	122
5.3. Stable Isotope Analyses	122
5.3.1. Samples and Procedures.....	122
5.3.2. Results	124
• Calcite Population	124
* $\delta^{18}\text{O}$	124
* $\delta^{13}\text{C}$	126
• Ankerite/Dolomite Population	126
* $\delta^{18}\text{O}$	126
* $\delta^{13}\text{C}$	126

5.3.3. Interpretation.....	127
• Calcite Population.....	127
* $\delta^{18}\text{O}$	127
* $\delta^{13}\text{C}$	128
• Outlier Carbonate	129
* $\delta^{18}\text{O}$ and $\delta^{13}\text{C}$	129
• Ankerite/Dolomite Population	130
* $\delta^{18}\text{O}$	130
* $\delta^{13}\text{C}$	130
5.3.4. Trends in $\delta^{18}\text{O}$ / $\delta^{13}\text{C}$	131
5.3.5. Synopsis	133
5.4. Radiogenic Isotopic Analyses.....	136
5.4.1. Samples and Procedures.....	136
5.4.2. Results.....	139
• $^{87}\text{Sr}/^{86}\text{Sr}$ and $\delta^{18}\text{O}$	139
5.4.3. Interpretation.....	139
5.4.4. Trends in $^{87}\text{Sr}/^{86}\text{Sr}$ versus $\delta^{18}\text{O}$	140
5.4.5. Synopsis	141
5.5. Paragenetic Sequences	142
5.5.1. Introduction	142
• Near-Basinal Lithofacies A, AD, B, C.....	142
• Lithofacies F, G, and GE	144
5.6. Conclusions	145
6. Chapter 6 - Aquitard Integrity and Fluid Migration Pathways.....	147
6.1. Introduction and Objectives	147
6.2. MICPM.....	148
6.2.1. Introduction and Sampling Techniques.....	148
6.2.2. Pressure Definitions and Calculations of Breaching Potential	148
6.2.3. Results	154
6.2.4. Discussion.....	154
• Normal and Overpressured Reservoirs.....	158
6.3. Magnetic Susceptibility	158
6.3.1. Introduction	158
6.3.2. Sample Selection and Results	159
6.3.3. Discussion.....	160
6.4. Fluid Flow Migration Patterns	163

6.4.1. Introduction	163
6.4.2. Cross Section A-A'	166
6.4.3. Cross Section B-B'	166
6.4.4. Cross Section C-C'	169
6.4.5. Cross Section D-D'	169
6.4.6. Cross Section E-E'	172
6.4.7. Cross Section F-F'	175
6.5. Summary	175
7. Chapter 7 - Conclusions	177
References	180
Appendix 1 - Details of core descriptions, and stable and radiogenic isotope analyses results	187
Appendix 2 - Detailed Stratigraphic and Structural Descriptions of Cross Sections A-A' to F-F'	191
Appendix 3 - Methodology	213
Appendix 4 - MICPM data	220

List of Tables

Chapter 4

Table 4.1: Tally of minerals identified in mineralogical facies	75
Table 4.2: Summary of lithofacies and depositional environments	102
Table 4.3: Summary of mineralogical facies and depositional environments	104

Chapter 5

Table 5.1: Chemical compositions of various clay minerals	117
---	-----

Chapter 6

Table 6.1: Data for samples taken for MICPM tests	150
Table 6.2: MICPM pressure data and hydrocarbon column height data	153

List of Figures

Chapter 1

- Figure 1.1: Map of Devonian Paleogeography and study area 3
Figure 1.2: Close-up of study area, core examined, and stratigraphic interval 4

Chapter 2

- Figure 2.1: Map of Western Canada Sedimentary Basin 9
Figure 2.2: Stratigraphic and hydrostratigraphic chart 11
Figure 2.3: Schematic of depositional environments - Woodbend Group 14
Figure 2.4: Schematic of depositional environments - Winterburn Group 18
Figure 2.5: Cross section of megahydrostratigraphic units; Alberta Basin 22

Chapter 3

- Figure 3.1: Map of cross sections A-A' to F-F' constructed in the study area 26
Figure 3.2: Stratigraphic cross section A-A' 30
Figure 3.3: Structural cross section A-A' 31
Figure 3.4: Stratigraphic cross section B-B' 33
Figure 3.5: Structural cross section B-B' 34
Figure 3.6: Stratigraphic cross section C-C' 35
Figure 3.7: Structural cross section C-C' 36
Figure 3.8: Stratigraphic cross section D-D' 38
Figure 3.9: Structural cross section D-D' 39
Figure 3.10: Stratigraphic cross section E-E' 40
Figure 3.11: Structural cross section E-E' 41
Figure 3.12: Stratigraphic cross section F-F' 43
Figure 3.13: Structural cross section F-F' 44

Chapter 4

- Figure 4.1: Depositional environments of lithofacies of Woodbend Group 47
Figure 4.2: Depositional environments of lithofacies of Winterburn Group 48
Figure 4.3: Typical core samples and thin sections of lithofacies A 51
Figure 4.4: Graph of whole-rock carbonate percentages of lithofacies 52
Figure 4.5: Typical core samples and thin sections of lithofacies B 55
Figure 4.6: Typical core samples and thin sections of lithofacies AD 57
Figure 4.7: Typical core samples and thin sections of lithofacies AE 60
Figure 4.8: Typical core sample and thin sections of lithofacies C 63
Figure 4.9: Typical core sample and thin sections of lithofacies G 66
Figure 4.10: Typical core sample and thin sections of lithofacies GE 69

Figure 4.11:	Typical core sample and thin sections of lithofacies F	72
Figure 4.12:	Core sample and thin sections of A & F, B & F, and C & F	74
Figure 4.13:	Map of mineralogical facies distribution	78
Figure 4.14:	Distribution of lithofacies in core 6-13-58-18W5	81
Figure 4.15:	Distribution of lithofacies in core 10-21-62-18W5	82
Figure 4.16:	Graph of carbonate percentages relative to stratigraphy	84
Figure 4.17:	Distribution of lithofacies in core 7-5-59-18W5	85
Figure 4.18:	Distribution of lithofacies in core 14-2-69-21W5	86
Figure 4.19:	Distribution of lithofacies in core 4-13-56-23W5	88
Figure 4.20:	Distribution of lithofacies in core 15-23-53-21W5	89
Figure 4.21:	Distribution of lithofacies in core 8-26-55-22W5	90
Figure 4.22:	Distribution of lithofacies in core 9-35-48-12W5	92
Figure 4.23:	Distribution of lithofacies in core 5-17-56-8W5	93
Figure 4.24:	Distribution of lithofacies in core 8-19-66-12W6	94
Figure 4.25:	Distribution of lithofacies in core 2-22-51-7W5	96
Figure 4.26:	Distribution of lithofacies in core 6-6-46-15W5	97
Figure 4.27:	Distribution of lithofacies in core 6-5-51-7W5	98
Figure 4.28:	Distribution of lithofacies in core 9-17-50-10W5	99
Figure 4.29:	Distribution of lithofacies in core 6-28-61-26W5	101

Chapter 5

Figure 5.1:	Photomicrographs of various calcite components and phases	109
Figure 5.2:	Core photo and photomicrographs of carbonate and pyrite phases	111
Figure 5.3:	Photomicrographs of infilling and replacement dolomite	114
Figure 5.4:	Core photo & photomicrographs of quartz, pyrite, dolomite, celestite	116
Figure 5.5:	Core photo & photomicrographs of sulphates and stylolites	120
Figure 5.6:	Photomicrograph of a coated grain and anhydrite	123
Figure 5.7:	Plot of $\delta^{18}\text{O}$ vs. $\delta^{13}\text{C}$ of calcites and dolomite populations	125
Figure 5.8:	Plot of $\delta^{18}\text{O}$ vs. $\delta^{13}\text{C}$ of calcites relative to stratigraphy	132
Figure 5.9:	Plot of $\delta^{18}\text{O}$ vs. $\delta^{13}\text{C}$ of dolomite population relative to stratigraphy	134
Figure 5.10:	Plot of $\delta^{18}\text{O}$ vs. $\delta^{13}\text{C}$ of dolomite population relative to disturbed belt	135
Figure 5.11:	Plot of $\delta^{18}\text{O}$ vs. $^{87}\text{Sr}/^{86}\text{Sr}$ of carbonates and sulphates	138
Figure 5.12:	Paragenetic sequences for near-basinal and near-reef lithofacies	143

Chapter 6

Figure 6.1:	Photo of drill core plug taken for MICPM	149
Figure 6.2:	Profiles of capillary pressure vs. pore volume of mercury saturation	152
Figure 6.3:	Profiles of capillary pressure vs. incremental pore volume mercury	155
Figure 6.4:	Initial entry pressure for sample CCS 11 in core 10-16-69-5W6	157
Figure 6.5:	Graph of the magnetic susceptibilities of whole-rock samples	161
Figure 6.6:	Profile of percent carbonate vs. magnetic susceptibility	162
Figure 6.7:	Magnetic susceptibilities plotted on structural cross section D-D'	164
Figure 6.8:	Magnetic susceptibilities plotted on structural cross section F-F'	165
Figure 6.9:	Potential fluid migration pathways in structural cross section A-A'	167
Figure 6.10:	Potential fluid migration pathways in structural cross section B-B'	168
Figure 6.11:	Potential fluid migration pathways in structural cross section C-C'	170
Figure 6.12:	Locations of cross-formational fluid flow in structural cross section D-D'	171
Figure 6.13:	Locations of cross-formational fluid flow in structural cross section E-E'	173
Figure 6.14:	Locations of cross-formational fluid flow in structural cross section F-F'	174

1. Chapter 1 - Introduction

1.1. Introduction and Previous studies

Throughout a large area of the Western Canada Sedimentary Basin (WCSB), carbonate platforms, banks, and reefs (buildups and pinnacles) of the Devonian system are present and contain major economic resources of oil, natural gas, as well as bitumen, sulphur, lead, and zinc (Wendte, 1992). This Devonian system contains an estimated total of about $1.4 \times 10^9 \text{ m}^3$ (8.9×10^9 bbls) of conventional crude oil, which is about 51% of the conventional crude oil in the basin, and about $840 \times 10^9 \text{ m}^3$ ($30 \times 10^{12} \text{ ft}^3$) of natural gas, which is about 23% of all marketable gas in the basin (Hay, 1994). In addition, the Devonian hosts a giant unconventional petroleum resource of about $42 \times 10^9 \text{ m}^3$ (264×10^9 bbls) of heavy oil/bitumen (Hay, 1994). To maximize the evaluation of the hydrocarbon resources, it is well known that a thorough understanding of (1) the sources of the hydrocarbons; (2) the reservoir(s) in which the hydrocarbons are emplaced; (3) the migration path from the source to the reservoir; and (4) the sealing and trapping mechanisms of the reservoir(s) are essential (e.g. Selley, 1985).

Several studies have been and are currently being conducted on the carbonate reservoirs and on regional aquifers in the Devonian system of the Alberta Basin, a sub-basin of the WCSB, e.g., Mountjoy et al., 1992; Patey, 1995; Horrigan, 1996; Huebscher, 1996; Machel et al., 1996; and Duggan, 1997. Jointly, these studies have revealed a better understanding of (paleo-)fluid migration pathways and constraints leading to the development of reservoirs within Devonian aquifers of the Alberta Basin. Analogous research regarding (paleo-)fluid flow in the deep part of the Alberta Basin adjacent to the disturbed belt of the Rocky Mountains is ongoing (McKenzie, 1999; Green, 1999; B.E. Buschkuehle and K. Michael, Ph.D. theses in progress, University of Alberta; S.W. Smith, M.Sc. thesis in progress, McGill University).

In studies conducted within Devonian carbonate reservoirs and aquifers close to the disturbed belt of the Rocky Mountains, anomalously high $^{87}\text{Sr}/^{86}\text{Sr}$

ratios have been identified in late-diagenetic, coarse-crystalline, calcite cements. These anomalous isotope ratios were first discovered in the Obed region of the Wild River Basin (Figures 1.1 and 1.2) (Patey, 1995; Machel et al., 1996) and, more recently, in late-stage carbonate cements within Devonian aquifers close to the disturbed belt, i.e., in studies completed within the Simonette Reef Complex (Duggan, 1997; Rock, 1999), the Leduc fringing reef of the Peace River Arch (McKenzie, 1999), and in Kaybob (Green, 1999), and also in graduate research currently in progress within the Southesk Caim Complex (B.E. Buschkuehle, Ph.D. thesis in progress, University of Alberta).

It has been proposed that during diagenesis, i.e., during smectite to illite transformation, Devonian shale aquitards could have provided the source for the elevated $^{87}\text{Sr}/^{86}\text{Sr}$ ratios within the adjacent carbonate aquifers Duggan et al. (1998) and Duggan (1997). However, geochemical analyses of some selected shales (Cavell and Machel, 1997) suggest that a basin-external source is more likely. Proterozoic metasedimentary rocks, similar to those located in the Jasper townsite of the Rocky Mountain Main Ranges, approximately 100 km southwest of the Obed area, have been proposed as the source for the ^{87}Sr -enrichment in these late calcites of the Obed region. Fluids responsible for transporting the high $^{87}\text{Sr}/^{86}\text{Sr}$ signatures to the Obed region were likely tectonically expelled during the Laramide orogeny and travelled laterally, northeastward through the Southesk Caim Complex (Figure 1.2). On the other hand, the source of anomalous $^{87}\text{Sr}/^{86}\text{Sr}$ signatures in the Simonette area (Duggan, 1997) may have been Cambrian strata or the Precambrian crystalline basement underlying the Devonian system in the WCSB. The fluids could have been transported via sub-vertically controlled faults, or by other methods. The hypothesis that shale and marl aquitards could have provided the source for the elevated $^{87}\text{Sr}/^{86}\text{Sr}$ ratios forms the foundation of the thesis.

Additionally, it is recognized that shale and marl aquitards, which repeatedly act as stratigraphic and structural seals to the intervening carbonate aquifers in the Devonian system, are generally not as well studied in comparison to the reservoir intervals. The only comprehensive studies of the hydraulic

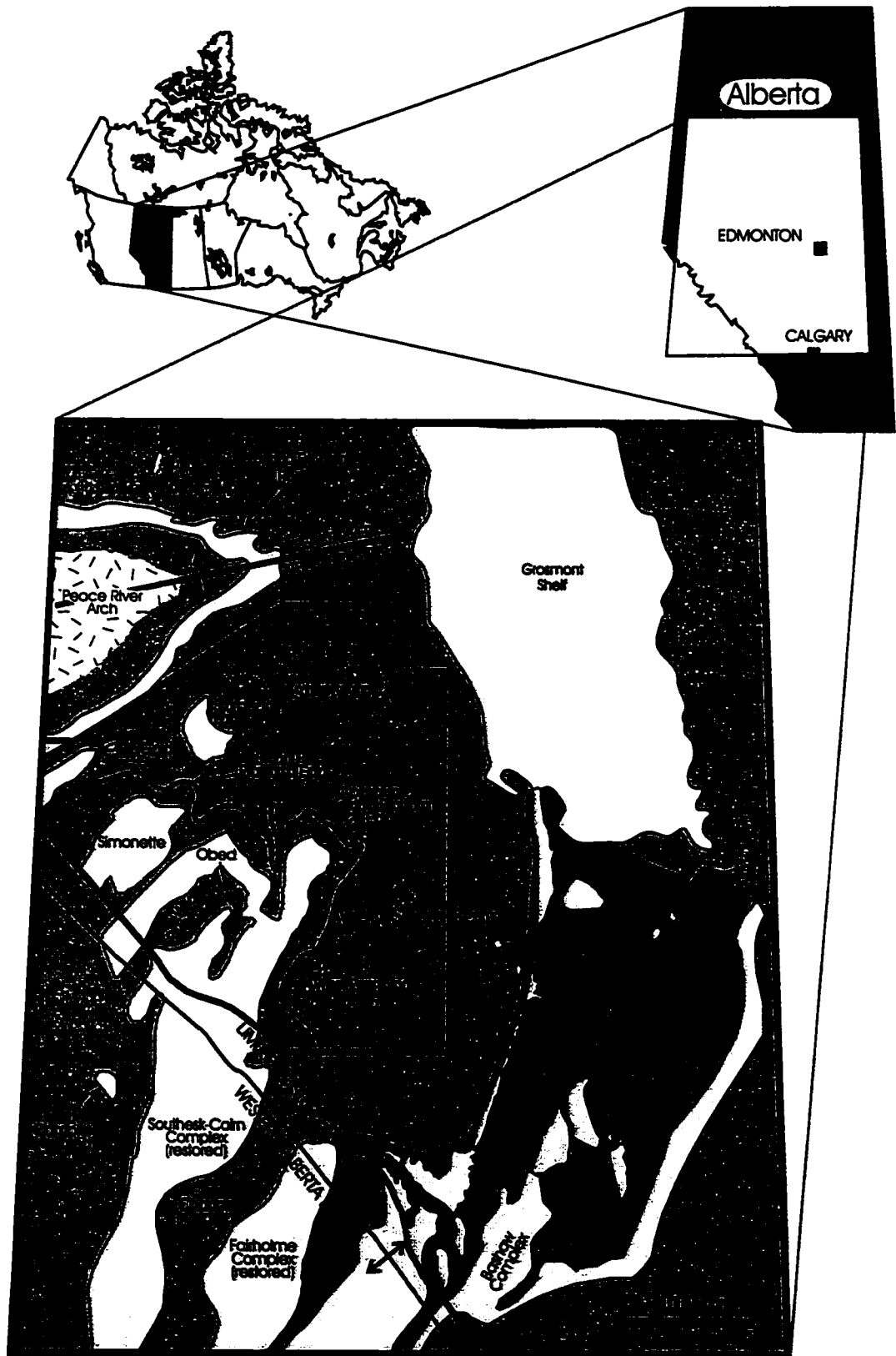
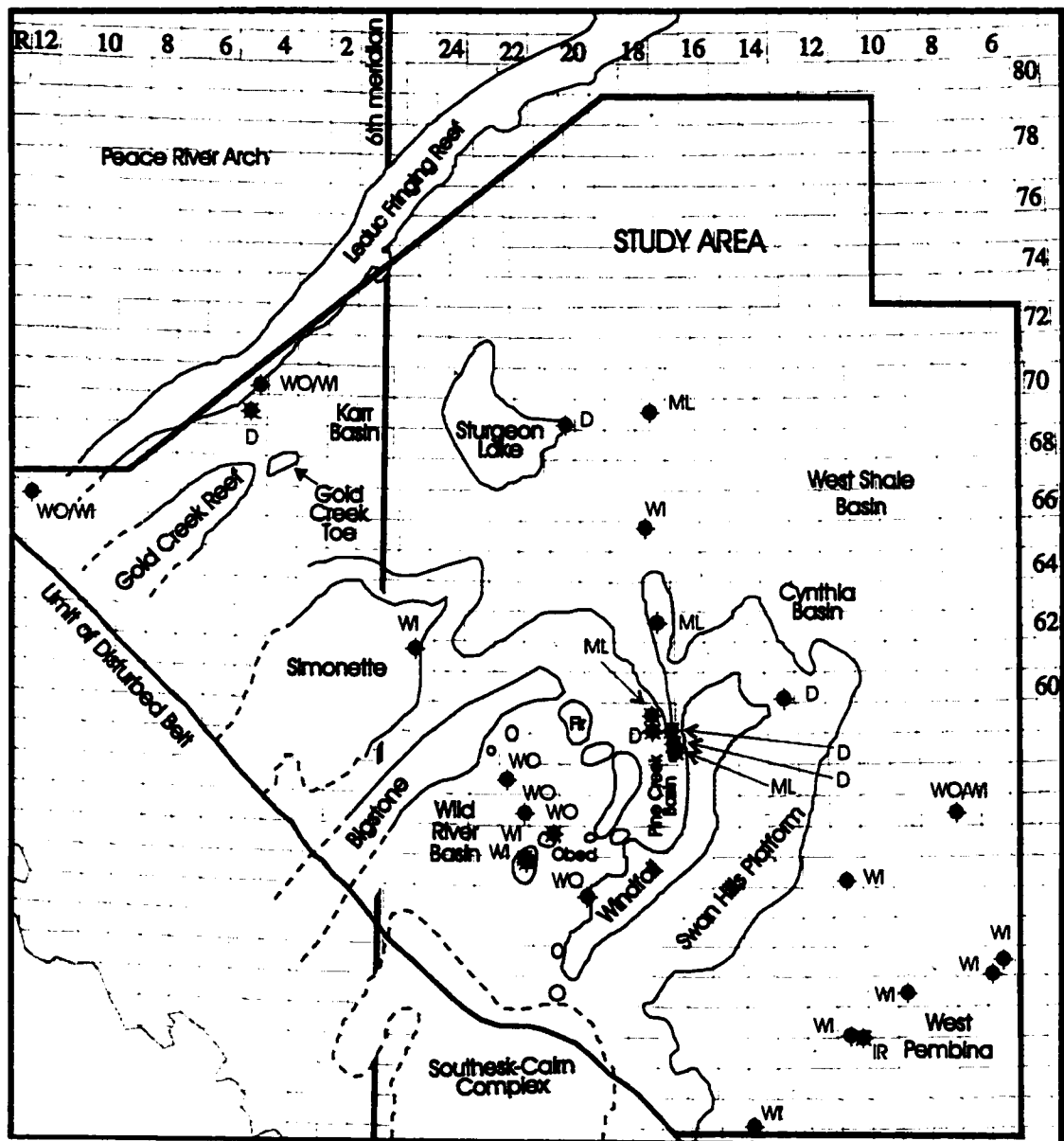


Figure 1.1: Devonian paleogeography map of Central Alberta including the location of the study area. Carbonate complexes and channels to the west of the disturbed belt have been palinspastically restored (Modified from Switzer et al., 1994).



integrity of a Devonian aquitard, the Ireton Formation, was conducted in the east-central Alberta Basin in the Bashaw Reef Complex (Figure 1.1) (Rostron, 1995; Hearn, 1996). As Hearn (1996) indicated, the reason for the relative scarcity of research on aquitards in the WCSB is the fact that petroleum companies are primarily interested in the hydrocarbon reservoirs and carbonate aquifers. Nevertheless, several studies of the source rock potential (Stoakes and Creaney, 1984; Allen and Creaney, 1991; Chow et al., 1995), sedimentology and depositional history (McCrossan, 1961; Oliver and Cowper, 1963; Campbell and Oliver, 1968; Stoakes, 1980; Stoakes and Creaney, 1984 and 1985; Stoakes, 1992), and (bio-)stratigraphy of the shales (e.g. Weissenberger, 1988 and 1994; McLean and Klapper, 1998) have been conducted. These studies have provided a general understanding of the sources of hydrocarbons in the Devonian system, and of the depositional environments of the aquitards.

In the subsurface of west-central Alberta, however, the potential influence that aquitards might have on (paleo-)fluid flow patterns within the Devonian system has generally been neglected. It is one of the objectives of this project to determine the role that aquitards play(ed) in the dynamics of regional fluid-flow patterns within the Devonian system, e.g., how they interact(ed) with surrounding aquifers. Downey (1994) asserted that information concerning aquitard lithology, thicknesses, capillary properties, and lateral continuity can provide a better understanding of the trap geometry, the hydrocarbon column sustainable by the "seal", and the areas of potential breaching; which proved to be successful in Hearn's (1996) study.

1.2. Objectives of the Research Project

To date in the subsurface of west-central Alberta, extensive studies have not been conducted on the stratigraphy, structure, petrography, and sealing capabilities of Devonian aquitards, which inevitably play(ed) a role in the dynamics of regional fluid-flow within the Devonian system. These issues are addressed using; firstly, a regional stratigraphic and structural study of Upper Devonian shale and marl aquitards to delineate their lateral and vertical extent

throughout the study area, in addition to investigating the presence of faults, and; secondly, detailed studies focussing on Woodbend and Winterburn Group aquitards within the Upper Devonian. These detailed studies include the following:

- a) petrography to identify the lithofacies and mineralogical facies, which in turn provide an understanding of the sedimentary depositional environments for the aquitards;
- b) radiogenic isotopic analyses, which includes an expansion of the $^{87}\text{Sr}/^{86}\text{Sr}$ database to determine if the aquitards contributed to ^{87}Sr -enriched fluids that were responsible for precipitating highly radiogenic (^{87}Sr -enriched) late-stage calcite cements within adjacent Leduc Formation;
- c) stable isotopic analyses, which includes $\delta^{18}\text{O}$ and $\delta^{13}\text{C}$ of to determine if the aquitards are effective barriers to aqueous (paleo-)fluid flow;
- d) a diagenetic history of the aquitards; and
- e) mercury injection capillary pressure measurements and magnetic susceptibility tests to determine the sealing capacity of the aquitards to, and their potential interaction with, hydrocarbons.

Together, these regional and detailed studies are incorporated to provide an investigation of regional (paleo-) fluid flow patterns in the Devonian system.

1.3. Study Area and Core Control

The study area is centered around the Obed sour gas field and the Wild River Basin located in the Alberta Basin (between approximately 3,000-5,000 m in depth) (Figures 1.1 and 1.2). The study area is approximately 38,000 km² in size and is constrained to the west by the limit of the disturbed belt, to the north by the Peace River Arch, and extends east to include the West Pembina area.

Approximately 790 m of core from 28 wells, containing intervals of aquitards and intervening aquifers from the Woodbend and the Winterburn Groups were examined at the Core Research Centre of the EUB (Energy and

Utilities Board) in Calgary, Alberta (Appendix 1). These cores were located in the Wild River Basin, West Pembina area, the Pine Creek Basin, and other areas near the disturbed belt (Figure 1.2).

The aquitards, from which samples were collected for further analyses, range in thickness from 3 m to 315 m. About 160 representative samples of the various aquitards were taken for further analyses. Samples were taken of the various lithofacies and also from intervals which showed direct evidence for (paleo-)fluid flow through the “aquitards”, e.g., cement infilled fractures.

2. Chapter 2 - Regional Geological Setting and Depositional History

2.1. Western Canada Sedimentary Basin

The WCSB (Figure 2.1) is the general name given to the northeasterly tapering wedge of sedimentary units that gradually thicken southwestward from a zero-edge along the exposed margin of the Canadian Precambrian Shield to greater than 6 km near the Cordilleran foreland thrust belt (Ricketts, 1989). The northern boundary of the WCSB is delimited by the Tathlina High in the Northwest Territories, and although the geological basin does extend into the United States, for the purpose of this study the southern boundary is delimited by the 49th parallel. The western boundary of the WCSB is defined by exposed, deformed sediments of the ancestral North American margin, equating to the eastern limit of allochthonous terranes. This is usually located near the boundary between the Omineca and the Intermontane belts of the Cordillera (Figure 2.1) (Wright et al., 1994). The eastern boundary is along the exposed margin of the Canadian Shield.

The thickest and stratigraphically most complete part of the WCSB occurs within the eastern parts of the Rocky Mountain foreland thrust and fold belt and the Omineca belt. The WCSB is sub-divided into two major sedimentary basins (Figure 2.1); the northwest-trending trough in front of the Cordilleran fold and thrust belt called the Alberta Basin, and the intracratonic Williston Basin, centered in North Dakota, which extends into southern Saskatchewan and southwestern Manitoba (Wright et al., 1994). These two features are separated by a broad northeast-trending positive element, the Bow Island Arch. The study area of this project is located within the western half of the Alberta Basin (Figure 2.1).

2.2. Devonian Stratigraphy

The current study involves stratigraphic and structural analyses of five Middle to Upper Devonian Groups within the Alberta Basin. From base to top

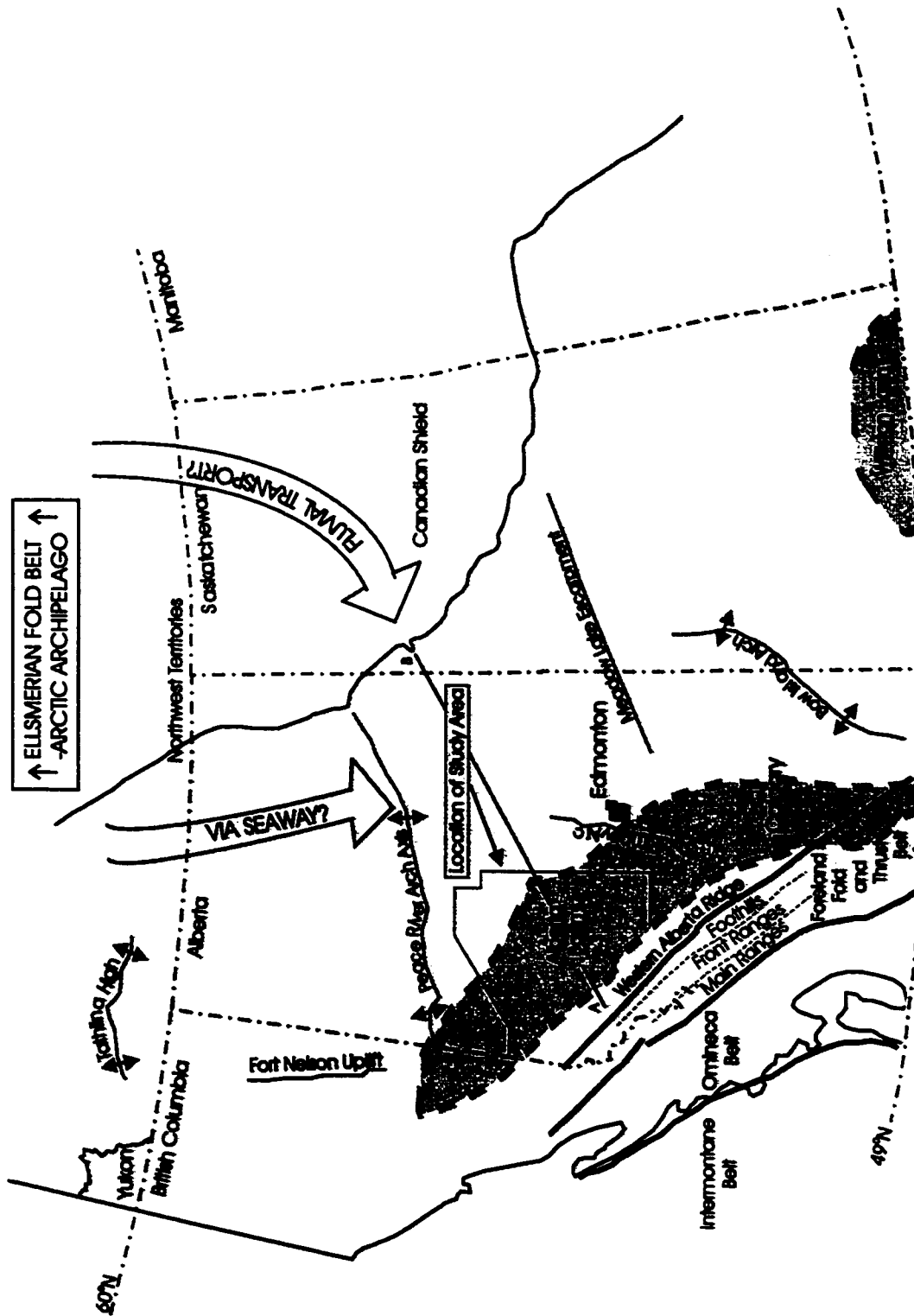


Figure 2.1: The Western Canada Sedimentary Basin including parts of the Alberta and Williston Basins and major structural trends and geological elements that influenced the deposition of shales and sands, and carbonate reef assemblages. The orientation of cross section A-B in Figure 2.2 is also indicated (Modified from Switzer et al., 1994, and Wright et al., 1994).

they include: the Elk Point, Beaverhill Lake, Woodbend, Winterburn, and Wabamun Groups (Figure 2.2). The Lower Carboniferous Exshaw Formation, capping the Wabamun Group, was used as a stratigraphically upper limit. The reasons for including the Exshaw Formation as part of this study is explained in Chapter 3.

Most work involves the stratigraphy and depositional history of the Woodbend and Winterburn Groups. Detailed accounts of the stratigraphy, depositional history and facies of other Groups can be found in Meijer Drees (1994), Oldale and Munday (1994), and Halbertsma (1994) and references therein.

2.3. The Alberta Basin

The Alberta Basin is that part of the WCSB north and northwest of the Bow Island Arch that extends up to the Tathlina High and east of an area defined as the Western Alberta Ridge (Figure 2.1) (Wright et al., 1994). The Alberta Basin can further be subdivided into the East and West Shale Basins (Figure 1.1), divided by the regionally extensive, approximately 560 km long, northeast-trending Rimbey-Meadowbrook reef chain. Since Cambrian time, two major highs in the Alberta Basin have existed: the Peace River Arch and the Western Alberta Ridge (Wright et al., 1994). Both play(ed) a significant role in the depositional pattern of Devonian strata.

2.3.1. West Shale Basin

Although the present research (Figures 2.1 and 1.1) is located within the West Shale Basin of the Alberta Basin, a discussion of the much larger WCSB is necessary to understand the depositional history within the study area.

2.4. WCSB Structures Influencing Devonian Stratigraphy

Major geological elements that directly or indirectly influenced the deposition of the Woodbend Group include: the Rimbey Arc; the Peace River (Athabasca) Arch; the Western Alberta Ridge; the Tathlina High; the Fort Nelson

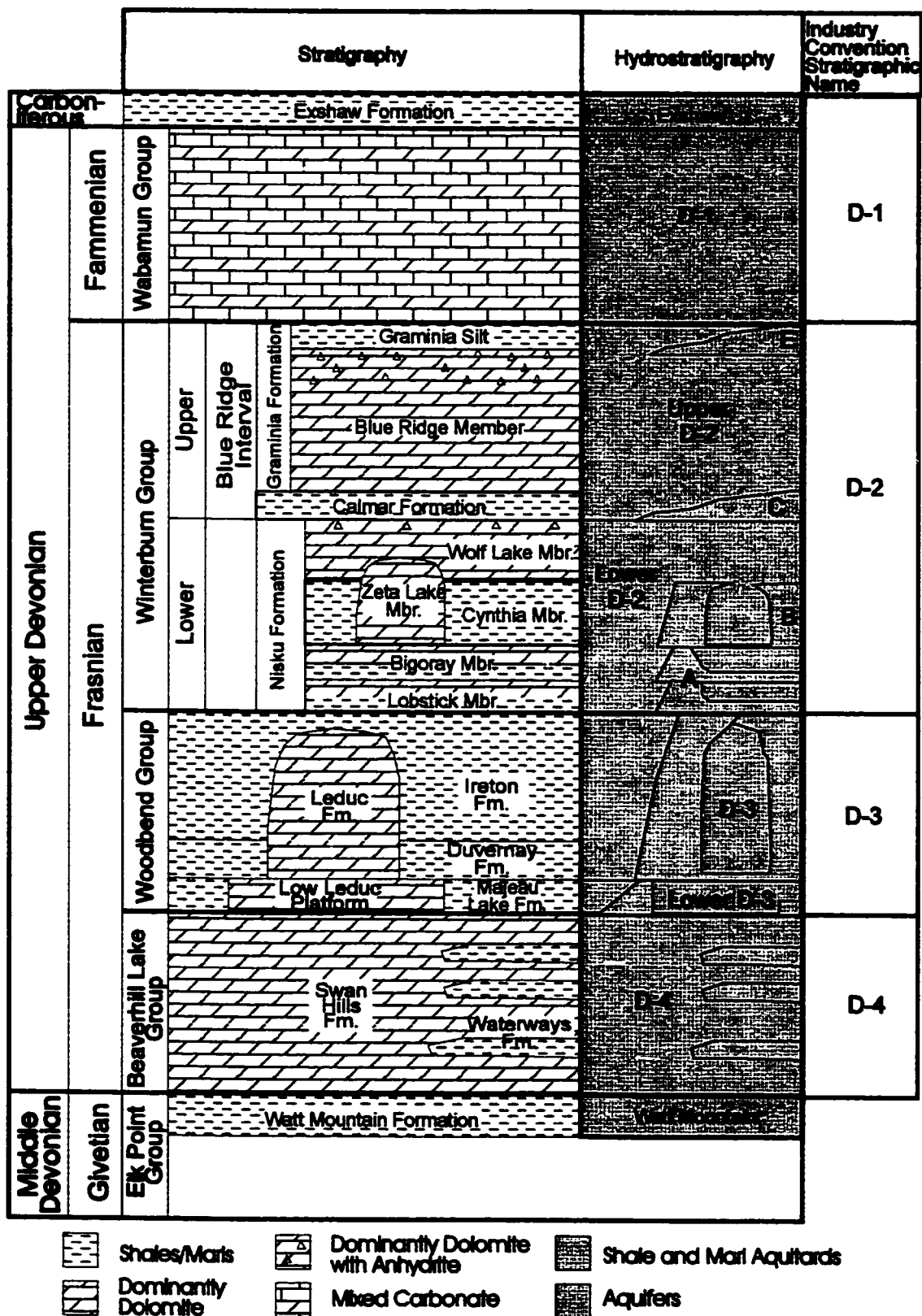


Figure 2.2: Generalized stratigraphic and hydrostratigraphic units (discussed in the text) pertaining to this study, including carbonate aquifers, and shale and marl aquitards. Woodbend and Winterburn Group strata modified from Switzer et al., (1994).

Uplift; and the Meadow Lake Escarpment (Figure 2.1) (Switzer et al., 1994). Some of these geological elements are Precambrian crystalline basement trends (topographic highs) that restricted Devonian marine incursion to the west (Burrowes and Krouse, 1987) and most likely controlled the location of several Devonian carbonate buildups (Moore, 1988; Mountjoy, 1980). These carbonate buildups, in turn, controlled the deposition of the clastic basin-fill units.

The Peace River Arch was a Precambrian granitic-basement landmass during deposition of the Woodbend and Winterburn Groups (Figures 2.1 and 1.1), and influenced subsidence and sedimentation patterns during the Devonian period. A narrow carbonate fringe of Leduc carbonates developed along the Peace River Arch during the Upper Devonian. In the Mississippian, the Peace River Arch subsided, and the region around it also subsided, largely through normal faulting (Burrowes and Krouse, 1987).

The Western Alberta Ridge (Figures 1.1 and 2.1) has a core that consists of an eroded lower Paleozoic sequence. The Ridge was mostly covered by the end of deposition of the Beaverhill Lake Group, but it still had an effect on Woodbend and Winterburn deposition, although at a progressively diminishing level. The ridge was a site of formation of a major Leduc Reef Complex during the Upper Devonian (Figures 1.1 and 1.2) (Switzer et al., 1994).

The Tathlina High, located in the Northwest Territories has a core of Precambrian granite. This high was completely buried by the Devonian Elk Point Group, and although it influenced Woodbend deposition in its vicinity, it probably had little affect on depositional patterns in the study area located to the south. The Tathlina High and Fort Nelson uplift remained submarine topographic highs against which basin-fill shales downlapped and thinned (Switzer et al., 1994).

The Meadow Lake escarpment, located northeast of the Bow Island Arch, is a major pre-Devonian erosional and structural feature. It is well known for its effect on Mid Devonian sedimentation, and also appears to have influenced many of the depositional changes in Upper Devonian strata (Switzer et al., 1994). The Meadow Lake escarpment coincides with both the southern bank

edge of Beaverhill Lake Group and also the southern Alberta Leduc shelf edge (Switzer et al., 1994).

2.5. Woodbend Group

2.5.1. Stratigraphy and Depositional history

The Woodbend stratigraphy was first defined within the East Shale Basin of the Alberta Basin, adjacent to the present study area. In the East Shale Basin, the Woodbend Group has a base of platform carbonates of the Cooking Lake Formation, which is covered by carbonate complexes and reefs of the Leduc Formation (Figures 2.2 and 2.3) (Switzer et al., 1994). In the West Shale Basin, and in the Peace River Arch area, the basal platform is called the Low-Leduc platform (Figures 2.2 and 2.3). Black, bituminous shales and dense argillaceous limestones of the Duvernay Formation conformably overlie the Cooking Lake Formation where the Leduc Formation is absent. The Majeau Lake Formation is the basinal equivalent of the Cooking Lake Formation; in places where the Duvernay Formation overlies the Majeau Lake Formation, these two are practically indistinguishable. The basinal Ireton Formation conformably overlies the Duvernay Formation, surrounding and eventually covering buildups of the Leduc Formation. During several early studies on the Ireton and Duvernay Formations, various lithologies and facies were recognized (McCrossan, 1957; Andrichuk, 1958; McCrossan, 1961; Oliver and Cowper, 1963; Campbell and Oliver, 1968). Most recently, Stoakes (1979, 1980) has provided one of the most detailed investigations of the lithofacies within these Formations in the East Shale Basin.

A distinctive and widespread wireline log marker within the thick Frasnian Ireton shales of west-central Alberta is the Z-marker (Wendte et al., 1995). It is a stratigraphically significant surface in the Ireton shales because it more closely approximates the division between the Woodbend and Winterburn Groups on the eastern shelf (proximal to the West Pembina area) than any other widespread, correlatable marker. In the west-central Alberta Basin, the Ireton shales above the Z-marker are stratigraphically equivalent to the Nisku

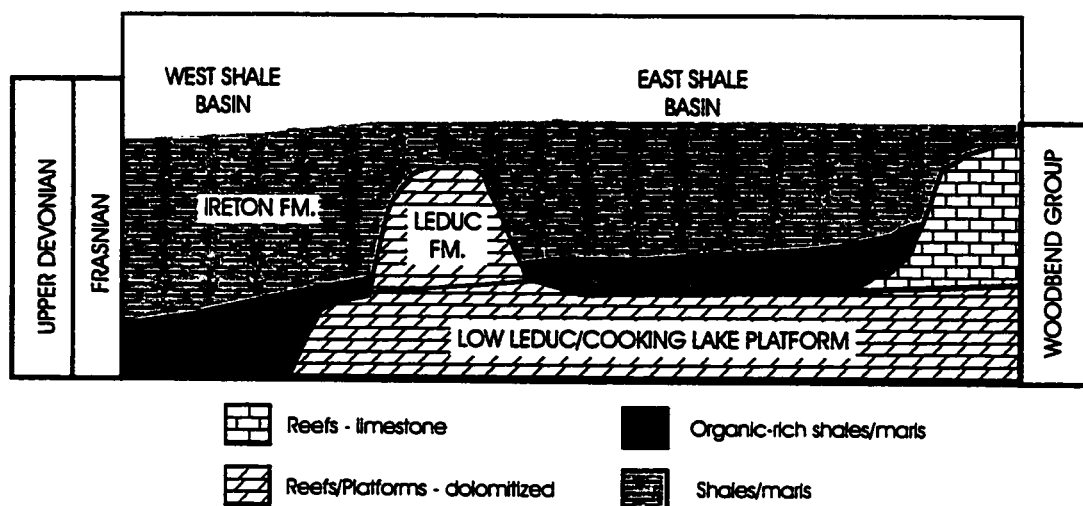


Figure 2.3: Generalized schematic diagram showing depositional environments and stratigraphy of the Woodbend Group in the West and East Shale Basins (Modified from Stoakes, 1980).

Formation and are not part of a basinally restricted wedge that predates most or all of the Nisku Formation. The correct recognition and correlation of this marker permits an understanding of basin evolution beyond that discernible from the existing lithostratigraphic nomenclature alone (Wendte et al., 1995).

Leduc Formation reef complexes of the Devonian deep basin, nearest the limit of the disturbed belt, show a relatively irregular distribution in contrast to the aligned trends of the eastern part and encircle a small sub-basin referred to as the Wild-River Basin (Figures 1.1 and 1.2). Between the Peace River Arch and the Wild River Basin, large isolated Leduc complexes, such as Sturgeon Lake and Gold Creek Reef, occur. Generally, the Leduc reefs in the deep basin appear to be aligned and oriented in a north/northeastern direction. This orientation may reflect structural trends within the Precambrian crystalline basement (Switzer et al., 1994 and references therein).

Sediments of the Woodbend Group comprise a single "mega" cycle of deposition consisting of a lower transgressive stage and an upper regressive stage. The beginning of the Woodbend coincides with a gradual deepening of the Alberta Basin, whereas the end of Woodbend deposition reflects a reduced rate of subsidence, along with a sea-level fall. At the end of Woodbend deposition, a significant portion of the Alberta Basin was infilled with shales.

The transgressive stage of the "mega" cycle is dominated by shallow-water platform and reefal carbonate during which only minor amounts of basinal sediment were added to basinal areas over most of the western Alberta Basin. The sea-level rise caused backstepping of carbonate platforms in both the East and West Shale Basins, e.g., backstepping of lower Leduc carbonate platforms over an underlying Swan Hills bank in the West Shale Basin (Stoakes, 1992) and the initiation and localization of isolate reefs and banks of the Leduc Formation (Figures 1.1 and 1.2), as well as onlap of several large Devonian bank complexes onto the Western Alberta Ridge.

The regressive phase is dominated by prograding, fine-grained calcareous and argillaceous basin-fill units of the Duvernay and Ireton Formations in addition to the formation of thin, carbonate platform units (Stoakes, 1992). The major

portion of basin fill took place following deposition of the uppermost middle Leduc Formation (Switzer et al., 1994). Asymmetric filling of the Alberta basin occurred from east to west. This depositional style was succeeded on the east side by forestepping carbonate platform units extending progressively over shale clinoforms. Only a small increment of basinal Ireton deposits was added to the West Shale Basin during this phase because this Basin was far removed from the advancing clinoforms of the Ireton Formation. For example, only a very thin increment of basinal sedimentation occurs around the base of Leduc Reefs in the Wild River Basin and around the Peace River Arch to the north (Switzer et al., 1994). The lack of terrigenous influx and hence, better water quality in the West Shale Basin, allowed many reefs and carbonate banks to sustain growth during the entire regressive phase. By the end of Woodbend deposition, the WCSB was almost filled by shale and carbonates.

2.6. Winterburn Group

2.6.1. Stratigraphy and Depositional History

The Winterburn Group differs in several ways from underlying Woodbend and Beaverhill Lake Groups including: (a) the extension of carbonate shelf complexes much farther basinward than underlying shelf complexes of either the Woodbend or Beaverhill Lake Groups; (b) the development of smaller pinnacle reefs and reef trends; (c) the general lack of more robust stromatoporoid morphotypes in addition to a predominance of corals in an open-marine setting; and (d) the introduction and extensive distribution of larger grain-sized siliciclastics (Cynthia, Calmar and Graminia siltstones to be discussed subsequently) (Switzer et al., 1994).

The Winterburn Group consists of carbonate platforms, ramps, and so called "pinnacle reefs" in addition to basin-filling lime mudstones and shales. Deposition of the Winterburn Group was characterized by an overall shallowing and continued infilling of the Alberta Basin after Woodbend Group deposition, so that by latest Frasnian time (equated to the end of deposition of the Graminia

Silt) little or no accommodation space was available over most of the Alberta Basin except to the extreme west and northwest. The Winterburn Group is divisible into an Upper and a Lower Group (Figure 2.4), and within each division, a smaller order transgression followed by a regression is represented.

- *Lower Winterburn Group*

The Nisku Formation of the Lower Winterburn Group started with an apparent rise in relative sea level (lower transgressive stage) and ended in a regression (upper progradational stage). The transgressive stage formed widespread carbonate buildups in the shallower part of the basin, to the east of the Rimbey-Meadowbrook reef chain, where the Nisku and the Grosmont shelves formed. At the same time, in deeper water areas to the west, e.g. within the study area, sets of backstepping carbonate ramps formed (Switzer et al., 1994). Local carbonate production kept pace with sea-level rise, which resulted in the formation of downslope isolated pinnacle reefs such as those of the Zeta Lake Member (Figure 2.4). The Lobstick, Bigoray, Zeta Lake, and Lower Cynthia Members are all part of this transgressive stage. During an ensuing period of relative sea-level stasis, prograding shales of the Upper Cynthia Member largely infilled the area between the isolated reefs and the shelf margin complex. In proximal portions of the Cynthia ramp towards the southeast and east, the predominantly carbonate sediments are termed the Dismal Creek Member (Figure 2.4) (Machel, 1983).

The regressive stage is represented by prograding carbonate and fine-grained clastic sedimentary wedges under conditions of diminishing accommodation space. In addition to isolated reefs, tidal flat sediments of the Wolf Lake Member were deposited across the Cynthia Basin (Figures 1.2 and 2.4).

- *Upper Winterburn Group*

The overlying Blue Ridge Interval (after Switzer et al., 1994) of the Upper Winterburn Group represents the last carbonate cycle within Frasnian time and

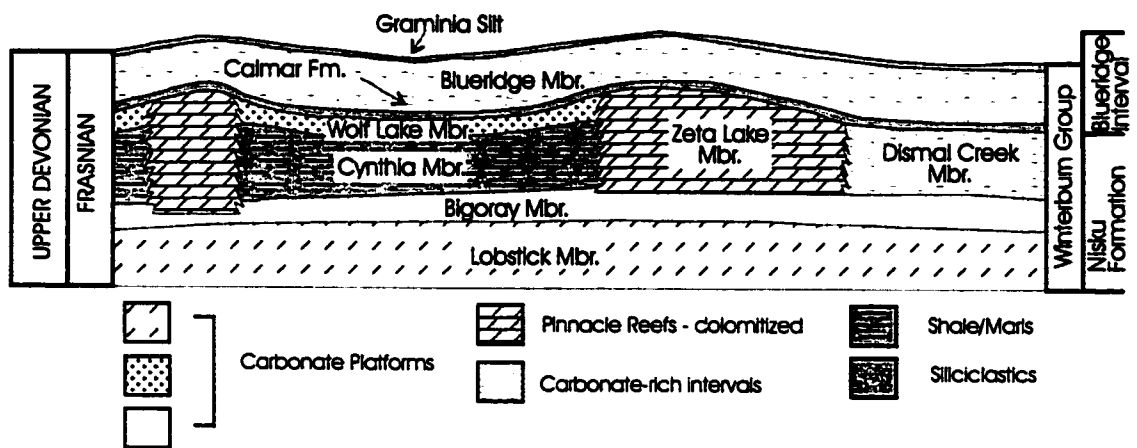


Figure 2.4: Generalized schematic diagram showing depositional environments and stratigraphy of the Winterburn Group typical in the West Pembina area (Modified from Machel, 1983 and Manzano, 1995).

consists of the Calmar Formation, the Blue Ridge Member, and the Graminia Silt (after Switzer et al., 1994) (Figure 2.2 and 2.4). This Interval is similar to the Nisku Formation in that it consists of a transgressive depositional phase followed by a phase of progradation and basin infilling. In particular, the Blue Ridge Member marks a relative sea-level rise. Underlying silts of the Calmar Formation form a distinctive and commonly employed log marker over much of the Alberta Basin. Unfortunately, little is known about the sedimentology and the depositional controls of this unit. In the West Pembina area (Figure 1.2), the Calmar Formation is represented by silty shale and carbonate mudstone. The Graminia Silt, which caps the Blue Ridge Member, is interpreted as representing reworked detrital and/or windblown material originally deposited in the basin during relative sea-level lowstand (Switzer et al., 1994).

In the Karr Basin (Figure 1.2), the lack of a recognizable Calmar silt makes definition of the base of the Blue Ridge Interval difficult. Also within the western part of the study area, particularly in the Karr Basin, evaporitic carbonates occur in the Blue Ridge Member. Thick Graminia Silt intervals are widespread in the Karr Basin area and probably indicate regional salt dissolution that preceded, or was coeval with, Graminia Silt deposition. The end of the Blue Ridge Interval coincides with the end of the Frasnian, which also marks a major global extinction event of many shallow water invertebrates (Switzer et al., 1994 and references therein).

2.7. Basin Fill Units

In the Woodbend and Beaverhill Lake Groups two major sources contributed sediment to basin infilling; an intrabasinal source of carbonate derived from buildups; and, secondly, an extrabasinal source of fine terrigenous material (Wendte, 1992). Basin-fill units of the Woodbend Group have a significant clay-shale content in contrast to the basin-fill units of the underlying Beaverhill Lake Group composed dominantly of carbonate muds derived from coeval carbonate banks. This increased clay-shale content marks delivery of

terrigenous material into the East Shale Basin from an extrabasinal source (Stoakes, 1992).

There are several suggestions regarding the terrigenous source and deposition of the basin-fill within the Upper Devonian. Stoakes (1979, 1980) suggested that, despite being distant from the Alberta Basin, the Ellesmerian fold belt in the Arctic Archipelago appears to be the most likely major source for the Duvernay and Ireton Formations of the Woodbend Group (Figure 2.1). Stoakes (1980) stated that fluvial transport of sediments over the Canadian Shield could have introduced shale into the basin from the east. Stoakes (1992) later stated that it is also reasonable to postulate that they gained access to the Alberta Basin by marine currents in a seaway existing between the Peace River emergent landmass and the Grosmont shelf (Figures 1.1 and 2.1).

Switzer et al. (1994) suggested that the asymmetric pattern of Ireton basin fill indicates that fine argillaceous input was largely along the eastern side of the basin, and an easterly trade-wind belt was responsible for imparting a westerly progradational aspect for the shales. The following aspects of Middle and Upper Devonian strata in the WCSB support deposition in a trade-wind belt: (a) the extensive occurrence of evaporites (particularly in the East Shale Basin), indicating a dry, tropical climate; and (b) indicators of water circulation in a northeastern to southwestern pattern, consistent with an easterly trade-wind belt.

The source of Majeau Lake clastics (basinal equivalent of the Cooking Lake Formation or the Low Leduc Platform in the West Shale Basin) has not been determined; however, there is no evidence for any significant contribution of shale from the west or the Peace River emergent landmass (Switzer et al., 1994). The majority of the shale appears to have been introduced into the basin in the vicinity of the Athabasca Arch (Figure 1.1) and deposited along the northeastern edge of the basin, adjacent to the Canadian Shield (Switzer et al., 1994).

Basinal deposits can act as both sources and seals for the intervening, prolific hydrocarbon-producing pinnacle reefs, reef platforms, and banks. The Duvernay Formation, for example, is considered to be one of the major source

rocks for most of the conventional hydrocarbon accumulation in Upper Devonian reservoirs (such as that of the Leduc and Nisku Formations) in Alberta (Creaney and Allan, 1990) and functions as a seal to the underlying Swan Hills Formation of the Beaverhill Lake Group. The Cynthia Member of the Winterburn Group has been targeted as being a minor source for Nisku pinnacle reefs in localized areas (Creaney and Allan, 1990) and is a lateral and vertical seal for many of the intervening Nisku pinnacle reefs.

2.8. Hydrostratigraphic units of the WCSB

The Devonian system consisting of predominantly of marine deposits, i.e., regionally extensive carbonate platforms, ramps, and buildups such as pinnacle reefs, as previously discussed, form thick, carbonate-dominated aquifer systems (D-1 to the D-4) that are separated; by wedges of fine-grained, lime mudstones and argillaceous "deep-marine" sediments or basin-fill units that form aquitards (Figure 2.2); and also by evaporitic aquicludes. The basin-fill units may have a significant clay-shale content, but may also consist of carbonate muds derived from coeval carbonate banks, buildups, etc. (Stoakes, 1980).

This Devonian system forms part of the Paleozoic sequence, which is one of two megahydrostratigraphic successions in the Alberta Basin (labelled unit 4 in Figure 2.5). The Middle to Late Devonian basin-fill units that form shale and marl aquitards surrounding carbonate aquifers within the Paleozoic megahydrostratigraphic sequence is the focus of the current research. It is important to note that the most probable initial flow-driving mechanism and origin of high-salinity northeastward-flowing waters in the Paleozoic sequence (unit 4) is past tectonic compression along the western basin margin (Bachu, 1995 and references therein) (Figure 2.5). The subsequent sections discuss identification and subdivision of aquitards in the study area.

The second, younger, Mesozoic and Cenozoic sequence of rocks in the WCSB consisting of mainly continentally derived fluvial, near-shore deltaic, and shallow-marine clastic sequences forms thick, shaly aquitards and relatively thin sandstone aquifers. Although not discussed in this project, this sequence

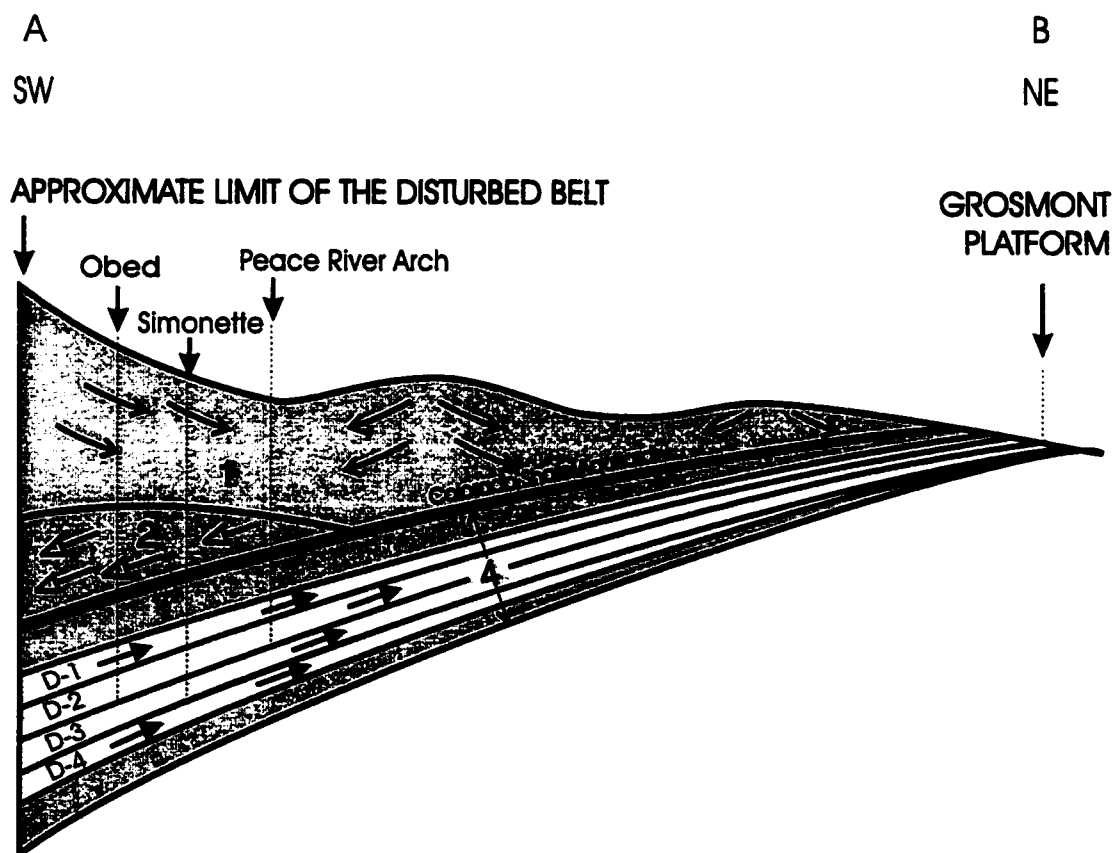


Figure 2.5: Dip Cross Section of two megahydrostratigraphic units in the Alberta Basin: the post-Jurassic (1 and 2); and the pre-Cretaceous (4). The location of the cross section is indicated in Figure 2.1. Unit 3 from Bachu (1995) is not included because the cross section passes north of it. The units are separated by a thick, regional Colorado Shale aquitard. Unit 4 contains regional Devonian aquifers (D1-D4), and shale and marl aquitards. Fluids within unit 4 are dominated by basin-scale tectonic flow. Fluids within units above the Colorado aquitard are dominated by local-scale topography driven flow (1) and by erosional rebound (2) (Modified after Bachu, 1995).

constitutes the second megahydrostratigraphic succession within the Alberta Basin (labelled units 1 and 2 in Figure 2.5) (Bachu, 1995).

2.9. Identification of Aquitards

The identification of Devonian and Lower Carboniferous shale and marl aquitards is based on gamma and sonic/acoustic geophysical well-log data where available. Aquitards are identified as units having; gamma log signatures corresponding to greater than 50 API (American Petroleum Institute) units, on a scale from 0 to 150 API units, and sonic or acoustic logs coinciding with less than 5% porosity, calculated using Schlumberger cross plots.

2.10. Shale and Marl Aquitards

2.10.1. Winterburn Group aquitards

Aquitards within the Lower and Upper Winterburn Groups are referred to as aquitards A and B, and C and E, respectively (Figure 2.2). Aquitard A most likely represents the basal Bigoray Member, but in places it appears to merge with the basal Lobstick Member. Aquitard B is equivalent to the Cynthia Member. Aquitard C is equivalent to the Calmar Formation. Aquitard E, equivalent to the Graminia Silt, is not labelled aquitard D because aquifers in the Devonian system, are partly labelled using this letter i.e., D-1 to the D-4. In more basinal areas these individual aquitards merge. When merged, they can be referred to as the Lower Winterburn Group aquitards, Upper Winterburn Group aquitards, or the Winterburn Group aquitards in general.

2.10.2. Woodbend/Winterburn aquitard

In areas where Winterburn Group aquitards directly overlie the Woodbend Group aquitard (see description below), the merged unit is referred to as the Woodbend/Winterburn aquitard (Figure 2.2).

2.10.3. Woodbend Group aquitard (s)

The Woodbend aquitard(s) generally include the Duvernay and Ireton Formations, however in locations where the Duvernay Formation directly overlies the Majeau Lake Formation, the latter is also included as part of the Woodbend Group aquitard (Figure 2.2).

2.10.4. Majeau Lake Formation aquitard

This aquitard can be mapped as a unit when separated from the Woodbend Group aquitard (Figure 2.2).

2.10.5. Beaverhill Lake Group aquitards

The Beaverhill Lake Group aquitards most likely represent the Waterways Formation (Figure 2.2).

2.10.6. Watt Mountain Formation aquitard

The Watt Mountain Formation forms an aquitard throughout the study area (Figure 2.2).

2.11. Carbonate Aquifers

Conventional use of the D-1 (Wabamun Group), the D-3 (Leduc Formation), and the D-4 (Swan Hills Formation) aquifers occurs (Figure 2.2). Although unconventional, it is useful in the present context to refer to the Low Leduc Platform as the L D-3 aquifer. Also, the D-2 aquifer, where possible, has been subdivided into the L D-2 (the Lower D-2) and the U D-2 (the Upper D-2) (Figure 2.2). The L D-2 refers to the aquifers interfingering the base of the Winterburn Group up to the Calmar Formation, and the U D-2 refers to the aquifers interfingering the Calmar Formation up to the Graminia Silt.

3. Chapter 3 - Stratigraphic and Structural Investigation of Middle to Upper Devonian Aquitards

3.1. Introduction and Objectives

Throughout the study area, twelve regional cross sections were constructed, six stratigraphic and six structural. They were generally constructed through Middle to Upper Devonian successions, including the Elk Point, Beaverhill Lake, Woodbend, Winterburn, and Wabamun Groups, up to the Lower Carboniferous Exshaw Formation (Figure 2.2). The main objective was to document the spatial and temporal relationships of Middle to Upper Devonian shale and marl aquitards and aquifers in the study area. Another objective in constructing cross sections was to indicate the stratigraphic distribution of core containing intervals of aquitards examined at the Core Research Centre in Calgary. The significance of the stratigraphic locations of the cores is detailed in Chapters 4 through 6.

The cross sections encompass an area of over 38,000 km² (Figure 3.1) and are centered around the Obed field and the Wild River Basin. The central part of the present study area overlaps that of Patey (1995), in which late-stage calcite cements of the Leduc Formation carry an anomalously high radiogenic strontium signature. The origin and pathways of the fluids responsible for these anomalous signatures are under debate, and are discussed in Chapters 5 and 6.

The construction of six stratigraphic cross sections (A-A' to F-F'), to be discussed subsequently, illustrate the distribution of Devonian aquitards, in particular their thickness and lateral continuity, during the time of deposition. The stratigraphic and geographic locations of discontinuously thin aquitards is discussed, and the locations where aquitards are absent have been identified. These locations are used to identify areas of interconnection of Devonian carbonate aquifers D-1 to D-4. Investigations of the distribution of aquitards and aquifers may contribute to an understanding of (paleo-)fluid flow patterns within Middle to Upper Devonian successions in Chapter 6.

In a series of six structural cross sections A-A' to F-F', analagous to the stratigraphic cross sections mentioned above, changes in the architecture of the strata since their deposition between 360 to 374 Ma are illustrated. Again, these six cross sections are discussed subsequently.

The Foreland fold and thrust belt and the Omineca belts, adjacent to the study area (Figure 2.1), formed during several several compressive deformation events between the Middle Jurassic to Eocene (Wright et al., 1994). Tectonic loading during the Late Cretaceous Laramide orogeny caused a depression to develop in front of the Laramide Foreland fold and thrust belt (Burrowes et al., 1987), resulting in a regional northeast-southwest trending dip of strata. This regional structural dip is evident in Figure 2.5, as well as in three structural cross sections constructed perpendicular to the limit of the disturbed belt (A-A' to C-C'). Structural features in the area, other than the regional northeast-southwest dip within the fore-deep, that possibly developed as a result of orogenesis, are identified. Three structural cross sections have also been constructed parallel to the limit of the disturbed belt (D-D' to F-F').

In this chapter, only the major results of the cross sections are summarized, which forms the basis for subsequent chapters. However, a detailed examination of aquitard distribution in both stratigraphic and structural cross sections A-A' to F-F' is documented in Appendix 2.

3.2. Cross Section Methods

The cross sections were constructed from logs of wells that have been sampled (Figure 1.2), and from additional logs that would allow for the construction of cross sections as close as possible to a perpendicular or parallel orientation of the regional northeast-southwest trending dip of the basin, respectively (Figure 3.1).

Due to poor well control in the area, it was not possible to construct ideal straight line cross sections. Wells more than approximately one township away from an ideal straight line were projected at 90 degrees onto this line (Figure

3.1). This compensated for an "apparent" dip of strata which would have been evident had the wells not been projected.

The cross sections form a grid-like pattern over the study area, with each dip section (A-A' to C-C') intersecting each strike section (D-D' to F-F') and having at least one well location in common between the two sections at the point of intersection (Figure 3.1). All cross sections, in this chapter, have been constructed with the same horizontal and vertical scale so as to allow direct comparison. On both stratigraphic and structural cross sections, intervals of shale and marl aquitards correspond to the shaded grey areas on well logs in addition to the intervals denoted in green between each well. Carbonate aquifers are denoted in blue.

Both stratigraphic and structural cross sections include well-log data from the Exshaw Formation, the Wabamun, Winterburn, Woodbend, and Beaverhill Lake Groups and quite frequently the top of the Elk Point Group (Watt Mountain Formation). However, some well logs do not contain information for all of these intervals (e.g., in the West Pembina area the majority of the well-log data only penetrates the top of the Woodbend Group).

3.3. Hydrocarbon Production in Wells

On both stratigraphic and structural sections, wells that produce or have produced hydrocarbons in the past, or those that have been injected or shut in with oil, gas, or water in the Devonian strata, are thus identified. Dry and abandoned wells are also indicated. On structural cross sections, the corresponding stratigraphic intervals are delineated with red, green, and blue bars indicating gas, oil, and water respectively.

3.4. Stratigraphic Cross Section Methods

All stratigraphic cross sections were constructed using the Lower Carboniferous Exshaw Formation as a datum because it is a regionally extensive persistent marker throughout the study area. It forms an aquitard overlying the Wabamun Group (D-1 aquifer).

Different datums have been used by other authors (e.g., Switzer et al., 1994; Wendte et al., 1995; and Wendte, 1998) to construct cross sections within the Devonian throughout the study area. In particular, the Graminia Silt, a thin unit within the uppermost Winterburn Group, has commonly been used (e.g., Wendte et al., 1995; Stoakes, 1992), but because it is discontinuous across the present study area, it was not suitable as a datum herein. Stratigraphically lower markers, such as the Middle Devonian Watt Mountain Formation, have also been used to eliminate the effect of compaction from overlying argillaceous deposits or distortion due to dissolution of overlying evaporites (Chow et al., 1995; Wendte, 1998; Wendte et al., 1995). Such Formations could not be used as reliable markers in this study because they were not present in the majority of well log data.

3.5. Structural Cross Section Methods

Structural strike cross sections have been constructed analogous to stratigraphic counterparts (D-D' to F-F'). Wells approximately one township away from the line of projection were shifted upwards or downwards until the Exshaw Formation formed a flat line across the cross sections. This eliminated the apparent offset in structural dip from wells that were updip (northeast) and downdip (southwest) from the projected line of section. Information regarding well adjustment is detailed in the figure captions affiliated with structural cross sections D-D' through F-F'.

3.6. Synopsis of Stratigraphic and Structural Investigations

3.6.1. Summary of Cross Sections A-A'

In sections A-A' (Figures 3.2 and 3.3) that traverse the West Pembina area, the Lower and Upper Winterburn Group aquitards are usually thin (<10 m), laterally continuous, and interlayered with carbonate aquifers of approximately the same thickness. In the center of the section, however, total interconnection of L D-2, U D-2, and also the D-1 aquifers exists because aquitards A to E are

A
SW

West Pembina Area

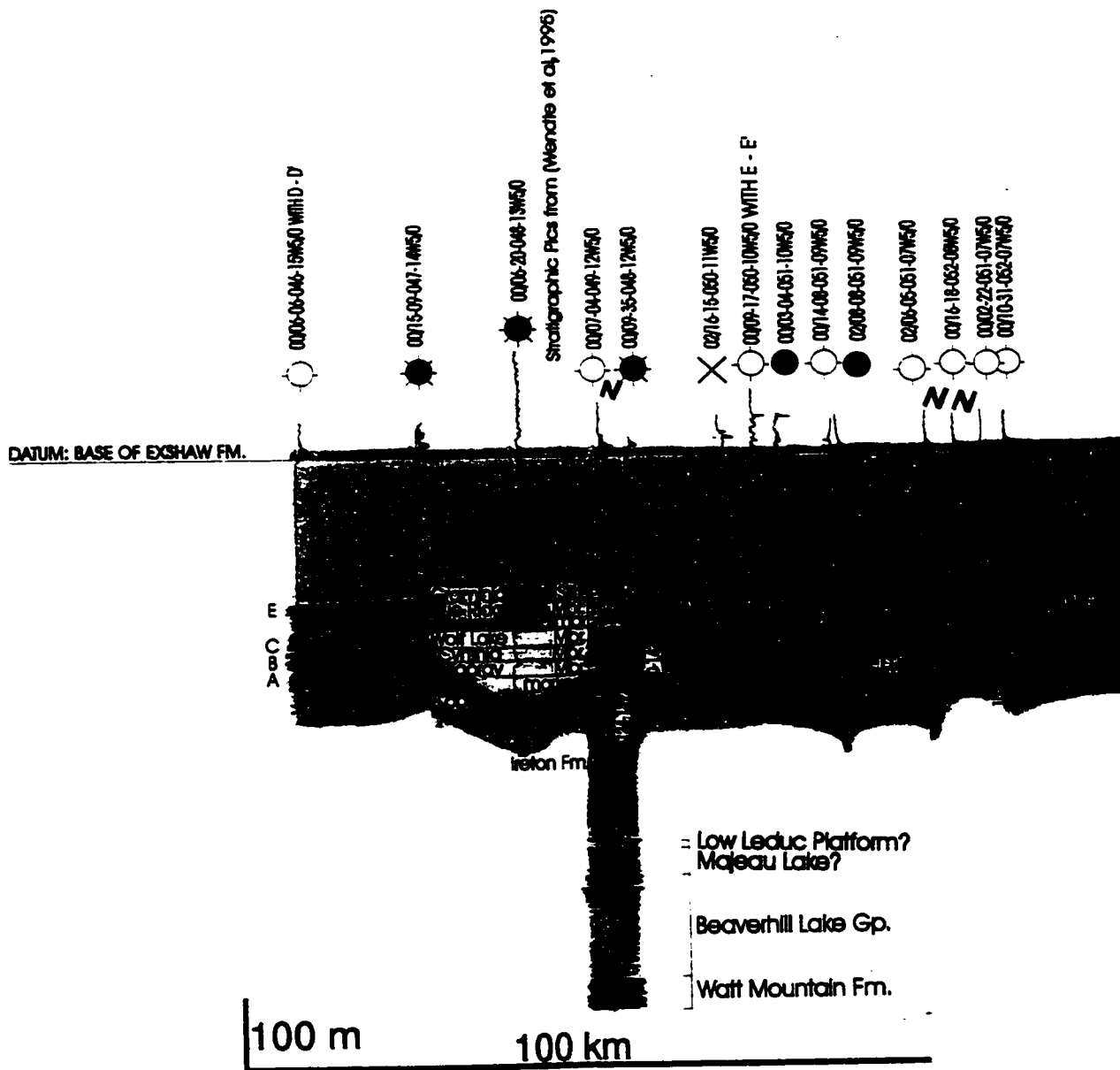
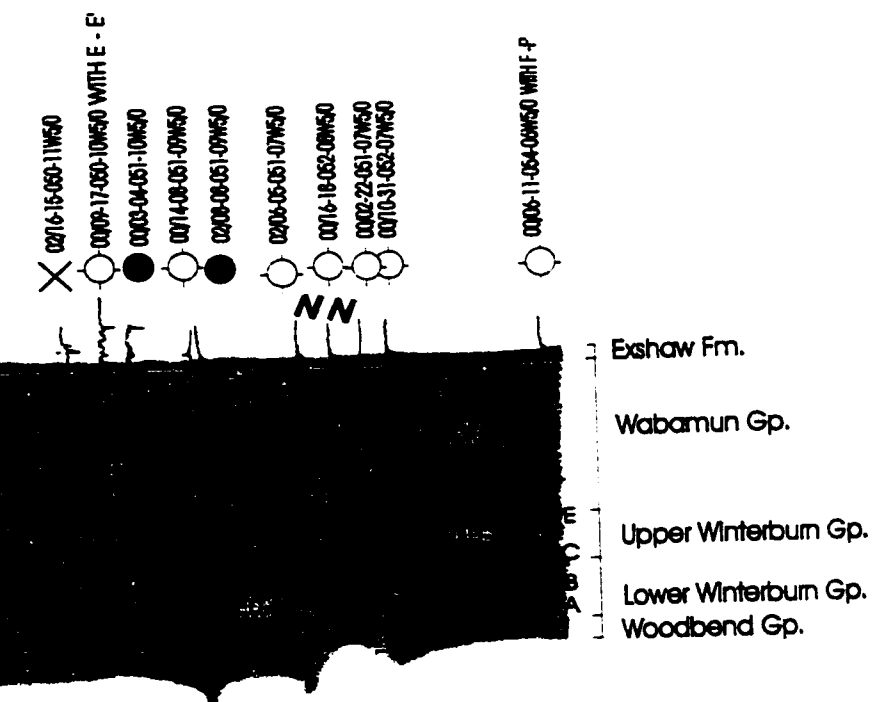


Figure 3.2: S

mbina Area

A'
NE



- Gas - producing
- Gas - injected
- Dry and abandoned
- Oil - producing
- × Water - injected

↗ Spacing
| Core

Figure 3.2: Stratigraphic Cross Section A-A'.

A
SW

West Pembina Area

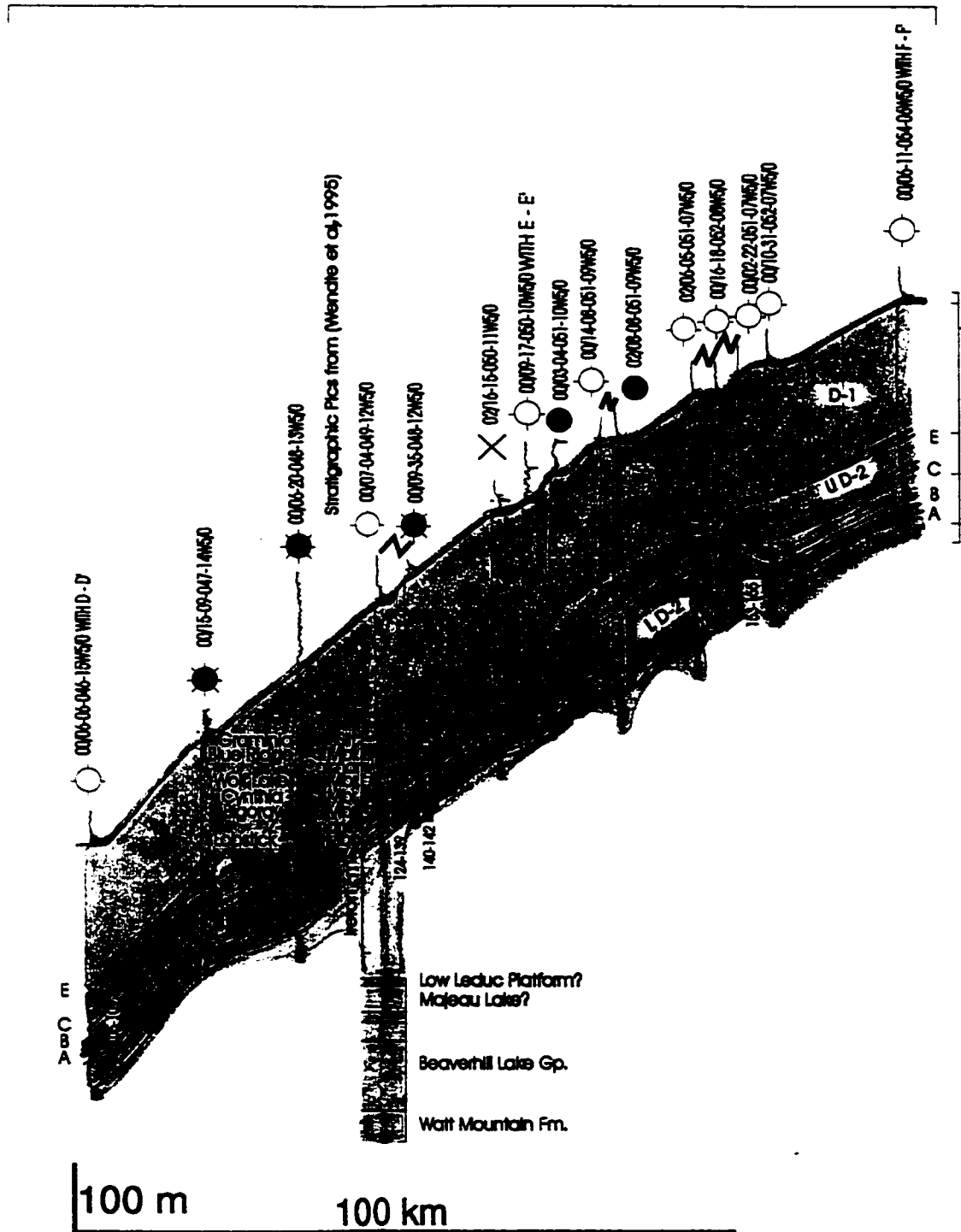


Figure 3.3

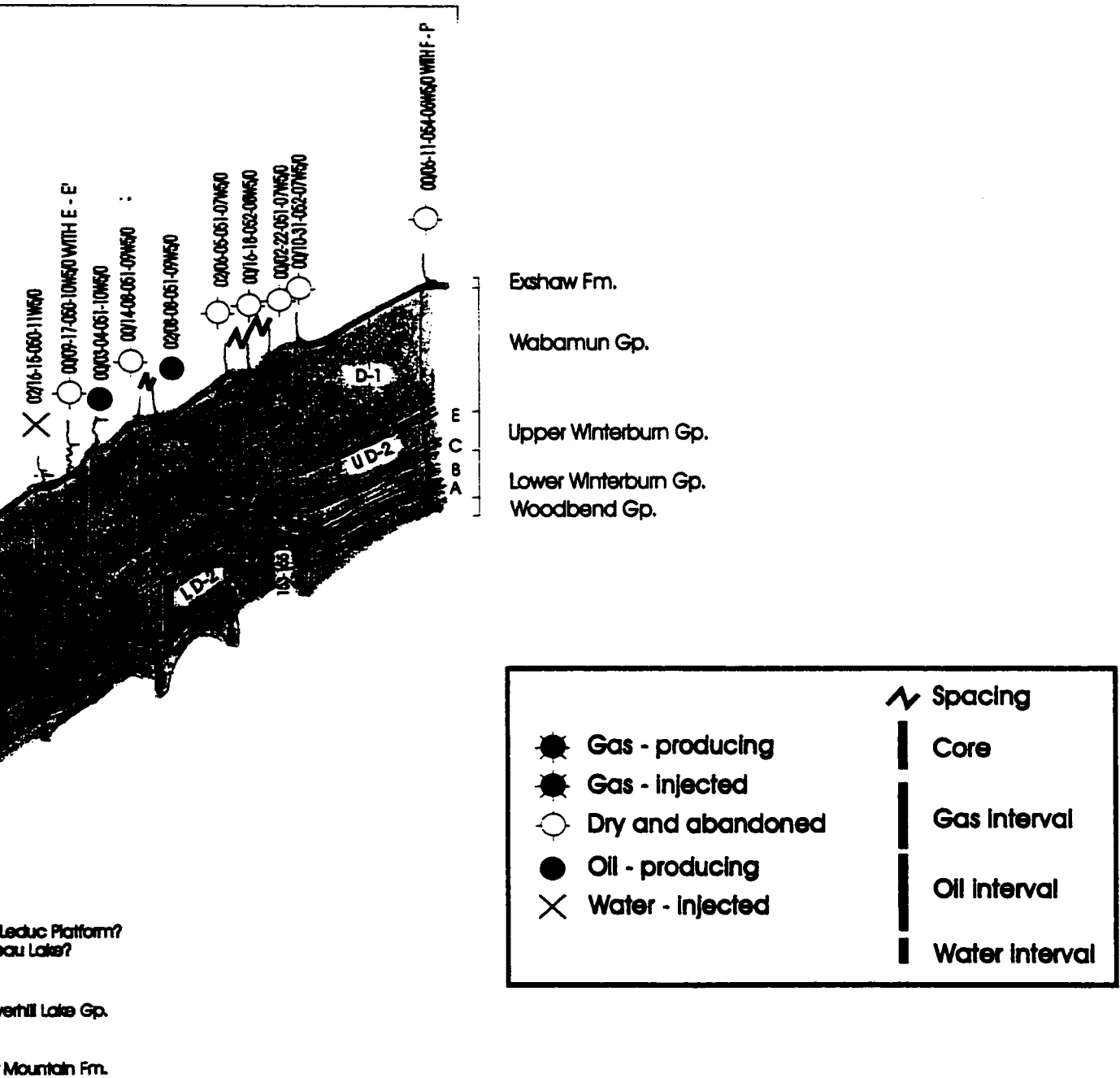


Figure 3.3: Structural Cross Section A-A'.

missing. In the structural cross section (Figure 3.3), a southwestern steeply dipping slope towards the limit of the disturbed belt, is present.

3.6.2. Summary of Cross Sections B-B'

In cross sections B-B' (Figures 3.4 and 3.5), the thick Woodbend/Lower Winterburn aquitard (refer to Appendix 2 for definition) and aquitard E, present in the northeast part of the section, pinch out towards the disturbed belt. These aquitards disappear in either the Obed or the Wild River Basin area. As such, in the Obed area and to the southwest, interconnection between the D-1 through to the D-4, exists. Aquifers in these sections are much thicker than in the West Pembina area in cross sections A-A' as they are merged. The D-4 aquifer is thick and ranges from 125 m and 150 m in thickness throughout the section. In the northeast part of the section, wedges of Beaverhill Lake Group aquitards are present.

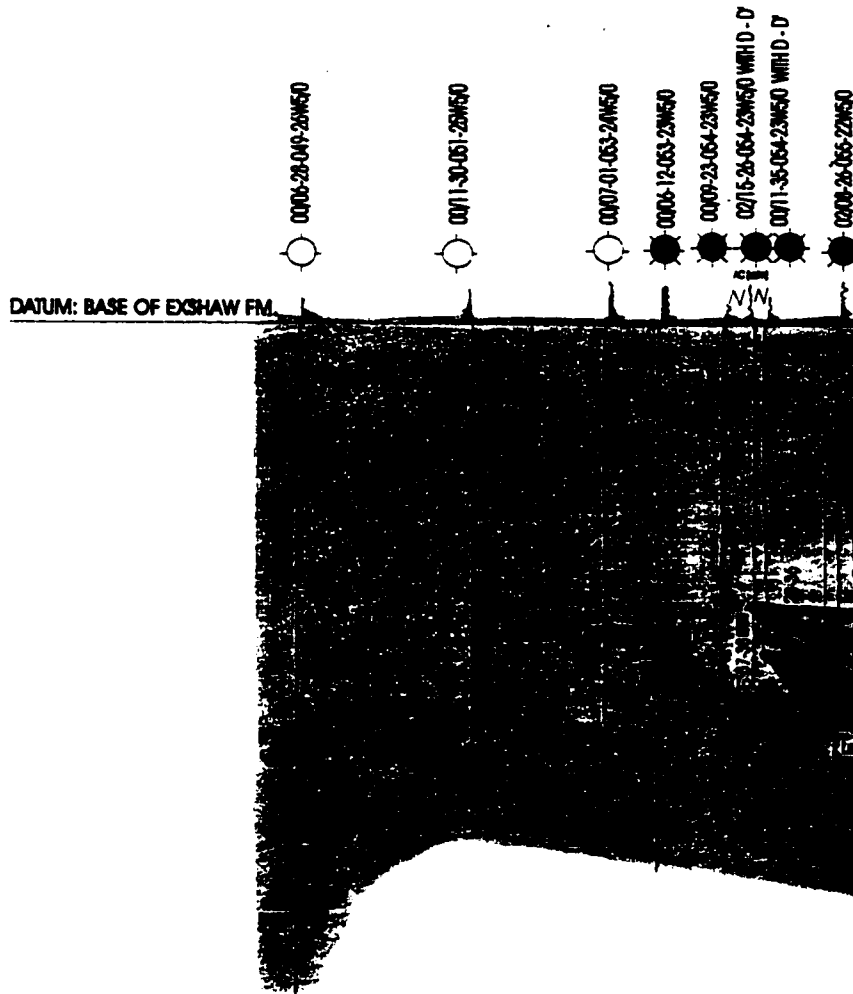
In the structural cross section (Figure 3.5), a steeply southwestern dipping slope towards the limit of the disturbed belt is apparent. The southwestern-most well of this cross section was drilled in the foothills. In this region, the strata were thrust several hundred meters updip, which explains the offset from the otherwise general southwestern dipping slope in the remainder of the section.

3.6.3. Summary of Cross Sections C-C'

In sections C-C', the thick Woodbend/Winterburn aquitard (refer to Appendix 2 for more detail) thins abruptly towards the limit of the disturbed belt (Figures 3.6 and 3.7), in contrast to sections B-B' where this aquitard thins gradually in the same direction. The D-1 and the D-2 aquifers are consistently interconnected, as there are no regional aquitards separating them. In comparison to cross sections A-A' and B-B', the D-4 aquifer in the present sections is considerably thin (less than 30 m). In the structural cross section (Figure 3.7), a steeply southwestern dipping slope towards the limit of the disturbed belt is present.

B
SW Southesk Calm Complex
near the limit of the
disturbed belt

Obed and
Surrounding
Fields



- Gas - producing
- Gas - suspended
- Gas - shut-in
- Gas - abandoned
- Dry and abandoned
- Oil - suspended

↗ Spacing
| Core

100 m

100

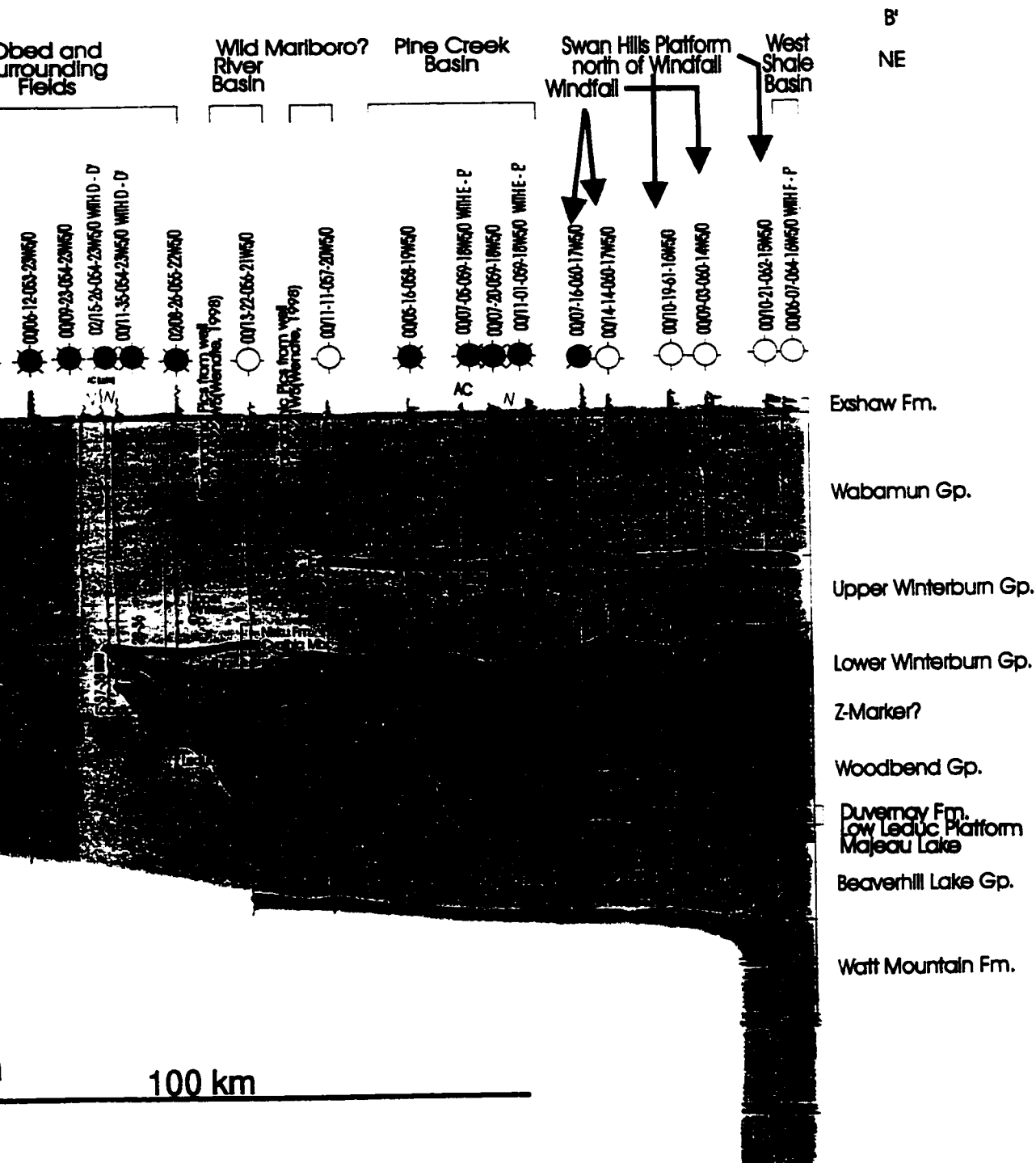


Figure 3.4: Stratigraphic Cross Section B-B'.

B Southesk Cairn Complex
SW near the limit of the
disturbed belt

Obed and
Surrounding
Fields

Wild Marlboro
River Basin

Pine Creek
Basin

Swan Hills Platform
north of Windfall

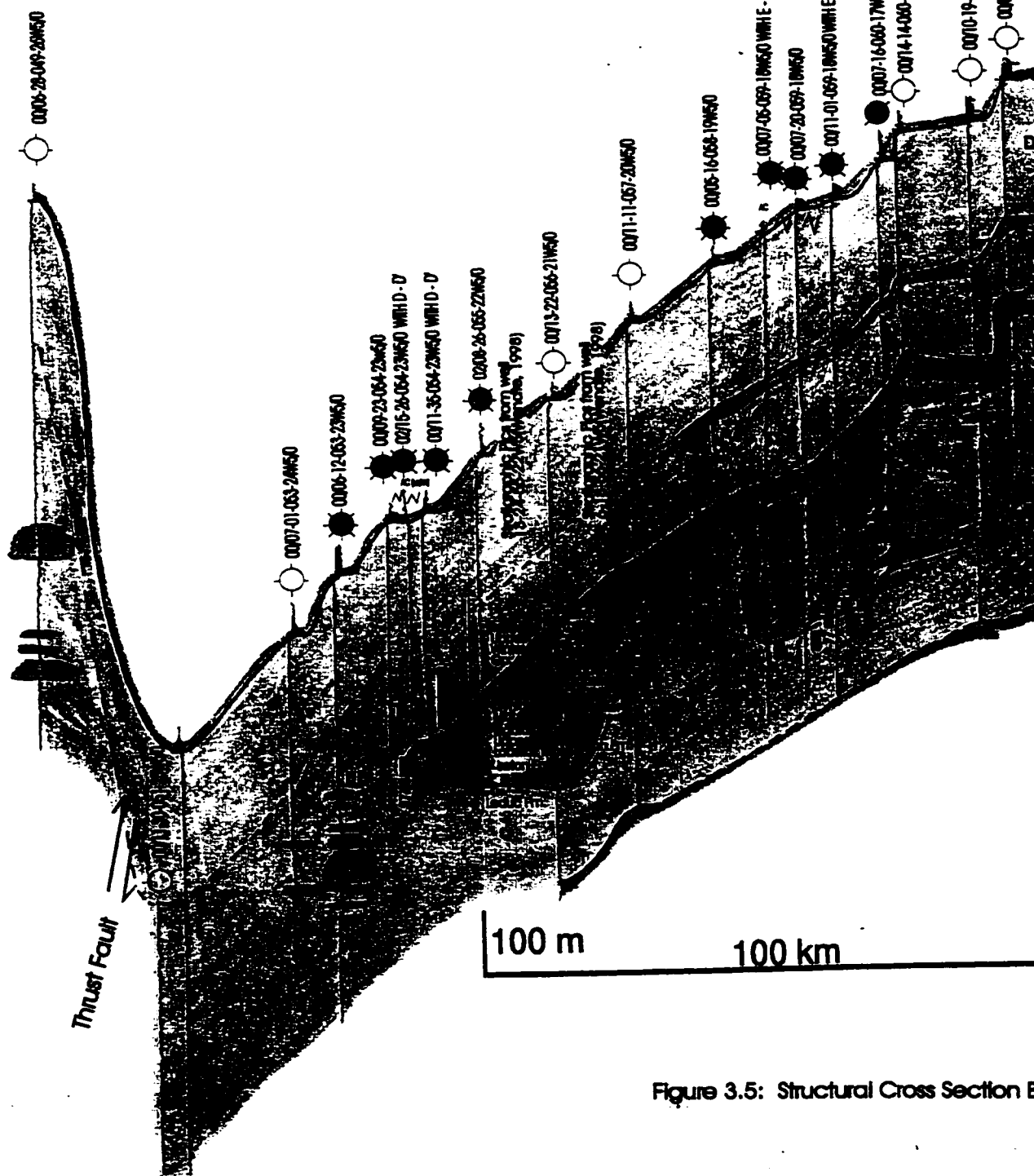


Figure 3.5: Structural Cross Section E

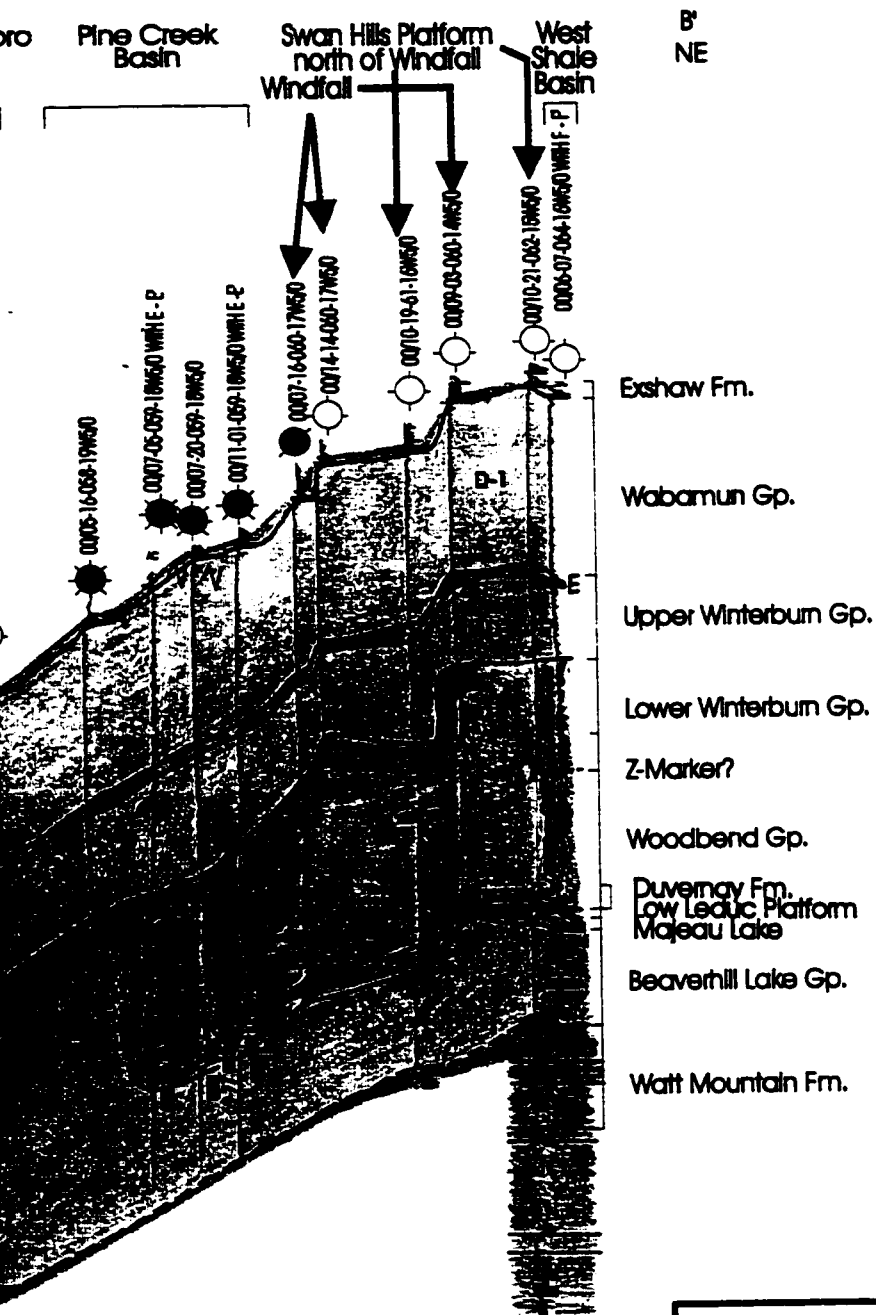
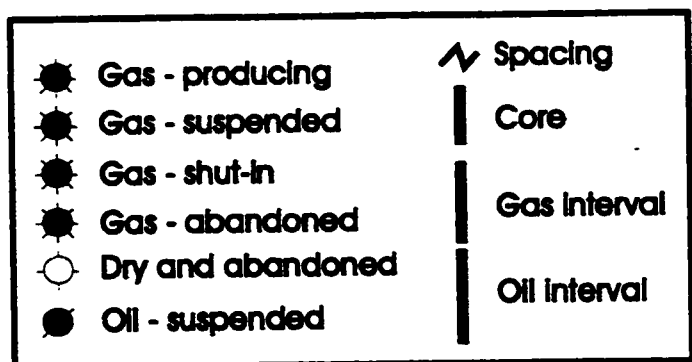


Figure 3.5: Structural Cross Section B-B'.



C

SW Gold Creek Reef

Adjacent to Peace River Arch - Leduc Fringe

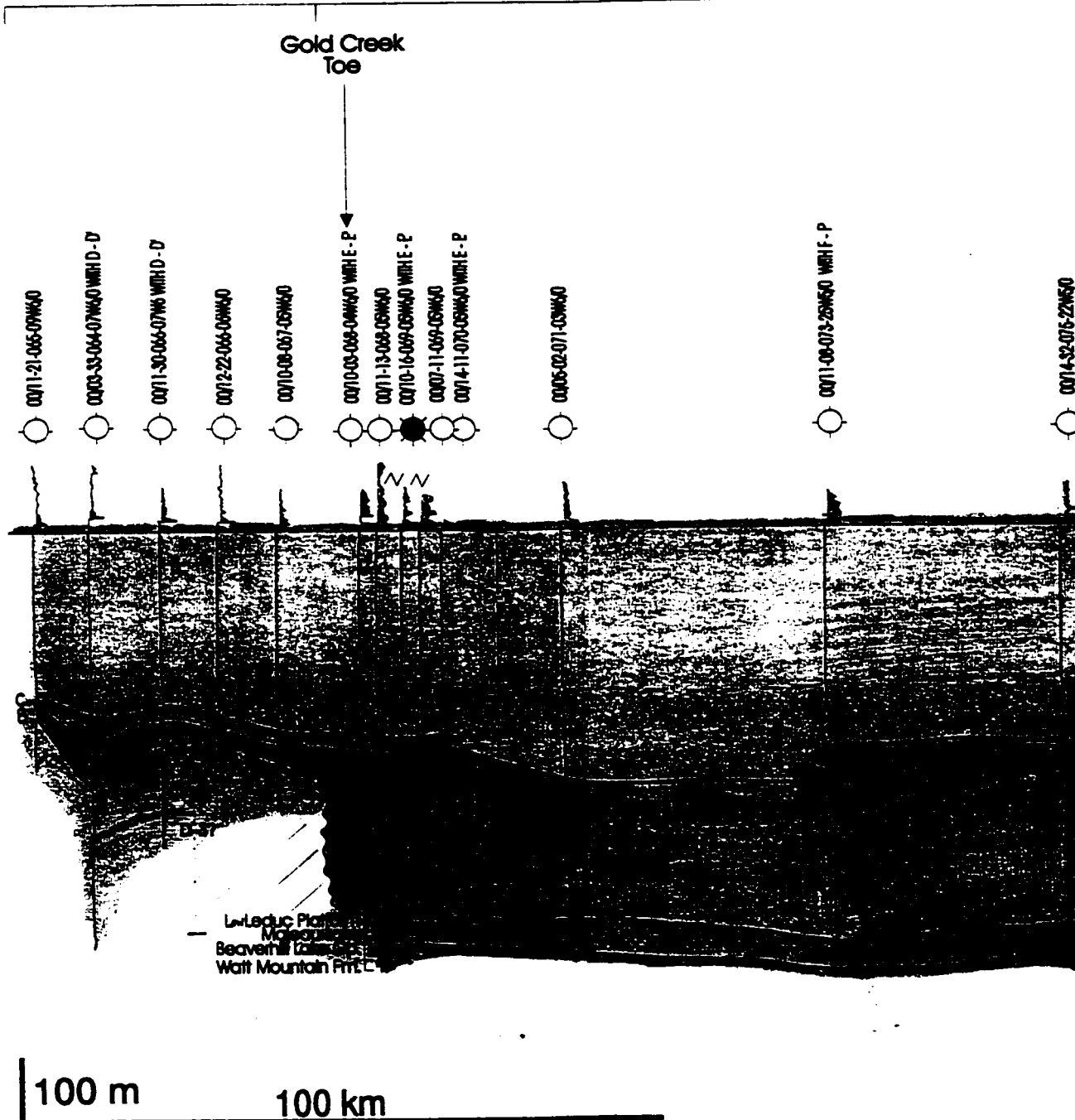


Figure 3.6: Stratigraphic Cross Section

C'

NE

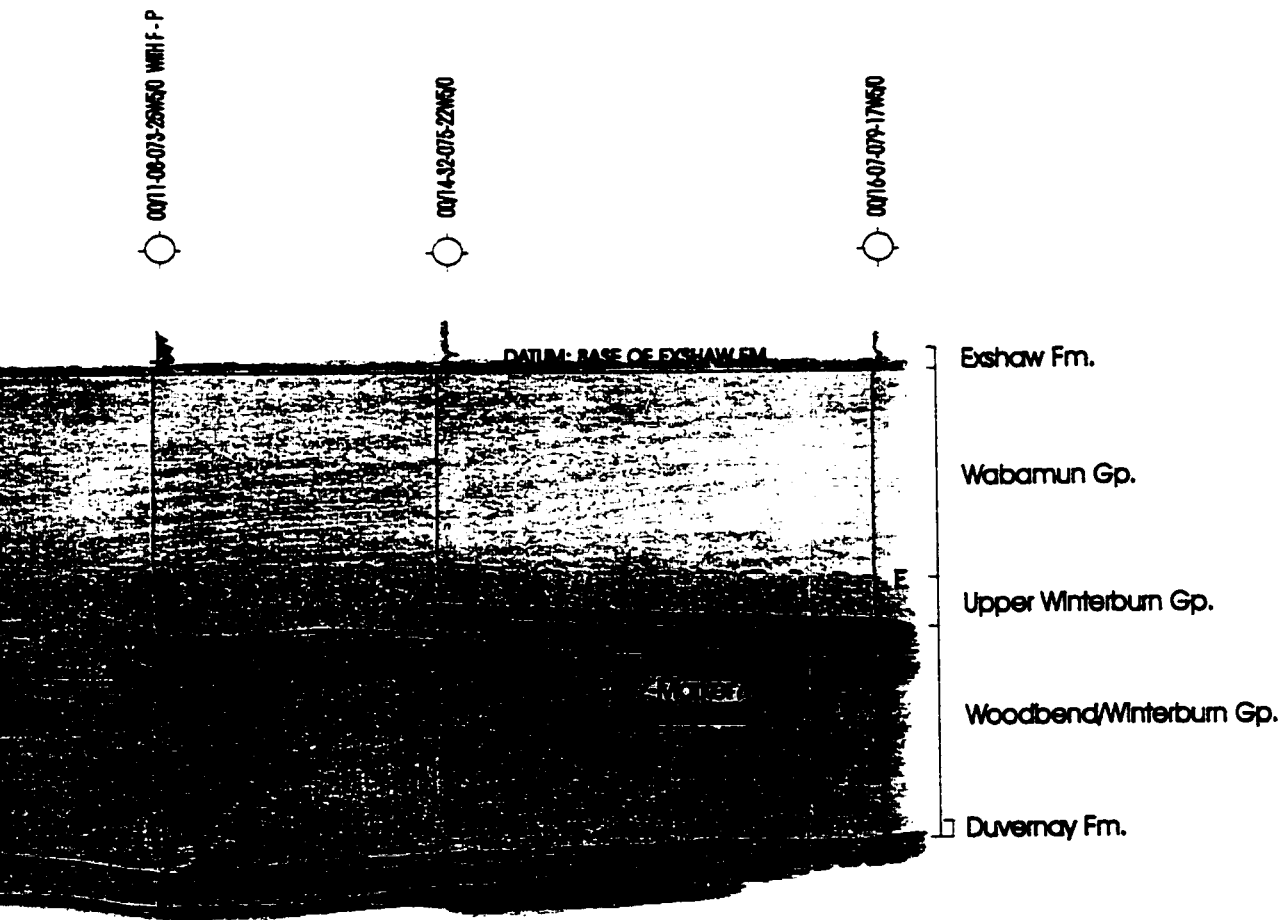
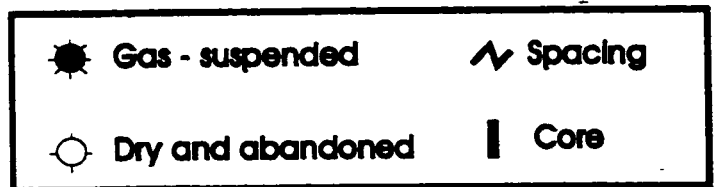


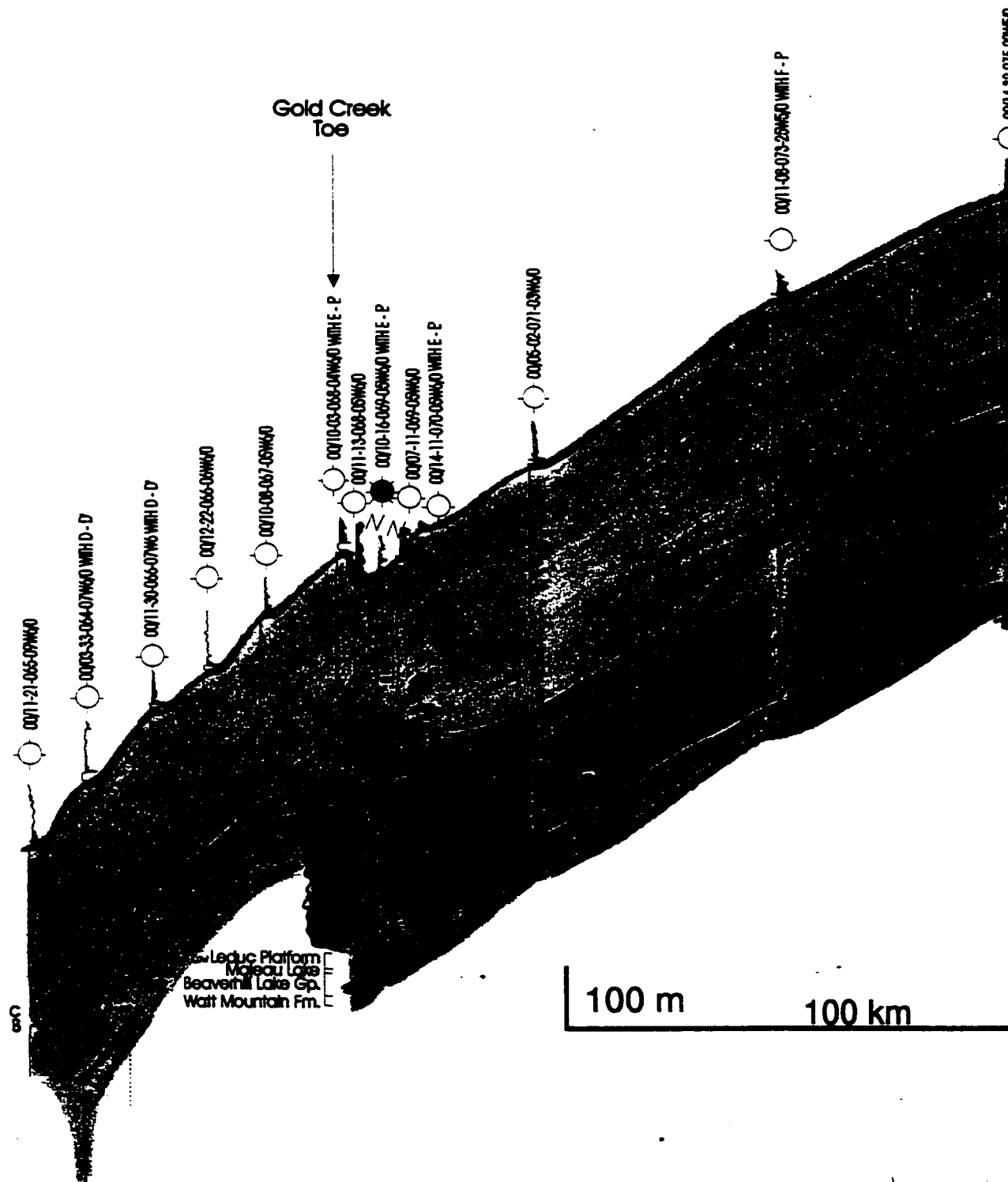
Figure 3.6: Stratigraphic Cross Section C-C'.



C
SW

Gold Creek Reef

Adjacent to Peace River Arch - Leduc Fringe



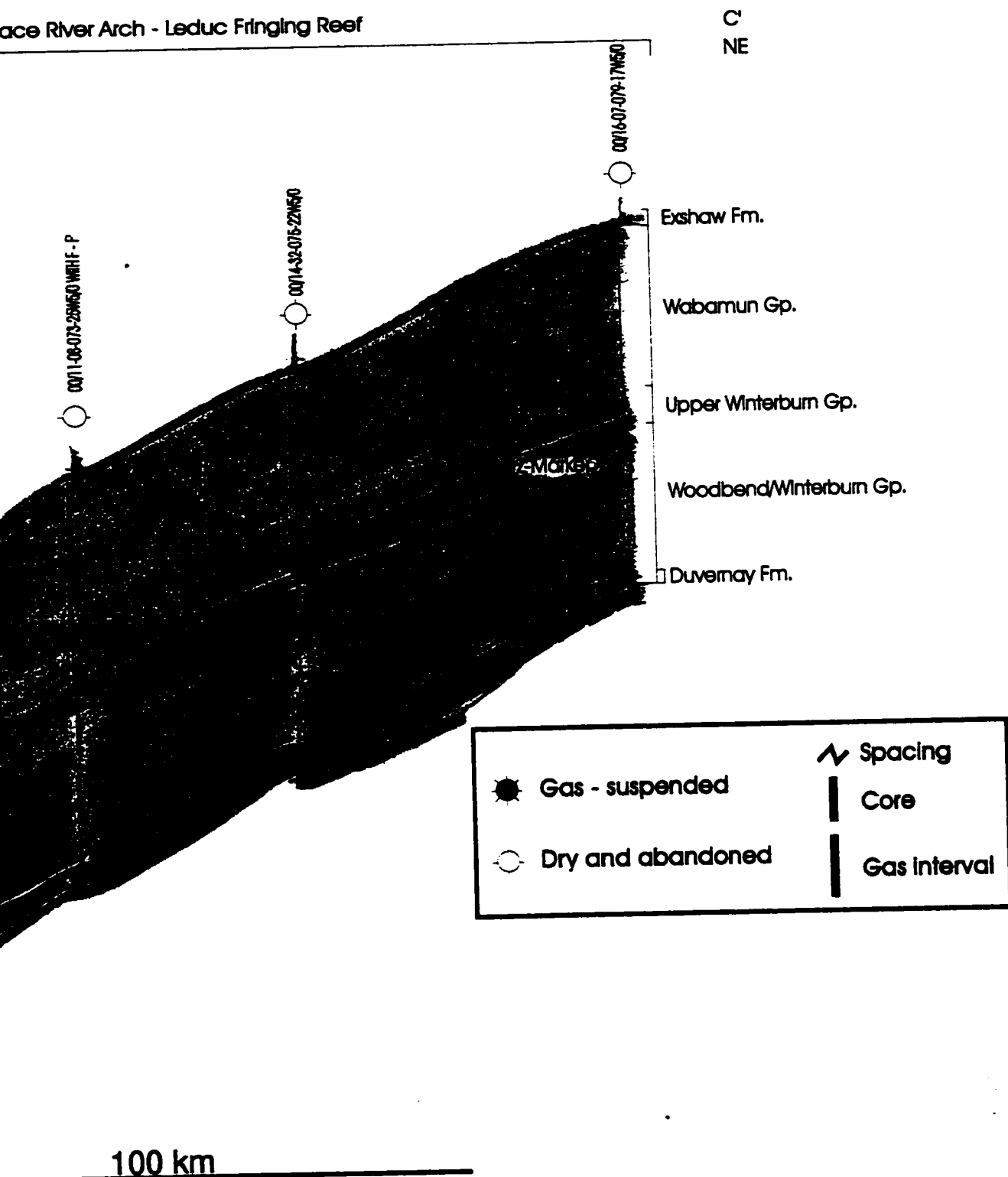


Figure 3.7: Structural Cross Section C-C'.

3.6.4. Summary of Cross Sections D-D'

Sections D-D', in and around the Obed area (Figures 3.8 and 3.9), show that the Woodbend/Winterburn aquitard (refer to Appendix 2 for more detail) is approximately 145 m in thickness. It gradually pinches out to the northwest so that in the Bigstone and Simonette Reefs, the aquitard has disappeared. As such, the D-1 through to the D-4 aquifers are interconnected in these areas. Also, in the majority of the sections, the L D-2, the U D-2, and the D-1 are often interconnected due to the absence of intervening aquitards, such as A to E. In the structural cross section (Figure 3.9), a gently dipping slope towards the direction of the Peace River Arch is present.

3.6.5. Summary of Cross Sections E-E'

The Woodbend/Winterburn aquitard (refer to Appendix 2 for more detail) does not pinch out to the northwest like that in cross sections D-D' because the section crosses through a basinal area, the Karr Basin, and does not intersect reefs such as Bigstone or Simonette (Figure 3.10 and 3.11). In the southeastern part of the sections, aquitard E separates the D-2 from the D-1 aquifer. However, on the northwestern edge of Pine Creek Basin, aquitard E pinches out, allowing for interconnection between the D-1 and the D-2 aquifers. Due to interfingering of thin aquifers and aquitards in the Swan Hills Platform and the Windfall areas, the hydraulic integrity of Lower Winterburn Group aquitards is probably quite low. In the Swan Hills Platform area, a potential for hydraulic interconnection exists between these thin (lower D-2) aquifers and the thicker (upper D-2) aquifer, and/or breaching of the aquitards, is possible. This is discussed further in Chapter 6. The D-4 aquifer thins considerably towards the Peace River Arch area, which is located to the northwest of the cross section and beyond. In this structural cross section (Figure 3.11), as in structural cross section D-D' (Figure 3.9), a gently dipping slope towards the Peace River Arch exists.

D
NW

Peace
River
Arch

Gold Creek
Reef

Simonette

Bigstone Wild R

0008-19-066-12W50



0071-30-066-07W6 WITH C - C



0003-33-064-07W50 WITH C - C



0002-08-082-04W50



0071-11-060-02W50



0006-28-061-28W50



0006-14-066-01W50



0006-01-061-27W50



0074-24-061-28W50



0009-23-061-25W50



DATUM: BASE OF EXSHAW FM.

100 m

100 km

Figure 3.8: Str

D'
SE

Stone Wild River Basin Obed area Windfall Swan Hills Platform southeast of Windfall West Pembina area

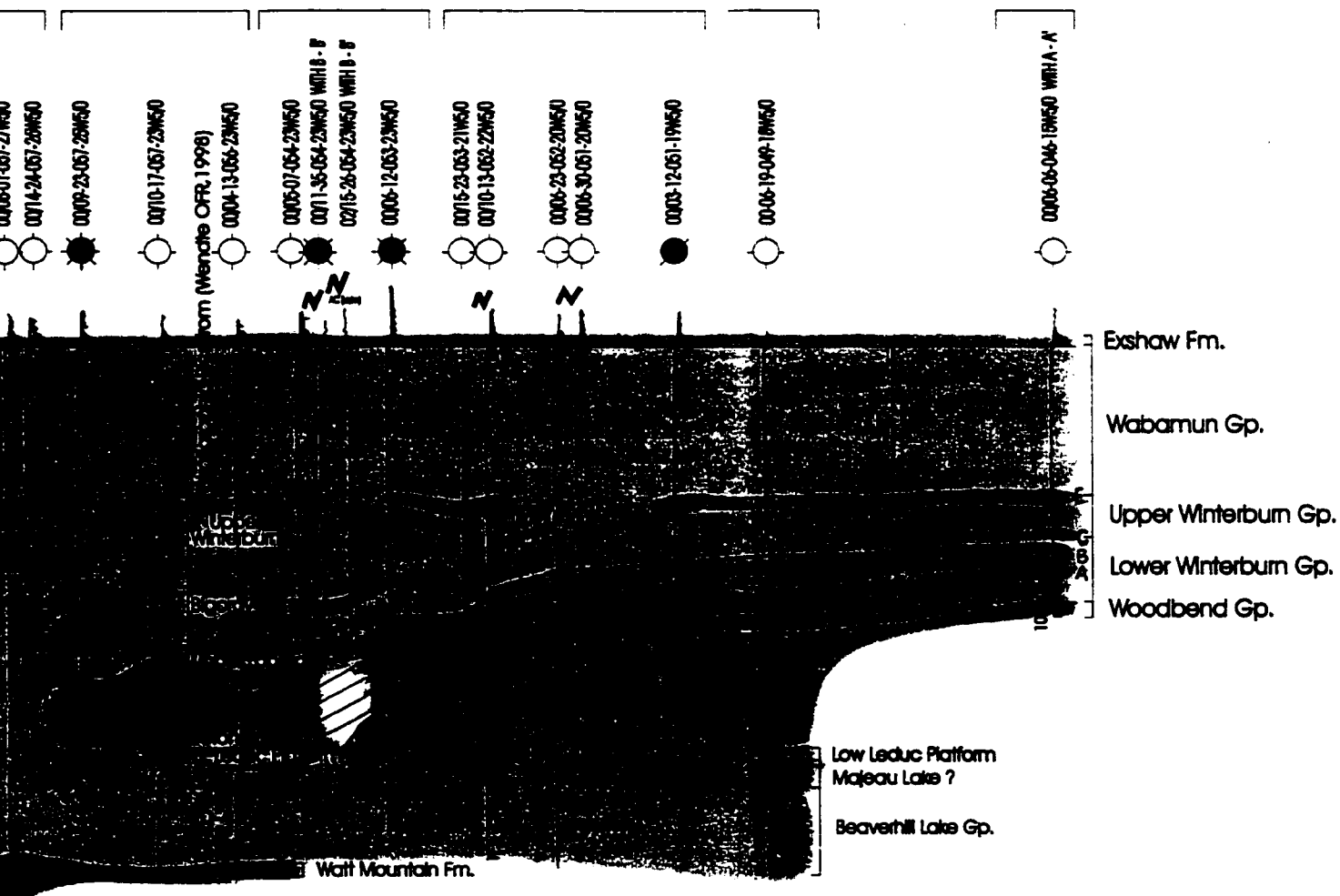


Figure 3.8: Stratigraphic Cross Section D-D'.

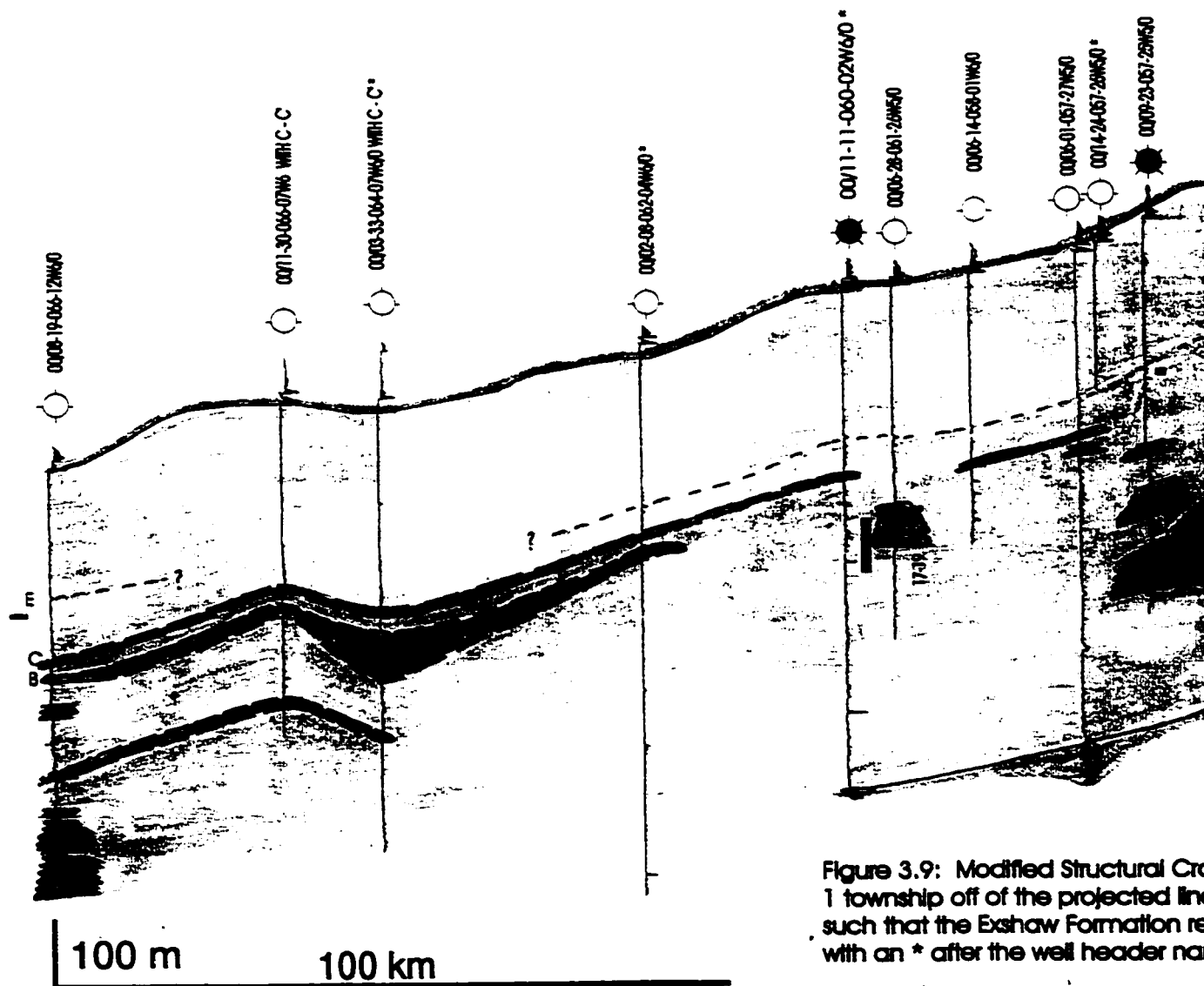
D
NW

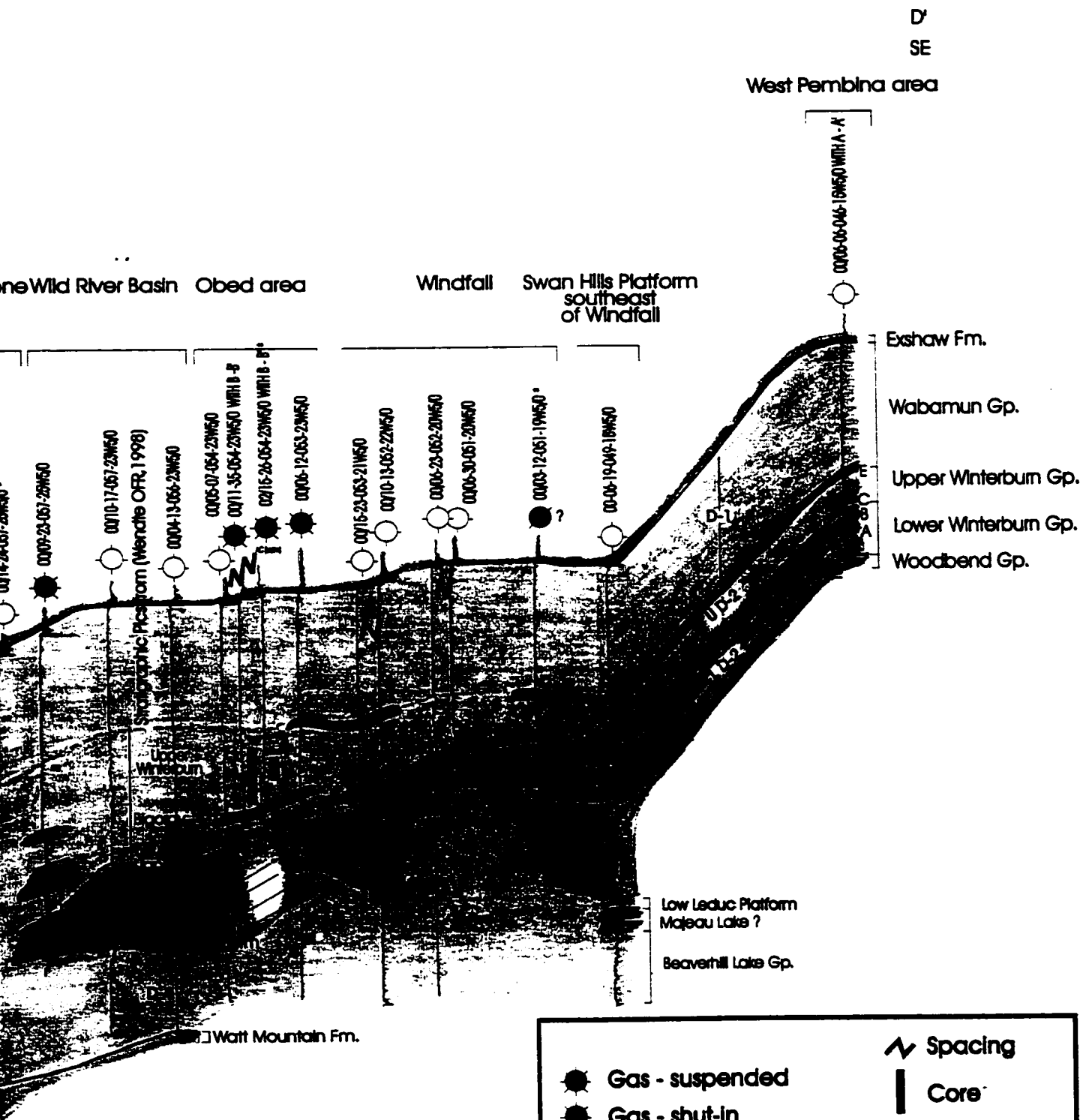
Peace
River
Arch

Gold Creek Reef

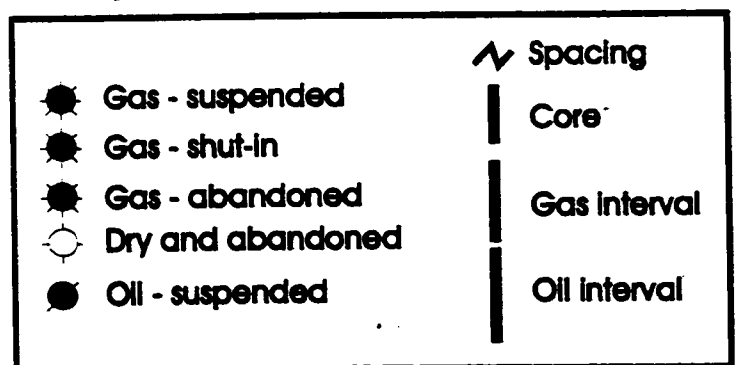
Simonette

Bigstone Wild R





Structural Cross Section D-D'. Wells that are more than
projected line of section have been adjusted
information remains flat. All wells except those
header name have been adjusted.



E

NW

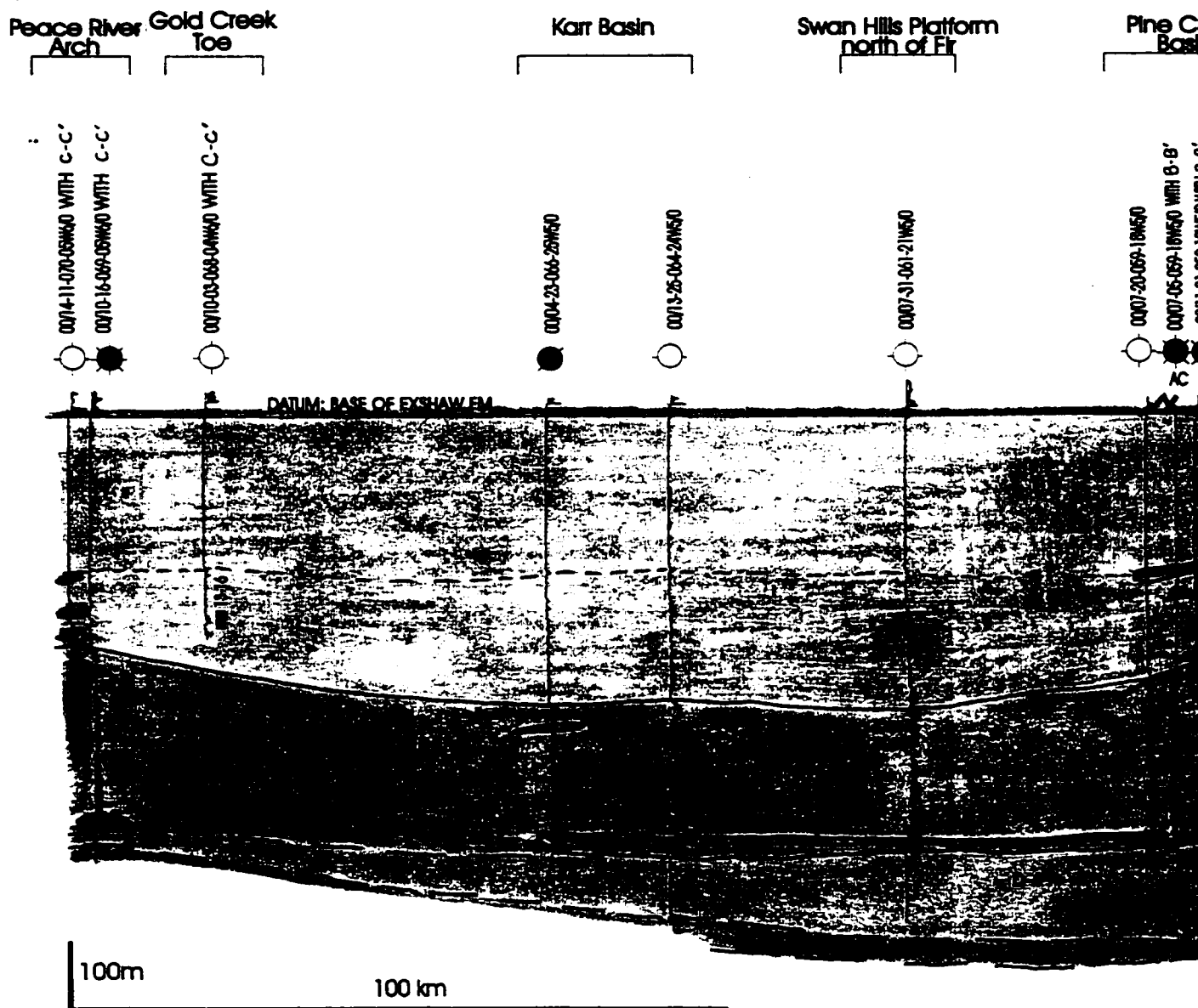
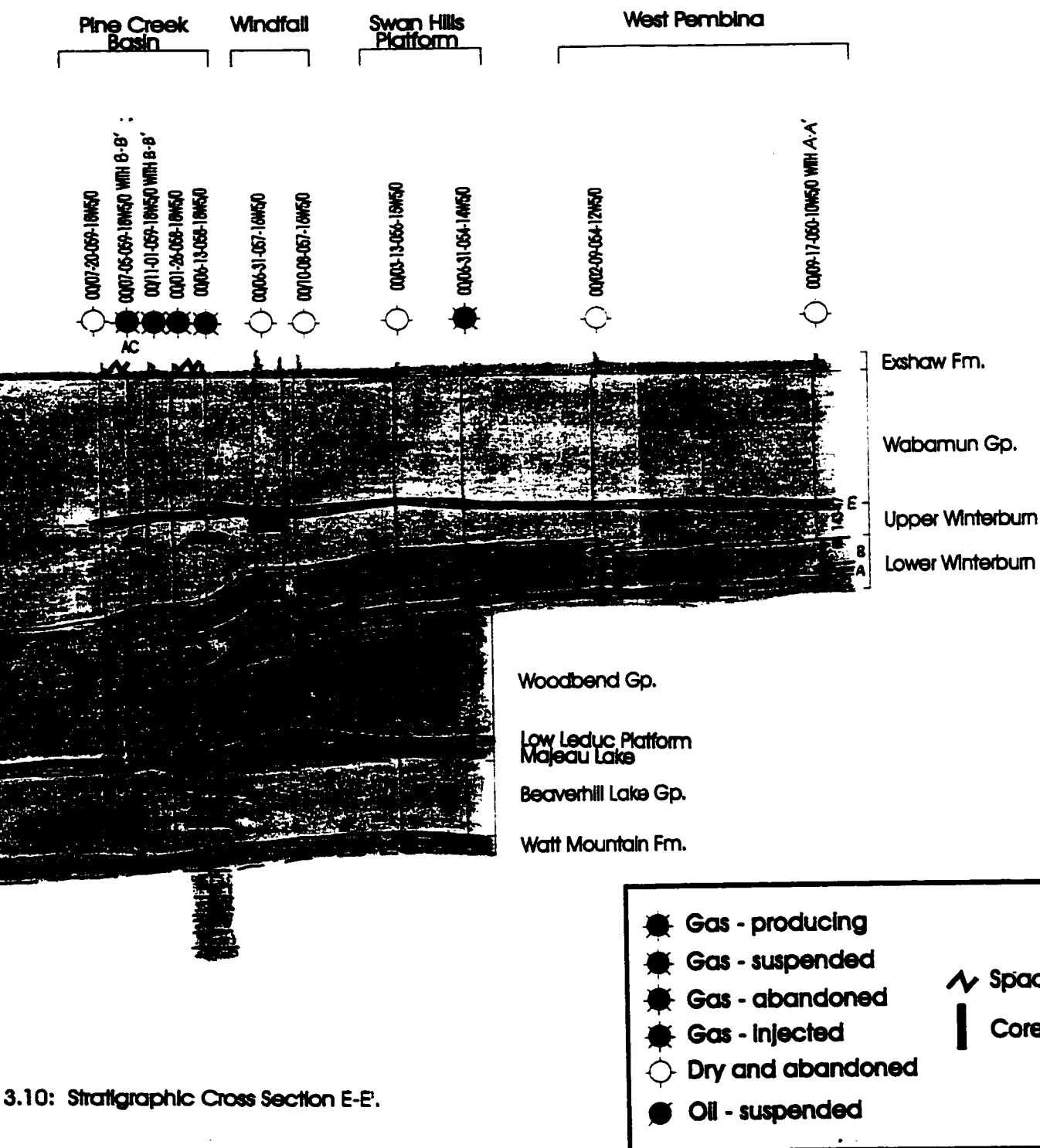


Figure 3.10: Stratigraphic

E

SE



3.10: Stratigraphic Cross Section E-E.

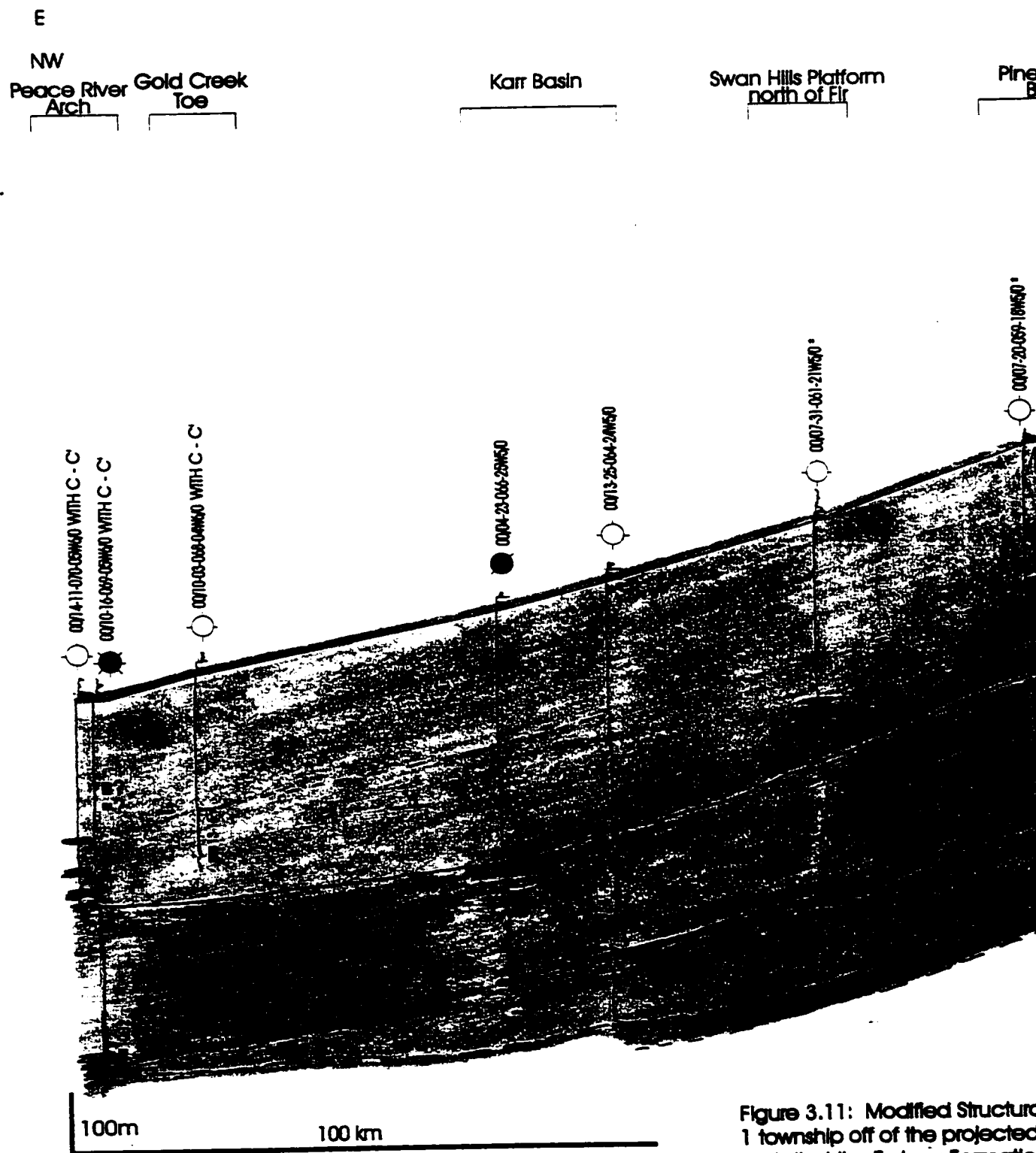
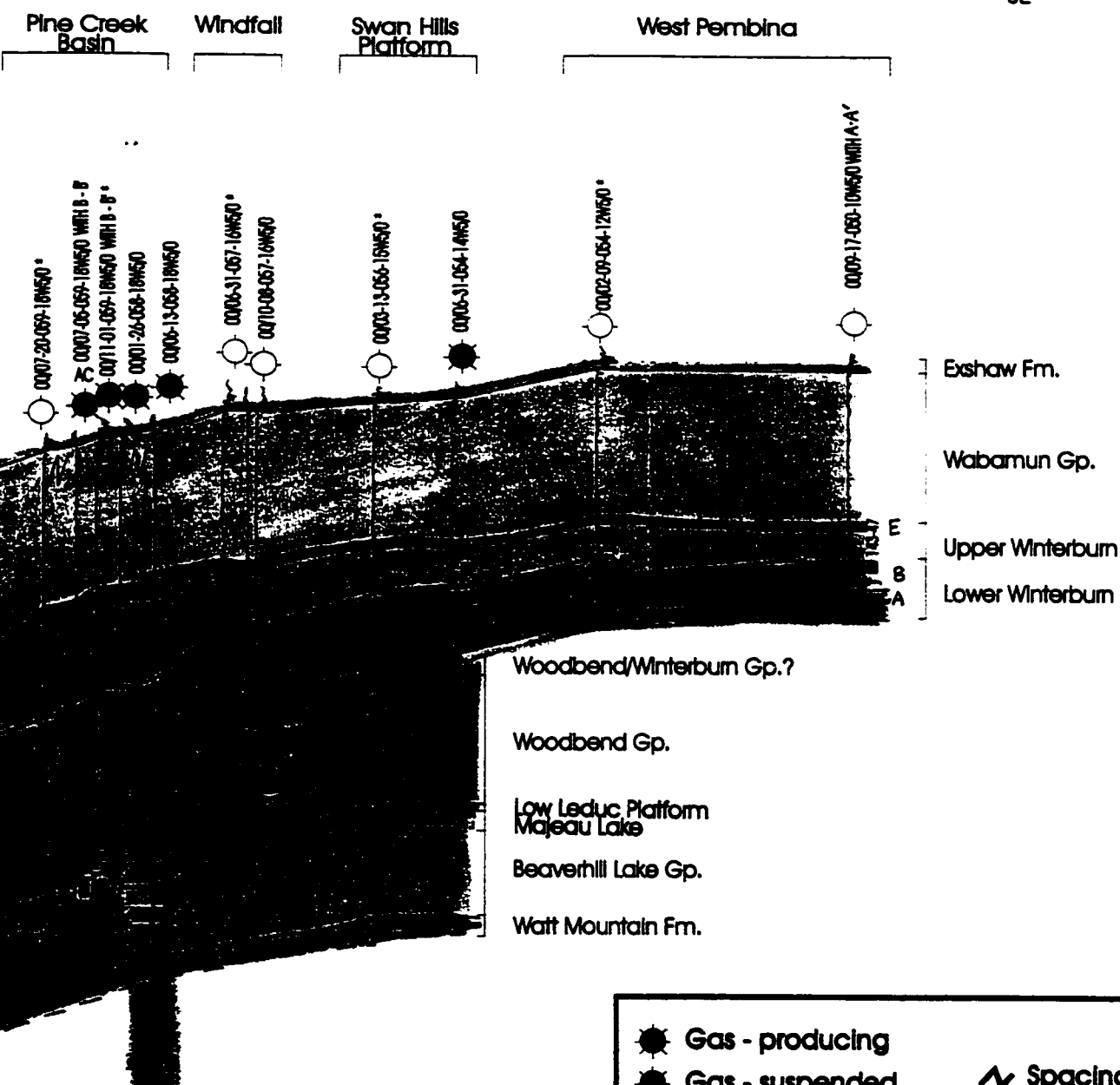


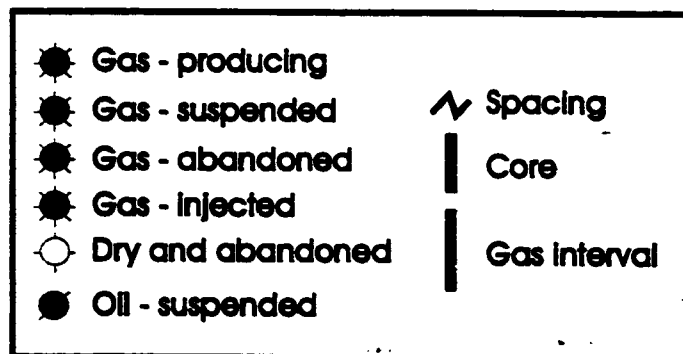
Figure 3.11: Modified Structural map of 1 township off of the projected map such that the Exshaw Formation is highlighted with an * after the well header

E'

SE



Structural Cross Section E-E'. Wells that are more than 100 feet from the line of section have been adjusted so that the section remains flat. All wells except those under name have been adjusted.



3.6.6. Summary of Cross Section F-F'

These cross sections are similar in appearance to cross sections E-E'. The L D-2 and U D-2 aquifers are intermittently separated by an aquitard in cross sections F-F' (Figures 3.12 and 3.13). In the Sturgeon Lake Reef and Peace River Arch areas, the D-1 aquifer is often found directly overlying the U D-2 aquifer, and direct communication between aquifers L D-2, U D-2, and D-1 exists. This is similar to the situation in the Karr Basin and adjacent to the Peace River Arch in cross sections E-E'. Again, comparable to sections E-E', aquifer D-4 also thins towards the Peace River Arch in this section. In the structural cross section (Figure 3.13), similar to findings in both cross sections D-D' and E-E', a gently dipping slope towards the Peace River Arch exists.

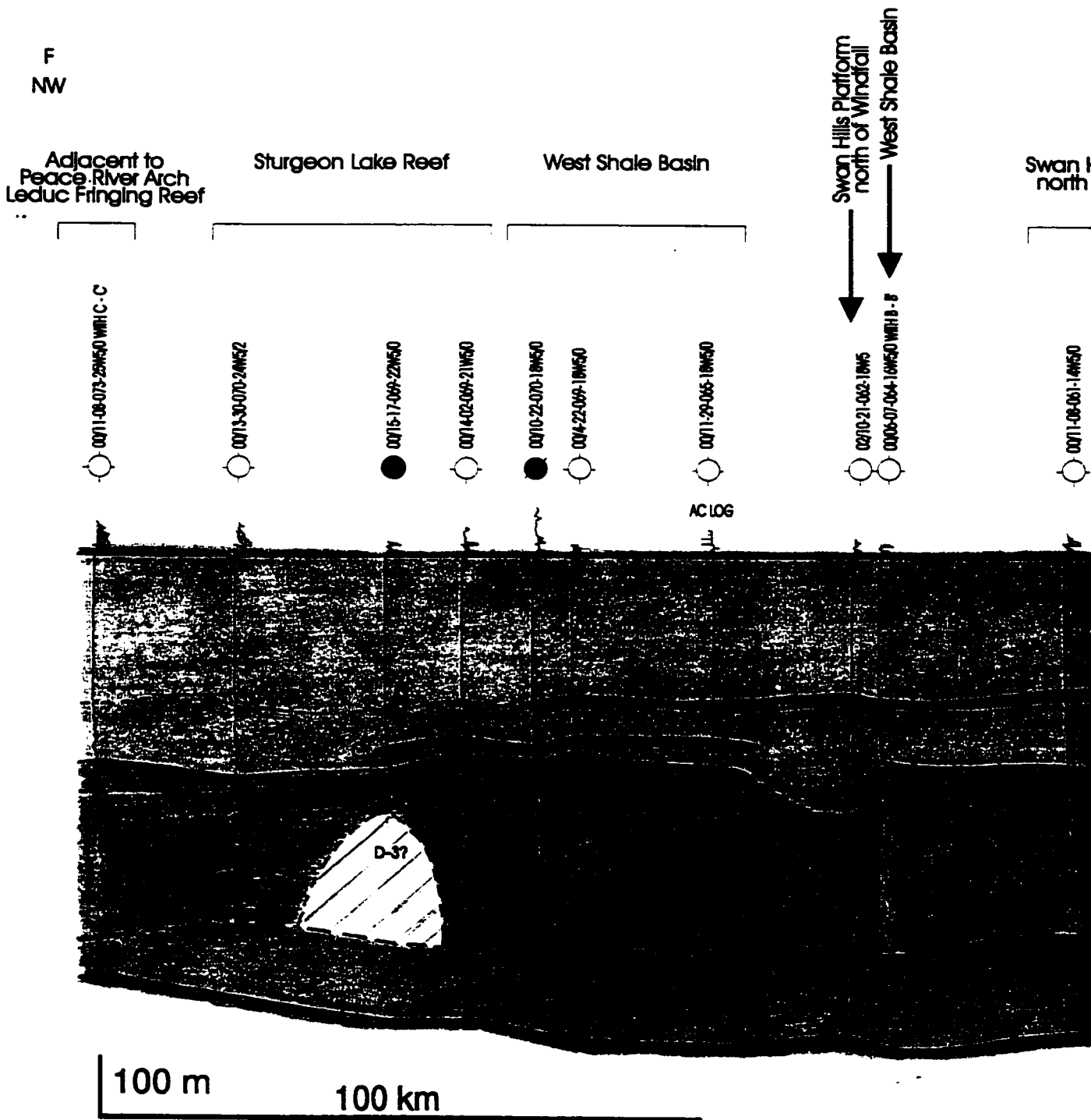


Figure 3.12:

0006-07-004-06W50 WH1A-A

P
SE

Swan Hills Platform
north of Windfall

West Shale Basin
West Pembina area

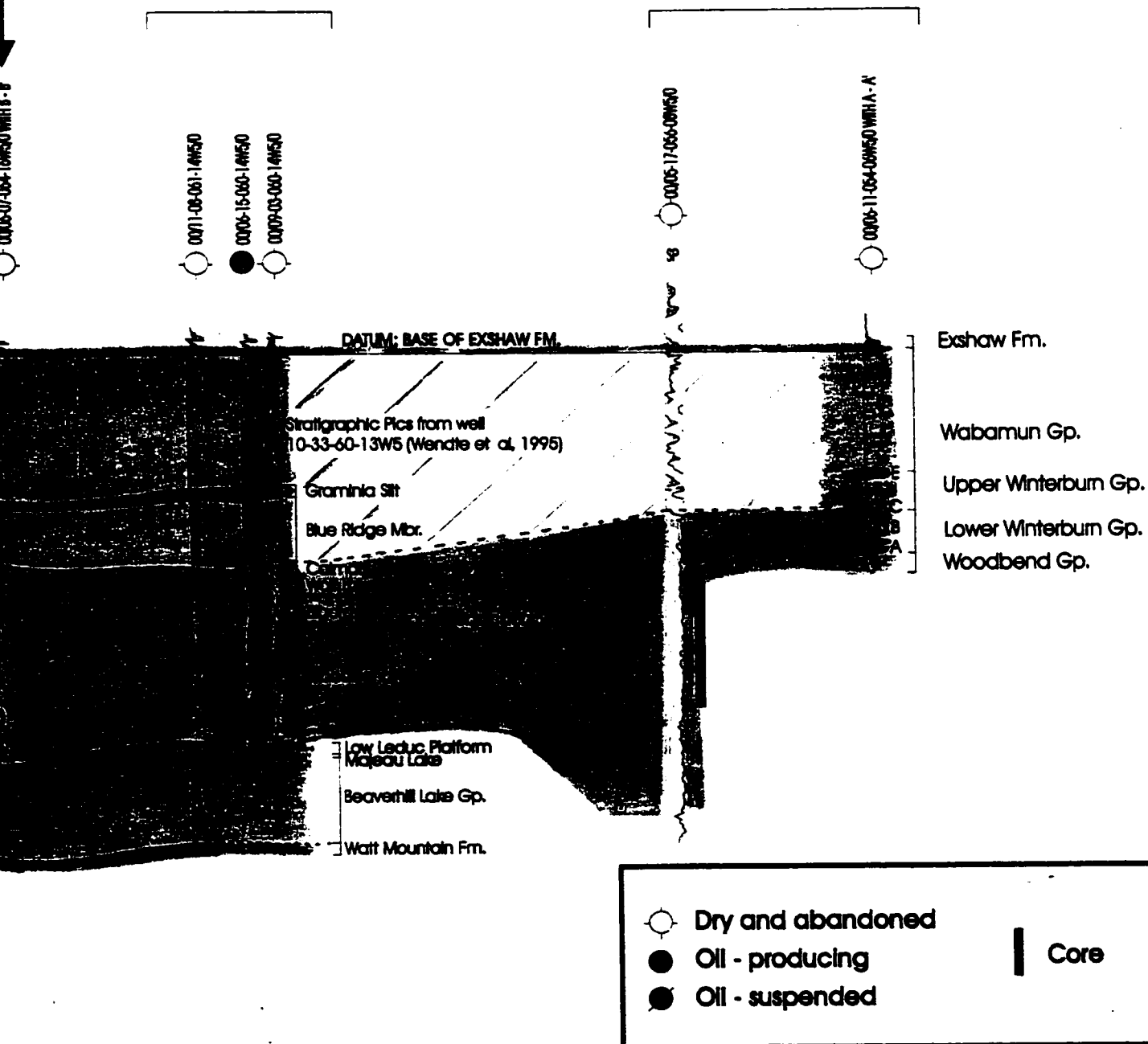


Figure 3.12: Stratigraphic Cross Section F-F.

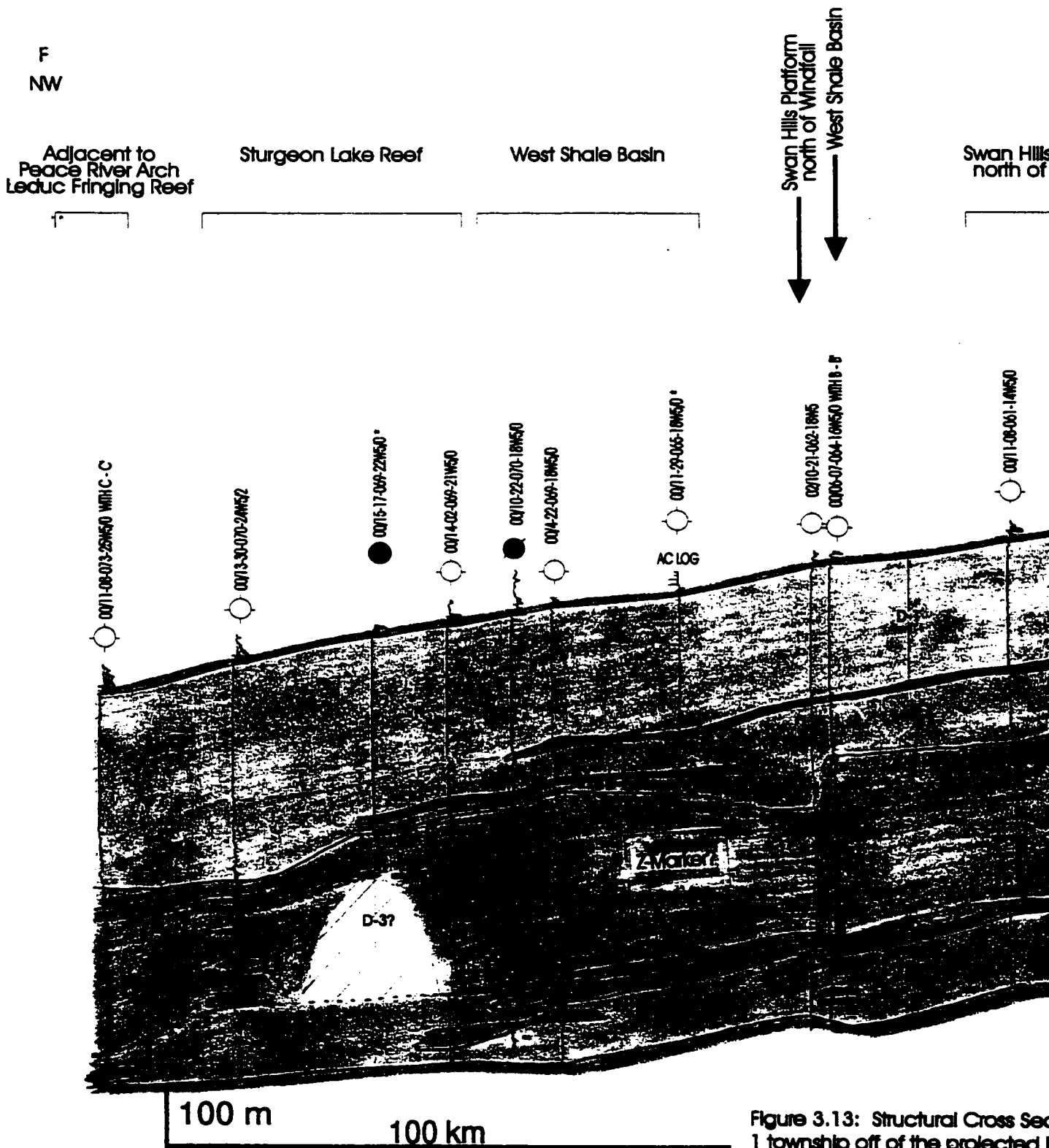
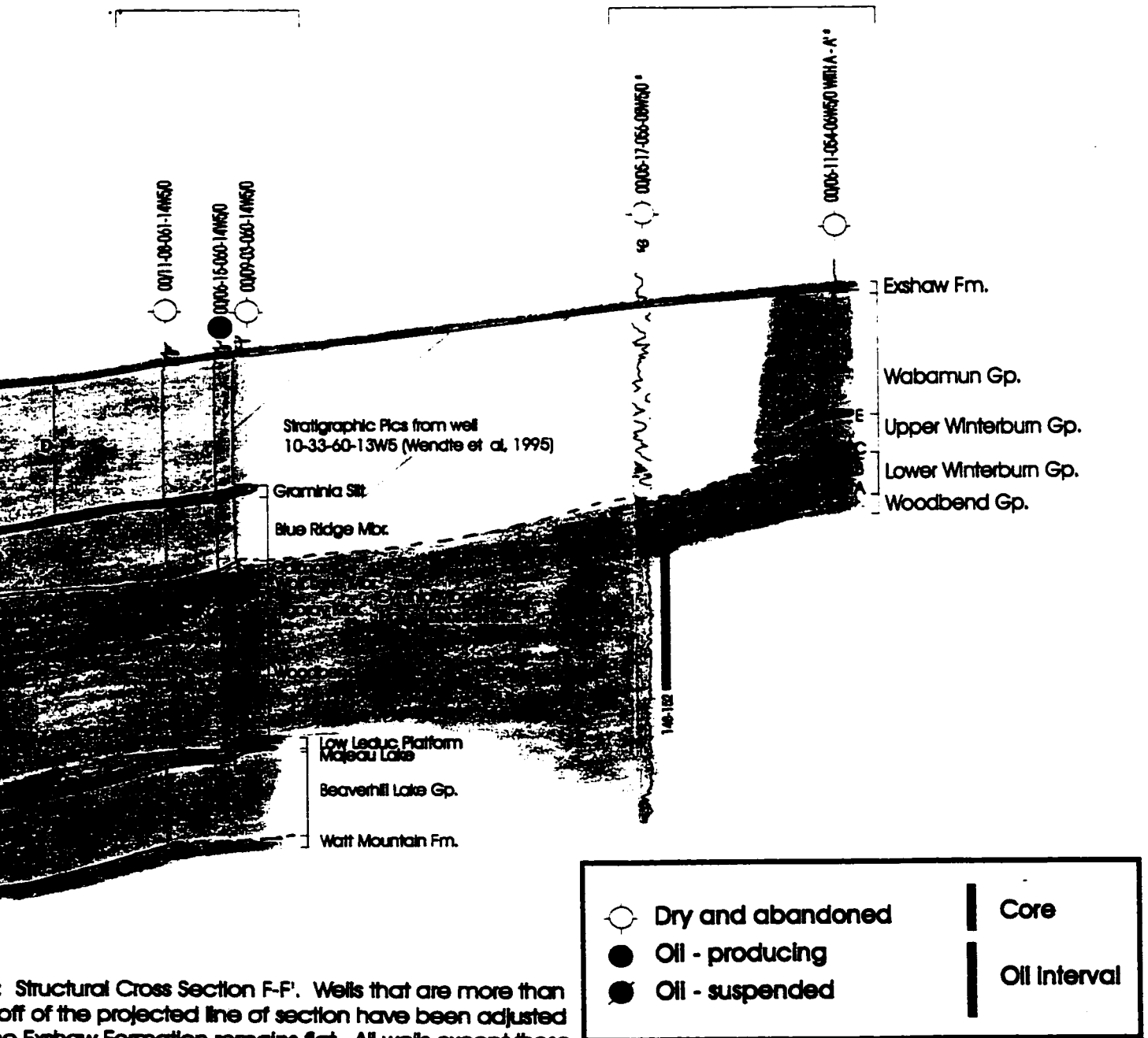


Figure 3.13: Structural Cross Section 1 township off of the projected Leduc Fringing Reef such that the Exshaw Formation is exposed with an * after the well header is

F
SE

Swan Hills Platform
north of Windfall

West Shale Basin
West Pembina area



Structural Cross Section F-F'. Wells that are more than 100 feet off of the projected line of section have been adjusted. The Exshaw Formation remains flat. All wells except those for the well header name have been adjusted.

4. Chapter 4 - Lithofacies and Mineralogical Facies of Regional Aquitards

4.1. Introduction

A total of 788 m of drill core in twenty-eight wells from west-central Alberta were analyzed at the Core Research Centre in Calgary (Appendix 1). The lithology and mineralogy of the aquitards are inhomogeneous and result in the subdivision of several facies within the aquitards. From initial core descriptions and detailed thin-section petrography of the aquitards, eight major lithofacies were identified. Using x-ray diffraction patterns, four mineralogical facies were identified.

Facies analyses of the aquitards is required to identify depositional environments, i.e., deposition in a platform-slope-basinal environment versus deposition in a carbonate ramp environment. But more importantly, the hydraulic integrity of the aquitards may be directly correlative with both lithological and mineralogical facies, as illustrated by Hearn (1996). The main objective of this section then, is to describe the major facies that can be identified within the core studied and to correlate them with stratigraphic and geographic locations.

Depositional environments play an important role in facies distribution, but are also important in controlling the lateral and vertical extent of shale and marl aquitards. Thin and discontinuous successions of aquitards interbedded with aquifers have been identified within the Winterburn Group, whereas in the undivided basinal Woodbend Group and combined basinal sections of the Woodbend/Winterburn Groups, thicker and relatively more laterally continuous intervals of aquitards have been identified. A more detailed discussion regarding the spatial and temporal distribution of these and other Upper Devonian aquitards is provided in Chapter 3 and Appendix 2. The combination of facies types and the vertical and lateral distribution of the strata with respect to hydraulic integrity of the aquitards is discussed in Chapter 6.

The Woodbend and the Winterburn Groups were deposited in different depositional environments, i.e., carbonate slope/basinal environments (Stoakes,

1980) and carbonate ramp environments (Watts, 1987), respectively. In this study, the Woodbend Group aquitards (including the Majeau Lake, Duvernay, and Ireton Formations where they can be subdivided) formed in a pattern similar to those of Stoakes (1980) and Hearn (1996). Deposited in a basinal to shale (or possibly carbonate) platform profile, four major environments of deposition (Figure 4.1) were identified: (1) a basinal environment and (2) toe of the slope; both of which are anaerobic and correlate with water depths of >100 m; (3) the middle foreslope environment which is dysaerobic and correlates with water depths of between 45-100 m; and (4) the upper foreslope and platformal environment which is aerobic and correlates with water depths of between 0-45 m.

The top of the Ireton Formation (end of the deposition of the Woodbend Group) coincides with the termination of a thick interval of fine-grained clastics and the onset of widespread carbonate ramps and localized reefs of the Winterburn Group (Switzer et al., 1994). Within the Winterburn Group, the Nisku Formation, in particular, formed in a homoclinal carbonate ramp (as defined by Ahr, 1973) with isolated shallow and downslope carbonate buildups (biostromes and bioherms) (Figure 4.2). Buildups, in comparison to the atoll-type reefs of the Leduc (of the Woodbend Group) and Swan Hills (of the Beaverhill Lake Group) Formations, are smaller and do not show the internal differentiation into foreslope, margin, crest, and back reef/lagoon areas (Watts, 1987 and references therein).

4.2. Lithological Facies

4.2.1. Introduction

The eight major lithofacies identified within Devonian aquitards include; A, B, AD, AE, C, G, GE, and F. The following sections describe the lithofacies and their depositional environments in sequential order from the deepest to the shallowest marine settings e.g., from basinal through slope, to near-reef environments.

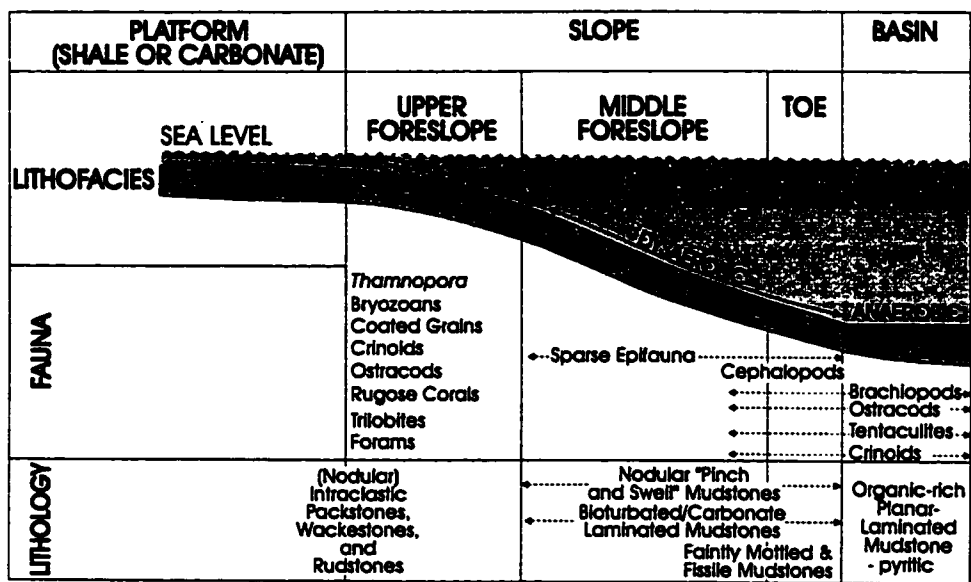


Figure 4.1: Depositional environments of lithofacies of the Woodbend Group in the study area. Lithofacies A to GE are explained in the text. Lithofacies F is not included in this model because an unambiguous depositional environment cannot be provided. The major lithological features and fauna present in the lithofacies are identified (modified by Stoakes, 1980 and Hearn, 1996).

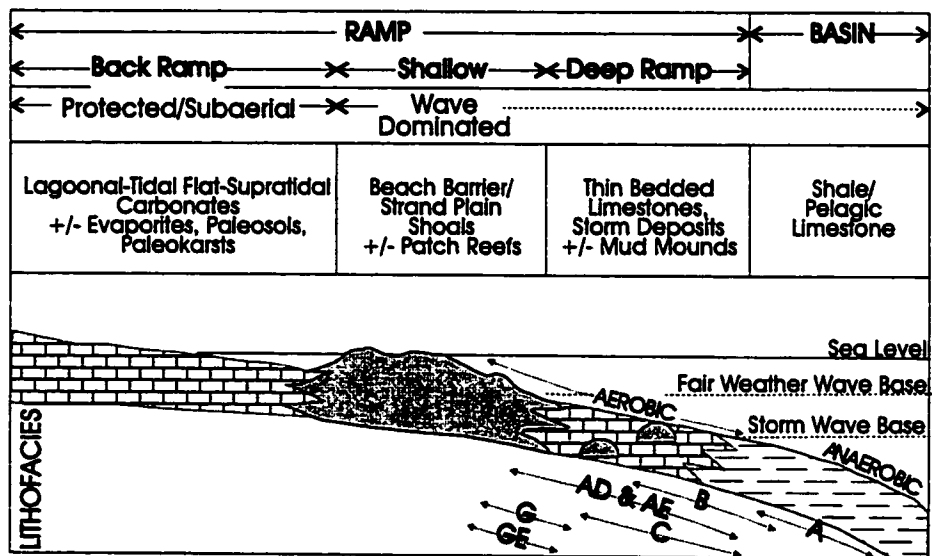


Figure 4.2: Depositional environments of lithofacies of the Winterburn Group in the study area (modified by Tucker and Wright, 1990 and Ahr, 1973). Lithofacies A to GE are explained in the text. Lithofacies F has not been included in this model because an unambiguous depositional environment cannot be provided.

4.2.2. Lithofacies A

The most common lithofacies present throughout the aquitards appears to be lithofacies A. It is a generally massive to planar-laminated, often pyritic, mudstone to wackestone (Figures 4.3 a, b, and c). Mineralogically, over half of the samples tested are shales (<35 weight % carbonate) and the remainder are marls (between 35-65 weight % carbonate) (Figure 4.4). The technique used to determine carbonate percentages is described in Appendix 3. Overall the samples contain an average of 30 weight % carbonate. Laminations contain microfossils such as tentaculites, ostracods and/or calcispheres. Larger (2-5 mm) fossils such as disarticulated brachiopods (and filaments), crinoids and/or echinoderm fragments, are sparse in mudstones yet common in wackestones (Figure 4.3 c-4). *Amphipora* are sparse but where present they form an *Amphipora* mudstone to floatstone (bottom of Figure 4.3 a).

Lithofacies A has several features that suggest it formed in a deep basinal environment, likely the deepest identified in this study. This facies is typically dark grey to black in color which suggests that it is quite rich in organic matter. Planar laminations, where present, indicate little disturbance by wave action and burrowing. The dark color and absence of bioturbation suggests formation in an anoxic environment. The epifauna typically consists of planktonic organisms such as ostracods which died and settled to the sea bottom as well as deep-marine organisms such as tentaculites. Disarticulated and fragmented brachiopods are present in patchy and wispy lenses of wackestones within massive, unfossiliferous mudstones. These wackestones could have formed when sediments and fauna were transported downslope into the basinal environment during storms.

This lithofacies is equivalent to Stoakes' (1980) "bituminous dark laminated limestone and shale facies". He suggested it formed in an anaerobic, basinal environment equating to the fondothem portion of Rich's model (1951). Stoakes and Creaney (1984) identified these laminated, bituminous mudstones as having the highest total organic carbon (TOC) values (5-10%) of all facies

Figure 4.3: Typical core samples and thin sections of lithofacies A - Massive to millimetre planar-laminated mudstones and wackestones.

a) Core sample of massive to slightly planar-laminated, black mudstone with sparse *Amphipora* in the bottom part of the core, which makes this core transitional from lithofacies A and F up to lithofacies A. Centimeter bar for scale. Sample taken from core 7-5-59-18W5, 11272.5' (3435.86 m).

b) Core sample of millimetre, planar-laminated, dark grey mudstone. Light-colored laminations mostly consist of microquartz grains and fossils such as tentaculites and ostracods, which cannot be seen at this scale. Centimeter bar for scale. Sample taken from core 7-5-59-18W5, 11310' (3447.29 m).

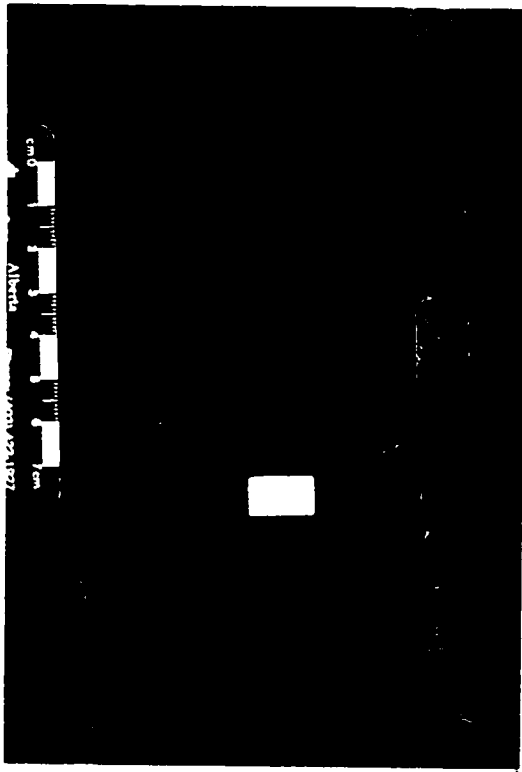
c) Photographs of thin sections showing the massive to planar-laminated texture of this lithofacies. This lithofacies commonly contains microfossils, however, they are generally not evident at the scale required to display the texture of this lithofacies. Thin sections have been stained on the left half of each slide with Alizarin Red-S dye and were also injected with a blue-stained epoxy. Dime for scale. Photographs were taken of the thin sections placed on a white piece of paper, illuminated by incident light, on a core photomicrograph stage.

c-1) Mudstone with ostracod and tentaculite. 4-13-56-23W5, 13547' (4129.12 m).

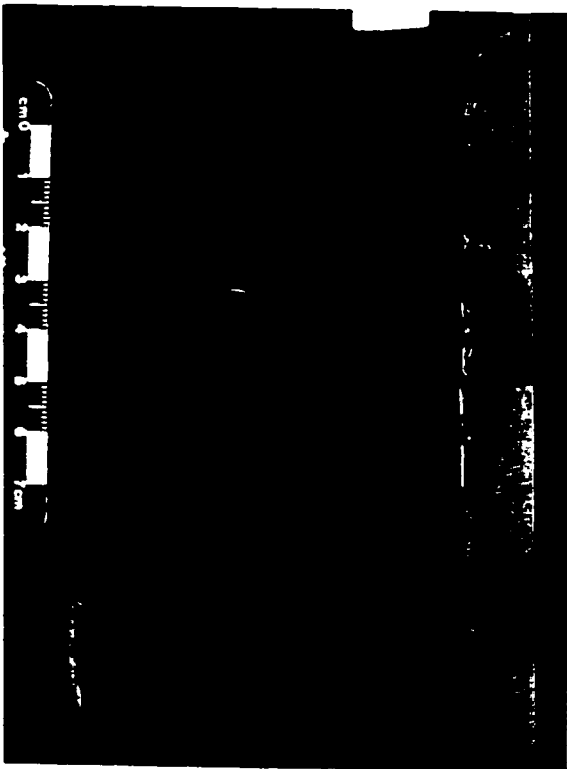
c-2) Slightly laminated, light-brown mudstone. 15-23-53-21W5, 13227.7' (4031.8 m).

c-3) Mudstone with white laminations of microquartz grains, ostracods, calcispheres, and tentaculites. 14-2-69-21W5, 9029.7' (2752.25 m).

c-4) Crinoid, and possibly thin-shelled embryonic brachiopod, wackestone to packstone. Fossils on the left part of slide are calcitic; see red-colored crinoid ossicles nearer the bottom. 10-17-57-23W5, 13137' (4004.16 m).



a



b

c

1



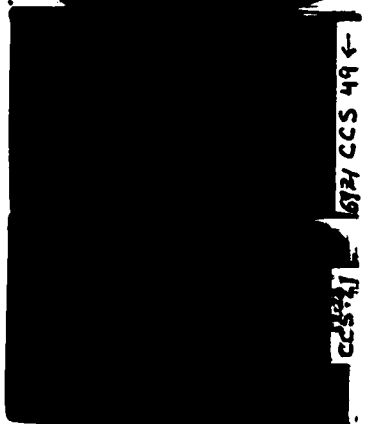
CCS 2536

2



CCS 53

3



CCS 49

4



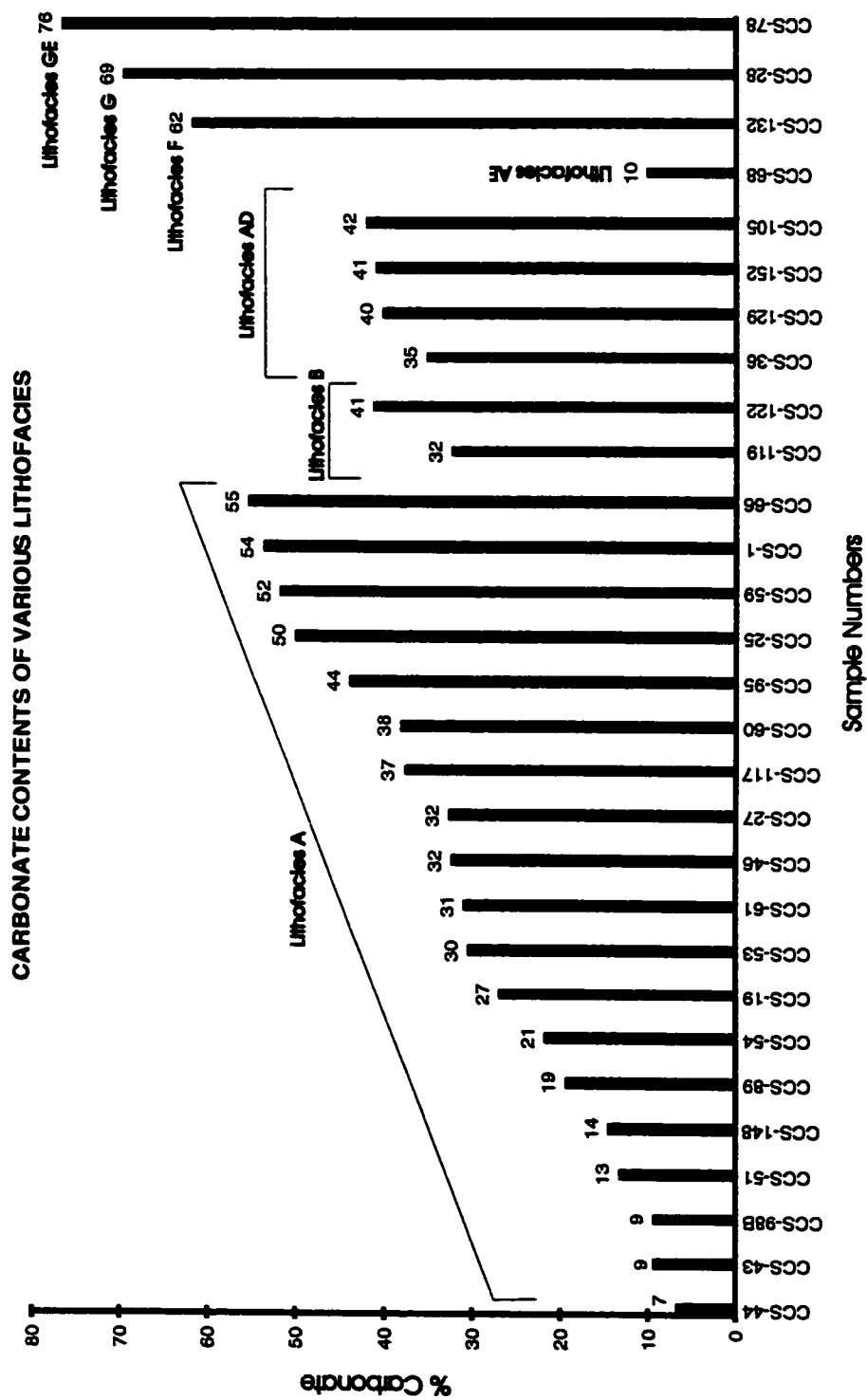


Figure 4.4: A graph showing carbonate percentages of whole-rock samples of the various lithofacies, as determined by chemical dissolution. Generally slope and near-reef facies AD, G, and GE have higher carbonate contents than the more basinal or deep-ramp facies A and B.

within the Duvernay and Ireton Formations, suggesting that it is the source rock for many Devonian reservoirs. Lithofacies A is common in Woodbend Group aquitards (including the Majeau Lake and Duvernay Formations), but it also occurs in the Winterburn Group. The stratigraphic distribution of facies A (and all other facies identified) will be discussed in further detail following the description of both lithological and mineralogical facies.

4.2.3. Lithofacies B

Lithofacies B is similar to the mudstones described in lithofacies A, in that epifauna are sparse and bioturbation is absent. However, lithofacies B is generally more carbonate-rich than lithofacies A (consisting of approximately 37 weight % carbonate); one sample tested is a marl (between 35-65 weight % carbonate), and the other is a shale (<35 weight % carbonate) (Figure 4.4). Lithofacies B is predominantly fissile in contrast to the more massive texture of lithofacies A (Figures 4.5 a, b, and c). Hand samples of this lithofacies, especially when wet, feel slimy to the touch. Compared to lithofacies A, this facies is lighter in color, usually a medium grey, indicating less amounts of organic matter.

Lithofacies B is interpreted to have formed in a moderately deep environment, but not so deep nor so oxygen-depleted as lithofacies A. Supporting evidence includes an increase in carbonate content in the matrix and a decrease in organic matter compared to lithofacies A. In the Woodbend Group, a possible depositional environment for this lithofacies is the toe of the foreslope (Figure 4.1). In the Winterburn Group, Watts (1987) envisaged a deep ramp to possible basinal margin setting for a similar lithofacies (Figure 4.2).

4.2.4. Lithofacies AD

Lithofacies AD is generally a massive, carbonate-rich, faintly mottled grey-to light grey-colored mudstone to wackestone. An average of 40 weight % carbonate was found in four marl samples (Figure 4.4). The faintly mottled texture may be evidence of bioturbation (Figures 4.6 a and b). Epifauna commonly found in wackestones include tentaculites, crinoids, ostracods, shell

Figure 4.5: Typical core samples and thin sections of lithofacies B - Fissile mudstones.

a) Core sample of medium grey-colored, moderately fissile mudstone. 2-9-54-12W5, 8435.70' (2571.2 m) Centimeter bar for scale.

b) Small core sample showing fissile texture of lithofacies B. 2-9-54-12W5, 8532.48' (2600.7 m). Centimeter bar for scale; each orange bar = 1 cm.

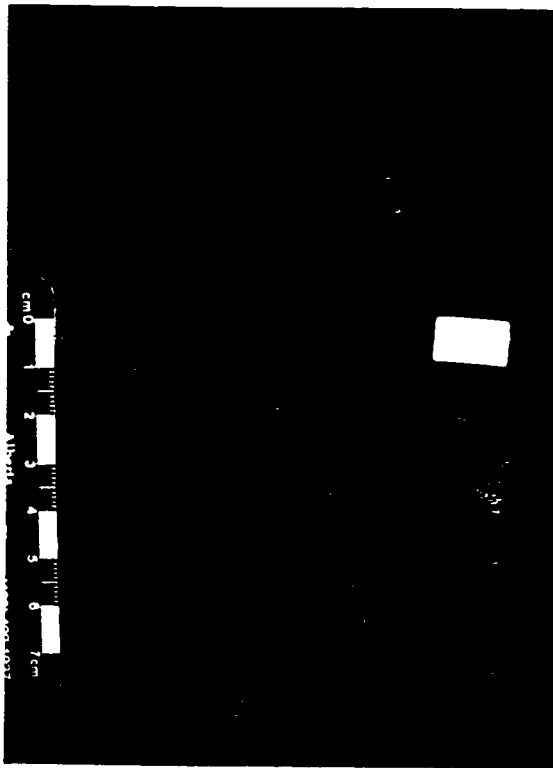
c) Photographs of thin sections showing the fissile texture of this lithofacies. These mudstones commonly contain microfossils, however, they are not evident at the scale required to display the fissile texture of the facies. All thin sections have been injected with a blue-stained epoxy and stained on the left half with Alizarin Red-S. Dime for scale. Photographs were taken of the thin sections placed on a white piece of paper, illuminated by incident light, on a core photomicrograph stage.

c-1) Fissile mudstone. 2-9-54-12W5, 8532.48' (2600.7 m).

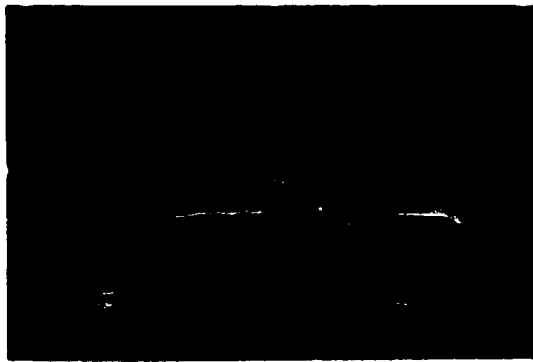
c-2) Fissile mudstone with small shell fragments, ostracods, and calcispheres. 2-9-54-12W5, 8530.51' (2600.10 m).

c-3) Fissile mudstone with small brachiopods. 2-9-54-12w5, 8410.76' (2563.6 m).

c-4) Fissile mudstone with small brachiopods and ostracods. 7-4-49-12W5, 10158.75' (3096.39 m).



a



Porta
logical Information Phone: (403
Calee

b

c

1

2

3

4

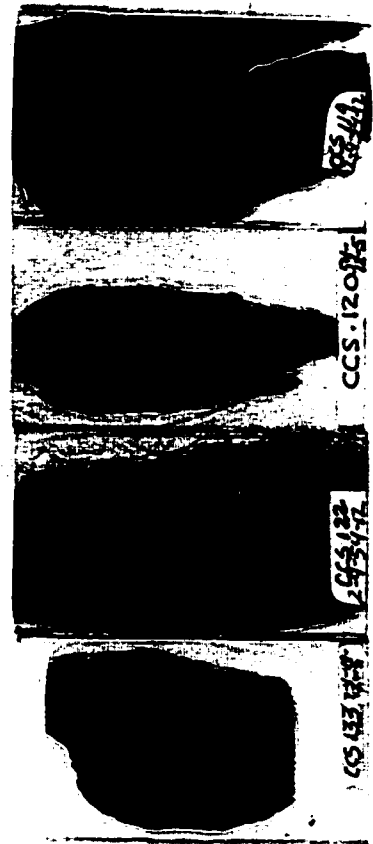


Figure 4.6: Typical core samples and thin sections of lithofacies AD - Faintly mottled mudstones and wackestones.

a) Core sample of mottled mudstone. 05-17-56-8W5, 7012' (2137.26 m). Centimeter bar for scale; an orange bar = 1 cm.

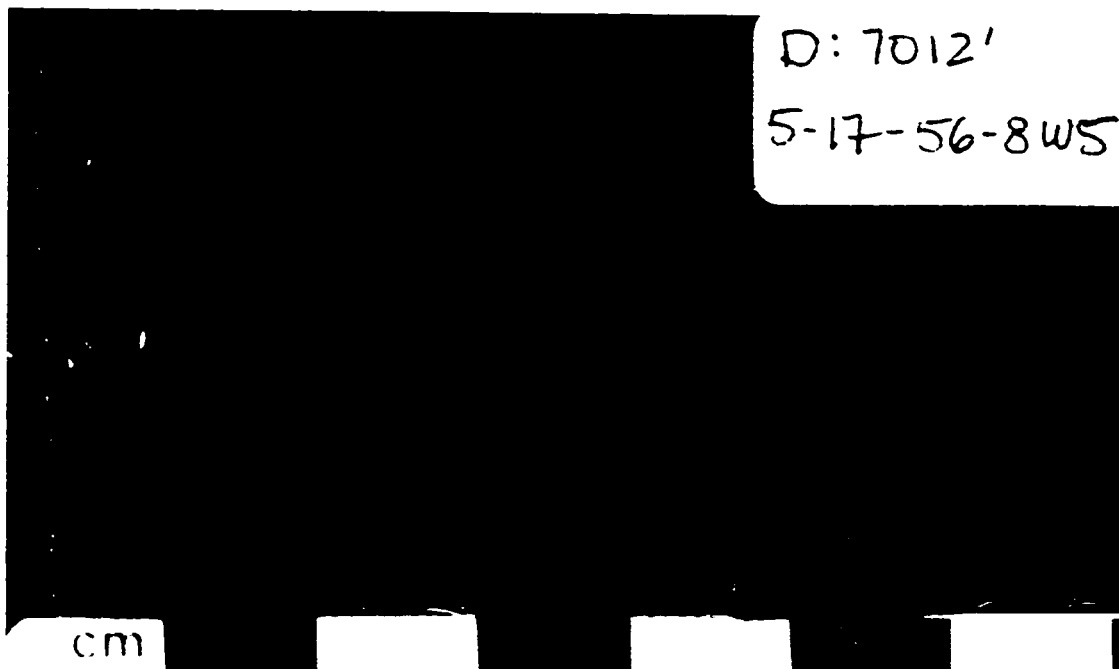
b) Photographs of thin sections showing the mottled texture of this mudstone. This facies may contain microfossils, however, they are not visible at the scale to show the faintly mottled texture of the facies. All thin sections have been stained on the left half with Alizarin Red-S, and injected with a blue-stained epoxy. Dime for scale. Photographs were taken of the thin sections placed on a white piece of paper, illuminated by incident light, on a core photomicrograph stage.

b-1) Bioturbated mudstone 6-6-46-15W5, 13549.9' (4130 m).

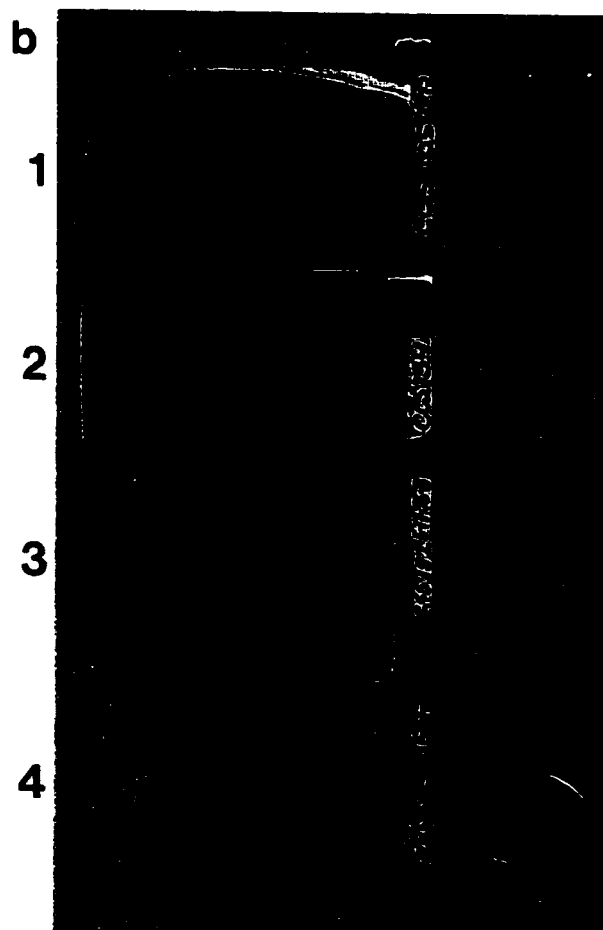
b-2) Mudstone to tentaculites, crinoid, shelly wackestone. 7-4-49-12W5, 10152' (3094.33 m).

b-3) Bioturbated mudstone 5-17-56-8W5, 7012' (2137.26 m).

b-4) Ostracod wackestone to mudstone. 6-5-51-7W5, 7678' (2340.25 m).



a



fragments, brachiopods (and possibly thin-shelled embryonic brachiopods), and minor amounts of cephalopods.

Possible evidence of bioturbation, minor amounts of epifauna, a lower organic content, and a generally higher carbonate content than lithofacies A and B, suggests that this lithofacies formed in a more oxygenated environment than lithofacies A or B. In the Woodbend Group, lithofacies AD is interpreted to have developed near the toe of the slope or in the lower-middle foreslope region (Figure 4.1); however of the core analyzed from the Woodbend Group (and subdivisions of this group), this lithofacies was not identified. In the Winterburn Group, a possible depositional environment is the deep ramp to the lower part of the shallow ramp (Figure 4.2).

4.2.5. Lithofacies AE

This lithofacies is generally represented by nodular mudstones. The macroscopic texture of this lithofacies, consisting of beige to dark-beige, carbonate-rich nodules or lens-like structures surrounded by "pinch and swell structures" (McCrossan, 1957) of a darker, more clay-rich matrix (Figures 4.7 a, b, and c), results from diagenetic processes. In some locations, it appears that the dark domains form stylolites in a horsetail-shaped pattern with evidence of carbonate dissolution. In other locations, the dark domains are so sparse and the nodules so large that the latter gradually merge into more continuous beds (Machel and Hunter, 1994) (Figure 4.7 a). Several authors have previously described similar textures and facies including "lenticular limestone masses or sedimentary boudinage structures" (McCrossan, 1957), "nodular limestones" (Stoakes, 1980), "nodular to nodular-banded lime mudstones" (Stoakes and Creaney, 1984), and "nodular mudstones" (Machel and Hunter, 1994). The difference between Stoakes' "nodular limestone facies" and lithofacies AE is the general absence of macroscopic skeletal grains.

The formation of this diagenetic "pinch and swell" texture is debatable. McCrossan (1957) suggests that they formed during the lateral plastic flow of newly deposited mud while its surface tended to conform to a horizontal plane,

Figure 4.7: Typical core samples and thin sections of lithofacies AE - Nodular mudstones.

a) Core sample showing diagenetic carbonate lenses and nodules surrounded by argillaceous-rich banding or "pinch and swell structures". The darker stripe down the centre of the core is an artifact of HCl staining. 11-29-65-18W5, 8394' (2558.5 m). Centimeter bar for scale.

b) Core sample showing the diagenetic nodular and "pinch and swell structures". Compared to Figure 2.6 a above, this sample is richer in organic matter, and the "pinch and swell structures" are larger and tend to close off the carbonate nodules. 5-17-56-8W5, 7050' (2148.84 m). Centimeter bar for scale; each orange bar = 1 cm.

c) Photographs of thin sections showing the diagenetic nodular and "pinch and swell structures" and texture. These nodular mudstones contain microfossils, however, they are not evident at the scale required to display the nodular texture. All thin sections have been stained on the left half with Alizarin Red-S and injected with a blue-stained epoxy. Dime for scale. Photographs were taken of the thin sections placed on a white piece of paper, illuminated by incident light, on a core photomicrograph stage.

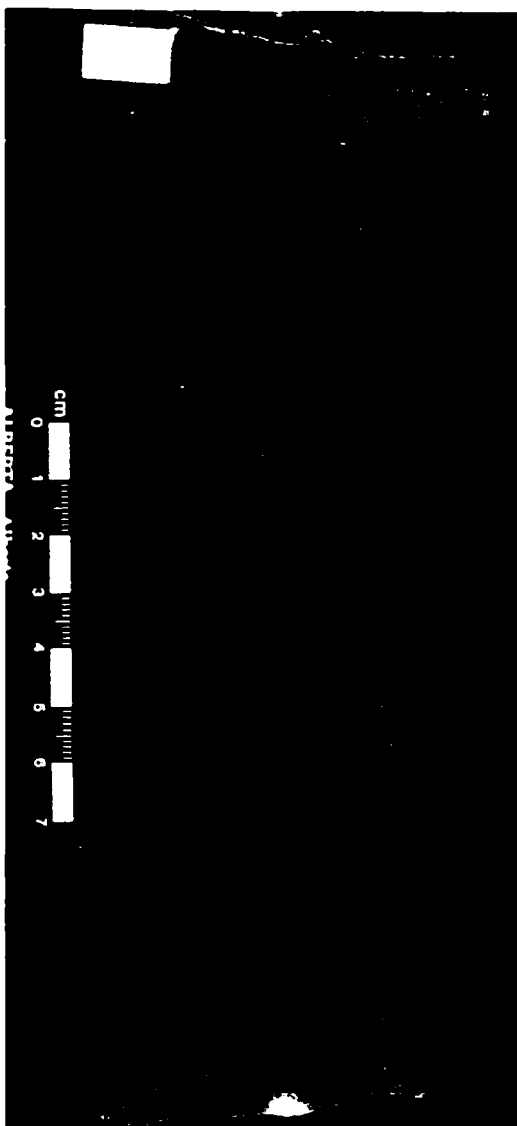
c-1) Nodular mudstone with minor amounts brachiopods, calcispheres, ostracods, tentaculites. 10-16-69-5W6, 12324' (3756.35 m).

c-2) Ostracod, tentaculites, coral? wackestone to mudstone. 10-22-70-18W5, 8548' (2605.43 m).

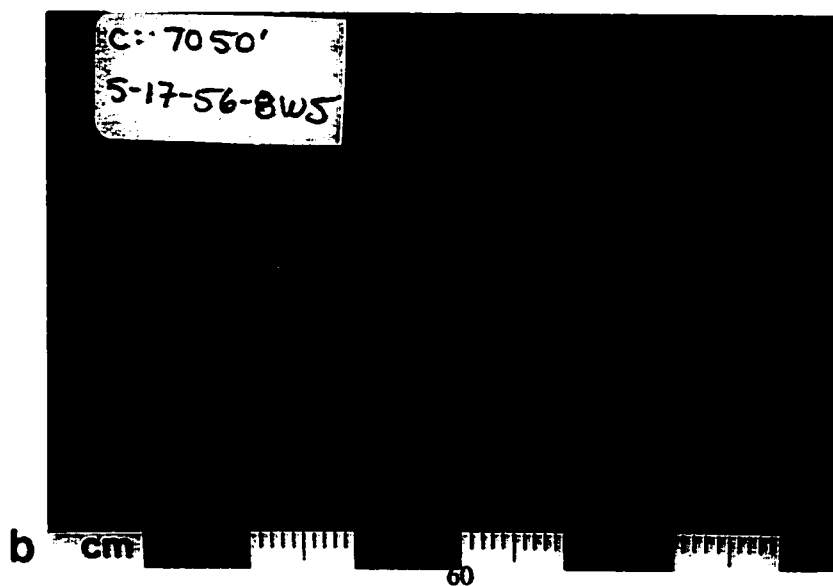
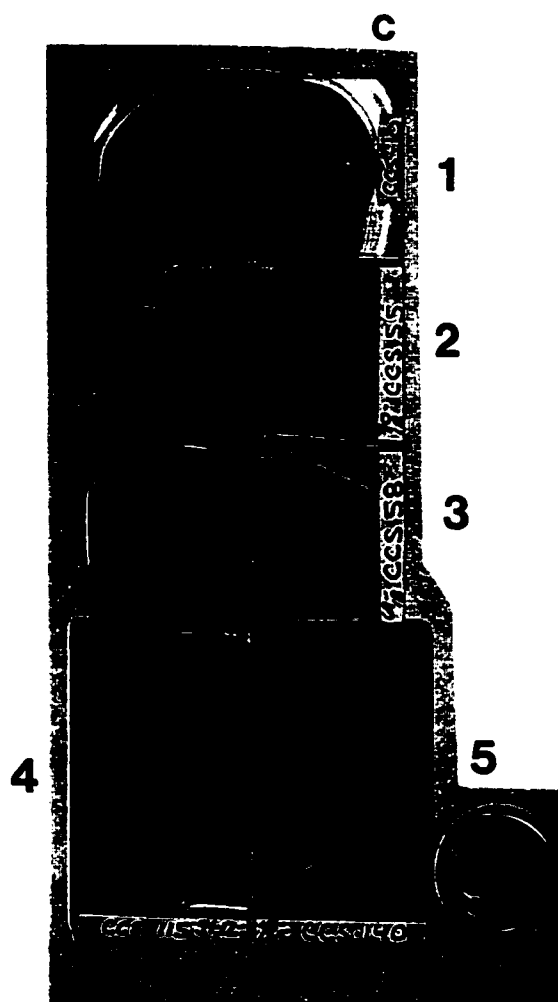
c-3) Nodular mudstone with small crinoids. 4-22-69-18W5, 9027' (2751.43 m).

c-4) Crinoid, tentaculites, ostracod, shell fragment wackestone to mudstone. 2-9-54-12W5, 8579.40' (2615 m).

c-5) Crinoid, brachiopod, wackestone alternating with wisps of mudstone. 9-35-48-12W5, 10361.5' (3158.18 m).



a



b

analogous to boudinage in metamorphic rocks. Accordingly, during compaction the more plastic beds (the calcareous shale beds) displaced the less plastic beds (the argillaceous granular limestones). On the other hand, Stoakes and Creaney (1984) assert that these textures formed from bioturbation and subsequent differential cementation of the sediments, and Machel and Hunter (1994) state that as carbonate content increases upwards on a carbonate ramp at the expense of clay content, the carbonate content gradually enlarges enough to form diagenetic nodules consisting of fine-crystalline carbonate in a shaley matrix. The nodular to nodular-banded lime mudstone facies identified by Stoakes and Creaney (1984) from the Duvernay and Ireton Formations in the east-central Basin produced TOC from 0.5 to 5%.

This macroscopic, diagenetically-formed texture is also present in lithofacies GE subsequently described. Although texturally similar, these two lithofacies are classified by features usually discernible only at the microscopic scale. In lithofacies AE, sparse epifauna including crinoids, brachiopods, calcispheres, and tentaculites, can be identified at this scale. A comparable fossil assemblage to lithofacies A and B, and possible evidence of varying degrees of bioturbation, suggests that lithofacies AE formed in an environment extending from the toe of the foreslope to the middle-foreslope in the Woodbend Group. The presence of higher clay contents in the lithofacies may indicate deposition nearer the toe of the slope (Figure 4.2). One clay-rich sample representing this lithofacies with a carbonate content of 10 weight % is a shale (Figure 4.4).

In the Winterburn Group, a depositional environment extending from the deep ramp to the shallow ramp is envisaged. From core analyzed however, this lithofacies was mostly identified in the Majeau Lake and Duvernay Formations, as discussed in subsequent sections.

4.2.6. Lithofacies C

Lithofacies C is a mudstone, laminated with carbonate lenses on a centimeter scale (Figure 4.8 a and b). In east-central Alberta this lithofacies is

Figure 4.8: Typical core sample and thin sections of lithofacies C - Bioturbated and/or carbonate-laminated mudstones.

a) Core sample of medium grey, and light grey to white laminated or bioturbated mudstone. 6-5-51-7W5, 7709.97' (2350 m) Centimeter bar for scale.

b) Photographs of thin sections showing the bioturbated or laminated texture of this lithofacies. This facies may contain microfossils, however, they are not evident at the scale required to display the bioturbation and/or laminations. Red staining of the carbonate layers indicate calcite. All thin sections have been stained on the left half with Alizarin Red-S, and injected with a blue-stained epoxy. Dime for scale. Photographs were taken of the thin sections placed on a white piece of paper, illuminated by incident light, on a core photomicrograph stage.

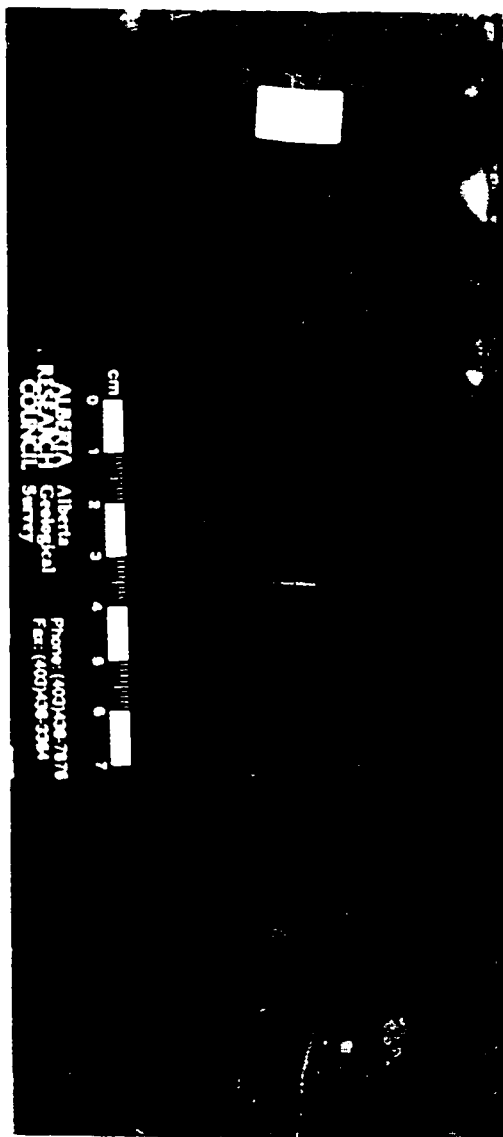
b-1) Calcite-rich laminated or bioturbated mudstone. 9-17-50-10W5, 8924.54' (2720.2 m).

b-2) Calcite-rich laminated mudstone with minor amounts of shell fragments and echinoderms. 5-17-56-8W5, 7590' (2313.43 m).

b-3) Calcite-rich laminated or bioturbated mudstone. 6-5-51-7W5, 7703.41' (2350 m) (sample taken from core in Figure 4.8 a).

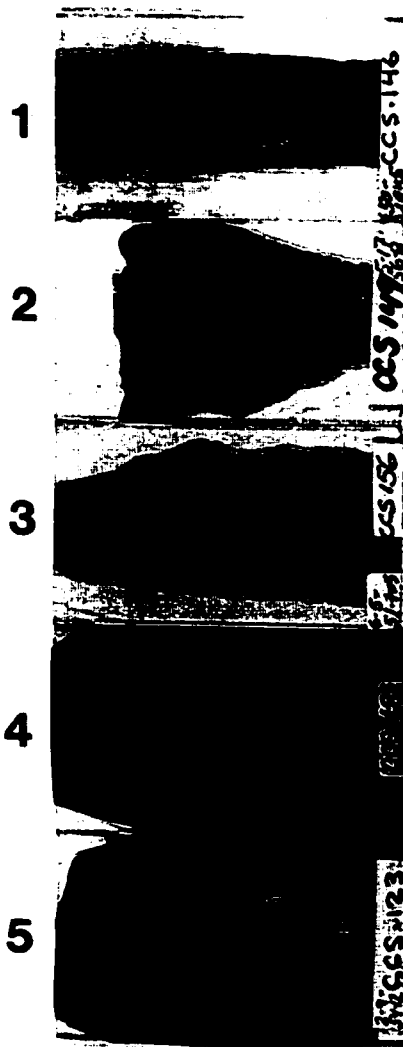
b-4) Bioturbated mudstone. 6-28-61-26W5, 12822.5' (3908.30 m).

b-5) Calcite-rich laminated or bioturbated mudstone. The calcite-rich horizons are composed of crinoid, foraminifera, brachiopod-rich wackestones to packstones. 2-9-54-12W5, 8392.39' (2558 m).



a

b



similar to that described by Stoakes (1980) as an "interbedded dense micritic limestone and calcareous shale facies"; however one of the major differences is the general absence of epifauna.

Stoakes (1980) suggested that the carbonate-rich lenses are related to material settling from hemipelagic suspension with low rates of accumulation. He also suggested that the environment of deposition of this facies was not conducive to the development of benthic epifauna, and that sediments appear to represent accumulation in relatively deep-water, low-energy conditions. It was also suggested that low-sedimentation rates allowed early diagenetic reorganization of calcite into nodules and layers.

Alternatively, the presence of carbonate lenses in this lithofacies could indicate bioturbation. If this is the case, this facies is interpreted to have formed in slightly more oxygenated waters than stated above, or suggested for lithofacies A or B. In the Woodbend Group, a suggested depositional environment is the toe of the foreslope to middle-foreslope region, similar to that of lithofacies AE (Figure 4.1); however, from the core analyzed, this lithofacies was identified only in the Winterburn Group. In the Winterburn Group, a possible depositional environment is the lower part of the deep ramp (Figure 4.2).

4.2.7. Lithofacies G

Lithofacies G is predominantly an intraclastic wackestone to packstone but in places is a rudstone (Figures 4.9 a, b, and c). This lithofacies appears equivalent to the intraclastic packstones to rudstones of Stoakes (1980). This facies contains a diverse fauna, most of which is very fragmented. Fauna includes; *Thamnopora* (and/or bryozoans), rugose corals, crinoids and echinoderm fragments, brachiopod and other shell fragments, trilobites, ostracods, foraminifera, peloids, and fragments of tabular stromatoporoids. As well, coated grains (oncolites) are present, many containing bioclastic nuclei. Anhydrite is typically present filling intraparticle pores of *Thamnopora* or bryozoan fragments. Dolomite (and/or ankerite) typically occurs in the matrix between calcitic fossils, and is also found replacing several fossils. One sample

Figure 4.9: Typical core sample and thin sections of lithofacies G - Intraclastic packstones to wackestones.

a) Crinoid-*Thamnopora* wackestone to packstone. 11-35-54-23W5, 13669.5' (4166.46 m) Centimeter bar for scale; each white bar = 1 cm.

b) Coated grain (with a large stromatoporoid for a nucleus), *Thamnopora* floatstone to rudstone. 9-3-60-14W5, 9795.93' (2681 m) Centimeter bar for scale; each white bar = 1 cm.

c) Photographs of thin sections of this lithofacies. All thin sections have been stained with Alizarin Red-S on the left half of the thin section except in Figure c-4 which has been stained on the right. They have also been injected with a blue-stained epoxy. Dime for scale. Photographs were taken of the thin sections placed on a white piece of paper, illuminated by incident light, on a core photomicrograph stage.

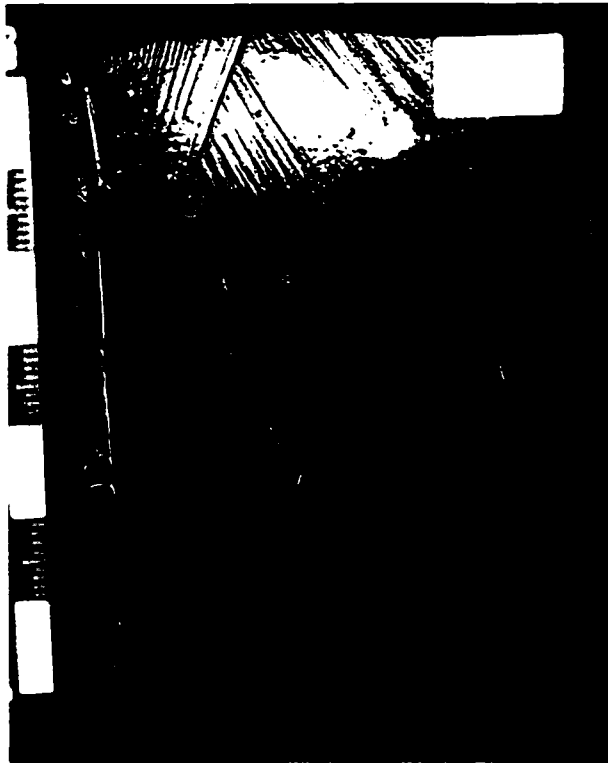
c-1) Crinoid, brachiopod, trilobite, *Thamnopora* lithoclastic wackestone to packstone. 14-11-70-5W6, 11141' (3395.78 m).

c-2) Nodular echinoderm wackestone to packstone. 15-23-53-21W5, 13257.55' (4040.9 m).

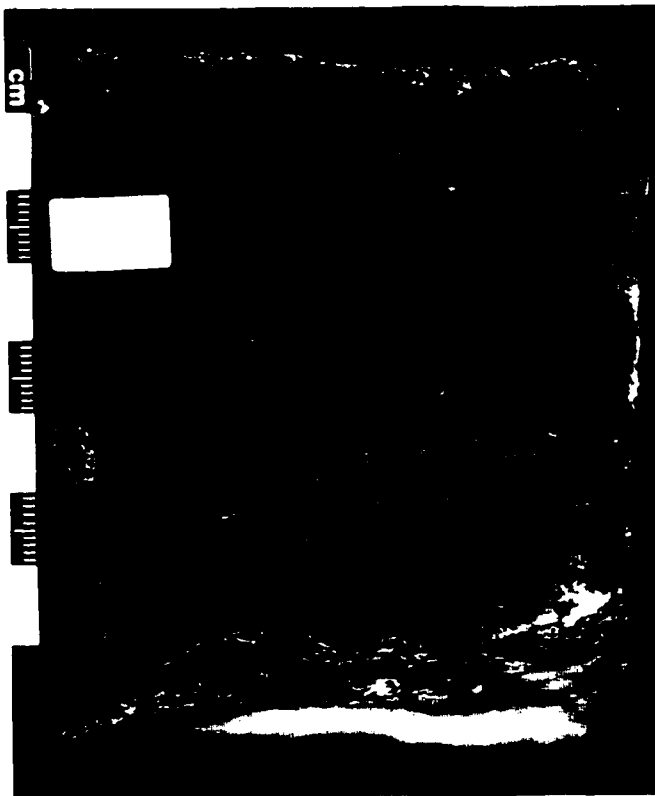
c-3) *Thamnopora* crinoid packstone. 9-3-60-14W5, 8792.65' (2680 m).

c-4) Brachiopod, *Thamnopora* packstone to rudstone. 7-4-49-12W5, 10074' (3070.56 m).

c-5) Tentaculites, brachiopod, bryozoan, *Thamnopora*, echinoderm, *Amphipora* packstone to wackestone. 11-35-54-23W5, 13675' (4168.14 m).

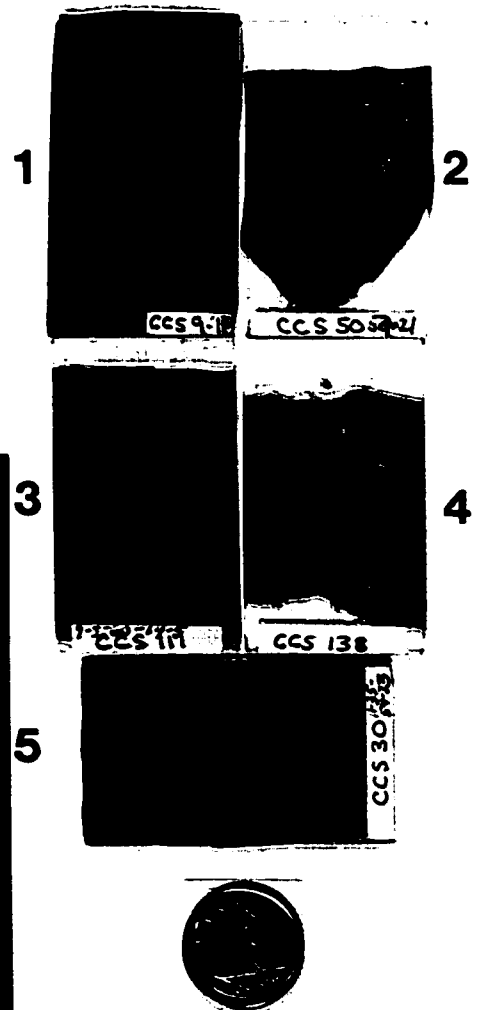


a



b

c



tested is 69 weight % carbonate, indicating it is between a carbonate-marl and a marl-carbonate, rather than a simply a marl (Correns, 1968) (Figure 4.4).

The macrofauna in this lithofacies was probably derived from near-reef environments during storms and incorporated with sediments from deeper marine environments. The depositional environment that Stoakes (1980) suggests for his intraclastic packstones to rudstones facies is a shale platform. Lithofacies G, in the Woodbend Group is interpreted to form in an upper-most foreslope to near-reef environment, close to the shale platform environment suggested by Stoakes (1980) (Figure 4.1). In the Winterburn Group, lithofacies G most likely formed in a shallow ramp or near-reef environment (Figure 4.2).

4.2.8. Lithofacies GE

Lithofacies GE is a nodular, intraclastic packstone, wackestone, to mudstone (Figures 4.10 a and b). Texturally, albeit not environmentally, it is actually a combination of lithofacies AE and G (Figures 4.7 a to c and 4.9 a to c). Lithofacies GE is similar to lithofacies AE in that it contains diagenetic sedimentary boundinage structures (pinch and swell structures). Also, lithofacies GE is similar to lithofacies G in that it contains identical (although not as abundant) fauna and typical anhydrite and dolomite cements. One sample of this facies tested consists of 76 weight % carbonate, indicating that it is a limestone (or marl-carbonate after Correns (1968)) (Figure 4.4).

In the Woodbend Group, a depositional environment in an upper-foreslope or near-reef region is interpreted for this lithofacies. This interpretation is based primarily on the near-reef fossil assemblage, high carbonate content, and comparison with Stoakes and Creaneys' (1994) "nodular limestone facies", and their interpretation of formation of in an upper-foreslope region (Figure 4.1). In the Winterburn Group, the facies was probably deposited in a near-reef setting correlative with the shallow ramp environment (Figure 4.2).

Figure 4.10: Typical core sample and thin sections of lithofacies GE - Nodular intraclastic wackestones to mudstones.

a) Core sample showing the typical nodular "pinch and swell structure" texture of this facies. This lithofacies appears similar to that of lithofacies AE; however, it is fossiliferous. 11-29-65-18W5, 8383.37' (2555.25 m) Centimeter bar for scale.

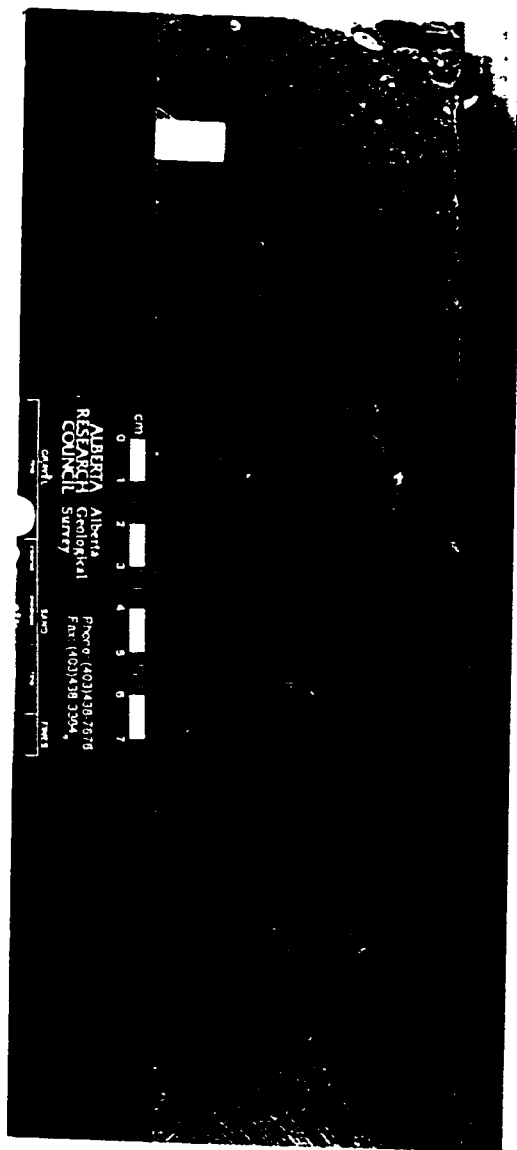
b) Photographs of thin sections of this lithofacies. This facies commonly contains microfossils, however, they are not evident at the scale required to display the nodular texture of this facies. All thin sections have been injected with a blue-stained epoxy and half stained on the left side with Alizarin Red-S except for Figure 2.10b-2 which has been stained on the right. Dime for scale. Photographs were taken of the thin sections placed on a white piece of paper, illuminated by incident light, on a core photomicrograph stage.

b-1) Echinoderm, *Thamnopora*, stylolitic, intraclastic packstone. 11-29-65-18W5, 8 385.83' (2556 m).

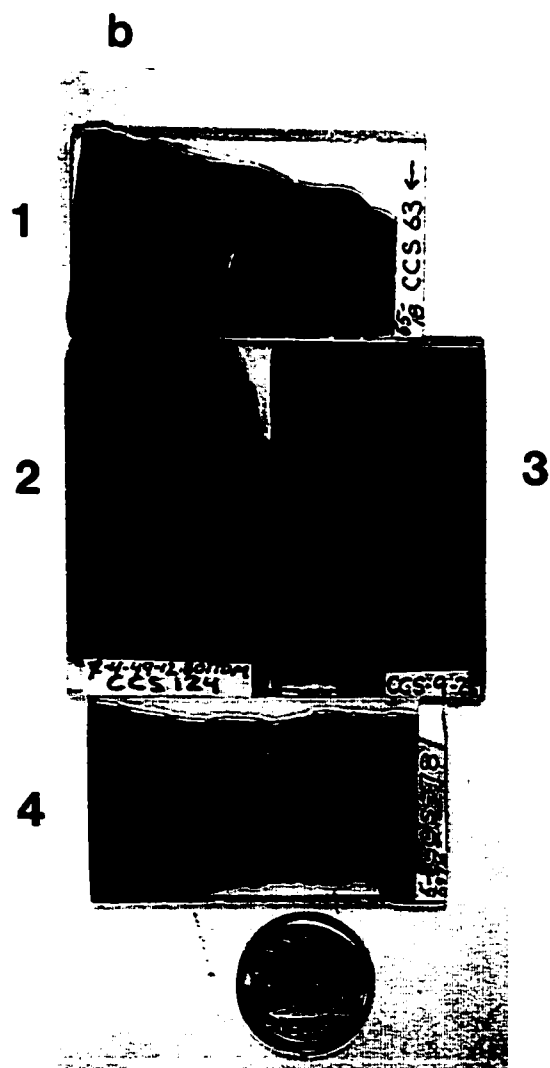
b-2) Crinoid, ostracod, *Thamnopora*, stylolitic packstone to wackestone. 7-4-49-12W5, 10299.5' (3139.29 m).

b-3) Crinoid, ostracoda, *Thamnopora*, wackestone to packstone. 14-11-70-5W6, 11141' (3395.78 m).

b-4) Echinoderm, brachiopod, stylolitic, intraclastic and nodular packstone to grainstone. 7-5-59-18W5, 11324.5' (3451.71 m).



a



4.2.9. "Lithofacies F"

Although not a real lithofacies, in that it is not mappable, it is important to distinguish it from the others. Lithofacies F consists of brachiopod floatstones and minor occurrences of *Amphipora* floatstones. This lithofacies contains a moderate amount, but only a limited type, of these epifauna. Lithofacies F (Figure 4.11 a and b) often occurs in combination with previously described lithofacies such as A, B, AD, C, and G (Figure 4.12 a, b, c). Considering this, the depositional environment for this lithofacies is ambiguous. This contrasts with proposed environment of deposition for a brachiopod floatstone facies within Slave Point deposits (of the Beaverhill Lake Group) by Craig (1987). This facies was suggested to have formed in an off-reef environment, in underturbulent to subturbulent wave conditions on the upper slope of a carbonate shelf.

4.3. Mineralogical Facies

4.3.1. Introduction

X-ray diffraction (XRD) data were obtained for fifty-one samples representing both whole-rock samples from several lithofacies, and specific parts of the more heterogeneous samples such as carbonate- cements, lenses, and nodules typical of lithofacies AE, C, and F within the various aquitards (Table 4.1). Prior to analyses, the samples were cleaned, and crushed or drilled (Appendix 3). The XRD methodology is also described in Appendix 3.

Mineralogical data obtained from whole-rock powder samples, and specific parts from several aquitards was used to identify the carbonate phase present and to semi-quantitatively estimate the amount of carbonate within the sample. This data was useful in choosing samples for later work in stable and radiogenic isotope analyses (discussed in Chapter 5).

Previous studies have examined the mineralogical content of aquitards in east-central Alberta (e.g., McCrossan, 1957; Campbell and Oliver, 1968), however, this study contains the first investigation of the mineralogical content of Devonian shale and marl aquitards in west-central Alberta. This section

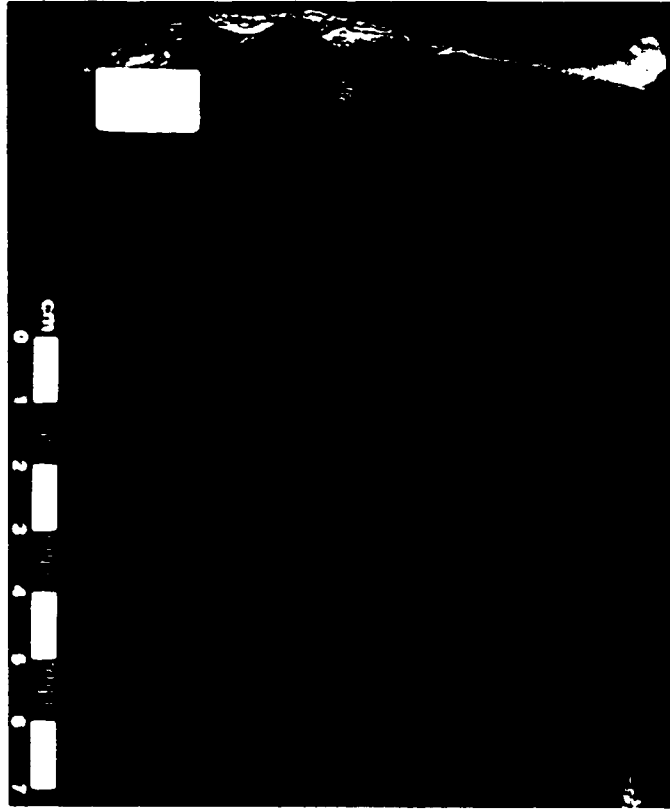
Figure 4.11: Typical core sample and thin sections of lithofacies F - Brachiopod floatstones.

a) Core sample of medium grey brachiopod floatstone. 7-4-49-12W5, 10224' (3116.28 m). Centimeter bar for scale.

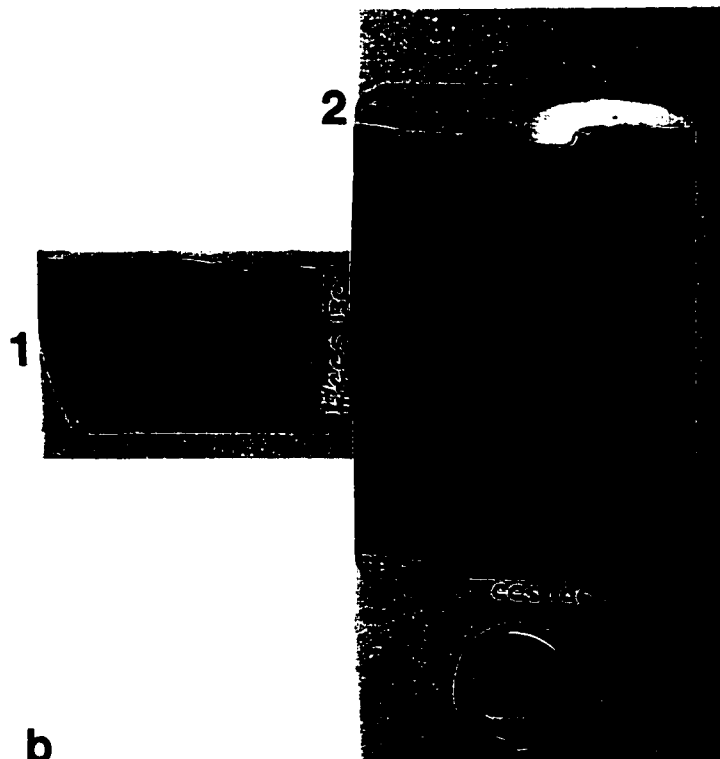
b) Photographs of thin sections of this lithofacies. All thin sections have been stained with Alizarin Red-S and injected with a blue-stained epoxy. Dime for scale. Photographs were taken of the thin sections placed on a white piece of paper, illuminated by incident light, on a core photomicrograph stage.

b-1) Articulated and disarticulated brachiopod floatstone with a calcite matrix (stained on the upper half). 7-4-49-12W5, 10224' (3116.28 m) (sample taken from core in Figure 4.11 a).

b-2) Articulated brachiopod floatstone with a matrix consisting of mainly quartz and ankerite (stained on the right half). The white spotted cement in one of the brachiopods on the upper right side is dolomite. The pure white cement in the brachiopod below it, unstained by Alizarin Red-S, is anhydrite. 6-6-46-15W5, 13544.62' (4128.4 m).



a



b

Figure 4.12: An example of a core sample and thin sections of combinations of lithofacies A and F, B and F, and C and F.

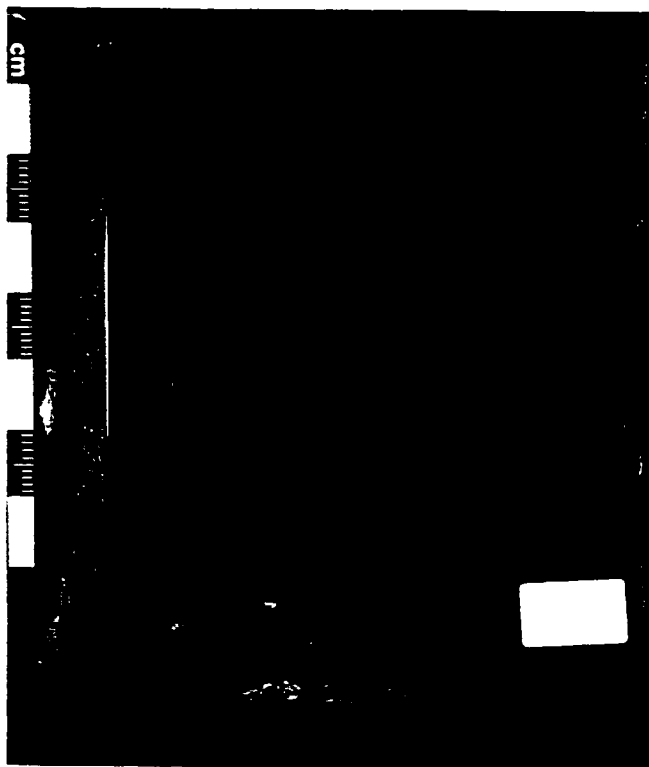
a) Core sample showing a transition from lithofacies F in the lower region, to lithofacies A in the upper part of the core sample. 7-20-59-18W5, 10490' (3197.35 m) Centimeter bar for scale; each white bar = 1 cm.

b) Core sample showing the combination of lithofacies C and F. This is an example of a calcite-rich, bioturbated, laminated mudstone interbedded with brachiopod floatstones. 2-9-54-12W5, 8391' (2557.6 m) Centimeter bar for scale; each white bar = 1 cm.

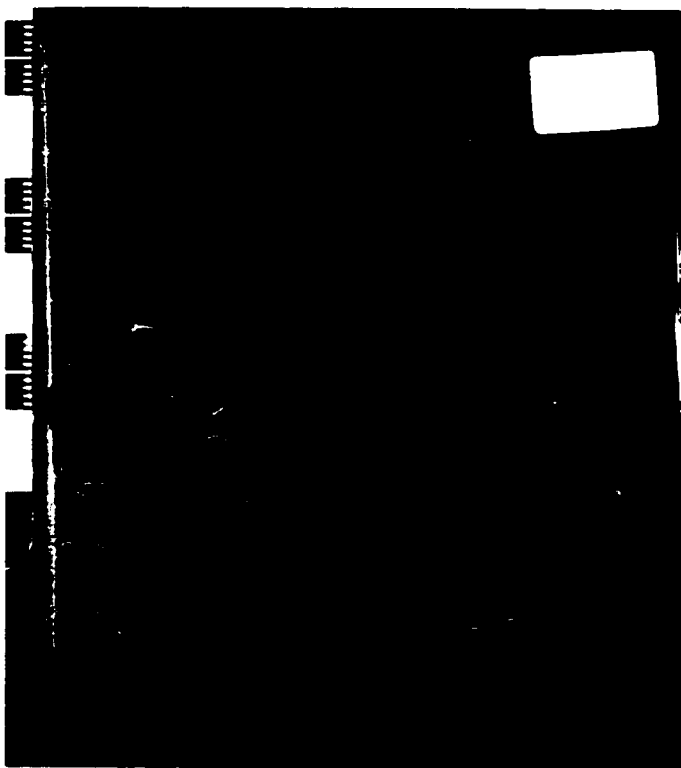
c) Photographs of thin sections showing combinations of lithofacies A and F. Thin section in Figure 2.11 c-1 has been half stained on the upper side with Alizarin Red-S and Figure 2.11 c-2 has been stained on the left half. All have been injected with a blue-stained epoxy. Dime for scale. Photographs were taken of the thin sections placed on a white piece of paper, illuminated by incident light, on a core photomicrograph stage.

c-1) Pyritized *Amphipora* floatstone to mudstone. 1-26-58-18W5, 11146' (3397.30 m).

c-2) Brachiopod floatstone to wackestone. Microfossils such as tentaculites and ostracods are common in this facies, however they are not evident at the scale which shows the floatstone classification of this facies. 10-22-70-18W5, 8542.5' (2603.75 m).

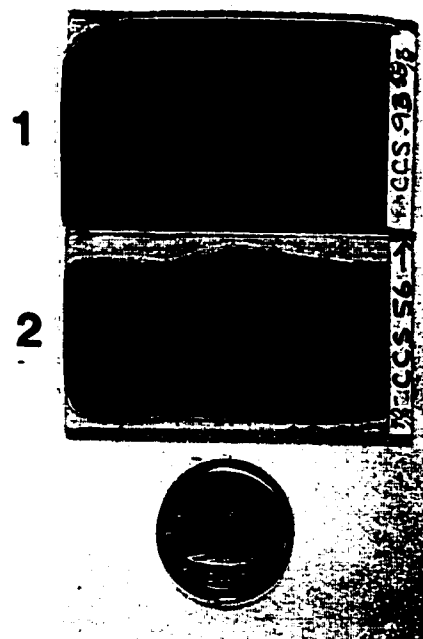


a



b

c



	Alkali-Feldspars			Talc	Illite	Chlorite	Muscovite	Calcite	Pyrite	Quartz	Dolomite	Ankerite	Anhydrite
	Albite?	Orthoclase?	Sandrine?										
CCS 87A								●	○	○			
CCS 149A								●	○	○			
CCS 22A								●	○	○			
CCS 73								●	○	○			
CCS 98								●	○	○			
CCS 358								●	○	○			
CCS 78				○	○	○	○	●	○	○		○	
CCS 66				○	○	○		●	○	○		○	
CCS 21							○	●	○	○		○	
CCS 28			○				○	●	○	○		○	
CCS 87B		○			○			●	○	○		○	
CCS 133 (1/2 SCAN)								●	○	○		○	
CCS 95			○					●	○	○			
CCS 36			○					●	○	○			
CCS 60						○	○	●	○	○		○	
CCS 25	○					○	○	●	○	○		○	
CCS 79		○				○	○	●	○	○		○	
CCS 27						○	○	●	○	○		○	
CCS 132						○	○	●	○	○		○	
CCS 53						○	○	●	○	○		○	
CCS 59						○	○	●	○	○		○	
CCS 35			○			○	○	●	○	○		○	
CCS 1					○		○	●	○	○		○	
CCS 38							○	●	○	○		○	
CCS 123								●	○	○		○	
CCS 10						○	○	●	○	○		○	
CCS 22B						○	○	○	○	○		○	
CCS 18 (1/2 SCAN)								○	○	○		○	
CCS 106B			○				○	○	○	○		○	
CCS 105			○			○	○	○	○	○		○	○
CCS 117			○			○	○	○	○	○		○	
CCS 152						○	○	○	○	○		○	
CCS 129			○			○	○	○	○	○		○	
CCS 19					○	○	○	○	○	○		○	
CCS 51						○	○	○	○	○		○	
CCS 89		○				○	○	○	○	○		○	
CCS 61							○	○	○	○		○	
CCS 46			○				○	○	○	○		○	
CCS 156A								○	○	○		○	
CCS 54					○	○		○	○	○		○	
CCS 119 (1/2 SCAN)						○		○	○	○		○	
CCS 20		○				○	○	○	○	○		○	
CCS 81			○				○	○	○	○		○	
CCS 11		○				○	○	○	○	○		○	
CCS 68						○	○	○	○	○		○	
CCS 98B							○	○	○	○		○	
CCS 148 (1/2 SCAN)								○	○	○		○	
CCS 48A			○			○	○	○	○	○		○	
CCS 47A			○				○	○	○	○		○	
CCS 43			○		○				○	○		○	
CCS 44					○				○	○		○	

XRD pattern counts	Estimated % based on carbonate dissolution
○ 0-1	≤10
○ >1-2	10-20
○ >2-3	21-30
○ >3-4	31-40
○ >4-5	41-50
○ >5-6	
○ >6-7	
○ >7-8	
○ >8-9	
○ >9-10	

Table 4.1: Tally of minerals identified in mineralogical facies Cq, CQp, QCP, and Qdp of Devonian aquitards using XRD patterns. XRD peak-height counts can be used to approximate the percentage of minerals present in the samples (left).

introduces a simplified mineralogy based on XRD. In Chapter 5, detailed descriptions of the mineralogy obtained by core and thin-section analyses will be used to explain the diagenetic history of the aquitards.

XRD analyses conducted on the Ireton and Duvernay Formations in east-central Alberta (McCrossan, 1957) identified the major minerals to be calcite, dolomite, illite, and fine quartz, along with minor amounts of pyrite and anhydrite. Later, Campbell and Oliver (1968) discovered the presence of chlorite in these Formations. McCrossan (1957) stated that the Ireton and Duvernay Formations in this area range in composition from 30 to 90 weight % calcium carbonate.

The present study of Woodbend and Winterburn aquitards in west-central Alberta reveals the presence of calcite, quartz, dolomite, ankerite, pyrite, and minor amounts of alkali feldspars (albite, orthoclase, and sanidine were identified), clay minerals (such as illite, chlorite, and talc), muscovite, and anhydrite (Table 4.1). Two major differences exist between the mineralogy of samples tested in west-central Alberta, of the present study, and that of studies in east-central Alberta (McCrossan, 1957; Campbell and Oliver, 1968). Firstly, ankerite has been identified in aquitards of the present study. Secondly, minor amounts of feldspars have been detected. It is recognized however, that difficulties exist in distinguishing feldspars from clay minerals using XRD when they occur in minor amounts (Table 4.1). In this study, shales, marls, and limestones (or marl-carbonates), ranging in carbonate contents between 9 and 76 weight % have been identified using whole-rock carbonate dissolution, which overlaps with that identified by McCrossan (1957).

In addition to the eight major lithofacies identified in the aquitards, four mineralogical facies were identified using XRD patterns and include facies QCp, Cqp, Cq, and Qdp (Table 4.1). The facies have been named using the first letter of each mineral which is abundant in them. For example, facies Cq contains major calcite (represented in the facies name by an upper case "C") and minor quartz represented by a lower case letter "q"). Each facies is gradational into the other facies. Three of the facies identified are representative of the whole-rock powder samples. Facies CQp contains major calcite, moderate quartz and minor

pyrite; facies QCp is mineralogically similar to facies CQp, but in this case, quartz is most abundant; and facies Qdp consists dominantly of quartz with minor dolomite and pyrite. "Facies Cq" is representative of the carbonate nodules, hardgrounds, and carbonate lenses and consists of major calcite with minor quartz. Although this is not a true facies, in that it does not represent whole-rock composition, it is important to distinguish it from the others.

4.3.2. Mineralogical Facies QCp

Twenty-three of the samples analyzed using XRD are classified in this category. In addition to the quartz, calcite, and pyrite that define this facies, about half of the samples also contain moderate to minor amounts of ankerite. A sheet silicate, muscovite and/or clay minerals (e.g. illite), are present in minor amounts as well (Table 4.1), the presence of illite is more probable and is further discussed in Chapter 5. Most of the samples are whole-rock powders, however, some samples have been taken from individual portions such as the matrix or organic-rich layers, or lenses. Samples analyzed are from the West Pembina area, the Pine Creek and Wild River Basins, the Obed field, the Simonette Reef, the Windfall (Lambert) Reef complex, east of the Sturgeon Lake Reef in the West Shale Basin, an area adjacent to the Peace River Arch-Leduc Fringing Reef, and from the Swan Hills Platform (Figure 4.13).

4.3.3. Mineralogical Facies CQp

Sixteen of the samples analyzed are classified in this category (Table 4.1). This mineralogical facies is defined by the presence of major calcite, quartz and minor pyrite, and may also contain minor to moderate amounts of ankerite. Also, a sheet silicate mineral (such as muscovite) is usually present in minor amounts (Table 4.1). Most specimens sampled are predominantly from whole-rock powders but one represents an organic-rich layer. Samples representing this facies are from the Pine Creek and the Wild River Basins, the Peace River Arch area, and also from the West Pembina area (Figure 4.13). The geographical distribution of this facies clearly overlaps with that of facies QCp. However, in the West Pembina area, fewer samples of this facies were identified

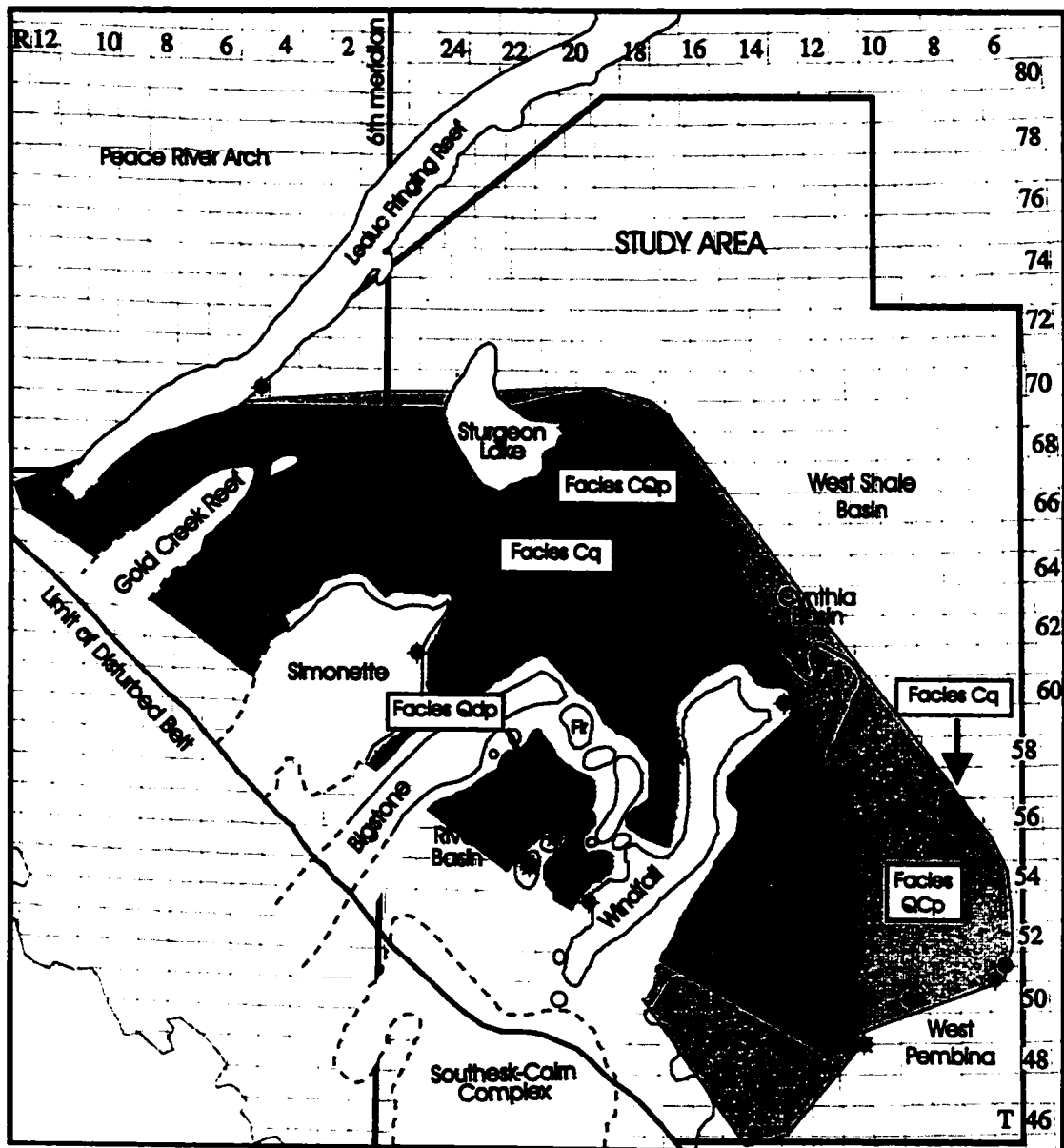


Figure 4.13: Distribution of mineralogical facies in the study area using XRD patterns of whole-rock powders, and individual components such as carbonate-rich horizons, lenses, or nodules within the aquitards. Mineralogical facies Qcp and Cqp are widespread in the study area, whereas facies Cq and Qdp are confined to smaller areas centralized in the Wild River and Pine Creek Basins. Mineralogical facies Qdp is confined to the Obed field (map is modified from Switzer et al., 1994).

compared to facies QCp. Facies CQp may be more concentrated in the Peace River Arch-Leduc Fringing Reef area.

4.3.4. "Mineralogical Facies Cq"

This mineralogical facies is represented by ten samples (Table 4.1). Most of which consist of carbonate or carbonate/chert hardgrounds, lenses, nodules, and layers within the whole rock. Three of the samples, however, are representative of whole-rocks.

Facies Cq, consists of major calcite with variable amounts of quartz. Minor amounts of pyrite are also usually present. In addition, a sheet silicate (such as muscovite), clay minerals (such as chlorite, illite, and talc), an alkali feldspar (identified as sanidine?), and ankerite have been detected (Table 4.1).

The majority of specimens from this group are from the Pine Creek and Wild River Basins and the Obed area. One sample is from the Swan Hills Platform region north of the Pine Creek Basin and Windfall Reef Complex. The geographic distribution of this facies, in contrast to the distribution of both QCp and CQp, is much smaller and is concentrated around the central part of the study area (Figure 4.13) with the exception of one sample from the West Pembina area. The central part of the study area is predominantly bounded by Leduc Reefs, and the large amount of carbonate within the samples is probably derived from these nearby reefs. The three whole-rock powder samples in this mineralogical facies were sampled from the Obed field, the Wild River Basin and the Swan Hills Platform north of the Pine Creek Basin.

4.3.5. Mineralogical Facies Qdp

Although only represented by two whole-rock samples, this mineralogical facies is different from the other facies in the absence of calcite, and presence of dolomite (Table 4.1). This could be similar to a finding in east-central Alberta, in which McCrossan (1957) identified dolomite (rather than calcite) as the predominant carbonate mineral in the upper part of the Ireton Member (now defined as a Formation).

XRD reveals major quartz, with minor dolomite and pyrite. Illite and an alkali feldspar (identified as sanidine?) are also present in minor amounts. Both samples are from the tip of the Obed field in the Wild River Basin (Figure 4.13).

4.4. Correlations of Lithological and Mineralogical Facies

4.4.1. Introduction

In the following sections, correlations of lithological and mineralogical facies with stratigraphic units and geographic areas will be presented. Due to the regional scope of this study, encompassing an area of approximately 38,000 km² and several stratigraphic units, as well as limited core control, the subsequent sections will present rather general conclusions regarding facies distribution within the stratigraphic units, as defined in Chapter 3, and geographic locations.

4.4.2. Majeau Lake Formation

This stratigraphic interval was studied in four cores from the following (paleo-)geographic areas: the West Shale Basin northeast of Sturgeon Lake, Pine Creek Basin, and just north of Pine Creek Basin on the edge of the Swan Hills Platform (Figure 1.2). Lithofacies A and AE are prominent in this stratigraphic unit. They occur as a thick interval of a single lithofacies, or of the two interbedded with each other (Figures 4.14 and 4.15).

The Majeau Lake aquitards are usually less than 20 m in thickness (see Chapter 3 and Appendix 2), and form the beginning stages of the major regression of sea level in the basin when major clastic input occurred for the first time (Switzer et al., 1994). They are associated with carbonate aquifers above (Low Leduc Platform), designated as reef facies (Figure 4.14), and below (the Swan Hills Formation of the Beaverhill Lake Group) (Figure 4.15). A transition from lithofacies GE to an interval of combined lithofacies F and A occurs at the base of the Majeau Lake Formation (Figure 4.15) where the lower carbonate reef facies (below the core analyzed) grades into the more basinal facies of the Majeau Lake Formation. In another well (not illustrated), transition from the

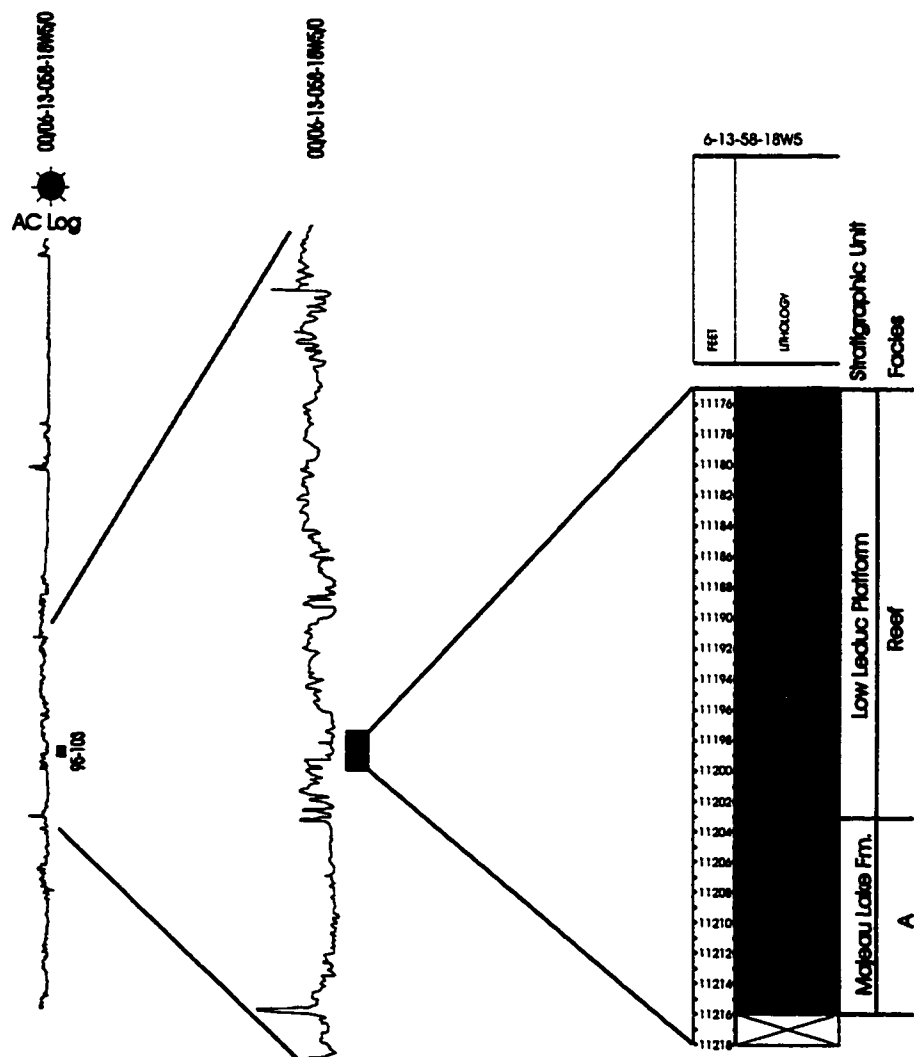


Figure 4.14: Interval of core investigated of the Majeau Lake Formation and Low Leduc Platform above and associated sonic (acoustic) log. Lithofacies A is prominent in this aquitard.

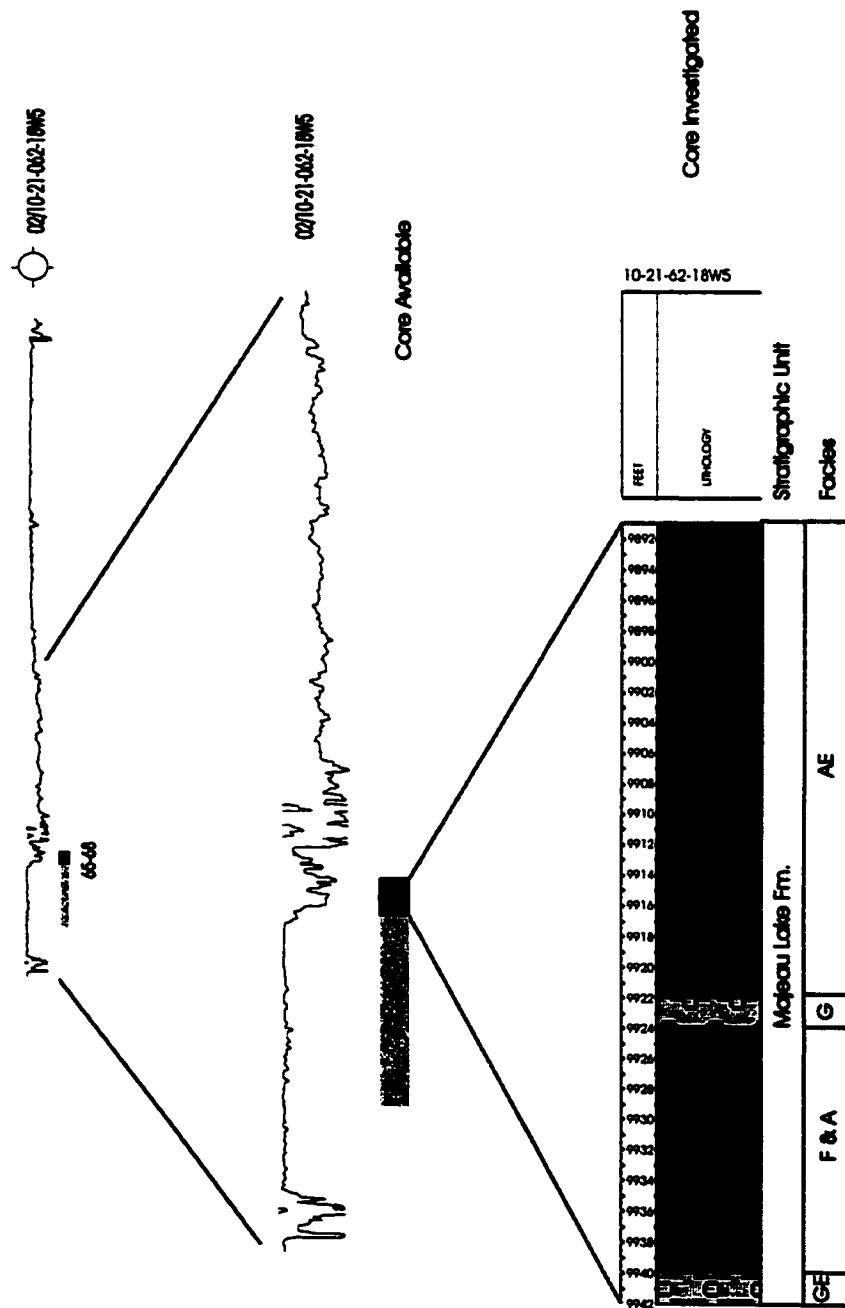


Figure 4.15: The interval of core investigated, in black, and associated gamma log of the Majeau Lake aquitard. Interfingering of lithofacies is prominent in the base which is overlain by a more massive, thick interval of lithofacies AE.

Swan Hills Reef interval into the Majeau Lake Formation occurs with interfingering of reef facies and lithofacies GE. The transition from the Majeau Lake Formation into the Low Leduc Platform appears to be sharper than the transition from the Swan Hills Formation to the Majeau Lake Formation (compare Figures 4.14 and 4.15).

With respect to mineralogical facies, nine samples from the Majeau Lake aquitards are equally represented by facies QCp, CQp, and Cq. One of the three Cq samples tested was a whole-rock powder, while the other two were carbonate (or carbonate-chert) nodules. Seven samples from the Majeau Lake Formation, representing lithofacies A were analyzed for carbonate content and ranged from 9 to 55 weight % with just over half of the samples being marls (between 35 and 65 weight % carbonate) (Figure 4.16).

4.4.3. Duvernay Formation

This stratigraphic interval was studied in six cores from the following (paleo-)geographic areas: three are located in the Pine Creek Basin; the others are in the Peace River Arch area, the Sturgeon Lake Reef, and on the edge or just to the northeast of the Windfall Reef complex (Figure 1.2). In the Duvernay Formation, lithofacies and transitions between facies are similar to those of the Majeau Lake Formation.

Lithofacies A is the major lithofacies present in the Duvernay Formation, however moderate amounts of lithofacies AE are also present. These two lithofacies occur as thick intervals (greater than 10' or 3 m) and can be found in association with one another (Figures 4.17 and 4.18). Lithofacies F occurs as thin bands associated with lithofacies A (e.g., in Figure 4.17). Moderate amounts of lithofacies G and minor amounts of GE are present.

The transition from a carbonate reef environment, e.g., of the Swan Hills Formation, upwards into the basinal Duvernay Formation, near-reef lithofacies occur. An example is lithofacies G (Figure 4.17). A similar example can be seen where an approximately 10' (3 m) thick interval of lithofacies A, present at the base of the Duvernay, is followed by an interval of interbedded carbonate reef

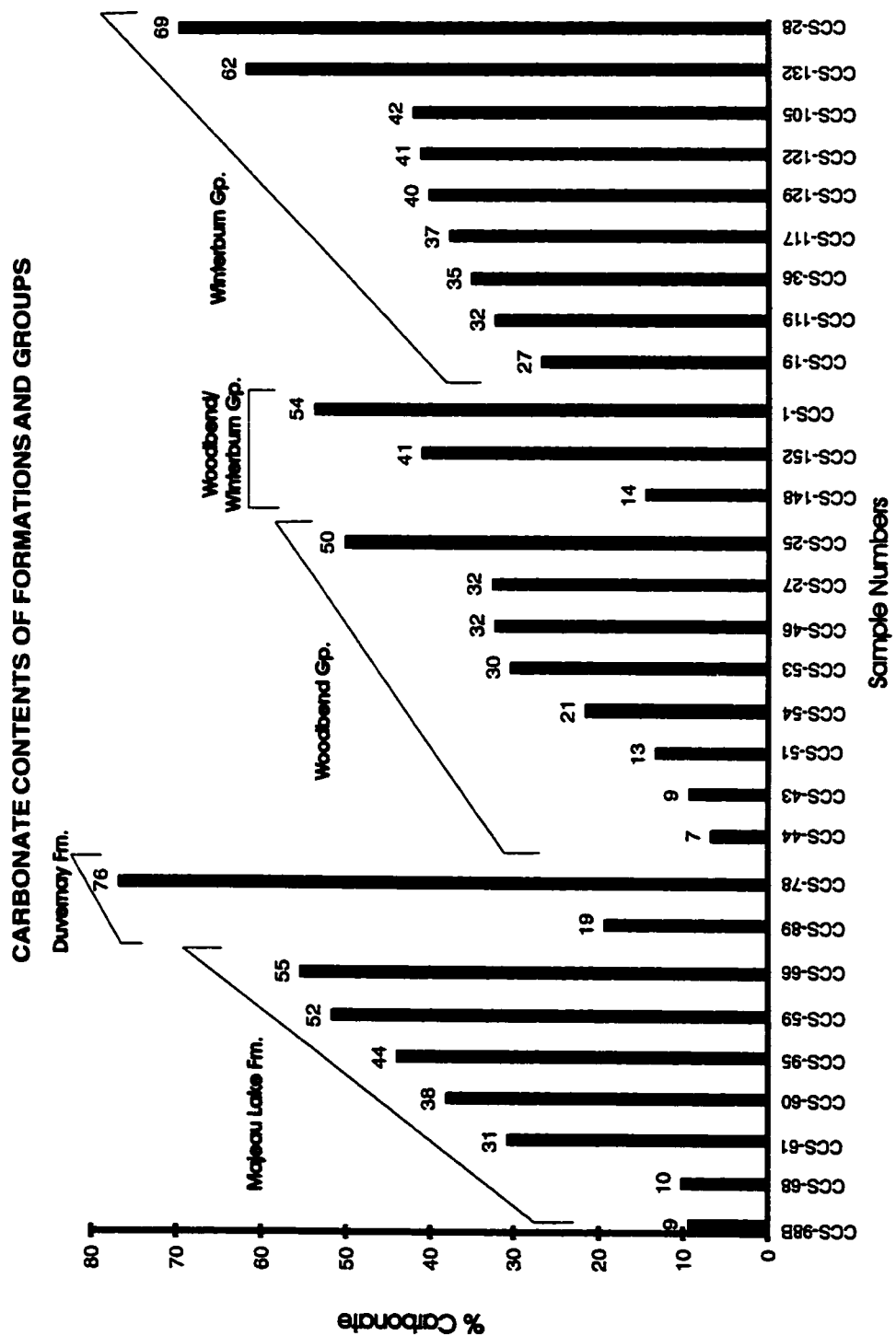


Figure 4.16: A graph showing the carbonate percentages of whole-rock samples of various Groups and Formations. The same data are plotted here as in Figure 4.4, however, this time the data are plotted with respect to stratigraphic context. Note the variable carbonate contents within each Formation and Group.

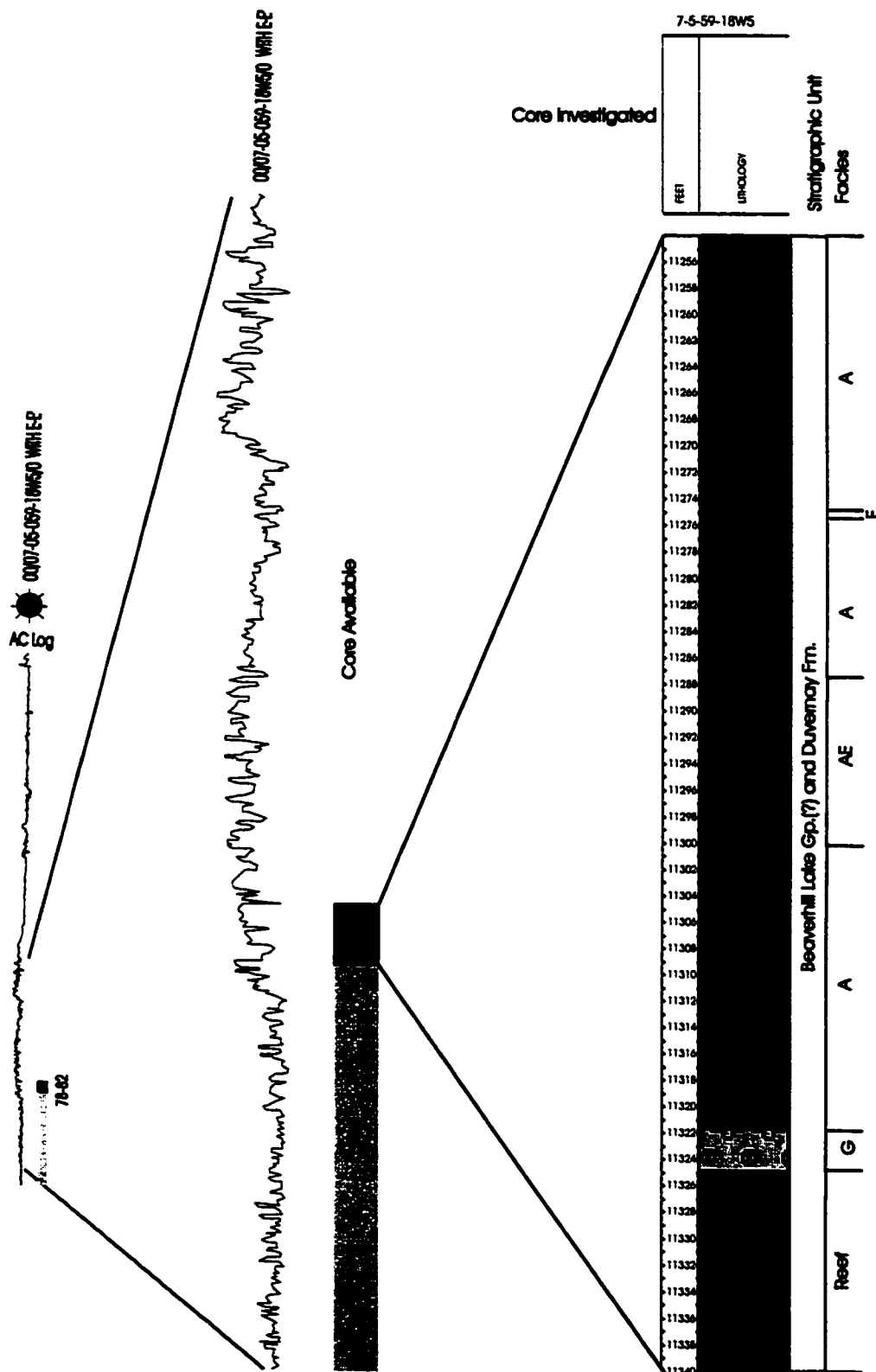


Figure 4.17: Interval of core investigated, in black, of the Duvernay Fm. and possibly the Beaverhill Lake Gp., and its associated sonic log. Lithofacies A and AE are present as prominent, thick packages. The base of the Formation is interfingered with reef facies. Lithofacies G is present in the transition from this interval into the more basinal facies.

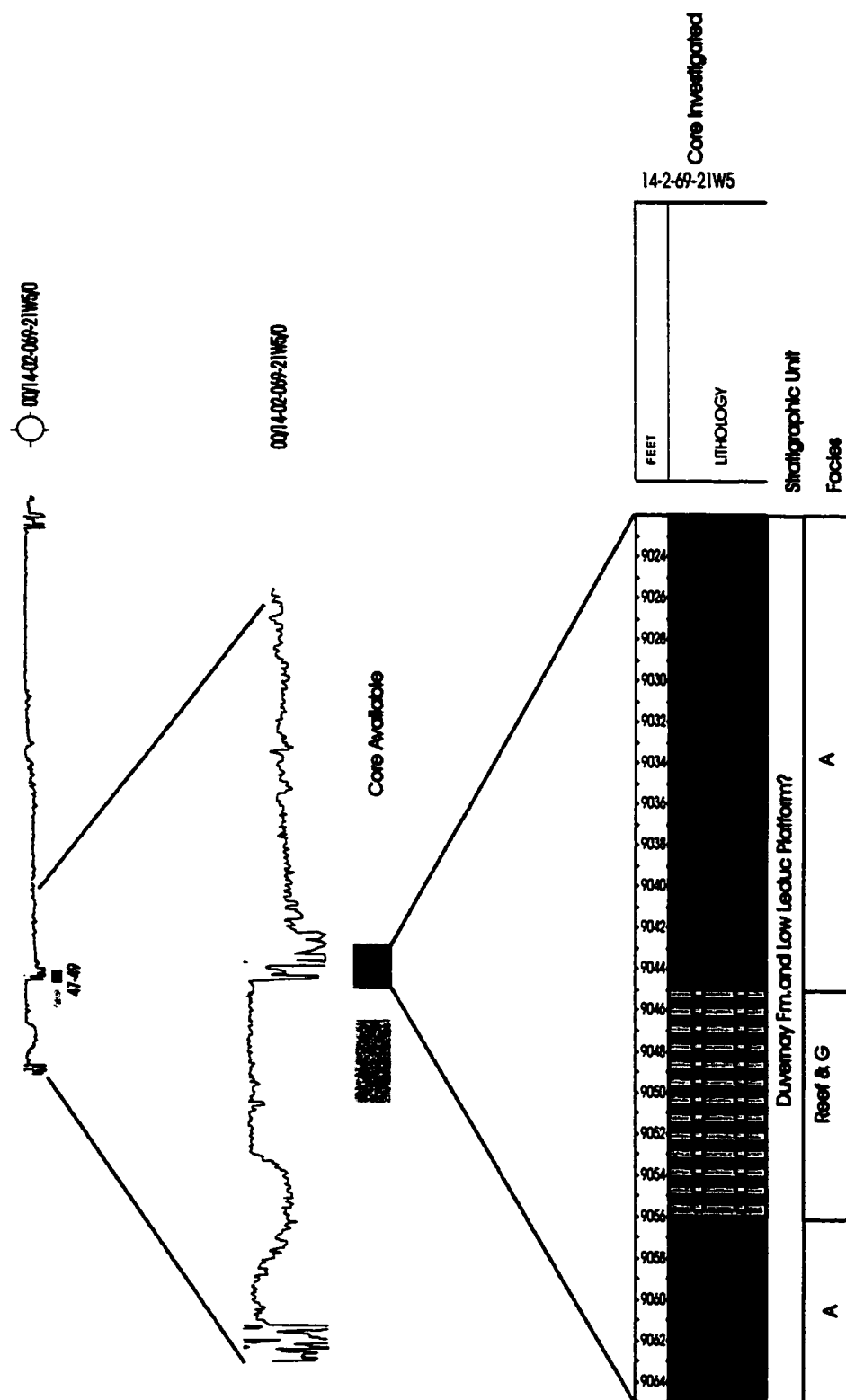


Figure 4.18: Interval of core investigated, in black, of the Duvernay Formation and interfingered Low Leduc Platform, and associated gamma log. Thick, massive intervals of Lithofacies A is prominent at the base and top of the core. The middle of the core is transitional between reef facies and lithofacies G.

facies and lithofacies G, which is subsequently followed by a thick (28 m) interval of lithofacies A (Figure 4.18). The presence of these interbeds again marks the transition from reef to basinal facies.

With respect to mineralogical facies, ten samples from Duvernay aquitards were tested for their mineralogical content. Five samples consist of mineralogical facies QCp, three of CQp, and two of Cq (one of which is a whole-rock powder). Two samples from the Duvernay Formation, representing lithofacies A and GE, produced carbonate contents of 19 and 76 weight % respectively (Figure 4.16).

4.4.4. Woodbend Group

In some cases, such as in basinal successions without intervening carbonate aquifers, the boundary between the Majeau Lake, Ireton and Duvernay Formations is difficult to locate (refer to Chapter 3 and Appendix 2). In such circumstances, the Woodbend Group has been left undivided. This occurred in four cores examined from the following locations: the Wild River Basin, the Obed field, and on the southwest limb of the Windfall Reef complex (Figure 1.2). The undivided Woodbend Group aquitard mainly consists of thick, (20-30' or 6-9 m) continuous intervals of lithofacies A (Figures 4.19 and 4.20). Near the base of one well studied, during the transition from carbonate reef facies of the underlying Leduc Formation (?) into the undivided Woodbend Group aquitard (Figure 4.20), lithofacies A and AE are interbedded with lithofacies GE (Figure 4.20) and minor reef facies. This interbedding is similar to that described for the transitions between carbonate reef facies and the subdivided Majeau Lake and Duvernay Formations. This core (Figure 4.20) is likely an aquitard, although in Chapter 3 it was not defined as such (see well location 15-23-53-21W5 in cross sections B-B' and D-D', Figures 3.4 and 3.8 respectively).

In one core of the undivided Woodbend Group, intervals of reef facies and basinal lithofacies A, both approximately 5-10' (1.5-3 m) in thickness, are present (Figure 4.21). In this core, lithofacies G, GE, and F are absent and the transition

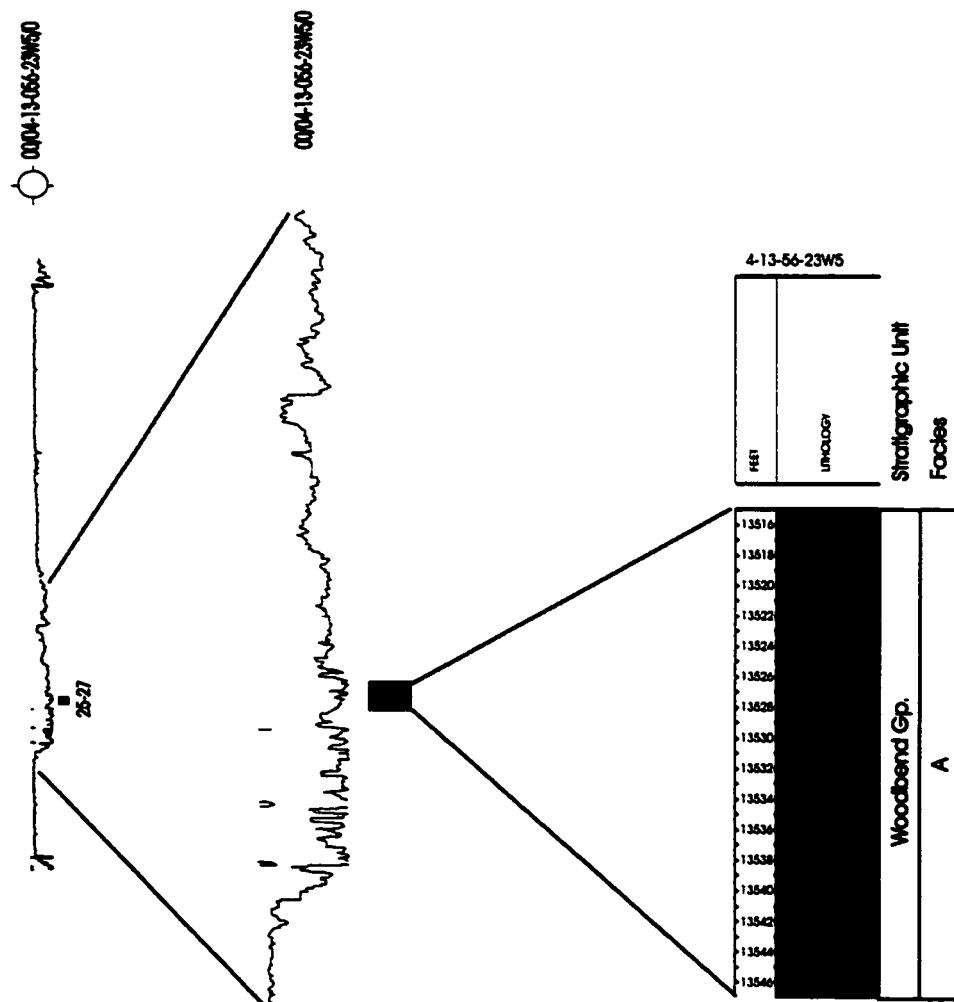


Figure 4.19: Interval of core investigated of the Woodbend Group, and associated gamma log. Lithofacies A dominates this core.

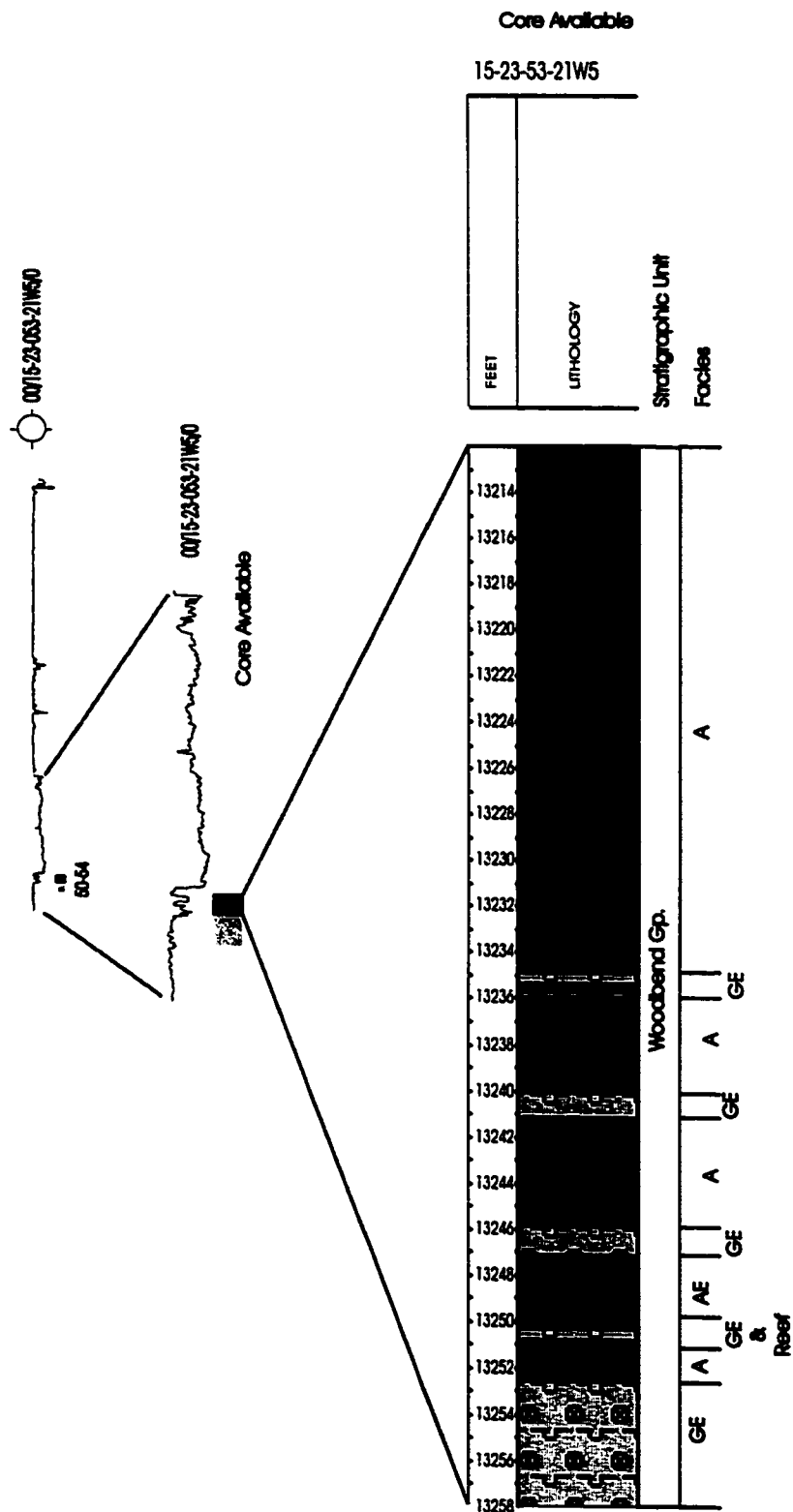


Figure 4.20: Interval of core investigated, in black, of the Woodbend Group, and associated gamma log. Lithofacies A is prominent in thick packages. Interfingering of thin near-reef and more basinal facies mostly occurs at the base of the core.

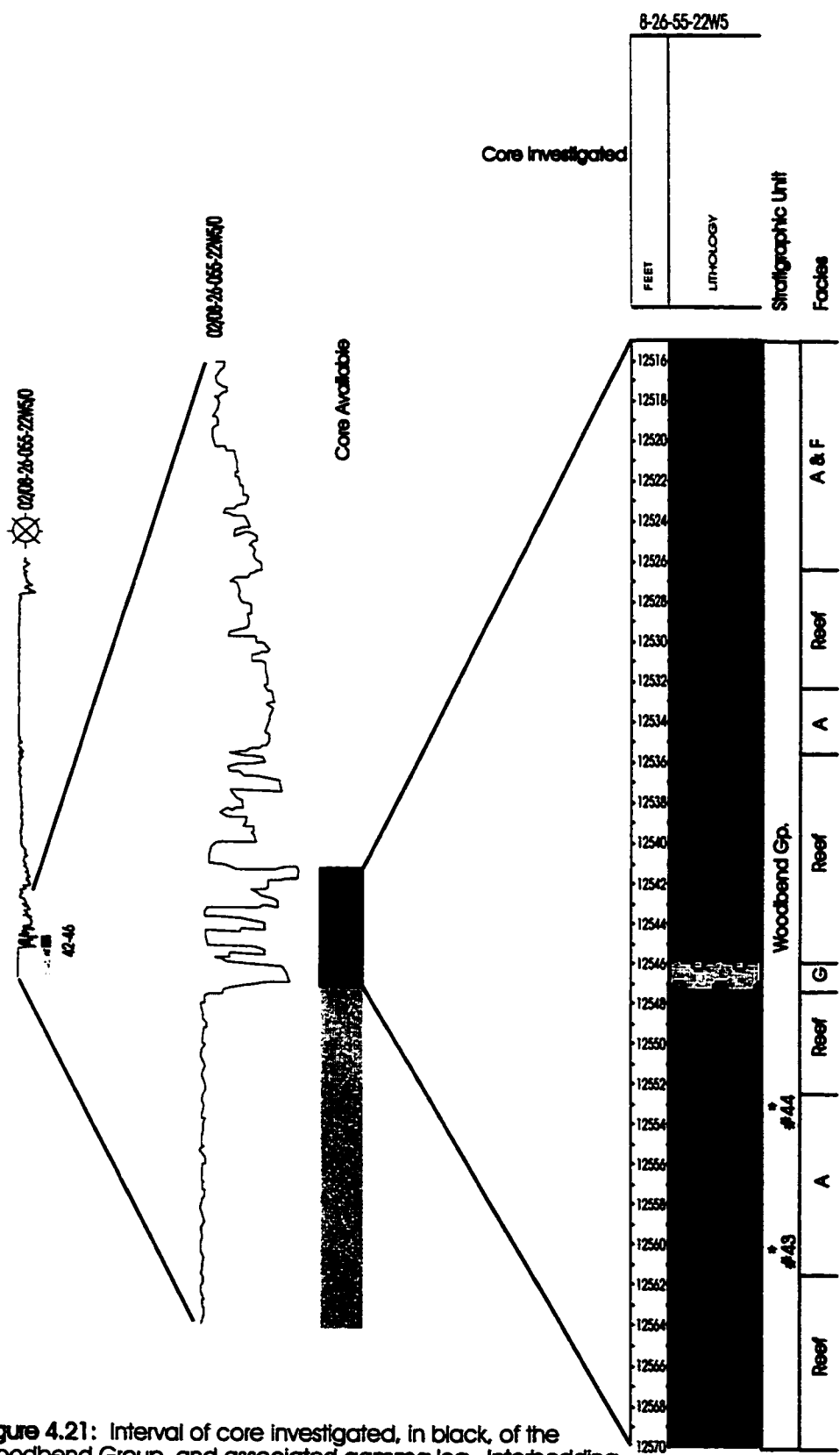


Figure 4.21: Interval of core investigated, in black, of the Woodbend Group, and associated gamma log. Interbedding of reef facies and basinal facies is common in this core. Core samples #43 and #44 are discussed in the text.

between basinal and reef facies is sharp, in contrast to the gradational transitions described above. Interfingering of lithofacies A and F occur at the top of this core.

With respect to mineralogical facies, the undivided Woodbend Group is represented primarily by mineralogical facies QCp, but moderate amounts of CQp and minor amounts of Cq (represented by calcite-rich lenses) are also present, as are the only two samples of mineralogical facies Qdp identified in this study. The two samples consisting of mineralogical facies Qdp are identified in Figure 4.21 (as numbers 43 and 44). Eight samples from the undivided Woodbend Group, all representing lithofacies A (Figure 4.16), range in carbonate contents from 7 to 50 weight %. One of the samples tested is a marl, but the remainder are shales.

4.4.5. Ireton Formation

In one core, from the West Pembina area, the uppermost part of the Ireton Formation could be distinguished from the undivided Woodbend Group. Interfingering of lithofacies F and A occurs in a thick package throughout most of the aquitard interval. It is overlain by an interval of lithofacies F (Figure 4.22). Two thin, interfingering intervals of lithofacies G and F are located in the core.

4.4.6. Woodbend/Winterburn Group

In some cases, using well log data, it is difficult to distinguish the boundary between the Winterburn and Woodbend Groups, such as in basinal sections where the Nisku Formation is absent (refer to Chapter 3 and Appendix 2). This happened in cores investigated from the Peace River Arch-Leduc Fringing Reef area and in the West Pembina area (Figure 1.2). These aquitards consist predominantly of thick (10-30' or 3-9 m) packages of lithofacies A and C, or interbedded lithofacies A and C, or B and C. Intervals of lithofacies AE and AD overlie the more basinal C and A lithofacies (Figure 4.23). A thick interval of lithofacies A and C is overlain by a thick package of combined lithofacies A and F, followed by a thin increment of lithofacies GE (Figure 4.24). This sequence of lithofacies defines the transition into a carbonate reef facies above. Lithofacies

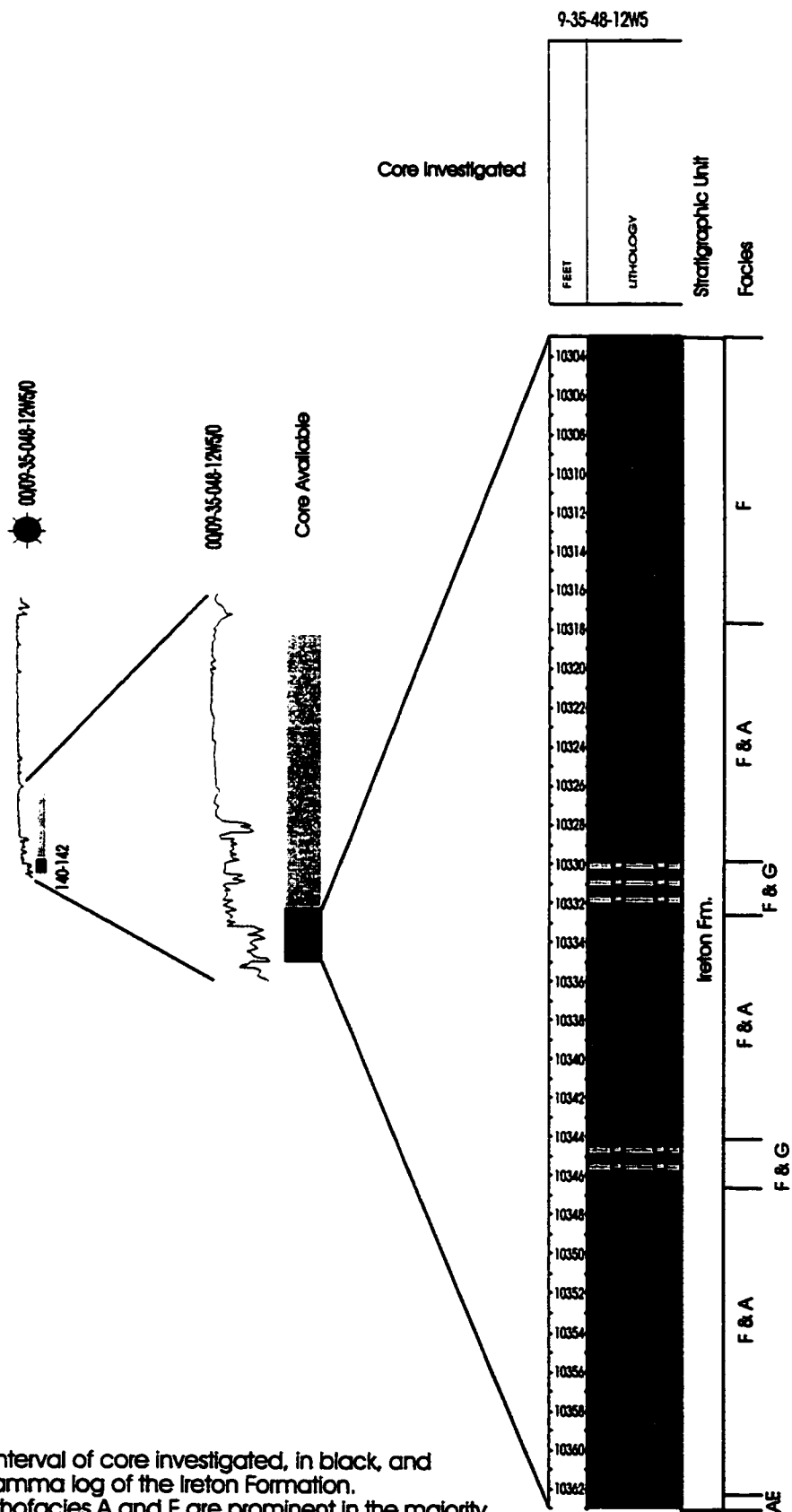


Figure 4.22: Interval of core investigated, in black, and associated gamma log of the Ireton Formation. Interbeds of lithofacies A and F are prominent in the majority of the core. The core is typified by near-reef facies.

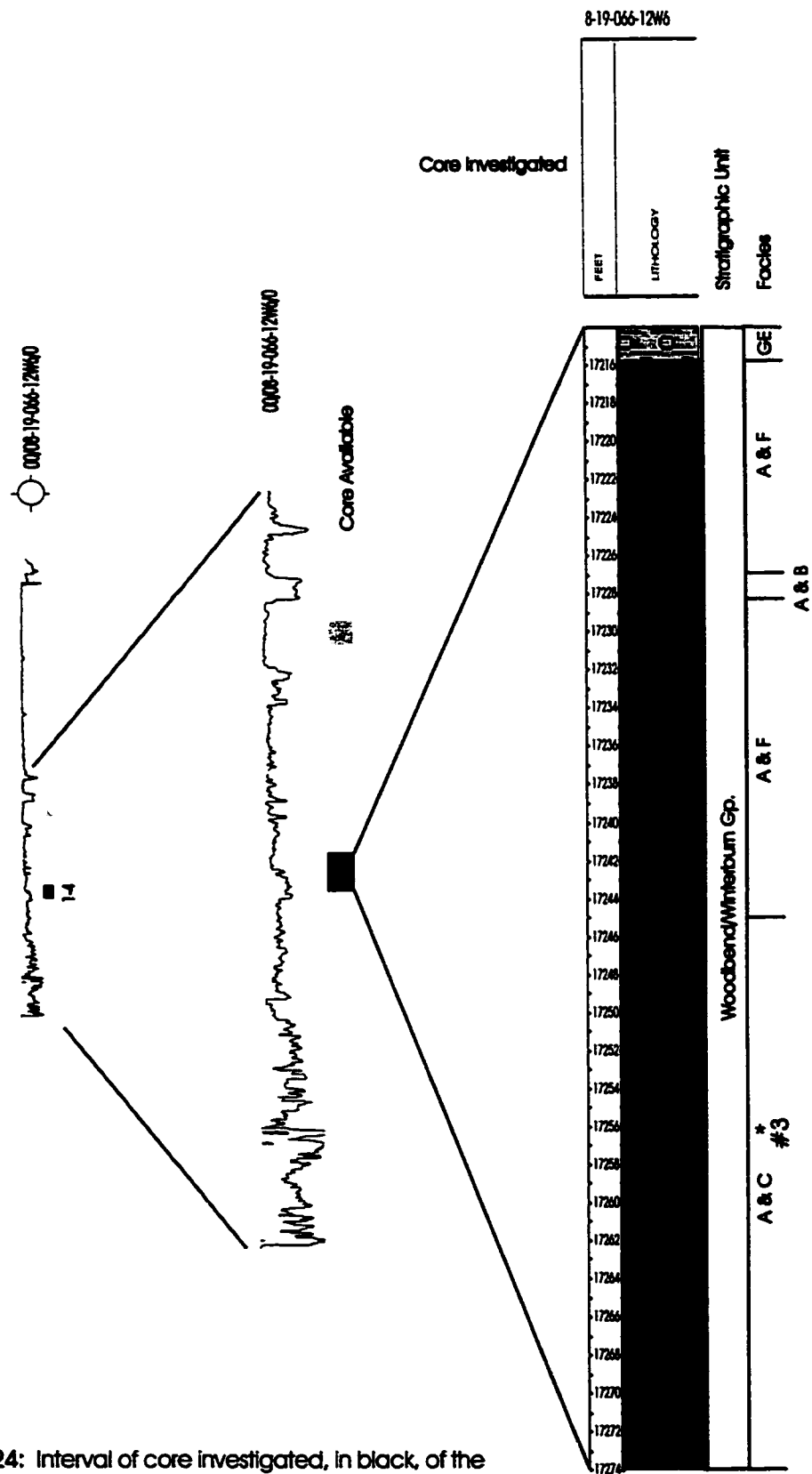


Figure 4.24: Interval of core investigated, in black, of the Woodbend/Winterburn Group, and associated gamma log. Interbedded intervals of lithofacies A and C and lithofacies A and F dominate the core. Core sample # 3 is discussed in the text.

C, B, and AD were not previously identified in core from the Majeau Lake, Duvernay, and Ireton Formations, or from the undivided Woodbend Group. They are most likely part of the Winterburn Group.

With respect to mineralogical facies, four samples from the undivided Woodbend/Winterburn Group were tested for their mineralogical content. Two samples from the Peace River Arch-Leduc Fringing Reef area represent mineralogical facies CQp, and two samples from the West Pembina area represent facies QCp. Three samples from the undivided Woodbend/Winterburn Group, two representing lithofacies A, and one lithofacies AD, ranged in carbonate contents from 14 and 54 weight %; one was a shale and the other two were marls (Figure 4.16).

4.4.7. Winterburn Group

Ten of twenty-eight cores analyzed in this study are from the Winterburn Group. These cores are from the following (paleo-)geographic areas: the West Pembina area, the West Shale Basin north of the Pine Creek Basin, Simonette Reef, and the Obed field (Figure 1.2).

Several lithofacies are present within the Winterburn Group aquitards. Common facies include F, AD, B, C, and A; minor facies include AE, G, and GE. Relatively thin intervals of lithofacies F combined with A, B, or G are also present, as are combinations of lithofacies B and C.

Aquitard A (equivalent to the Lower Lobstick or Bigoray Member) within the Winterburn Group is usually dominated by lithofacies F (Figure 4.25), but interfingers with intervals of lithofacies AD (Figure 4.26). Aquitard B (equivalent to the Cynthia Member) generally tends to be dominated by lithofacies C and AD (Figure 4.27), although may interfinger with lithofacies F (Figure 4.28). Where thin, aquitard B is dominated by slightly more basinal facies, B and AD. Where thick, it is dominated at the base by the same lithofacies (B and AD), which are overlain by more basinal lithofacies B and C. In the West Pembina area, in locations where aquitards A and B merge, the lower part of the aquitard (most

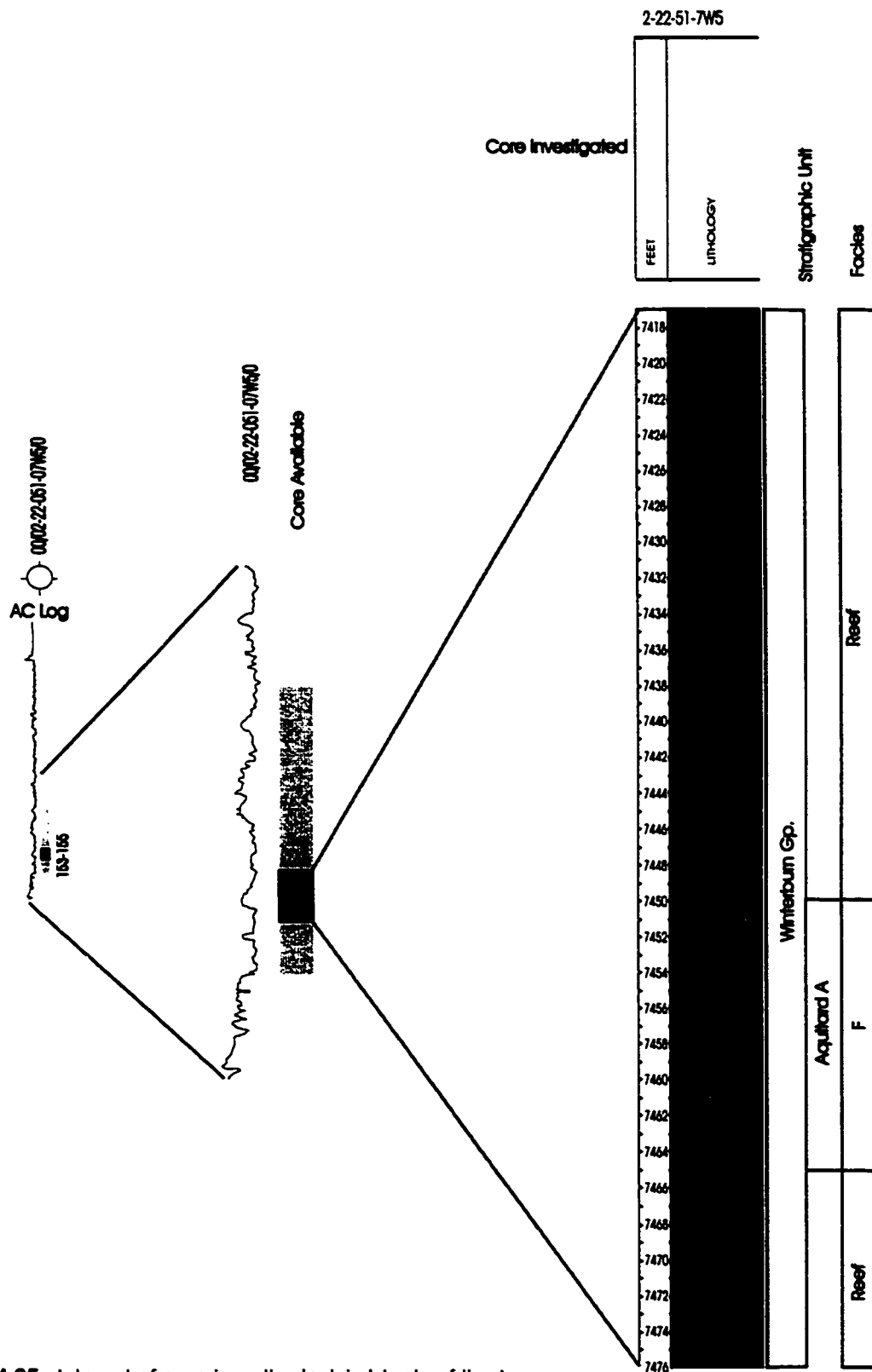


Figure 4.25: Interval of core investigated, in black, of the Lower Winterburn Group. and associated sonic log. Aquifard A in the lower half of this core is composed entirely of lithofacies F.

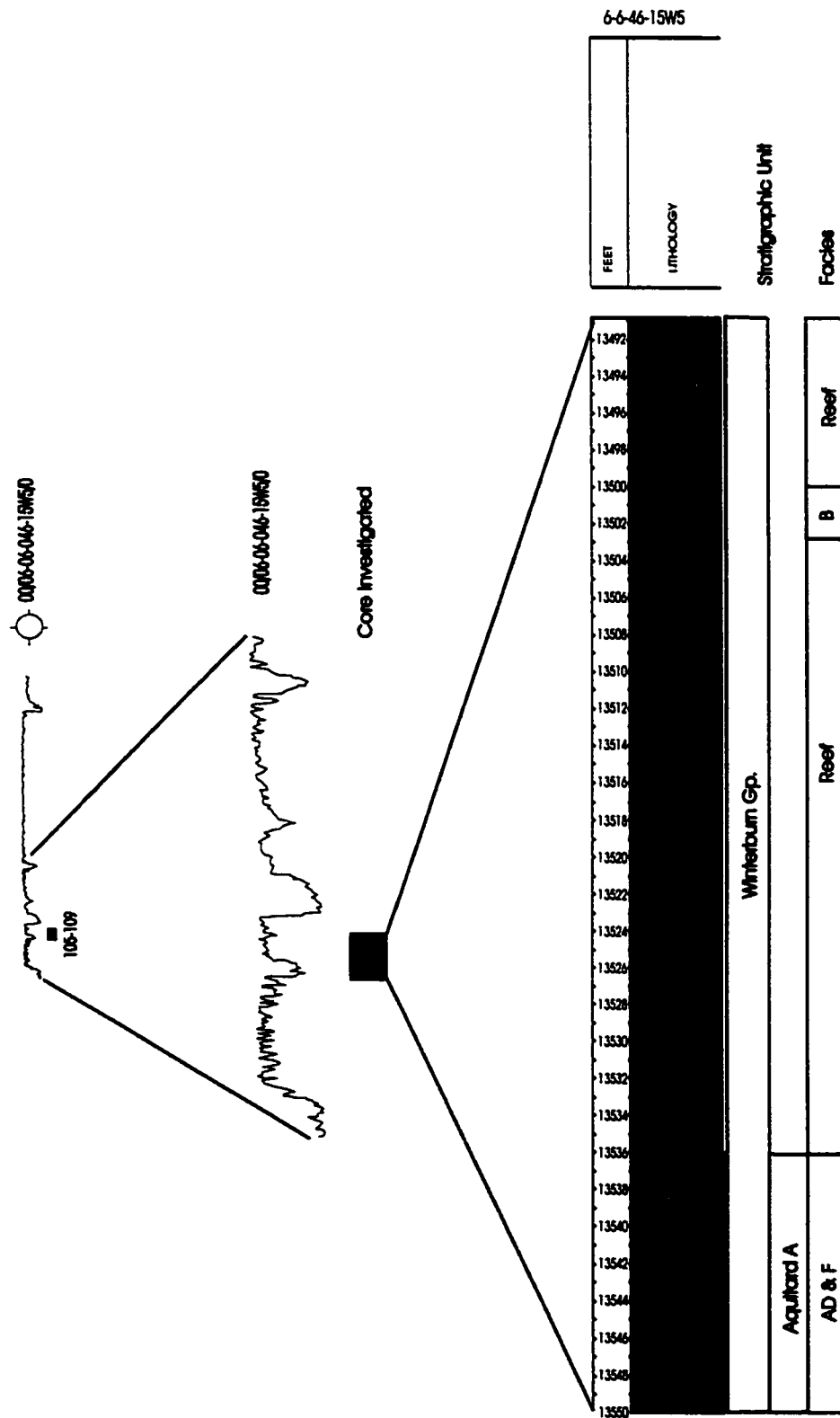
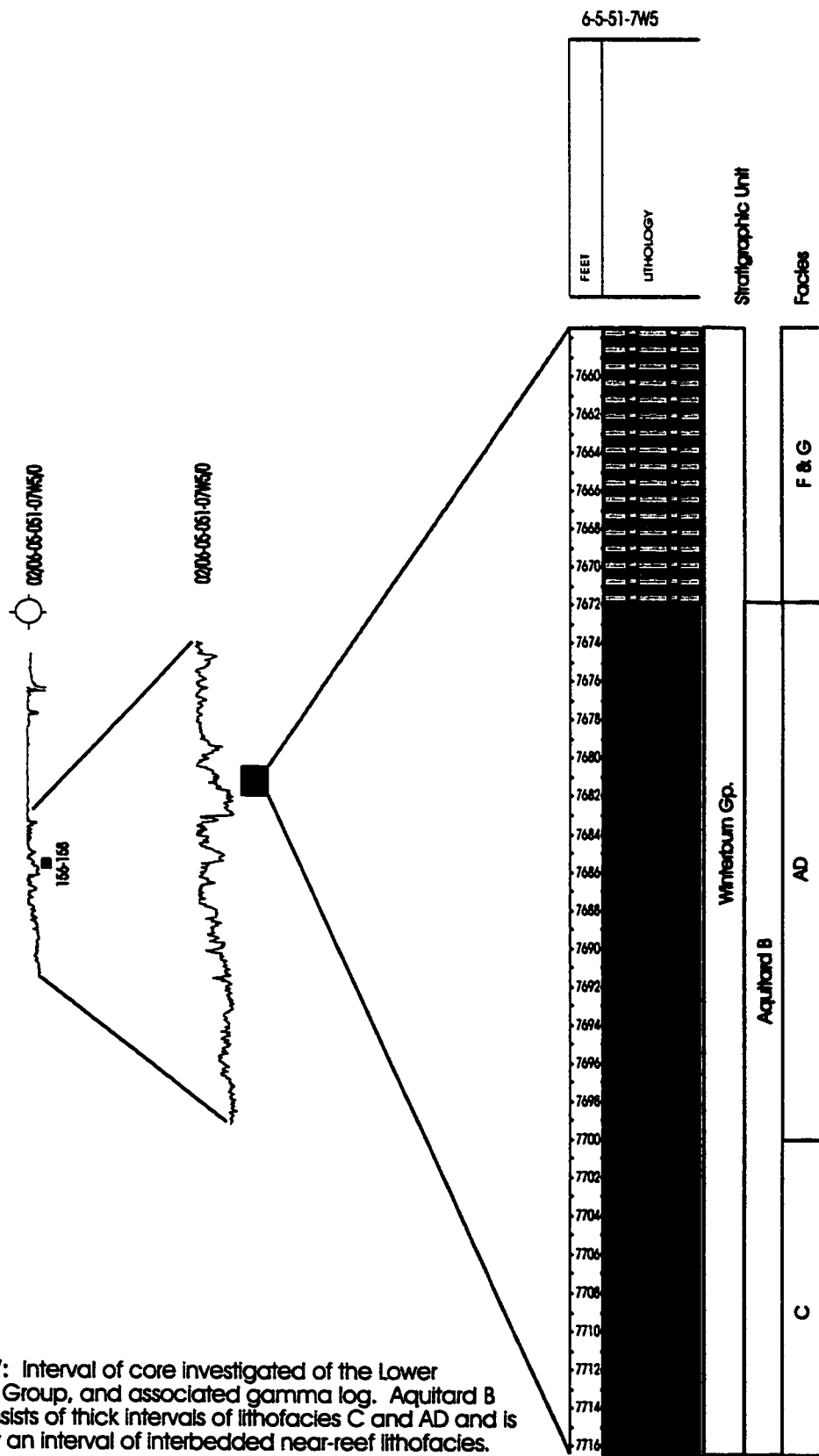


Figure 4.26: Interval of core investigated of the Lower Winterburn Group and associated gamma log. Aquitard A consists of interbedded lithofacies AD and F.

Figure 4.27: Interval of core investigated of the Lower Winterburn Group, and associated gamma log. Aquitard B mostly consists of thick intervals of lithofacies C and AD and is overlain by an interval of interbedded near-reef lithofacies.



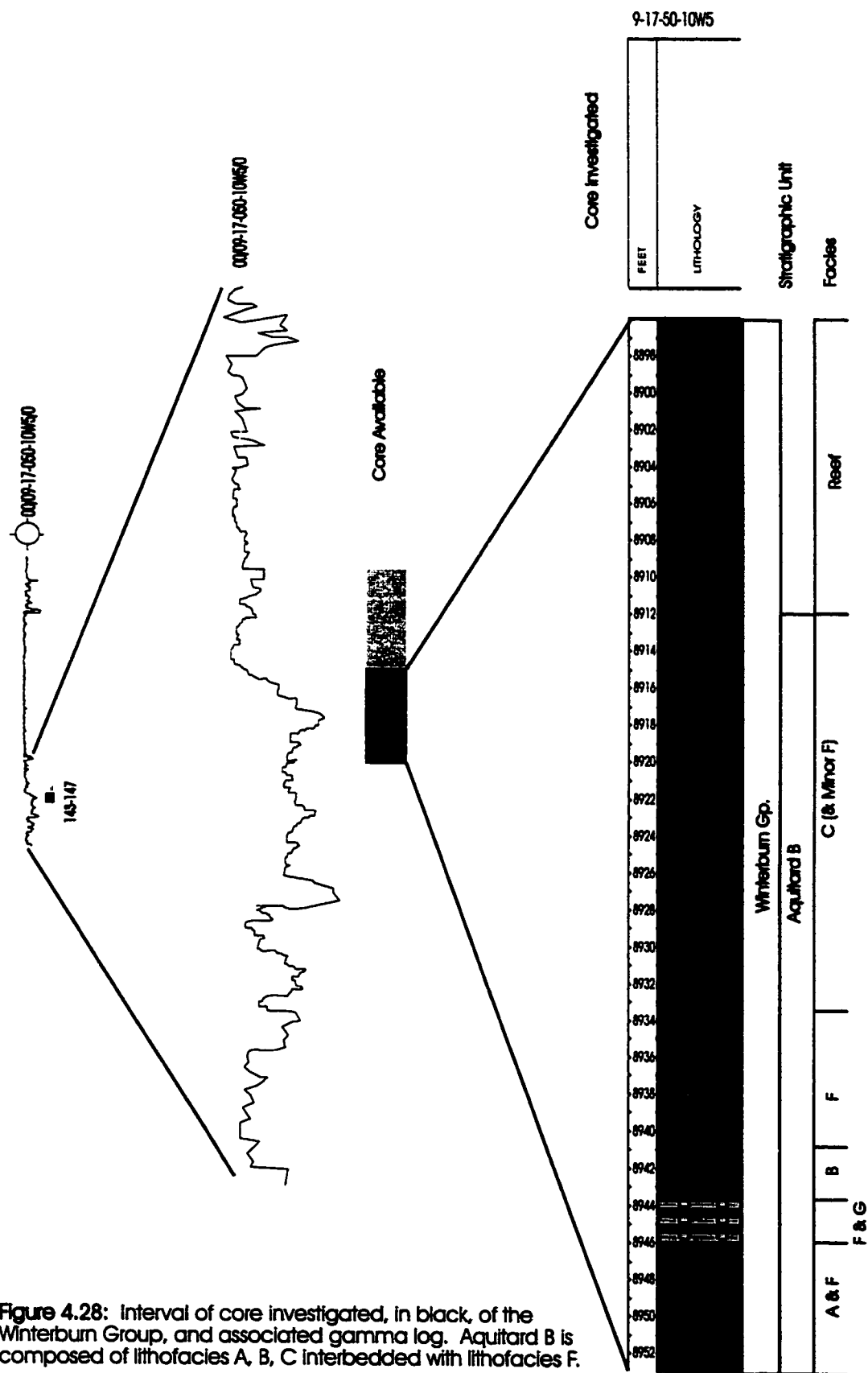


Figure 4.28: Interval of core investigated, in black, of the Winterburn Group, and associated gamma log. Aquitard B is composed of lithofacies A, B, C interbedded with lithofacies F.

likely equivalent to aquitard A) is dominated by lithofacies B and C, however, minor occurrences of lithofacies F are present near the base.

In one well, close to the disturbed belt, in the Simonette Reef, it appears that aquitard B is dominated by lithofacies A (Figure 4.29). In another well in the deep part of the basin, in the Obed field area, it appears that aquitard C similarly consists of a basinal facies, lithofacies A.

In summary; aquitard A is dominated by lithofacies F, whereas thin, overlying intervals of aquitard B are dominated by basinal lithofacies C and AD, or where thin, B and AD. Where thick, these same lithofacies are overlain by more basinal lithofacies B and C. From the core analyzed, a general conclusion can be drawn that up section, within Winterburn Group aquitards A and B, a transition from lithofacies F (basinal to near-reef?) to basinal lithofacies (e.g. AD, B, and C) occurs. It is interpreted that towards the limit of the disturbed belt, aquitard B becomes more basinal (lithofacies A becomes prominent).

With respect to mineralogical facies, sixteen samples from the Winterburn Group aquitards were tested for their mineralogical content. Eight of these samples represent mineralogical facies QCp, five represent facies CQp, and three represent facies Cq (one of which is a whole-rock powder). The samples have been taken from the West Pembina area, Obed field, and Simonette Reef. Nine samples from the Winterburn Group aquitards range in carbonate contents between 27 to 69 weight % with all the samples but two being marls (35 to 65 weight % carbonate) (Figure 4.16).

4.5. Synopsis and Significance

4.5.1. Lithofacies Summary

Table 4.2 summarizes the eight major lithofacies identified in the aquitards studied and their environments of deposition. Lithofacies F is often found in combination with the other lithofacies identified, such as A, B, and C, and also near-reef facies G and GE and a possible depositional environment for it is ambiguous. Rather it is the facies with which lithofacies F is associated that may be useful in indicating the depositional environment for the facies. The

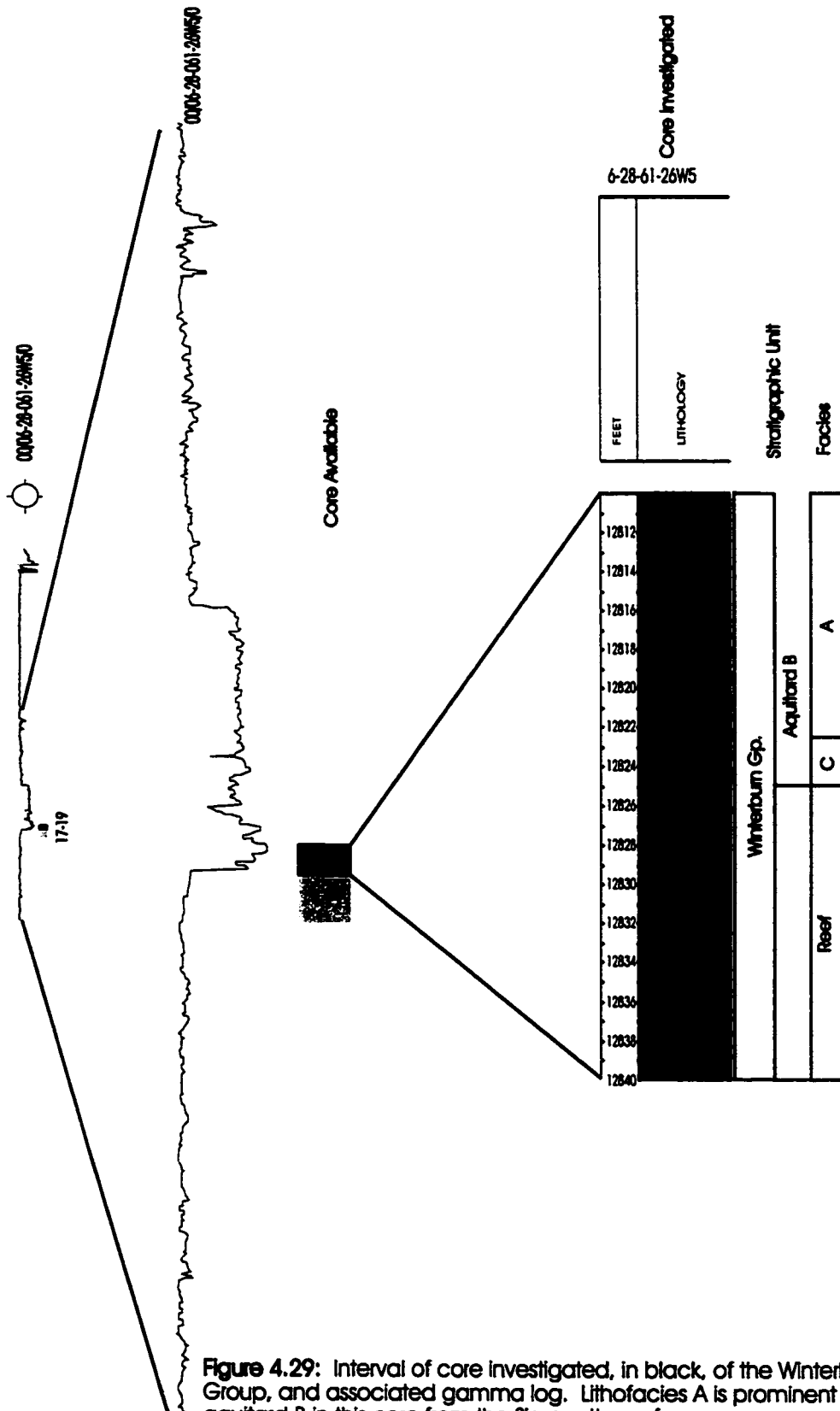


Figure 4.29: Interval of core investigated, in black, of the Winterburn Group, and associated gamma log. Lithofacies A is prominent in aquitard B in this core from the Simonette reef area.

depositional environments for the Majeau Lake, Duvernay and Ireton Formations and the undivided Woodbend Group can range from basinal, foreslope, to near-reef. In the Winterburn Group, depositional environments range from basinal, to deep- to shallow-ramp (near-reef).


<i>Lithofacies</i>	<i>General Description</i>	<i>Depositional Environment</i>
A	Massive to millimetre, planar-laminated mudstones and wackestones.	Basinal  Near-Reef
B	Fissile Mudstones.	
AD	Faintly mottled mudstones and wackestones.	
AE	Nodular mudstones.	
C	Bioturbated and/or carbonate laminated mudstones.	
G	Intraclastic packstones to wackestones.	
GE	Nodular intraclastic wackestones to mudstones.	
F	Brachiopod floatstones may occur in combination with all the above lithofacies.	Basinal to Near-Reef?

Table 4.2: General summary of major lithofacies identified in the Woodbend and Winterburn Group aquitards in this study.

4.5.2. Stratigraphic Correlations

The following section summarizes correlations between lithofacies and stratigraphic intervals.

- *Majeau Lake and Duvernay Formations*

These two Formations are dominated by relatively thick intervals of lithofacies A and AE. Thinner intervals of lithofacies G and GE are present during the gradual transition from the Swan Hills Formation or into Low Leduc Platform reef facies.

- *Woodbend Group*

In the undivided Woodbend Group, thick intervals of lithofacies A are dominant. Thick intervals of AE characteristic of the Majeau Lake and Duvernay Formations are not present. Interfingering of lithofacies A with F also occurs. In

one core, sharp transitions from aquitards to reef facies occur; however, the remaining three cores show a gradational transition from carbonate reef facies to aquitards, similar to that identified, for example, in the transition from the Swan Hills Formation into the Majeau Lake Formation.

- *Ireton Formation*

The Ireton Formation could be subdivided from the Woodbend Group in one core. Interbedding of lithofacies A and F occur, which is subsequently overlain by a thick interval of lithofacies F.

- *Woodbend/Winterburn Group*

In this aquitard, lithofacies C, B, and AD are present. These lithofacies have not been identified in cores where the Majeau Lake, Duvernay and Ireton Formations can be differentiated, or in sections where the Woodbend Group can be differentiated from the Winterburn Group. This strongly suggests that these three lithofacies are part of the Winterburn Group.

- *Winterburn Group*

Aquitard A is dominated by lithofacies F. Overlying intervals of aquitard B are dominated by basinal lithofacies C and AD, or where thin, B and AD. Where thick, these same lithofacies are overlain by more basinal lithofacies B and C. In the West Pembina area, where aquitards A and B merge, the lower part of the aquitard (most likely equivalent to aquitard A) is dominated by lithofacies B and C, however, minor occurrences of lithofacies F are present near the base.

From the core analyzed, a general conclusion can be drawn that up section, within Winterburn Group aquitards A and B, a transition from lithofacies F (basinal to near-reef?) to basinal lithofacies (e.g. AD, B, and C) occurs. It is interpreted that towards the limit of the disturbed belt, aquitard B becomes more basinal (lithofacies A becomes prominent).

4.5.3. Geographic Correlations

Except for aquitard B as described above, the paleogeographic distribution of lithofacies is largely uncorrelated. This is due to the regional scope of this study, encompassing an area of approximately 38,000 km² and several stratigraphic units, as well as limited core control.

4.5.4. Mineralogical Facies Summary

Four major mineralogical facies are present within the aquitards studied: QCp, CQp, Cq, and Qdp, as summarized in Table 4.3.

<i>Mineralogical Facies</i>	<i>General Description</i>
QCp	Major quartz, moderate calcite, minor pyrite and moderate to minor amounts of ankerite
CQp	Major calcite, moderate quartz, minor pyrite, and ankerite is often present
Qdp	Major quartz, minor dolomite and pyrite.
Cq	Major calcite, variable amounts of quartz, minor pyrite.

Table 4.3: General summary of major mineralogical facies identified in the Woodbend and Winterburn Group aquitards in this study.

From the data analyzed, mineralogical facies do not appear to have significant correlations with stratigraphy. Facies QCp and CQp are present in every stratigraphic interval. Facies Cq is absent in only the Woodbend/Winterburn Group. Facies Qdp, on the other hand, is present only in the Woodbend Group. The presence of mineralogical facies Cq correlates with the presence of carbonate-rich lenses such as laminations, but is not restricted to these intervals as it is also found representing whole-rock samples.

In contrast, mineralogical facies appear to have a significant correlation with geographic distribution. Facies QCp and CQp are widespread throughout the study area. Facies Cq occurs in a restricted area in and around the Obed field and Wild River and Pine Creek Basins. Facies Qdp is localized, appearing only in the Obed field (Figure 4.13).

4.5.5. Carbonate content

The carbonate content within the shale aquitards appears to be correlative with lithofacies, rather than with stratigraphy. Basinal lithofacies tend to have a lower carbonate content, whereas near-reef facies tend to have higher carbonate contents.

5. Chapter 5 - Diagenetic History of the Aquitards

5.1. Introduction and Objectives

A major objective of this chapter is to interpret the diagenetic history of the aquitards within the study area from detailed core descriptions, thin-section analyses, and geochemical techniques including stable ($\delta^{18}\text{O}$ and $\delta^{13}\text{C}$) and radiogenic ($^{87}\text{Sr}/^{86}\text{Sr}$) isotope analyses. In Chapter 4, simplified mineralogical descriptions were presented using XRD (Table 4.1). In this chapter, a more detailed mineralogical account of the aquitards is presented, as required to investigate the diagenetic history of the aquitards. Stable and radiogenic isotopic analyses of the whole-rock carbonate fraction of the aquitards, in addition to individual components within the aquitard, e.g., cements, fossils, and nodules, provide important information about the diagenetic history of these units.

A second objective of this chapter is to compare the diagenetic history of the aquitards with that of the adjacent carbonate aquifers. In particular, the potential for aquitards to be the source for ^{87}Sr -enriched late-stage calcite cements, such as those in the Leduc Formation within the Obed region (Patey, 1995; Machel et al., 1996), is evaluated.

5.2. Mineralogy

5.2.1. Introduction

To understand the diagenetic history of the aquitards, detailed petrographic and hand-specimen descriptions of the mineralogical components is required and is presented below. Diagenetic minerals are emphasized in these descriptions, but they are also considered in relation to detrital minerals, as the latter comprise a significant fraction of the aquitards.

5.2.2. Mineralogical Analyses from Core and Thin Sections

- *Carbonate Phases*

Two major carbonate phases (calcite and ankerite) and minor amounts of dolomite were distinguished within whole-rock powders by XRD (Table 4.1).

*** *Calcite***

Several forms of calcite have been identified in the aquitards. Fine-grained calcite forms between 10 to 75 weight % of the matrix of the aquitards (Figure 5.1 a, as well as Figures 4.6 b-4, 4.7 b-4 and b-5, and 4.8 b-2). This calcite is locally derived from intrabasinal carbonate buildups. Most skeletal debris and fossils are predominantly composed of calcite (Figures 5.1 b and c and Figures 4.3 c-4, 4.11 b-2, and 4.12 c-2), yet often appear recrystallized (Figure 5.1 d). Calcite also occurs in minor amounts as infilling cement (Figures 4.11 b-2 and 4.12 c-2). Minor calcite veins present in some of the lithofacies are associated with stylolitization (Figure 4.10 b-1).

In a study of the Ireton and Duvernay Formations in east-central Alberta, McCrossan (1957) identified at least two generations of calcite. Detrital calcite occurred as discrete grains, and secondary calcite mainly filling cracks. In this study, one localized vein system is present in which calcite is accompanied by pyrite and dolomite (Figures 5.2 a, b, and c). Two phases of calcite exist in this vein system, a fine-grained phase followed by a coarser grained ("c1" and "c2" in Figure 5.2 b). Both phases of calcite are associated with pyrite (Figure 5.2 a, and "p" in Figure 5.2 b) and minor amounts of dolomite ("d" in Figures 5.2 b and c). The largest vein containing calcite, dolomite, and pyrite is less than 0.5 cm in width and extends subvertically for approximately 10 cm; only part of this vein is shown in Figure 5.2 a. Minor veins are present on both sides of the central vein (Figure 5.2 a and c).

*** *Ankerite and Dolomite***

Of the aquitards examined in west-central Alberta, calcite is the dominant carbonate phase present, followed by ankerite, then dolomite. This is based mostly on XRD, but also partially on thin-section petrography. In this study, ankerite is distinguished from dolomite only through the use of XRD, as it is difficult to differentiate the two in thin section. Using XRD peak heights, and comparing them to percentages of carbonate determined chemically for whole-rock samples, a semi-quantitative estimate of ankerite within whole-rock powders

Figure 5.1 a

Thin section of a mudstone with pyritized *Amphipora*. Fine-grained matrix calcite, stained red by Alizarin Red-S, is visible in the upper right half of the photo. This is a combination of lithofacies A and F from the Duvernay Formation. Plane-polarized light. White scale bar = 0.5 mm. Sample taken from core 1-26-58-18W5, 3397.3 m (11146').

Figure 5.1 b

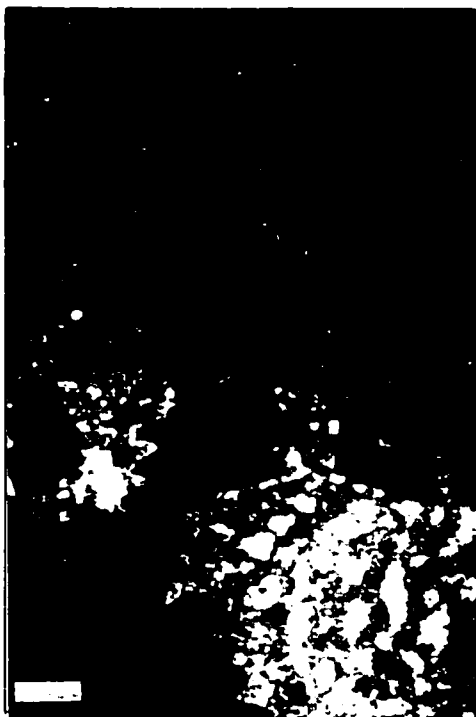
Thin section showing calcite-rich, fragmented and flattened ostracods, minor tentaculitids, and brachiopods in a dark, organic-rich matrix. From lithofacies A of the Woodbend Group. Stained with Alizarin Red-S. Plane-polarized light, White scale bar = 0.5 mm. Sample taken from core 4-13-56-23W5, 4119.5 m (13515.5').

Figure 5.1 c

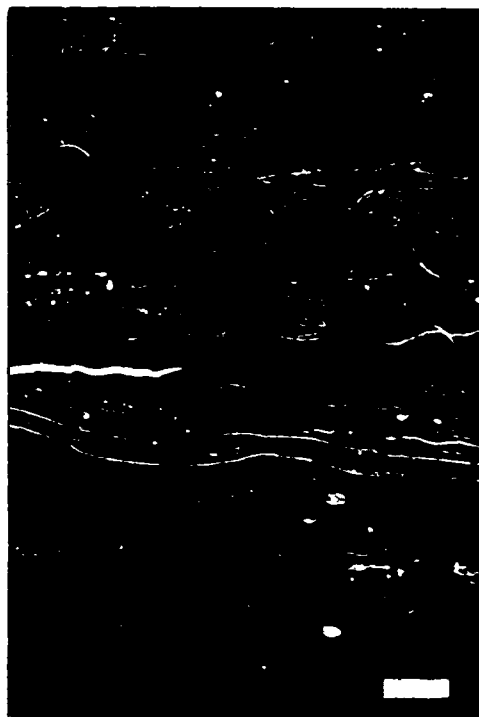
Thin section of a matrix of quartz silt, muscovite, and clinocllore with minor, calcitic skeletal matter (stained red by Alizarin Red-S) less than 1 mm in size. From lithofacies AD of the Winterburn Group. Plane-polarized light. White scale bar = 0.5 mm. Sample taken from core 7-4-49-12W5, 3099.8 m (10170').

Figure 5.1 d

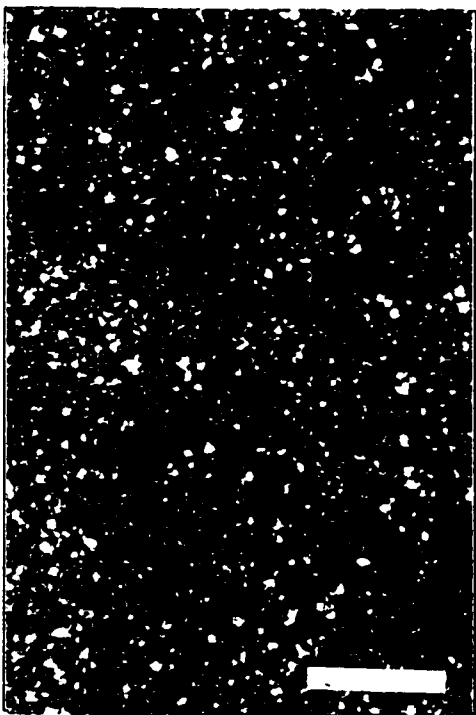
Thin section of a recrystallized, calcitic brachiopod stained with Alizarin Red-S in the upper right corner of the photo. From lithofacies F of the Winterburn Group. Cross-polarized light. White scale bar = 0.5 mm. Sample taken from core 2-22-51-7W5, 2271.5 m (7452.5').



A



B



C



D

Figure 5.2 a

A core sample showing a localized vein system of calcite, dolomite, and pyrite. The calcite and dolomite are difficult to distinguish in this photo, but are evident in thin section in Figures 5.2 b and c. On both sides of the major vein, two minor veins (of less than 1 mm in width) are visible and are associated with disseminated pyrite. Core is part of the undivided Woodbend Group. Way up is indicated with arrow. White scale bar = 1 cm. Sample taken from core 8-26-55-22W5, 3815.9 m (12519.3').

Figure 5.2 b

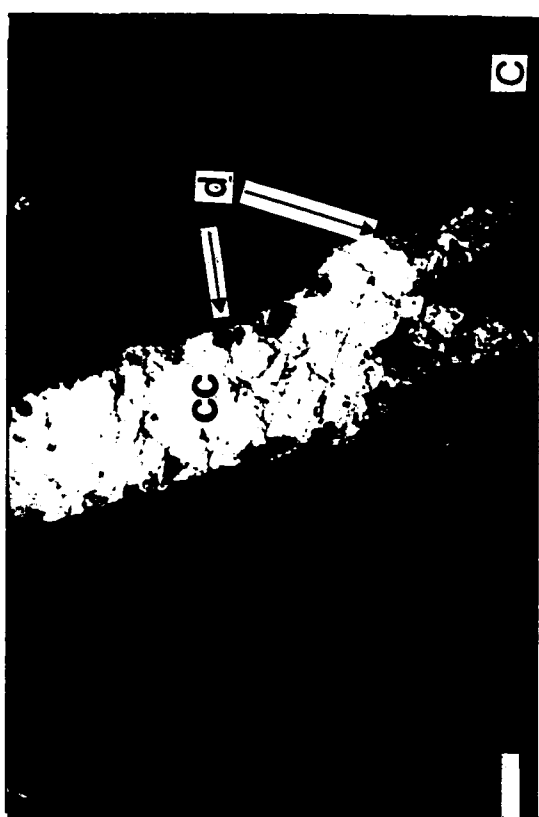
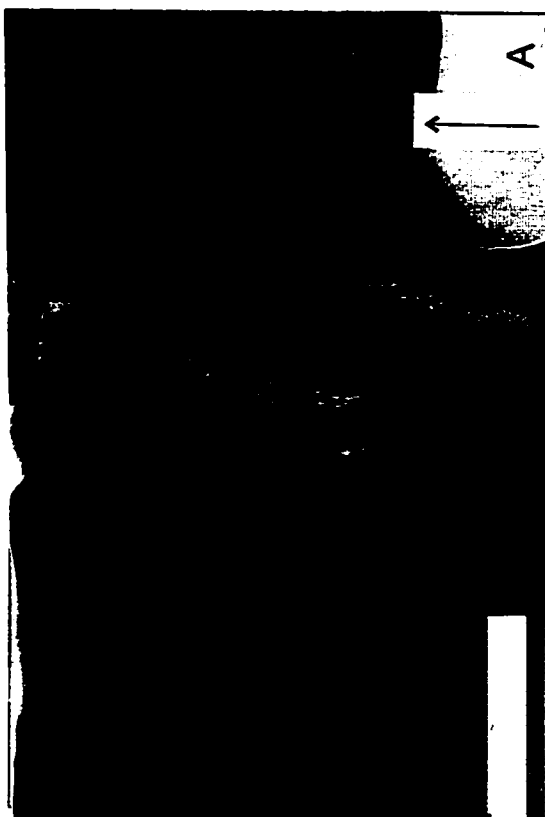
Thin section of the major vein shown in core in Figure 5.2 a. Two phases of pyrite are visible: an outer 1-1.5 mm wide pyrite (p) vein; and an inner, minor phase. At least two calcite phases (c-1 and c-2) are visible. The grey-shaded calcite (c-2) is coarse textured. Dolomite (d) is visible, lining the c-1 calcite. Cross-polarized light, stained with Alizarin Red-S and Potassium Ferricyanide. White scale bar = 0.5 mm. Sample taken from core 8-26-55-22W5, 3815.9 m (12519.3').

Figure 5.2 c

Thin section of a minor vein shown in core in Figure 5.2 a. The fracture is sparsely lined with dolomite (d) and infilled with a later stage of calcite (cc). Plane-polarized light, stained with Alizarin Red-S. White scale bar = 0.5 mm. Sample taken from core 8-26-55-22W5, 3815.9 m (12519.3').

Figure 5.2 d

Thin section of a slightly bioturbated, ankerite-rich silty marl from lithofacies C of the Winterburn Group. The XRD results for the specimen indicate that the carbonate in this whole-rock sample is about 40% ankerite. Plane-polarized light, stained with Alizarin Red-S. White scale bar = 0.5 mm. Sample taken from core 6-28-61-26W5, 3908.3 m (12822.5').



is estimated to range between 0 and 40 weight % (Table 4.1). Ankerite, present as approximately 40 weight % of one sample is difficult to identify without the use of XRD (Figure 5.2 d).

In east-central Alberta, McCrossan (1957) identified dolomite (rather than calcite) as the predominant carbonate mineral in the upper part of the Ireton Member (now defined as a Formation).

Dolomite in lithofacies F, G, and GE is visible as crystals ranging in size from 1-3 mm, mainly replacing matrix in *Thamnopora* floatstones (Figure 5.3 a and b). Dolomite is also associated with calcite and pyrite in the localized vein system described in the previous section. In this system, dolomite appears as sparse crystals developed inwards from pyrite and a fine-grained phase of calcite and a second phase of pyrite (Figure 5.2 b). Dolomite also lines minor fractures (Figure 5.2 c).

- *Quartz and Feldspars*

Mason (1966) stated that quartz and feldspars are generally the most abundant detrital minerals found within shales. At surface conditions, quartz is resilient to chemical attack and the amount of quartz in a shale may be directly correlative with shoreline proximity (Potter et al., 1980). Feldspars, due to their susceptibility to weathering, are not as abundant in shales as quartz (Mason, 1966). Part of the feldspar in a shale may be authigenic. However, it is difficult to distinguish authigenic from detrital feldspar in very fine-grained sedimentary rocks (Potter et al., 1980).

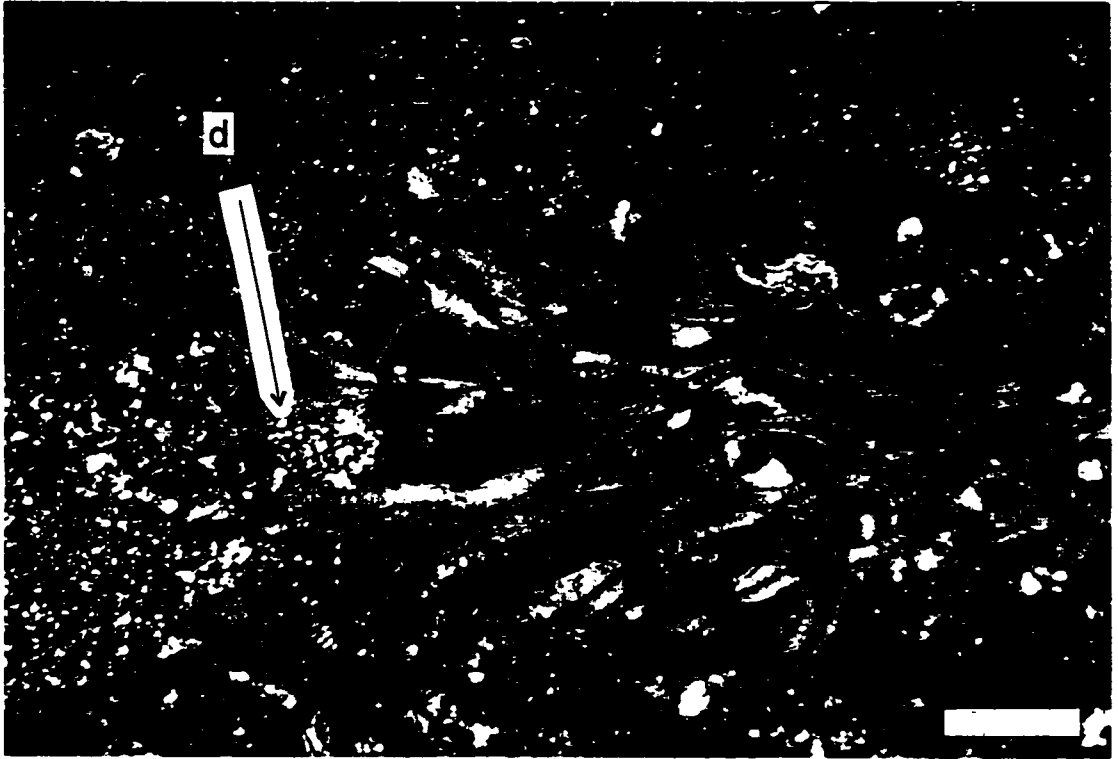
In this study, quartz is visible in thin section as minute, round grains within the matrix (Figure 5.2 d) and is abundant within laminations (Figure 5.4 a). Using the same method described for ankerite above, a semi-quantitative estimate of quartz within whole-rock samples ranges from 10 to 40 weight % (Table 4.1). A minor amount of this quartz occurs as microcrystalline chert replacing a rugose coral. Minor amounts of alkali feldspars have been detected by XRD in samples from the four mineralogical facies. However, because the feldspars are very fine-grained, they are almost impossible to identify in thin section.

Figure 5.3 a

Thin section of dolomite (d) replacing mainly the matrix in the left part of the photo. From lithofacies G of the Winterburn Group. Plane-polarized light, stained with Alizarin Red-S. Scale bar = 1 mm. Sample taken from core 11-35-54-23W5, 4171.2 m (13685').

Figure 5.3 b

Thin section of a floatstone consisting of calcitic *Thamnopora*, brachiopod spines, and possible mollusc fragments. The brachiopod shown is infilled with and surrounded by matrix dolomite (d) and calcitic fossil fragments (stained red with Alizarin Red-S). Some *Thamnopora* pores are infilled with anhydrite (a). Winterburn Group, lithofacies G. Plane-polarized light. White scale bar = 1 mm. Sample taken from core 7-4-49-12W5, 3070.6 m (10074').



A



B

Figure 5.4 a

Thin section of a quartz-rich laminated shale from lithofacies A of the Duvernay Formation. Plane-polarized light, not stained with Alizarin Red-S. White scale bar = 0.5 mm. Sample taken from core 14-2-69-21W5, 2752.25 m (9029.7').

Figure 5.4 b

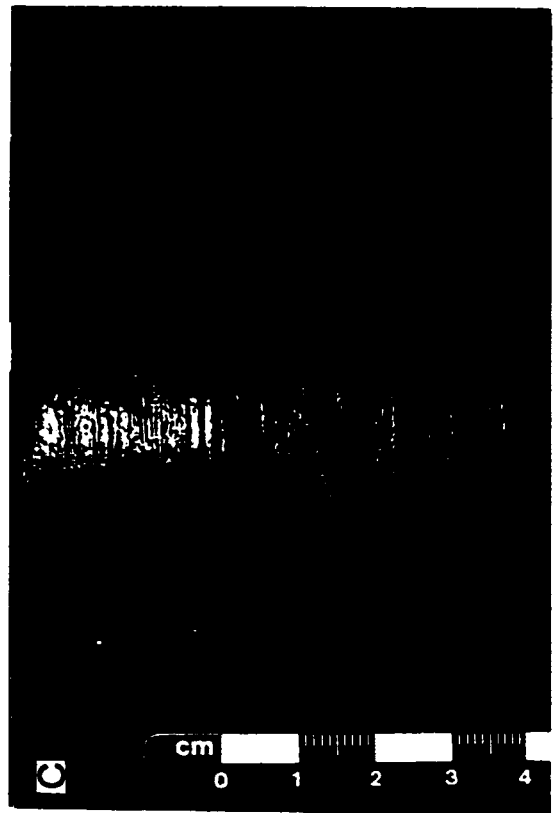
Thin section of pyrite replacing calcite around the rim of a large crinoid fragment. Pyrite also partially replaces several other calcite fossils such as brachiopods in the thin section. The dark color of the thin section is attributed to abundant pyrite within the matrix. Plane-polarized light, stained with Alizarin Red-S. White scale bar = 0.5 mm. Sample taken from the Woodbend Group, core 10-17-57-23W5, 4004.2 m (13137').

Figure 5.4 c

Core showing pyritized rims surrounding and replacing *Amphipora* fossils. Duvernay Formation, combination of lithofacies A and F. Centimeter bar for scale. Sample taken from core 1-26-58-18W5, 3397.3 m (11146').

Figure 5.4 d

Thin section of a celestite vein or infilled fracture (light blue to grey in color) with associated pyrite grains (black). Quartz silt and detrital calcite are present in the matrix. Thin section taken from core in Figure 5.5 a. Cross-polarized light, and partially stained with Alizarin Red-S on the left side. White scale bar = 0.5 mm. Sample taken from the Woodbend/Winterburn Group, core 8-19-66-12W6, 5259.6 m (17268').



- *Clay and Sheet Silicate Minerals*

The amount of clay and sheet silicate minerals present within whole-rock powders is semi-quantitatively estimated to be between 10 and 20 weight % (Table 4.1), using the same method described above for ankerite. Interference by the strong quartz reflection affects the values obtained. Minor amounts of chlorite and muscovite have been identified by XRD. However, the minor amount of muscovite identified using XRD is more likely illite. This assumption is supported by the following: (1) illite and muscovite have similar XRD patterns and chemical compositions (Table 5.1); (2) the presence of illite rather than muscovite agrees with results obtained from studies on the Ireton Formation and Woodbend Group in the East Shale Basin (McCrossan 1957, 1961; Campbell and Oliver, 1968); (3) illite has been identified as the most common clay material in marine sediments and sedimentary rocks and probably forms as a result of surface weathering of silicates, principally feldspars, to form detrital illite; and (4) diagenesis is proven to promote the formation of illite and chlorite at the expense of kaolinite and montmorillonite (smectite) (Mason, 1966) (refer to Table 5.1 for the chemical compositions of these minerals). Consequently, illite and chlorite are likely the two most abundant clay minerals in the aquitards. They probably formed diagenetically, although part of the illite may be detrital.

Kaolinite	$\text{Al}_4[\text{Si}_4\text{O}_{10}](\text{OH})_8$
Smectite	$(1/2\text{Ca}, \text{Na})_{0.7}(\text{Al}, \text{Mg}, \text{Fe})_4[(\text{Si}, \text{Al})_8\text{O}_{20}](\text{OH})_4.n\text{H}_2\text{O}$
Chlorite	$(\text{Mg}, \text{Fe}^{2+}, \text{Fe}^{3+}, \text{Mn}, \text{Al})_{12}[(\text{Si}, \text{Al})_8\text{O}_{20}](\text{OH})_{16}$
Illite	$\text{K}_{1.5-1.0}\text{Al}_4[\text{Si}_{6.5-7.0}\text{Al}_{1.5-1.0}\text{O}_{20}](\text{OH})_4$
Muscovite	$\text{K}_2\text{Al}_4[\text{Si}_6\text{Al}_2\text{O}_{20}](\text{OH}, \text{F})_4$

Table 5.1: Chemical composition of four clay minerals and a sheet silicate mineral. Kaolinite and smectite are common in younger shales, but diagenetically alter to chlorite and illite in older (e.g., Paleozoic) shales. Muscovite and illite have similar chemical compositions.

- *Sulfides*

- * *Pyrite*

Potter et al. (1980) stated that iron sulfides, such as crystalline pyrite or marcasite, are the only abundant sulfides in shales. They also stated that iron

sulfide is much more abundant in marine than in continental shales, and that both pyrite and marcasite indicate strongly reducing conditions either at the sediment-water interface or within the sediment.

Pyrite has been detected as a minor component, using XRD, in the majority of whole-rock samples (Table 4.1). It is clearly visible in core and thin section in variable amounts and in several forms. Given this, it is likely that several events of pyritization occurred throughout the diagenetic history of the aquitards. In one sample pyrite is associated with celestite (strontium sulphate) (Figure 5.4 d), the latter assumed to be related to an early-stage event (discussed below). In a second sample, pyrite is associated with a localized, possibly late-stage, calcite-dolomite vein system (Figure 5.2 a and b) (discussed subsequently).

The amount of pyrite appears to be directly related to the organic matter present within the aquitards. Pyrite is present in all of the lithofacies, but is most abundant in lithofacies A, the organic-rich basinal facies. Pyrite is commonly found disseminated throughout the matrix, and is also concentrated in laminations. It commonly occurs as euhedral crystals, and in shapes such as blebs and rosettes. Associated with fossils, it is present in three forms: (1) on the inside edges of calcitic fossils, nodules, and lenses (Figure 5.4 b); (2) completely or nearly completely replacing calcite fossils; and (3) completely rimming fossils such as *Amphipora* (Figure 5.4 c). In a study of the Ireton and Duvernay Formations in east-central Alberta, McCrossan (1957) identified a minor amount of pyrite as a fine-grained replacement of calcite.

- *Sulfates*

- * *Celestite*

Celestite has been identified in one of the cores examined. It occurs as a vein or fracture fill within a thin (approximately 10 m thick) Woodbend/Winterburn Group aquitard (Figures 3.8 and 3.9, well location 08-19-66-12W6, and Figure 4.24) in the Leduc Fringing Reef of the Peace River Arch area. Celestite (Figures 5.5 a and b and 5.4 d) may have precipitated during soft sediment deformation, however, it may have also formed subsequent to a fracture event.

Figure 5.5 a

Core showing celestite veins. Core is from lithofacies A of the Woodbend/Winterburn Group. Centimeter bar for scale on the left side of photo, each white bar = 1 cm. Sample taken from core 8-19-66-12W6, 2215 m (17268').

Figure 5.5 b

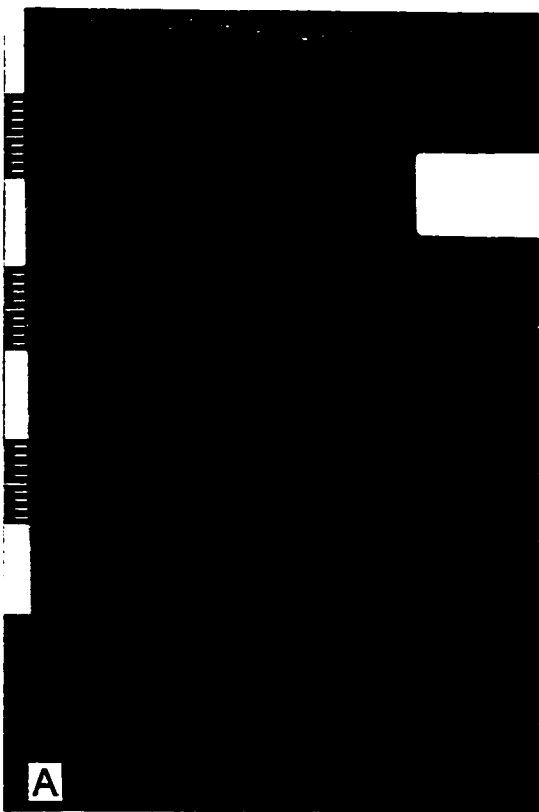
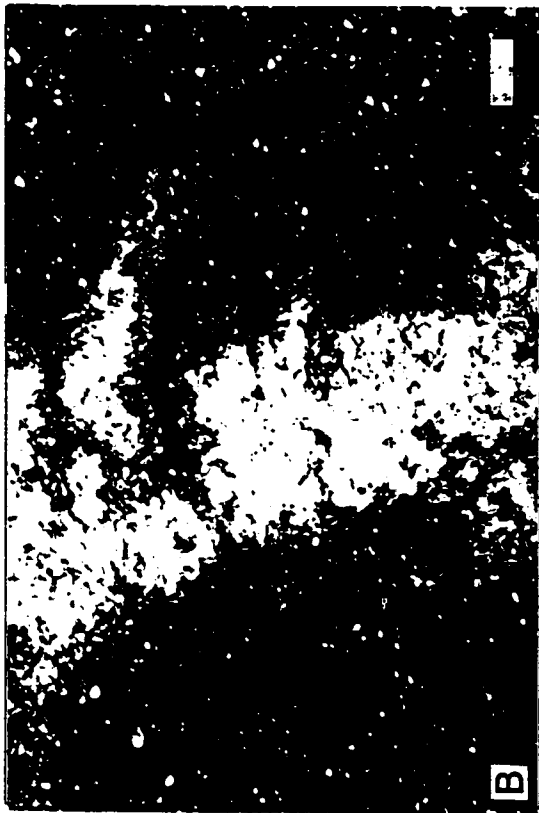
Thin section of a celestite vein rimmed by a clay mineral (possibly clinochlore). Thin section is from lithofacies A of the Woodbend/Winterburn Group. The sample is taken from core in Figure 5.5 a. Cross-polarized light, stained with Alizarin Red-S. White scale bar = 0.5 mm. Sample taken from core 8-19-66-12W6, 5259.6 m (17268').

Figure 5.5 c

Thin section of a calcitic *Thamnopora* fragment (calcite is stained red by Alizarin Red-S), partially replaced with anhydrite. Thin section is from lithofacies G of the Woodbend/Winterburn Group. Cross-polarized light. White scale bar = 0.5 mm. Sample taken from core 14-11-70-5W6, 3395.8 m (11141').

Figure 5.5 d

Thin section of calcite-rich *Thamnopora*, brachiopod spines, and other fossil fragments, some that are partially replaced with anhydrite, and intersected by wispy horsetail-like dissolution seams or stylolites. Thin section is from lithofacies GE of the Winterburn Group. Cross-polarized light, stained with Alizarin Red -S. White scale bar = 0.5 mm. Sample taken from core 7-4-49-12W5, 3139.3 m (10299.5').



XRD of sediment surrounding the vein or infilled fracture yielded no trace of dispersed celestite.

Celestite is frequently associated with shallow-water evaporite deposits such as gypsum and barite, e.g., in the anhydrite zone of the evaporites of Eskdale, Yorkshire and also in deposits of rock salt (Stewart, 1949). Celestite deposits have also been discovered in Newfoundland, Nova Scotia, New Brunswick, Ontario, and British Columbia associated with evaporite minerals (Andrews and Collings, 1991). However, the occurrence of celestite in deep-sea sediments (below approximately 100 and 300 m of the sediment-water interface) is rare, and has been reported by Baker and Bloomer (1988). In core examined from the Woodbend/Winterburn Group, a significant amount of evaporites was not identified. It is possible, therefore, that celestite formed under conditions similar to those described by Baker and Bloomer (1988).

The common occurrence of celestite in shallow-water environments is correlative with the presence of aragonite, which tends to contain abundant strontium (e.g., Bush, 1973). In pelagic sediments where aragonite is not as abundant, celestite is not commonly precipitated. In the sediments that Baker and Bloomer (1988) studied, celestite formed by the diagenesis of biogenic calcite, predominantly coccoliths enriched in strontium relative to recrystallized calcite precipitated during burial diagenesis. During recrystallization, strontium was released into the porewaters. When the rate of carbonate accumulation and recrystallization is high (high strontium in porewaters) and the rate of microbial sulfate reduction is low (high sulfate in porewaters), celestite can form. Porewater strontium was found to increase with increasing burial depth.

* *Anhydrite*

In a study of the Ireton and Duvernay Formations in east-central Alberta, McCrossan (1957) identified anhydrite as fracture fillings. In this study, anhydrite was found as a replacement of calcitic fossils and also as a cement in fossils within upper foreslope and near-reef lithofacies G and GE, as well as in within lithofacies F. Specifically, anhydrite infills pores and replaces fragments of calcitic *Thamnopora* and/or bryozoans, *Amphipora*, and brachiopods (Figures

5.5 c and d, 5.3 b, 5.6, and Figure 4.11 b-2). Minor anhydrite veining is associated with the formation of coated grains and it is likely that the replacement and vein filling anhydrite post-dates the formation of coated grains (Figure 5.6). It is uncertain how many phases of anhydrite exist, but it is likely that anhydrite is not primary or syngenetic, but rather it likely formed during shallow, moderate, to deep burial diagenesis.

- *Structures*

- * *Coated Grains*

Coated grains occur in, and are typical of, near-reef lithofacies G and GE. Fossils such as brachiopod spines can form the nucleus of the coated grain, whereas several other smaller bioclasts may also be present (Figure 5.6). They are likely syndepositional, and formed as a result of symbiosis with microbial organisms.

- * *Pinch and Swell Structures*

The details of pinch and swell structures were described in Chapter 4. To reiterate, these structures are predominantly associated with lithofacies AE and GE. They likely formed as a result of diagenesis during the reorganization of sediment into a carbonate-rich domains and more silicate-rich domains of the aquitards (Machel and Hunter, 1994). The structures, in addition to stylolites and dissolution seams, appear to post-date the formation of anhydrite replacement in fossils within the lithofacies (Figure 5.5 d).

5.3. Stable Isotope Analyses

5.3.1. Samples and Procedures

$\delta^{18}\text{O}$ and $\delta^{13}\text{C}$ ratios were determined for forty-two whole-rock samples containing carbonate fractions such as calcite, ankerite, and dolomite in addition to nine specimens of calcite fossils, nodules, cements, layers, lenses, and hardgrounds from within the aquitards (Appendix 1). The methodology is described in Appendix 3. Calcite, the predominant carbonate phase in the



Figure 5.6

Thin section of a coated grain (arrows pointing to its margin), with a nucleus consisting of a brachiopod spine. Anhydrite has infilled the center and replaced part of the spine. A narrow anhydrite vein on the left (largely within the coating) appears to have formed. Thin section of lithofacies GE from the Woodbend/Winterburn Group. Stained with Alizarin Red-S on the left. XPL. White scale bar = 1 mm. Sample taken from 14-11-70-5W6, 3395.8 m (11141').

whole-rock samples, was analyzed in thirty-eight whole-rock samples, whereas the less abundant ankerite and dolomite phases were only analyzed in twelve whole-rock samples. Additional ankerite whole-rock fractions were analyzed but unfortunately the data obtained from them was not useful. Ankerite, which contributed less than 10 weight % (Table 4.1) to the whole-rock fraction, typically produced the same isotopic signature as that of the predominant calcite whole-rock fraction of the same sample.

Stratigraphically, samples were selected from the Majeau Lake, Duvernay, and Ireton Formations, in addition to the Woodbend, Woodbend/Winterburn, and Winterburn Group aquitards. Geographically, samples were selected from near the disturbed belt (e.g., from the Obed field, Wild River and Pine Creek Basins, Leduc Fringing Reef of the Peace River Arch, East of Sturgeon Lake, Windfall, and Simonette Reefs, and the Swan Hills Platform north of the Pine Creek Basin), as well as distant from the disturbed belt in the West Pembina area.

5.3.2. Results

Stable isotopic analyses ($\delta^{18}\text{O}$ and $\delta^{13}\text{C}$) have been plotted in Figure 5.7. Two distinctive fields of data are evident: (1) a calcite population consisting of whole-rock calcites in addition to all but one of the individual components such as calcite fossils, nodules, cements, etc.; and (2) an ankerite/dolomite population consisting of whole-rock ankerites and dolomite fractions. The one outlier in Figure 5.7 is a carbonate lens from the Woodbend Group within the Wild River Basin. The calcite and ankerite/dolomite fields overlap and both show a slight positive correlation between $\delta^{18}\text{O}$ and $\delta^{13}\text{C}$; as the $\delta^{13}\text{C}$ becomes more negative, so does the $\delta^{18}\text{O}$.

• *Calcite Population*

* $\delta^{18}\text{O}$

The $\delta^{18}\text{O}$ ratios of the calcite population range between -5.9 and -9.5‰ PDB. These ratios are up to 5.5‰ more negative than hypothetical Upper

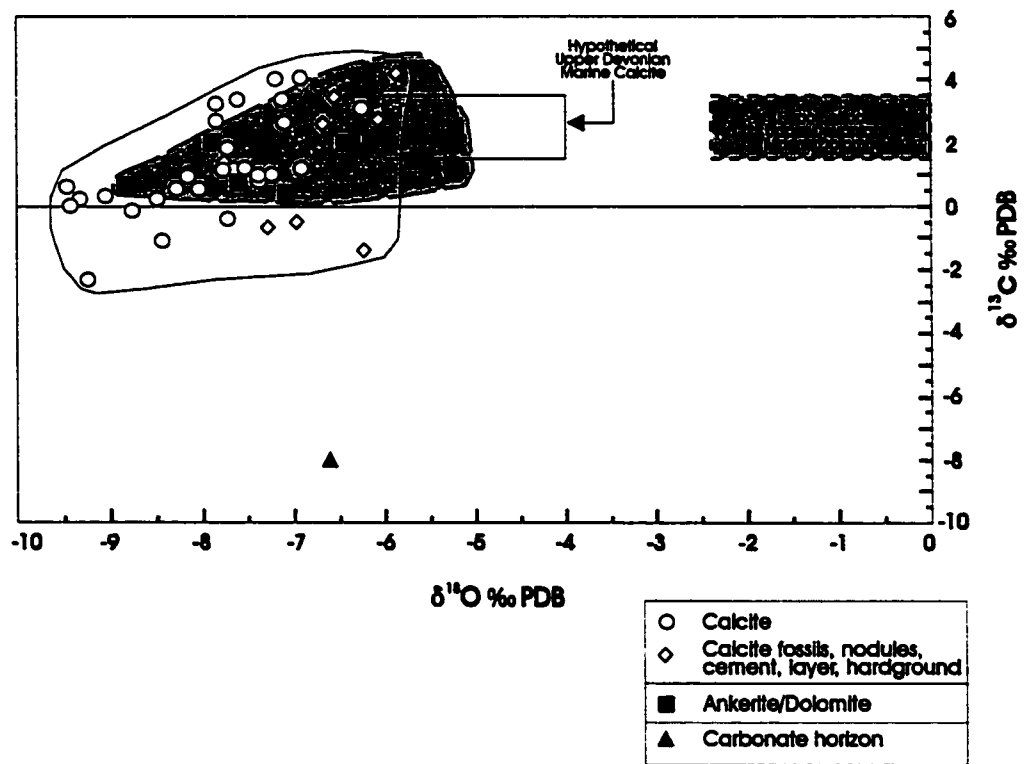


Figure 5.7: Plot of $\delta^{18}\text{O}$ (PDB) versus $\delta^{13}\text{C}$ (PDB). White and grey rectangular boxes indicate hypothetical marine calcites and dolomites respectively (after Amthor et al., 1993 and references therein). Two fields of data representing a calcite population (field outlined in black) and an ankerite/dolomite population (grey colored field) are evident. One outlier, representing a carbonate lens, is depleted in $\delta^{13}\text{C}$ relative to the rest of the calcite population.

Devonian marine calcites (Figure 5.7) that range from approximately -4 to -6‰ PDB (Amthor et al., 1993 and references therein). The calcite population likely represents a combination of marine-equilibrated calcites in addition to recrystallized marine-equilibrated calcites at higher temperatures.

$$\ast \quad \delta^{13}\text{C}$$

The $\delta^{13}\text{C}$ ratios of the calcite population range from +4.2 to -2.3‰ PDB, and overlap with those estimated for hypothetical Devonian marine calcites (+1.5 to +3.5‰ PDB) (Amthor et al., 1993 and references therein). However, samples can be slightly depleted or enriched in $\delta^{13}\text{C}$ relative to hypothetical marine calcites (Figure 5.7). The majority of the calcite population tends to be slightly more depleted in $\delta^{13}\text{C}$ (enriched in ^{12}C) (up to 3.8‰) relative to hypothetical marine calcites.

• *Ankerite/Dolomite Population*

$$\ast \quad \delta^{18}\text{O}$$

The $\delta^{18}\text{O}$ ratios of the ankerite/dolomite population range from -5.3 to -8.9‰ PDB and generally overlap with $\delta^{18}\text{O}$ ratios of the calcite population (Figure 5.7). The $\delta^{18}\text{O}$ of the ankerite/dolomite population is between 2.9 to 8.9‰ PDB more negative than hypothetical Upper Devonian marine dolomite (0 to -2.5‰ PDB) (Amthor et al., 1993 and references therein).

$$\ast \quad \delta^{13}\text{C}$$

The ankerite/dolomite population ranges in $\delta^{13}\text{C}$ between +4.4 and +0.4‰ PDB, which overlaps with the calcite population and with hypothetical Upper Devonian marine dolomites (+1.5 to +3.5‰ PDB) (Amthor et al., 1993 and references therein) (Figure 5.7). The twelve samples of ankerite and dolomite all have positive $\delta^{13}\text{C}$ ratios, in contrast to the negative ratios of some of the calcite population.

5.3.3. Interpretation

- *Calcite Population*

- * $\delta^{18}\text{O}$

Although the $\delta^{18}\text{O}$ composition of marine waters is unknown, if it is assumed that the fluids from which the calcites precipitated were of Late Devonian marine parentage, then the paleotemperature of formation or recrystallization of the carbonate phases can be estimated from $\delta^{18}\text{O}$. From the range in $\delta^{18}\text{O}$ values for the calcite population (between -5.9 and -9.5‰ PDB), and a reasonable estimate for the isotopic composition of Upper Devonian seawater of $\delta^{18}\text{O} \approx -1\text{‰}$ to -2.5‰ SMOW (Standard Mean Ocean Water) (Amthor et al., 1993 and references therein), using the calcite-water fractionation equation

$$\delta^{18}\text{O}_{\text{calcite}} - \delta^{18}\text{O}_{\text{fluid}} = 2.78 \times 10^6 T^{-2} - 2.89$$

of Friedman and O'Neil (1977) (T = temperature in $^{\circ}\text{K}$) valid for a temperature range of 0-500°C, a temperature of formation for the calcite population is estimated to range between 30 and 61°C. Using a surface temperature of approximately 25°C during the Late Devonian (Carpenter et al., 1991) and a geothermal gradient of 25°C/km within the Alberta Basin (the average of geothermal gradients typical in the area; after Bachu and Burwash, 1994), the calculated temperature range corresponds with that estimated for depths of between 200 m and approximately 1.4 km. However, if one was to use a surface temperature as high as 30°C and a geothermal gradient as high as 30°C/km, the calculated temperature range corresponds with that estimated for Late Devonian seawater to burial depths of approximately 1 km of depth. Using burial curves from the Swan Hills region (Duggan, 1997 and references therein), the Rimbey-Meadowbrook Reef trend (Horrigan, 1996), and the Bashaw Reef Complex (Hearn, 1996), depths up to 1.8 km were most likely reached by the end of the Late Devonian/Early Carboniferous.

* $\delta^{13}\text{C}$

Carbon isotopic fractionation is relatively insensitive to temperature compared to oxygen, therefore, carbon isotopes are of little use as geothermometers. Instead, carbon isotopes are useful in understanding the origin of carbon in the carbonate. Other than carbonate inorganically or microbially precipitated from seawater, three other carbon sources may contribute to carbonates. The first consists of a reduced organic carbon derived from marine (and land) plants (Tucker and Wright, 1990) during shallow burial. The second and third sources are produced during deep burial of organic matter and include biogenic methane, produced at temperatures below 70°C by bacterially mediated processes; and thermogenic methane generated by thermal breakdown of kerogen and oil.

To contribute to carbonate at shallow depths, reduced, organic carbon (the first source) must first be oxidized (Emery and Robinson, 1993). There are two pathways by which this may occur. Firstly, organic matter containing a certain but small amount of oxygen can be liberated as carbon dioxide or organic acids. Secondly, bacteria can oxidize organic matter using oxygen, nitrate, manganese, iron oxides, and sulfate (Froehlich et al., 1979). The by-product of these reactions is bicarbonate which retains an isotopic composition similar to that of the precursor organic matter (e.g., -20 to -25‰ PDB).

If organic matter is buried beyond the sulfate reduction zone it is degraded by methanogenic bacteria. This process occurs at temperatures of up to about 70°C by either acetate fermentation or carbon dioxide reduction; the latter is dominant in saline water (Tucker and Wright, 1990) and is pertinent to this study. Isotopically light (-50 to -90‰ PDB) biogenic methane is produced from these reactions (the second source). Isotopically heavier (-20 to -55‰ PDB) thermogenic methane is produced by the thermal breakdown of kerogen and oil above 70°C (up to 100°C?) (the third source). The end result is a highly variable carbon isotopic composition of carbon dioxide in the biogenic and thermogenic methane zones; most values are between +2 and -22‰ PDB (Emery and Robinson, 1993).

Above 100°C, hydrocarbons can be converted to carbon dioxide by reaction with mineral oxidants such as sulphate or ferric iron. The best known of these reactions is thermochemical sulphate reduction (TSR), which produces bicarbonate with an isotopic composition similar to that of the reactant methane (-35 to -60‰ PDB).

In this study, it appears that a combination of carbon sources contributed to the calcite population. As most of the calcites are not significantly enriched or depleted relative to those of marine carbonates, most of the carbon represents marine carbonate. The depleted $\delta^{13}\text{C}$ values are attributed to processes occurring at relatively low temperatures (up to 61°C calculated using $\delta^{18}\text{O}$ for the formation of calcites), such as the oxidation of reduced organic carbon, which produces bicarbonate with an isotopic composition similar to precursor organic matter (e.g., -20 to -25‰ PDB), or during degradation by methanobacteria in the biogenic zone, likely by carbon dioxide reduction rather than acetate fermentation, which can produce a composition of carbon dioxide in these zones down to approximately -22‰ PDB. On the other hand, the enrichment of $\delta^{13}\text{C}$ in samples from the calcite population may also be attributed to carbon dioxide reduction in the biogenic zone, which can produce carbon dioxide isotopic compositions with values up to approximately +2‰ PDB. Processes above approximately 60°C are unlikely to attribute carbon to calcites in this study, e.g., those involving thermogenic methane or thermochemical sulphate reduction reactions.

- *Outlier Carbonate*

- * $\delta^{18}\text{O}$ and $\delta^{13}\text{C}$

A carbonate from the Woodbend Group in the Wild River Basin has a $\delta^{18}\text{O}$ ratio of -6.6‰ PDB, which is within the range of calcite population previously described. However, a low $\delta^{13}\text{C}$ ratio of -8.0‰ PDB differentiates it from the calcite population (Figure 5.7). Enrichment in ^{12}C (depletion in $\delta^{13}\text{C}$) in this outlier is most likely attributed to marine carbonate recrystallizing in the presence of oxidation of reduced organic carbon (-20 to -25‰ PDB) or

degradation by methanobacteria in the biogenic zone during carbon dioxide reduction (+2 and -22‰ PDB).

- *Ankerite/Dolomite Population*

- * $\delta^{18}\text{O}$

A reasonable estimate for the isotopic composition of Upper Devonian seawater is $\delta^{18}\text{O} \approx -1\text{‰}$ to -2.5‰ SMOW (Amthor et al., 1993 and references therein) (refer to discussion in the previous section on calcite population). From the range in $\delta^{18}\text{O}$ values for the ankerite/dolomite population (between +5.3 and -8.9‰ PDB), and using the dolomite-water fractionation equation

$$\delta^{18}\text{O}_{\text{dolomite}} - \delta^{18}\text{O}_{\text{fluid}} = 2.78 \times 10^6 T^{-2} + 0.11$$

of Fritz and Smith (1970) (T = temperature in °K), a temperature of formation for the ankerite/dolomite population is estimated to range between 43 and 77°C. Assuming a surface temperature of approximately 25°C (Carpenter et al., 1991), and a geothermal gradient of 25°C/km (average of geothermal gradients in the area after Bachu and Burwash, 1994), the entire population, with the exception of the sample with the most depleted $\delta^{18}\text{O}$ value (-8.85), most likely formed and/or recrystallized at depths of between 720 m and 1.8 km within the basin. However, if one was to use a surface temperature as high as 30°C and a geothermal gradient as high as 30°C/km, the calculated temperature range corresponds with that estimated for burial depths of between 433 m and 1.6 km. Using burial curves from the Swan Hills region (Duggan, 1997 and references therein), the Rimbey-Meadowbrook Reef trend (Horrigan, 1996), and the Bashaw Reef Complex (Hearn, 1996), these depths were most likely reached by the end of the Late Devonian/Early Carboniferous.

- * $\delta^{13}\text{C}$

Similar to the calcite population, the carbon in the ankerite/dolomite population is not significantly enriched or depleted relative to those of marine

carbonates. However, the slight depletion noted in several samples is attributed to processes occurring at low temperatures (below 77°C calculated using $\delta^{18}\text{O}$ of the carbonate fraction), such as the oxidation of reduced organic carbon, which produces bicarbonate with an isotopic composition similar to precursor organic matter (e.g., -20 to -25‰ PDB), or during degradation by methanobacteria in the biogenic zone by carbon dioxide reduction (e.g., +2 to -22‰ PDB). However, the enrichment of $\delta^{13}\text{C}$ in one sample may also be attributed to processes involving degradation by methanobacteria in the biogenic zone by carbon dioxide reduction (e.g., +2 to -22‰ PDB).

5.3.4. Trends in $\delta^{18}\text{O}$ / $\delta^{13}\text{C}$

The $\delta^{18}\text{O}$ and $\delta^{13}\text{C}$ of both the calcite and ankerite/dolomite populations have been correlated with their corresponding (1) stratigraphic and geographic locations, (2) lithofacies and mineralogical facies and, (3) depths to reveal any significant trends. In a plot of $\delta^{18}\text{O}/\delta^{13}\text{C}$ of the calcite population (Figure 5.8), calcites from the Duvernay Formation and the Woodbend Group appear to be depleted in $\delta^{18}\text{O}$ and $\delta^{13}\text{C}$ relative to the rest of the calcite population, whereas calcites from the Winterburn Group tend to be more enriched with respect to both $\delta^{18}\text{O}$ and $\delta^{13}\text{C}$ relative to the rest of the calcite population. However, calcites from the Majeau Lake Formation that plot between those from the Winterburn Group and Duvernay Formation and Woodbend Group (Figure 5.8) do not fit this pattern. It is possible, therefore, that a relationship does not exist with respect to stratigraphic level. The depleted $\delta^{18}\text{O}$ and $\delta^{13}\text{C}$ ratios of calcites from the Duvernay Formation may otherwise be explained by or related to the source rock quality of the Formation (with total organic carbon contents of between 5 and 10% (e.g., Stoakes and Creaney, 1984)) e.g., the Duvernay calcites formed and/or recrystallized in the presence of an abundance of originally organic carbon, which caused depletion in the $\delta^{13}\text{C}$ isotopic signature. Ankerites from the Winterburn Group, most of which represent lithofacies AD

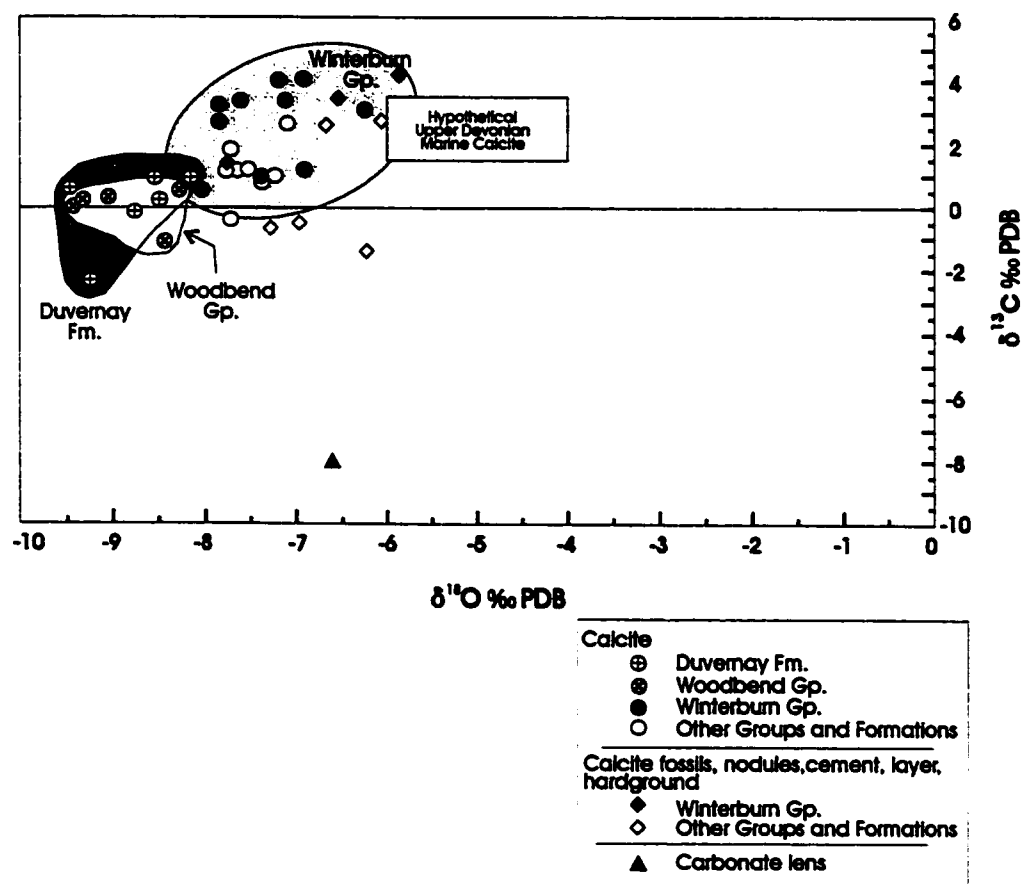


Figure 5.8: Calcite samples in a plot of $\delta^{18}\text{O}$ (PDB) versus $\delta^{13}\text{C}$ (PDB) with respect to stratigraphic units from which the samples have been taken. The white rectangular box indicates hypothetical marine calcites (after Amthor et al., 1993 and references therein). It is apparent that calcites from the Duvernay Fm. and the Woodbend Gp. are depleted in $\delta^{13}\text{C}$ and $\delta^{18}\text{O}$, whereas calcites from the Winterburn Gp. are enriched.

(Appendix 1), are generally more enriched in $\delta^{18}\text{O}$ than samples from the Woodbend/Winterburn and Woodbend Groups (Figure 5.9). This is similar to the relationship identified with the calcite population.

Fluids, tectonically expelled during the Laramide orogeny and proposed to have migrated through the Southesk Cairn Complex (Machel et al., 1996; Cavell and Machel, 1996, 1997), must have had the greatest potential to interact with aquitards near the disturbed belt. In a plot of the $\delta^{18}\text{O}/\delta^{13}\text{C}$ of the ankerite/dolomite population, ankerites distant from the disturbed belt, e.g. in the West Pembina area, relative to ankerites and dolomites near the disturbed belt, appear slightly more enriched in $\delta^{18}\text{O}$ (Figure 5.10). This could indicate that ankerites recrystallized at slightly lower temperatures in the West Pembina area than those nearer the disturbed belt. However, this enrichment may also be stratigraphic- or lithofacies- dependent, as most of these samples are from the Winterburn Group (Figure 5.9) and lithofacies AD. No significant trend was identified with the calcite population.

The $\delta^{18}\text{O}$ values of the calcite and ankerite/dolomite population, when plotted with respect to mineralogical facies did not reveal any significant correlations. As well, with respect to the current depths of the samples, no significant correlations were identified despite the approximately 2.7 km range in depths between the samples.

5.3.5. Synopsis

The calcite population most likely formed in isotopic equilibrium with Upper Devonian seawater and also recrystallized from marine-equilibrated carbonates at higher temperatures. The $\delta^{18}\text{O}$ of the calcites have been altered from their marine values, and the $\delta^{13}\text{C}$ has been affected by shallow burial processes such as the oxidation of organic carbon.

The ankerite/dolomite population, which formed from the recrystallization of marine carbonate is generally more depleted relative to hypothetical Upper Devonian Marine dolomites than the $\delta^{18}\text{O}$ of the calcite population is relative to hypothetical Upper Devonian marine calcites. The ankerite/dolomite population,

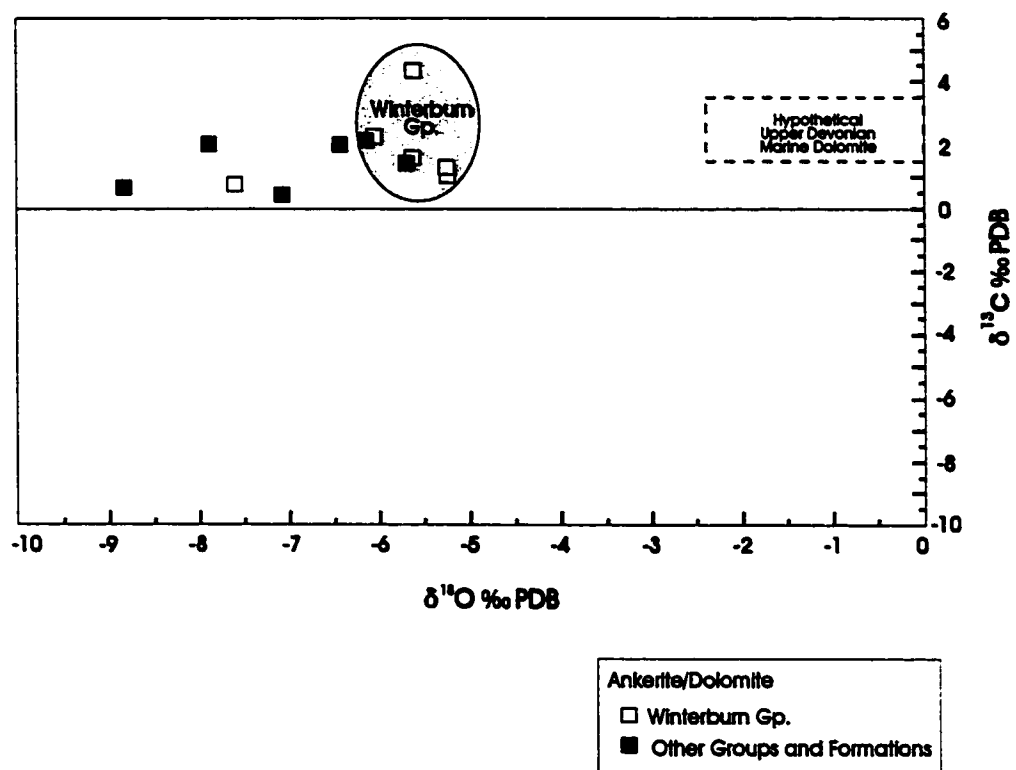


Figure 5.9: Ankerite and dolomite samples in a plot of $\delta^{18}\text{O}$ (PDB) versus $\delta^{13}\text{C}$ (PDB) with respect to stratigraphic units from which the samples have been taken. The white rectangular box with dashed lines indicates hypothetical marine dolomites (after Amthor et al., 1993 and references therein). From the data analyzed, it is apparent that all but one of the ankerites from the Winterburn Gp. are more depleted in $\delta^{13}\text{C}$ and $\delta^{18}\text{O}$ than the other samples.

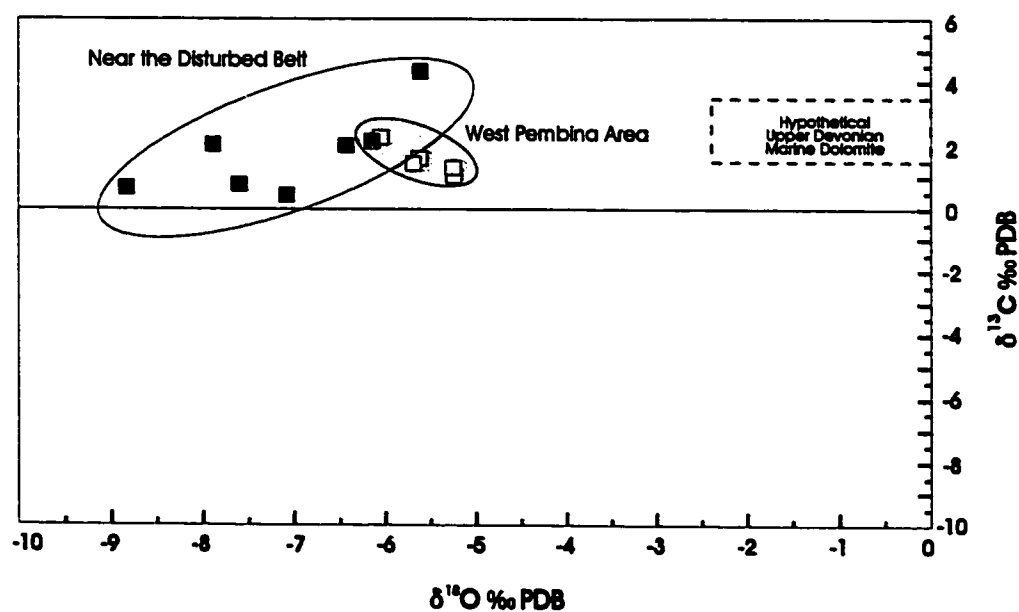


Figure 5.10: Ankerite and dolomite samples in a plot of $\delta^{18}\text{O}$ (PDB) versus $\delta^{13}\text{C}$ (PDB) relative to distance from the limit of the disturbed belt. The white rectangular box with dashed lines indicates hypothetical marine dolomites (after Amthor et al., 1993 and references therein). Samples from the West Pembina area, i.e., distant from the disturbed belt, tend to be enriched in $\delta^{18}\text{O}$ relative to those near the disturbed belt. The enrichment in the West Pembina samples may be stratigraphic- or lithofacies-dependent rather than dependent on proximity to the disturbed belt.

thus, has been calculated to form under slightly more elevated temperatures than the calcite population, and similar to the calcite population, its $\delta^{13}\text{C}$ has also been affected by shallow burial processes e.g., degradation by methanobacteria and oxidation of organic carbon.

Combined, both populations formed and/or recrystallized at relatively low temperatures (between 30 and 77°C), coinciding with temperatures estimated for Devonian sea water and at relatively shallow burial depths of up to approximately 1.8 km in the Alberta Basin. Presently the aquitards are buried to depths of between approximately 2.6 km and 5.3 km. The temperatures and depths of formation or recrystallization, derived from stable isotopic analyses indicate, therefore, that the carbonate fraction of the aquitards, including individual calcite fossils, nodules, etc. within the aquitards, have not isotopically re-equilibrated with respect to present-day diagenetic conditions. This implies that the aquitards have been generally impermeable to aqueous formation fluids since the Late Devonian/Early Carboniferous. This is the first, major conclusion of this study toward achieving an objective of this study (refer to Chapter 1).

5.4. Radiogenic Isotopic Analyses

5.4.1. Samples and Procedures

$^{87}\text{Sr}/^{86}\text{Sr}$ analysis was completed on twenty-one samples, a subset of those analyzed for $\delta^{18}\text{O}$ and $\delta^{13}\text{C}$. Most of these samples represent whole-rock calcite and ankerite fractions. Additionally, five samples representing carbonate nodules, laminations, etc., and one sample of celestite were also analyzed (Appendix 1). Only three whole-rock samples, CCS 35', 152, and 3B, contain a combination of both calcite and ankerite in their whole-rock matrices (Appendix 1 and Table 4.1). Whereas in stable isotope analyses it was possible to chemically separate and analyze both the calcite and ankerite fractions in a single sample (other than for those described in Section 5.3.1), in $^{87}\text{Sr}/^{86}\text{Sr}$ analyses, because the two phases of carbonate could not be mechanically separated from each other, the total carbonate content (e.g., a combination of calcite and ankerite)

was used. An acid-leaching process (described in Appendix 3) after Cavell and Machel (1997), was followed to ensure that strontium was extracted from only the carbonate fraction of the whole-rock samples since this is the only fraction that could have released strontium under the prevailing diagenetic conditions (Cavell and Machel, 1997). Where the $^{87}\text{Sr}/^{86}\text{Sr}$ ratios of the three samples containing a combination of whole-rock calcite and ankerite are plotted against $\delta^{18}\text{O}$ values of the individual calcite and ankerite phases, two separate $\delta^{18}\text{O}$ analyses (representing calcite and ankerite) are present for every $^{87}\text{Sr}/^{86}\text{Sr}$ analysis (representative of the a combination of calcite and ankerite, or total carbonate).

The highest $^{87}\text{Sr}/^{86}\text{Sr}$ ratio from the West Pembina area is 0.7120, a value recently been defined as *MASIRBAS* - the *MAXimum Strontium Isotope Ratio of the BASinal Shale* (Cavell and Machel, 1997). This value serves to define the $^{87}\text{Sr}/^{86}\text{Sr}$ background delivered by the clastic sedimentary units in the basin. Cavell and Machel (1996 and 1997) and Machel et al. (1996) interpreted higher strontium isotope signals as either tectonic, i.e., from tectonically expelled fluids from the disturbed belt, or from the basement, i.e., from fluids which ascended via faults from the crystalline basement.

Unlike $\delta^{18}\text{O}$ and $\delta^{13}\text{C}$, $^{87}\text{Sr}/^{86}\text{Sr}$ is not significantly fractionated so it may be used to study provenance. $^{87}\text{Sr}/^{86}\text{Sr}$ ratios reflect the contributions from: (1) the host rock (limestone, dolomite, and impurities); (2) any fluids from external sources; and (3) the degree of water-rock interactions (e.g. Banner, 1995). In Figure 5.11, *MASIRBAS* and the $^{87}\text{Sr}/^{86}\text{Sr}$ composition of Late Devonian seawater, which varies between approximately 0.7079 to 0.7084 (Burke et al., 1982), have been plotted. The latter, combined with proposed values for the $\delta^{18}\text{O}$ of dolomites and calcites in isotopically equilibrium with Late Devonian seawater (-4 to -6‰ PDB for calcites and 0 to -2.4‰ PDB for dolomites (Amthor et al., 1993 and references therein)), provides an estimate of the fluid compositions of marine equilibrated calcites and dolomites during the Late Devonian.

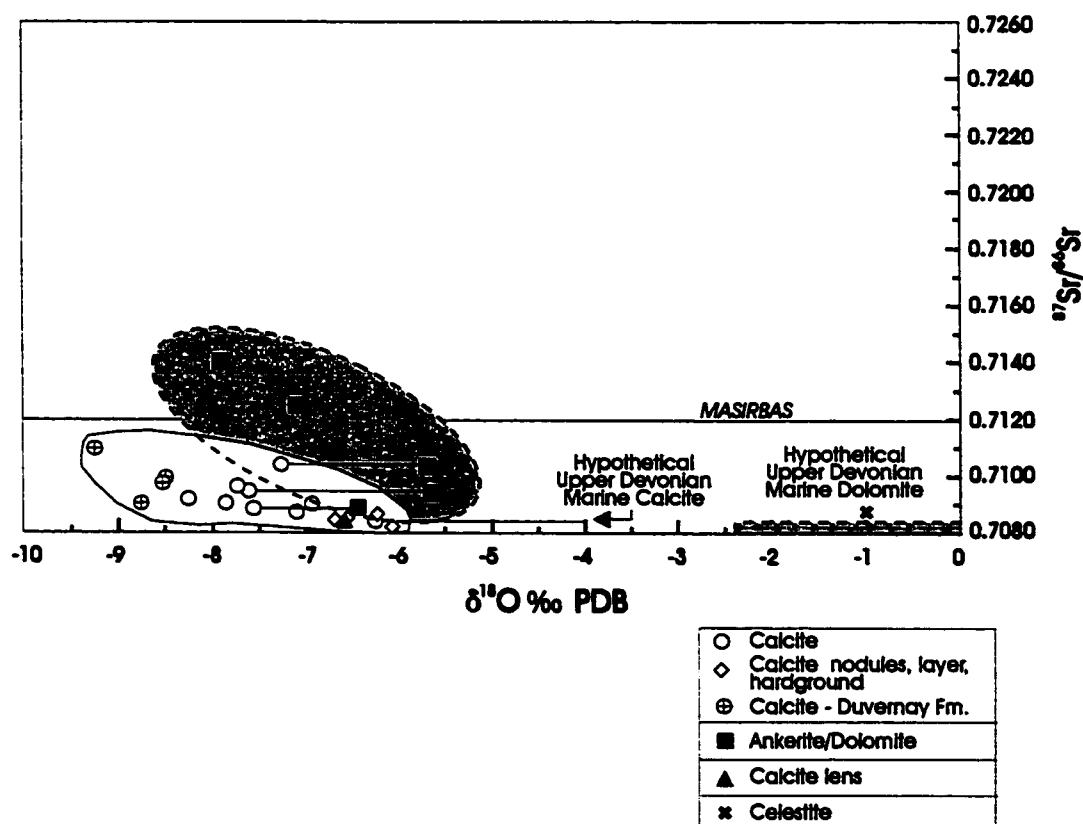


Figure 5.11: Plot of $\delta^{18}\text{O}$ PDB versus $^{87}\text{Sr}/^{86}\text{Sr}$. Rectangular boxes indicate hypothetical marine calcites and dolomites (after Burke et al., 1982; and Amthor et al., 1993 and references therein). Two fields of data representing a calcite population and an ankerite/dolomite population are evident. The two carbonate phases within these three samples, with separate $\delta^{18}\text{O}$, but common $^{87}\text{Sr}/^{86}\text{Sr}$ ratios, are connected with tie-lines. One sample of celestite was analyzed for $^{87}\text{Sr}/^{86}\text{Sr}$ however, was designated a $\delta^{18}\text{O}$ ratio of -1 ‰ PDB. See text for explanation.

5.4.2. Results

• $^{87}\text{Sr}/^{86}\text{Sr}$ and $\delta^{18}\text{O}$

A $\delta^{18}\text{O}$ versus $^{87}\text{Sr}/^{86}\text{Sr}$ plot was constructed for twenty-four samples, a subset of the samples analyzed for $\delta^{18}\text{O}$ and $\delta^{13}\text{C}$ (Figure 5.11). The carbonate samples plot in two distinctive fields. The $^{87}\text{Sr}/^{86}\text{Sr}$ ratio for the calcite population ranges from 0.7083 to 0.7110 with $\delta^{18}\text{O}$ ranging from -6.1 to -9.3‰ PDB, and the $^{87}\text{Sr}/^{86}\text{Sr}$ ratio for the ankerite/dolomite population ranges from 0.7089 to 0.7140 with $\delta^{18}\text{O}$ ranging from -5.6 to -7.9‰ PDB. The celestite sample has a $^{87}\text{Sr}/^{86}\text{Sr}$ ratio of 0.7088. The celestite sample was not analyzed for $\delta^{18}\text{O}$, but instead was designated a $\delta^{18}\text{O}$ ratio of -1, in order to be included in the plot of $\delta^{18}\text{O}$ versus $^{87}\text{Sr}/^{86}\text{Sr}$ (Figure 5.11).

5.4.3. Interpretation

Three samples; including a carbonate nodule, a calcite-rich lamination, and a whole-rock calcite fraction have $^{87}\text{Sr}/^{86}\text{Sr}$ within the estimated range for Upper Devonian seawater (Figure 5.11 and Appendix 1). The celestite sample and remainder of the calcite and ankerite/dolomite populations are slightly more enriched in $^{87}\text{Sr}/^{86}\text{Sr}$ relative to Upper Devonian seawater. This enrichment indicates that during burial, to depths of 1.6 km, Devonian marine parentage fluids and/or the carbonate fractions interacted with the silicate fraction of the shales.

Two samples from the ankerite/dolomite population with $^{87}\text{Sr}/^{86}\text{Sr}$ ratios of 0.7125 and 0.7140 plot above *MASIRBAS* and are anomalous to the rest of the data set. These two samples consist of a whole-rock dolomite fraction from the Obed region and a whole-rock ankerite fraction from the Wild River Basin. Values above *MASIRBAS* have been interpreted to be tectonic in origin, i.e., from tectonically expelled fluids, or from the basement, i.e., from fluids which ascended from the crystalline basement via faults (Cavell and Machel, 1997;

Machel et al.,1996). As such, these fluids may have interacted with the shales, percolating through faults and interacting with the shales, within and around the Obed area and Wild River Basin. Supporting this is evidence of a possible late-stage fracture associated with a calcite-dolomite-pyrite vein system in the same core from which the most radiogenic sample has been analyzed. However, it is possible that the enrichment in radiogenic strontium may be accounted for otherwise. Although significant measures were taken to ensure that strontium was extracted from only the carbonate fraction during the chemical leaching process, it is possible that because these two samples have significantly low carbonate percentages (9 and 13 weight %), radiogenic strontium from the silicate fraction may have also been leached. In a plot of carbonate content (completed by acid dissolution) versus $^{87}\text{Sr}/^{86}\text{Sr}$, a slight negative correlation between these two variables is present. Another explanation for the enrichment is that during recrystallization of the carbonate fraction, which for these two shales occurred at slightly higher temperatures (indicated by the relatively depleted $\delta^{18}\text{O}$ ratios) relative to the remainder of the ankerite/dolomite population, interaction between the silicate and the carbonate portion of the two shales may have occurred.

5.4.4. Trends in $^{87}\text{Sr}/^{86}\text{Sr}$ versus $\delta^{18}\text{O}$

The sample (or outlier) with the most depleted $\delta^{13}\text{C}$ ratio of all the samples (-8.0‰ PDB $\delta^{13}\text{C}$) (Figure 5.7), does not have an anomalous $^{87}\text{Sr}/^{86}\text{Sr}$ ratio, rather its $^{87}\text{Sr}/^{86}\text{Sr}$ ratio correlates with calcite equilibrated with Late Devonian seawater.

Within $^{87}\text{Sr}/^{86}\text{Sr}$ versus $\delta^{18}\text{O}$ plots, the $^{87}\text{Sr}/^{86}\text{Sr}$ of both the calcite and ankerite/dolomite populations have been correlated with their corresponding stratigraphic levels. From the samples analyzed, only the calcite samples from the Duvernay Formation show any interesting results. Four of the five samples representing the Duvernay Formation appear more depleted in $\delta^{18}\text{O}$ than the other Formations and Groups, the one that is not depleted represents a

carbonate hardground. A more detailed explanation regarding the likely cause for depletion was provided in Section 5.3.4..

5.4.5. Synopsis

In a pilot study by Cavell and Machel (1997), the strontium isotopic compositions of the carbonate fractions of three basinal shales; the Ireton, Duvernay, and Cynthia samples (included in this study as CCS-35', 81', and 132' respectively) (Appendix 1), were found to be well within the most common range for adjacent, early, dolomitized reefal carbonates. From this it was inferred that calcite recrystallization and minor dolomitization within the shale and marl aquitards probably occurred at about the same time as early, regional, pervasive dolomitization of matrix limestones in the adjacent carbonate aquifers. The majority of samples in this study that were analyzed for $^{87}\text{Sr}/^{86}\text{Sr}$ are depleted in $\delta^{18}\text{O}$ (by up to 7.9‰) and slightly enriched in $^{87}\text{Sr}/^{86}\text{Sr}$ (by up to 0.0061) relative to those that equilibrated with Devonian seawater (Figure 5.11). This suggests that in this study, formation or recrystallization occurred under conditions similar to that proposed by Cavell and Machel (1997). In contrast to late-calcite cements in adjacent carbonate aquifers, such as that identified in the Leduc Formation in the Obed area with ratios of up to 0.7255 (Patey, 1995), the $^{87}\text{Sr}/^{86}\text{Sr}$ ratios of the carbonate fraction within the shale and marl aquitards are not nearly as radiogenic, with a maximum $^{87}\text{Sr}/^{86}\text{Sr}$ of 0.7140.

Mountjoy et al. (1992) and Duggan (1997) proposed a number of sources for radiogenic strontium identified within late-stage cements occluding porosity in the Leduc Formation; including adjacent illitic shales, Precambrian basement rocks, and the underlying metasedimentary strata. Cavell and Machel (1997) explained that under the prevailing diagenetic conditions the shales (and marls) could not have produced the necessary amount of ^{87}Sr to contribute to the cements in adjacent aquifers of the Leduc Formation. Rather, metamorphic conditions would have to be encountered before the radiogenic strontium would be released from the silicate fraction to contribute to the cements in adjacent aquifers of the Leduc Formation (Cavell and Machel, 1997). No fluid with a

$^{87}\text{Sr}/^{86}\text{Sr}$ ratio above 0.7120, was produced from the shales and marls to form the Obed area calcite cements. A more probable source is an external, non-basinal source for ^{87}Sr of tectonically expelled fluids, during the Laramide orogeny, or hydrothermal to metamorphic fluids from metasedimentary units, either Proterozoic or Paleozoic, which underlie the Devonian sequence (Machel et al., 1996; Machel and Cavell, 1999).

5.5. Paragenetic Sequences

5.5.1. Introduction

Using core, thin section, and geochemical analyses, two relatively simple paragenetic sequences have been developed for the aquitards; one for the generally more basinal lithofacies such as A, AD, B, and C and another for the near-reef lithofacies such as G and GE and also lithofacies F (Figure 5.12).

- *Near-Basinal Lithofacies A, AD, B, C*

A paragenetic sequence is presented for lithofacies A, AD, B, and C that form in basinal areas, on the toe of the foreslope, and middle foreslope regions (Figure 5.12). Geochemical analyses of several phases of calcite, whole-rock ankerites and dolomites, and also of one celestite sample within these lithofacies, strongly suggest that these phases formed and/or recrystallized at a relatively early diagenetic stage, i.e., during the Late Devonian to Early Carboniferous. The matrix ankerite and dolomite probably formed and/or recrystallized at a slightly later diagenetic stage under higher temperatures (between 43 and 77°C), and at greater depths (between approximately 433 m and 1.8 km) than the calcite population that formed and/or recrystallized between 30 and 61°C, which coincides with burial depths of between approximately 200 m and 1.4 km (Figure 5.12). Several stages of pyrite have formed throughout the diagenetic history of these lithofacies. Pyrite that occurs disseminated throughout the matrix, concentrated in laminations, completely or nearly completely replacing calcite fossils, on the inside edges of nodules and

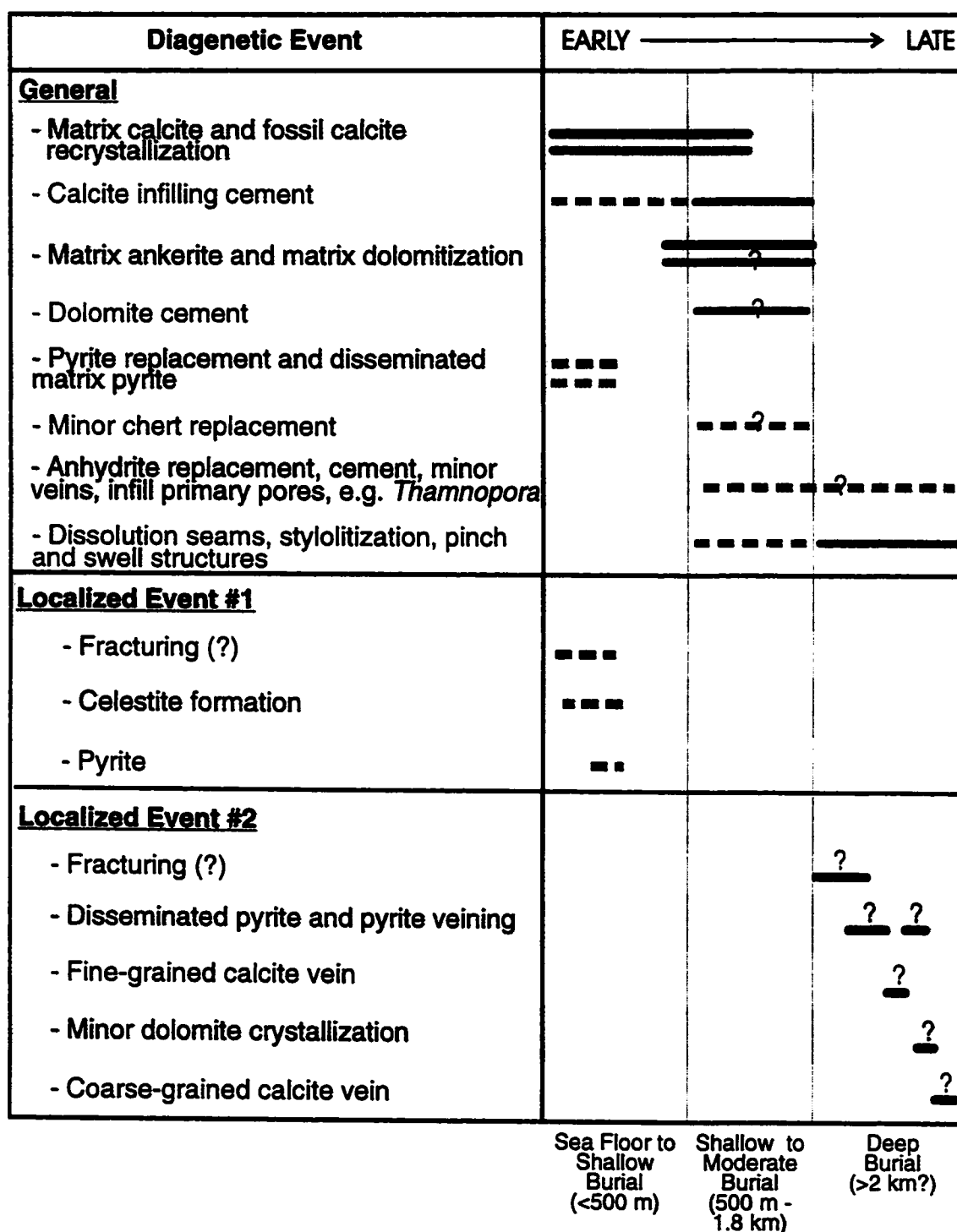


Figure 5.12: Paragenetic sequences for basinal and near-basinal lithofacies A, AD, B, C indicated with black lines and for near-reef lithofacies G, GE, and also lithofacies F and to some extent AE, indicated with grey lines.

lenses, and completely rimming fossils, likely formed at a relatively early stage, as a by-product of bacterial sulfate reduction, which commonly occurs at depths of below 200 m (Machel, pers. comm.).

Two localized diagenetic events are evident within near-basinal facies. In one core, a celestite vein or fracture fill is present. The pyrite associated with this vein or fracture fill of celestite formed at a relatively early stage, but after the formation of celestite, again most likely as a by-product of bacterial sulfate reduction. Another core contains a calcite-pyrite-dolomite vein system that likely represents the latest diagenetic event within these lithofacies. This vein system likely formed during deep burial (e.g., > 2 km), although geochemical analyses could not be completed on the carbonate fractions of this vein filling event to confirm this interpretation. However, elevated ^{87}Sr present within the whole-rock carbonate fraction of a Woodbend Group shale in the same core less than 35' beneath this vein system, supports the interpretation that this vein system is related to a late-stage event. The relative ages of the calcite, pyrite, and dolomite phases within the vein are known (Figure 5.12).

- *Lithofacies F, G, and GE*

A paragenetic sequence for the generally upper foreslope and near-reef lithofacies such as G and GE, as well as for lithofacies F and AE, is set apart from the paragenetic sequence described above for the near-basinal lithofacies. Although the near-reef lithofacies have experienced a similar diagenetic history as near-basinal lithofacies, with the exception of the two localized events described above, the near-reef lithofacies have been exposed to further diagenetic alteration. The presence of chert, secondary anhydrite, coated grains, dolomite cement, stylolites, dissolution seams, and pinch and swell structures within this near-reef lithofacies paragenetic sequence, are absent and separates it from the near-basinal paragenetic sequence.

Stable and radiogenic isotopic analyses conducted on individual carbonate portions within these lithofacies, such as fossils, nodules, and cements, and also on the whole-rock carbonate fractions, indicate that

recrystallization occurred at an early stage, i.e., before the Early Carboniferous, and that they have not re-equilibrated since this time, although dolomites and ankerites appear to have formed and/or recrystallized at higher temperatures and depths than the calcite population. The minor presence of secondary anhydrite in these lithofacies suggests that a later, but minor, fluid event interacted with the shales. However, this late-fluid event that precipitated the highly radiogenic calcites and dolomites in Devonian carbonate aquifers, did not influence the aquitards.

5.6. Conclusions

Stable isotope analyses of several calcite forms, and whole-rock ankerites and dolomites, indicate that shale and marl aquitards have most likely acted as effective barriers to aqueous fluids since the Late Devonian/Early Carboniferous. The $^{87}\text{Sr}/^{86}\text{Sr}$ ratios of three calcites are analogous with the ratio of calcites equilibrated with Upper Devonian seawater. Most other calcites, and all ankerites and dolomites are slightly more radiogenic. However, they are not nearly as radiogenic as late-stage calcite cements present in adjacent Leduc Formation in the Obed area with $^{87}\text{Sr}/^{86}\text{Sr}$ ratios of up to approximately 0.7255, where ^{87}Sr appears to have been derived from tectonically induced fluids associated with the Laramide orogeny or from fluids ascending from the Precambrian crystalline basement through subvertical faults. It is unlikely that these external fluids strongly interacted with the aquitards, either near or distant from the disturbed belt. This is the second major conclusion of this study toward achieving the objectives of this study. A potential exists for localized interaction of these fluids with shales from within the Obed area and Wild River Basin, where elevated ^{87}Sr carbonate fraction of shales exist. However, other reasons may account for this enrichment, such as the leaching of radiogenic strontium from the silicate fraction.

Two simplified paragenetic sequences have been developed for the aquitards; one for the generally near-basinal lithofacies, and a second for the generally near-reef lithofacies. The near-basinal lithofacies consists of matrix

calcite and fossil calcite recrystallization, matrix ankerite and matrix dolomite, pyrite replacement and formation of matrix pyrite, which formed during early to moderate burial in the paragenetic sequence. In addition, two localized diagenetic events including a celestite vein and a calcite-pyrite-dolomite vein system are evident. The latter of these two most likely represents a late stage (> 2 km) event.

The paragenetic sequence of the near-reef lithofacies is similar to that of the near-basinal lithofacies, with the exception of the two localized diagenetic events. The near-reef lithofacies paragenetic sequence differs from the near-basinal sequence in that chert, anhydrite, coated grains, stylolites, dissolution seams, and pinch and swell structures are present. The presence of secondary anhydrite indicates a potential minor interaction with late-stage fluids.

6. Chapter 6 - Aquitard Integrity and Fluid Migration Pathways

6.1. Introduction and Objectives

In recent studies of the Bashaw Reef Complex in the east-central Alberta Basin, breaching of the Ireton aquitard by hydrocarbons was interpreted to occur where the aquitard was either less than 4 m in thickness, or up to 10 m but with a carbonate content of greater than 80% (Hearn, 1996; Rostron and Toth, 1996; and Rostron et al., 1997). The potential for these aquitards to be breached was supported by physical evidence, such as hydrocarbon staining in aquitard fractures, and with mercury injection capillary pressure measurements (MICPM). Breached aquitards produced significantly lower initial entry pressures those that were effective seals.

This chapter presents MICPM data from Upper Devonian aquitards in west-central Alberta. This data is used to predict the seal integrity of the aquitards, by calculating the hydrocarbon column heights sustainable by the aquitards.

Magnetic susceptibility, an uncommon technique used to predict hydrocarbon migration pathways through various media (e.g., Elmore et al., 1989; Machel, 1996), was applied to a small data set of effectively sealed aquitards as well as breached aquitards by Hearn (1996). Unfortunately, this technique did not reveal any signal related to oil seepage, i.e., potential hydrocarbon migration pathways through the aquitards. Magnetic susceptibilities from a larger data set of samples from aquitards in the west-central Alberta Basin are presented in this chapter, in a further attempt to predict hydrocarbon pathways through, or breaches within, the aquitards.

Finally, a general set of migration pathways for brines and hydrocarbons within the Devonian system have been developed using results from MICPM and magnetic susceptibilities presented in this chapter, combined with stratigraphic and structural cross sections presented in Chapter 3, and from geochemical analyses presented in Chapter 5.

6.2. MICPM

6.2.1. Introduction and Sampling Techniques

MICPM tests have been in use for about fifty years to simulate the migration of hydrocarbons through core (Jennings, 1987). In these tests, mercury, which acts as a nonwetting phase, is injected into an uncovered sample, conventionally one inch in diameter by one inch in length, in a stepwise fashion (Appendix 3). Conventionally, vertically drilled core plugs of shale cap-rocks or seals are taken for MICPM; however, most plugs taken for MICPM in this study have been drilled horizontally (Figure 6.1).

One of the main objectives for conducting MICPM tests was to identify the sealing capacity of aquitards to hydrocarbons. However, samples selected for MICPM were taken from aquitards not presently functioning as hydrocarbon seals. These results may, with limitations, be applied to aquitards acting as hydrocarbon seals where core has not been drilled. A set of samples representative of (near-)basinal facies, selected from several stratigraphic units over a widespread geographic area, was found to be adequate for testing (Table 6.1).

6.2.2. Pressure Terminology and Calculations of Breaching Potential

Several types are associated with data from MICPM, e.g., initial entry, threshold, closure, breakthrough, leakage, and displacement (e.g., Hearn, 1996; Krushin, 1997; and Sneider et al., 1997). These terms can often be misleading if not initially defined. In this project, only initial entry pressures are discussed.

Initial entry pressure (closure pressure) is defined as the pressure at which mercury first enters the pore system of the rock (Sneider et al., 1997). When the combined driving forces on hydrocarbons, which are provided by buoyancy and hydrodynamic flow, exceed the resistive forces of the aquitard, hydrocarbon leakage occurs (Rostron and Toth, 1996). Initial resistance to leakage through the aquitard is provided by the difference in initial entry

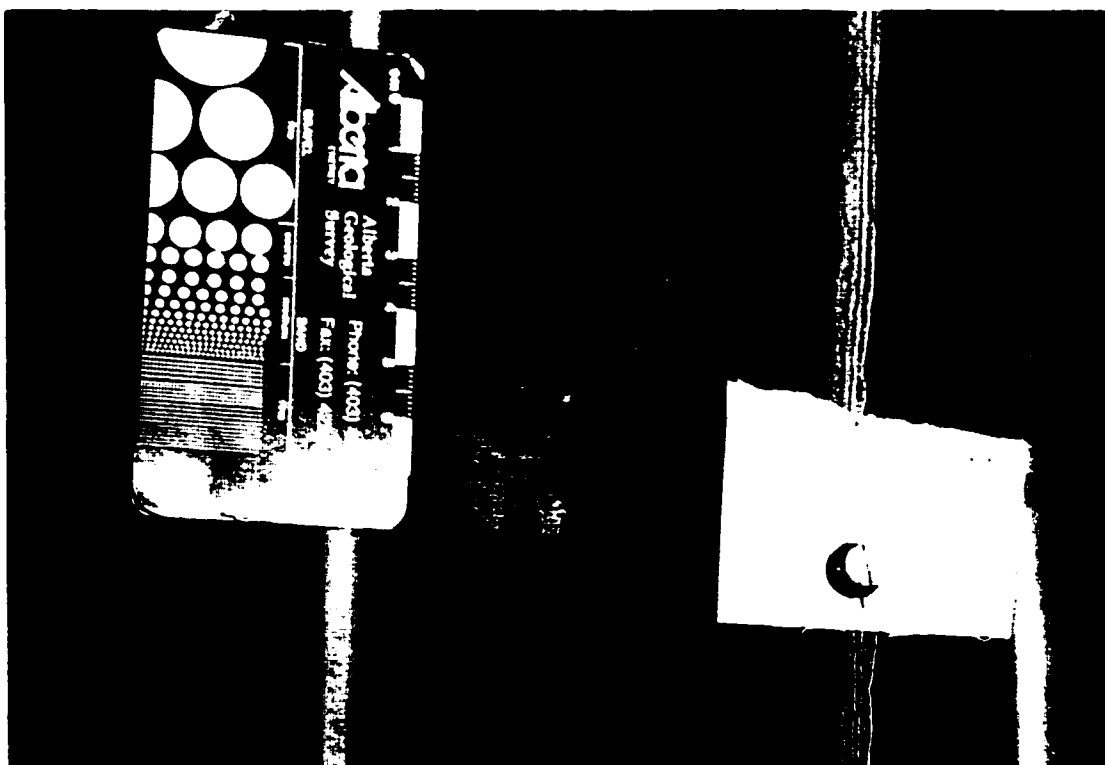


Figure 6.1: Horizontal drill core plug taken for MICPM tests. Drill core is from the Woodbend Group; well 8-26-55-22W5, 12516.2' (3814.9 m).

Sample #	Carbonate Percentage	Lithologies	Mineralogical Notes	Stratigraphic Unit	Thickness Approximate	Location
CCS 3B	~55	A (interfingered with C)	CQp	Woodbend/ Winterburn Gp.	10 m	adjacent to Peace River Arch
CCS 46	32	A (interfingered with F)	QCp	Woodbend Gp.	80 m	Obed
CCS 66	55	A (interfingered with F)	Cq	Majeau Lake Fm.	18 m	Swan Hills Platform north of Pine Creek Basin
CCS 11	~10	A	QCp	Duvernay Fm.	256 m	adjacent to Peace River Arch
CCS 105	42	AD (interfingered with F)	CQp	Winterburn Gp.	10 m	West Pembina
CCS 22B	~40-50	A	QCp	Woodbend Gp.	150 m	Wild River Basin
CCS 68	10	AE	QCp	Majeau Lake Fm.	18 m	Swan Hills Platform north of Pine Creek Basin
CCS 51	13	A	QCp	Woodbend Gp.	8-10 m	Windfall
CCS 20	~20-30	A	QCp	Woodbend Gp.	150 m	Wild River Basin
CCS 61	31	A	QCp	Majeau Lake Fm.	30 m	East of Sturgeon Lake - West Shale Basin
CCS 1	54	A (interfingered with C)	CQp	Woodbend/ Winterburn Gp.	10 m	adjacent to Peace River Arch

Table 6.1: Data from eleven samples taken for MICPM tests.

pressures of the reservoir and the aquitard. The resistive force can be expressed in terms of the hydrocarbon column height (H_o) sustainable by the aquitard using the following equation (Schowalter, 1979):

$$H_o = \frac{P_{db} - P_r}{(\rho_w - \rho_h)g} \quad \text{Equation 1.}$$

where; P_{db} is the subsurface hydrocarbon-water breaching pressure (psi) of the aquitard; P_r is the subsurface hydrocarbon-water breaching pressure of the reservoir rock (for a good quality reservoir rock this value is assumed to be 0 (Krushin, 1997)); ρ_w is the water density (≈ 1 g/cc); ρ_h is the hydrocarbon density in the reservoir (≈ 0.7 g/cc for oil and ≈ 0.1 g/cc for gas); and g is the hydrostatic gradient of fresh water (0.433 psi/ft). The hydrocarbon column height sustainable by the seal, H_o (in feet), provides a useful measure of sealing capacity of the aquitard. To initiate leakage in a hydrostatic system, the vertical component of the hydrocarbon column must exceed the H_o .

Before Equation 1 can be calculated, mercury initial entry pressures (from MICPM curves such as in Figures 6.2 a, b, and c; and also documented in Table 6.2) must be converted to a hydrocarbon breaching pressure (P_{db}) using the following equation (after Purcell, 1949):

$$\frac{P_{CHg/a}}{P_{CHc/w}} = \frac{-(\delta_{Hg/a}) (\cos\theta_{Hg/a})}{(\delta_{Hc/w}) (\cos\theta_{Hc/w})} \quad \text{Equation 2.}$$

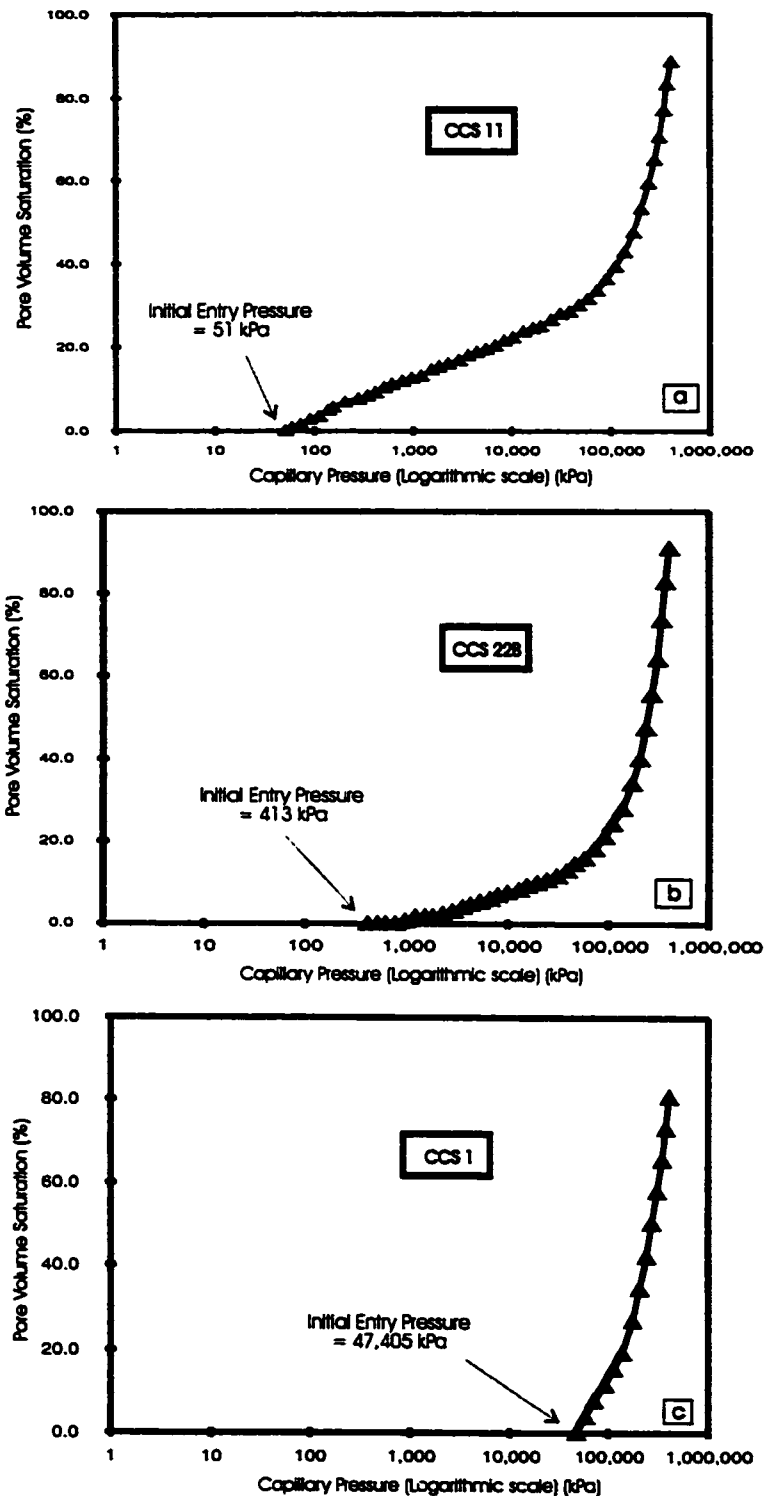
where

$\delta_{Hg/a}$ = 480 dynes/cm, surface tension of Hg/air

$\delta_{Hc/w}$ = ≈ 32 (oil), ≈ 70 dynes/cm (gas), surface tension of hydrocarbon/water

$\theta_{Hg/a}$ = 140° , contact angle of Hg/air

$\theta_{Hc/w}$ = 0° , contact angle of hydrocarbon with water



Figures 6.2 a, b, and c: Capillary pressure versus pore volume mercury saturation profiles. Data have been corrected in that the amount of mercury injected at low pressures (refer to Figures 6.3 a, b, and c) has been subtracted prior to construction of these profiles. On each profile, the initial entry pressures of the MICPM curves are indicated with arrows. Sample CCS 11 represents an ineffective barrier to hydrocarbons, whereas CCS 228 and CCS 1 are relatively effective barriers. See text for further explanation. These pressures are used to calculate oil and gas column heights, H_{og} , sustainable by the aquitards.

Sample	Initial Entry Pressure at CO ₂ Breakthrough (psia)	Porosity (%)	Pore Volume Trapped by Hg (%)	Porosity Ratio (mmHg)	Oil Column Height calculated from initial entry pressure (ft)	Gas Column Height calculated from initial entry pressure (ft)
CCS 3B	—	tiny	nil	tiny	?	?
CCS 4B	—	tiny	nil	tiny	?	?
CCS 6B	—	tiny	nil	tiny	?	?
CCS 11	51 (7.4)	3.6	89	0.011-0.135	1.5 (5)	1 (4)
CCS 105	206 (30)	1.3	82	0.006-0.011	6 (20)	5 (15)
CCS 22B	413 (60)	4.7	91	0.005-0.009	12 (40)	9 (29)
CCS 68	1,853 (269)	3.7	94	0.009-0.021	55 (180)	40 (131)
CCS 51	2,268 (320)	1.4	74	0.006-0.011	65 (214)	48 (156)
CCS 20	8,255 (1,197)	3.6	88	0.004-0.007	244 (801)	178 (585)
CCS 61	16,137 (2,340)	2.4	87	0.006-0.008	477 (1,566)	349 (1,144)
CCS 1	47,405 (6,874)	0.9	81	0.004-0.005	1,403 (4,602)	1024 (3,360)

Table 6.2: Data and values obtained from MICPM experiments, in addition to the oil and gas column heights sustainable by the aquitard samples.

Application of Equation 2, for an average oil and gas, results in a value of $P_{CHg/a} / P_{CHc/w}$ of 11.5 for oil and 5.25 for gas. Therefore, mercury initial entry pressures (in psi) (taken from MICPM curves and presented in Table 6.2) are simply divided by the gas or oil value to provided a value for P_{ab} prior to calculating H_o in Equation 1.

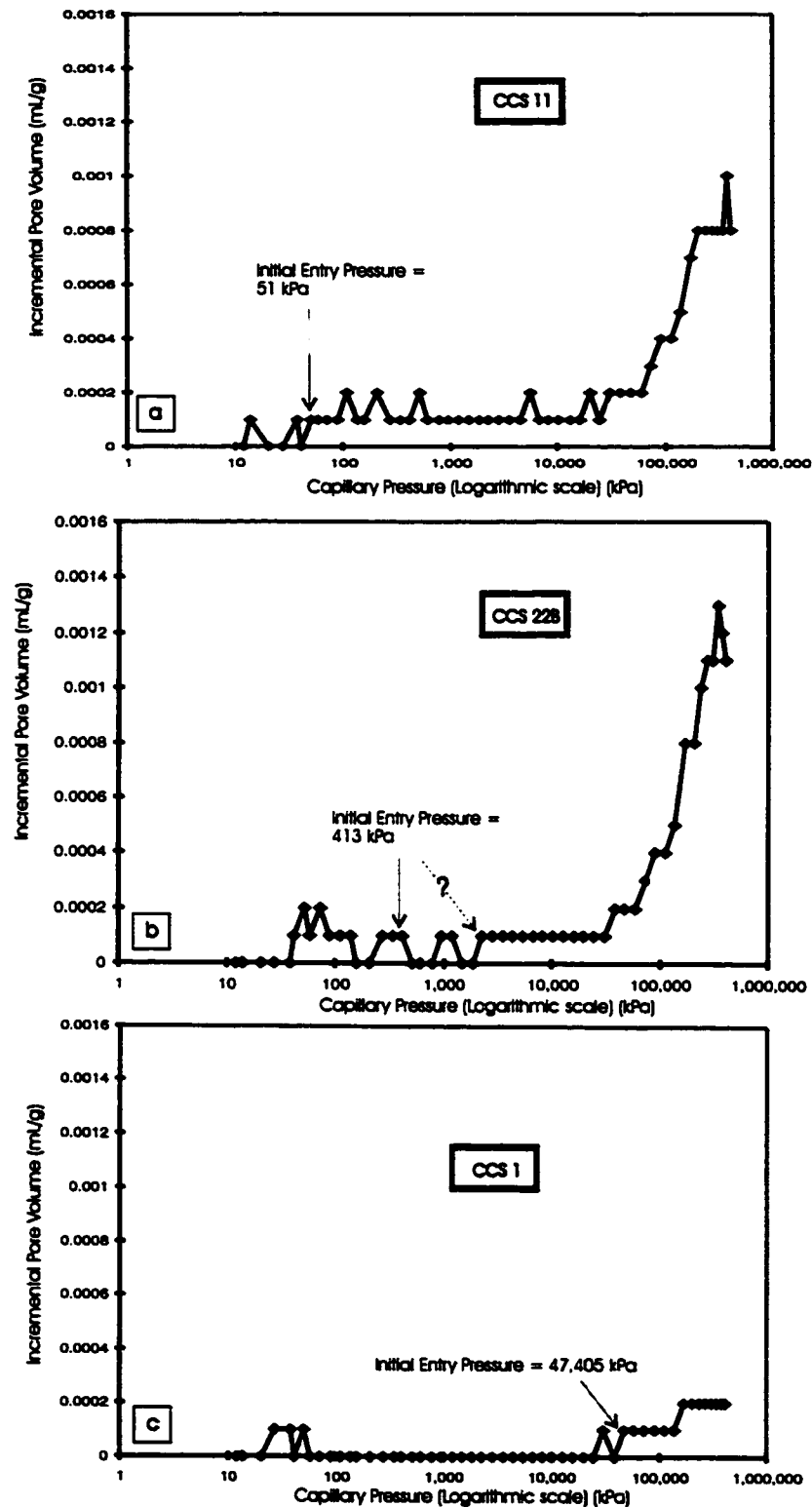
6.2.3. Results

The mercury initial entry pressure results for eight samples tested and the corresponding hydrocarbon column heights, H_o , sustainable by the aquitard samples are presented in Table 6.2. Three samples could not tested (the first three samples in Table 6.2) for MICPM due to their low porosity (considered to be below 0.9%, the lowest porosity tested in this study) and small pore size. The stratigraphic location of the ten of the eleven samples selected for MICPM, along with the corresponding initial entry pressures are indicated in cored well logs in Appendix 4.

6.2.4. Discussion

Initial entry pressures, such as those shown in Figures 6.2 a, b, and c are selected by the engineer from the "raw data" shown in Figures 6.3 a, b, and c, which, in these cases, correlates with a significant amount of mercury (≈ 0.0001 mg/L) entering the samples. It is possible that erroneous picks were chosen by the engineer for three of the eight samples tested (as suggested in sample CCS 22B in Figure 6.3 b, and also for CCS 105 and CCS 51).

Within the area of interest within the Alberta Basin, Devonian oil and gas pools (e.g., in fields such as Simonette, West Pembina, and Obed) can average between 10 m and 100 m (33' - 333') in thickness (e.g., White, 1960; Larson, 1969; and Rose, 1990). The aquitard samples not be able to withstand these hydrocarbon column heights, i.e., have oil and gas column heights of approximately 10 m or less (Table 6.2), would include CCS 11, CCS 105, and CCS 22B. However, it must be noted that the latter two of these samples likely have lower initial entry pressure than they actually should have, e.g., the



Figures 6.3 a, b, and c: Profiles of capillary pressure versus incremental pore volume of mercury injected. On each profile, the approximate locations of initial entry pressures of mercury, picked by the engineer in charge, are indicated. An erroneous pick is possible for sample CCS 228, and a suggested new pick is indicated with a dashed line. The spikes in the curves at pressures lower than initial entry pressures result from mercury entering surface irregularities and fissility in the samples. Compare these profiles to those in Figures 6.2.

pressures were erroneously picked as previously mentioned (refer to Figure 6.3 b). Therefore, it is only certain CCS 11 is an ineffective barrier to hydrocarbon column heights typically found in the study area. All other samples, including the three that could not be tested due to their low porosity and small pore size are considered to be effective barriers to fluid, and can withstand hydrocarbon column heights typically found within the Alberta Basin (of ≈ 10 m - 100 m).

Detailed investigations of the location of sample CCS 11 (Figure 6.4), show that the sample location from which CCS 11 has been taken is actually a very thin aquitard. It is important to note that this thin aquitard, although it has a low initial entry pressure (51 kPa), is overlain by a much greater aquitard of approximately 250 m in thickness, with only a thin intervening aquifer separating the two. Hydrocarbons are unlikely to pass through this overlying 250 m thick aquitard.

When comparing the relative oil column heights to gas column heights for each of the aquitard samples, it has been calculated that the aquitards can withstand greater oil columns relative to gas columns (Table 6.2). However, it should be noted that a given rock can seal a larger gas column than an oil column (Schowalter, 1979). The reason for this unexpected relation is that the high interfacial tension of the gas-water system compared to the oil-water system counteracts the higher buoyant pressure generated by gas-water systems.

Krushin (1997 and references therein) states that mercury entering the samples at pressures lower than the initial entry pressures (refer to Figures 6.3 a, b, and c), is attributed to mercury infilling surface irregularities such as nicks, gouges, and vugs. Such surface irregularities could form as a result of sampling procedures. As well, mercury entering the samples at such low pressures could partly be attributed to fissility. Fissility likely formed as a result of exposure of drill core to surface conditions, i.e., in a process comparable to isostatic rebound. It is unlikely that the samples are fissile at confining pressures of depths of approximately 2 to 5 km in the subsurface. However, an estimated 1.4 to 3.5 km of sediments have been eroded from the WCSB during the Tertiary (e.g., Magara, 1976; Bustin, 1991; Kalkreuth and McMechan, 1996; Duggan, 1997),

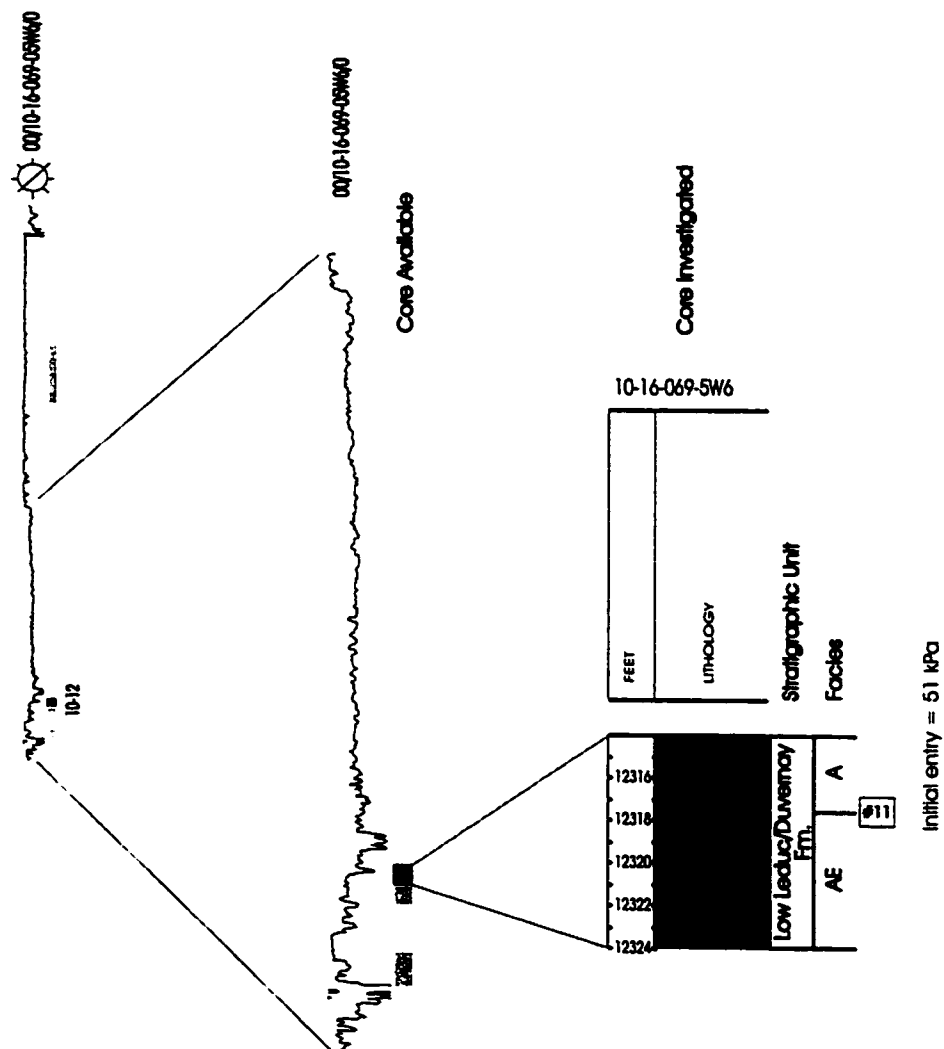


Figure 6.4: Interval of core investigated (in black) of the Low Leduc Platform and Duvernay Formation aquitard, and associated gamma log. The initial entry pressure derived from MICPM is included for sample #11. This is a suspended gas well.

which may have resulted in at least some isostatic rebound, possibly resulting in fissile shales and marls in the subsurface.

Although one might expect that MICPM tests would have resulted in leaky type signatures from upper foreslope/near-reef facies such as G and GE, due to their high carbonate percentage, because these facies were often sandwiched by near-basinal facies e.g., in the transition from carbonate aquifers into overlying aquitards, they were not tested. Had they occurred as thin, isolated aquitards, they would have been selected for MICPM. Moreover, these facies were often too fragile to obtain a core plug with the dimensions necessary for MICPM. Similarly, other lithofacies such as B and F were too fragile to obtain a core plug with the correct dimensions for MICPM, and therefore were not tested. The fragility of the samples is believed to be an artifact of alteration of the core from exposure to surficial conditions.

- *Normal and Overpressured Reservoirs*

The natural formation fluid pressures encountered within Devonian gas and oil reservoirs in the study area range from approximately 30,000 to 40,000 kPa (Wendte et al., 1998). Within the Wild River Basin, abnormally pressured gas reservoirs of the Leduc Formation exist, with formation fluid pressures of between 90,000 and 100,000 kPa (Wendte et al., 1998). These pressures are approximately 2 to 3 times in excess of the "normal" fluid pressures stated above. The question arises as to what effect these pressures have on enhancing hydrocarbon movement through the aquitards, which have significantly lower initial entry pressures of the sampled aquitards. This question remains to be answered and is beyond the current scope of the project.

6.3. Magnetic Susceptibility

6.3.1. Introduction

Magnetic susceptibility is a technique that has the potential to locate hydrocarbon breaches and delineate hydrocarbon migration pathways through various types of media, including solid rock and soil (Machel, 1996). The

rationale is based on the fact that hydrocarbons can generate or destroy magnetic minerals, creating anomalous magnetic signatures and resulting in either positive or negative contrasts (corresponding to enhanced or reduced total magnetization, respectively) to that of the background signature prior to hydrocarbon interaction (Machel, 1996; Hearn, 1996; and references therein). Thermodynamic modeling suggests that magnetic contrasts are likely to become more positive with depth and with closer proximity to hydrocarbon sources (Burton et al., 1993; Machel, 1996).

In an attempt to locate potential aquitard breaches, or possible hydrocarbon migration pathways through the aquitards, a series of measurements at room-temperature low-field susceptibility were conducted on twenty-eight whole-rock powders representing aquitards of variable thicknesses and lithofacies throughout the study area. This was conducted under the guidance of M.E. Evans in the Department of Physics at the University of Alberta (Appendix 3). Although XRD of the powdered samples (Table 4.1) did not reveal the presence of commonly magnetic minerals as magnetite, titanomagnetite, hematite, or pyrrhotite, the samples revealed low-frequency magnetic susceptibility. In a recent study of using magnetic susceptibilities as a lithological indicator near and within a magmatic intrusion, Grzymala (1995) isolated chlorite, a mineral not commonly associated with magnetism, in addition to magnetite, as the two most likely sources of the bulk of magnetic susceptibility. In this study, it follows that chlorite may have accounted for some of the low-frequency magnetic susceptibilities. However, it is more likely that the more common magnetic minerals, aforementioned, account for the low-frequency susceptibilities. It is probable that these minerals were not detected using XRD because they are present in quantities below their detection limits.

6.3.2. Sample Selection and Results

Most of the samples chosen for magnetic susceptibility represent near-basinal facies, similar to the population selected for MICPM. The majority of the samples represent lithofacies A (n=19), the remainder of the samples tested

(n=10) represent lithofacies AD, AE, B, F, and GE. The samples have been taken from a diverse assemblage of Formations and Groups (Figure 6.5). Low-frequency values of the twenty-eight samples tested range from 0.35 to $5.42 \times 10^{-8} \text{ (m}^3\text{kg}^{-1}\text{)}$.

6.3.3. Discussion

Magnetic susceptibilities have been tested from aquitard samples above and below producing and suspended gas fields, suspended oil fields, and also from dry (non-productive) intervals within the Devonian system. Unfortunately no meaningful trends between magnetic susceptibility and productive, non-productive, and hydrocarbon-bearing intervals exist. Secondly, no apparent trends between magnetic susceptibility and thin (<10 m in thickness) versus thick aquitards exist, as postulated from the fact that hydrocarbon migration is more likely to occur through thin, rather than thick intervals. Lastly, no apparent trends in magnetic susceptibility and present depth of the samples from the aquitards (as proposed by Machel, 1996) are evident.

Although magnetic susceptibilities do not reveal possible interactions with hydrocarbon migration patterns, they do reflect some other interesting trends. Firstly, correlations of magnetic susceptibilities with proximity to hydrocarbon sources such as the Duvernay Formation may exist. Samples from the Duvernay Formation have two of the lowest susceptibilities (Figure 6.5). Secondly, with the exception of three values, a weak negative correlation ($R=-0.39$) between magnetic susceptibility and carbonate content is present (Figure 6.6). This is a much weaker negative correlation than that identified by Hearn ($R=-0.91$), who suggested that increased magnetic susceptibilities, corresponding with samples of lower carbonate content, may be accounted for by an increase in detrital magnetic minerals associated with terrigenous clastics. In a study of sediment cores from the Hudson Strait and Hatton Basin conducted by Manley et al. (1993), it was proposed that higher magnetic susceptibilities could reflect the delivery of sediment derived from glacial erosion of Precambrian granites and gneisses. These authors also proposed that a concentration of a

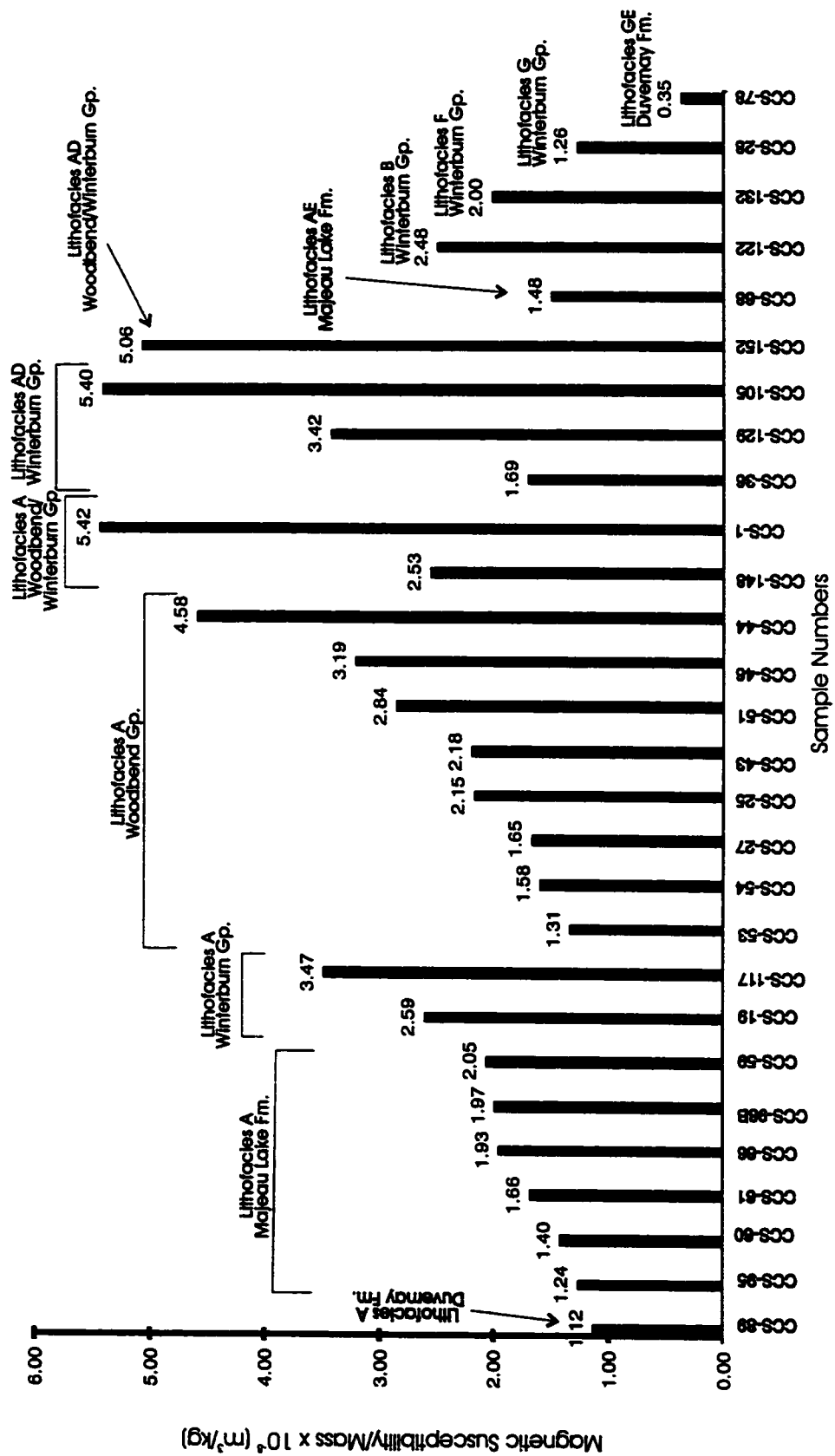


Figure 6.5: Low-Frequency Magnetic Susceptibilities of whole-rock samples representing various lithofacies, Formations and Groups.

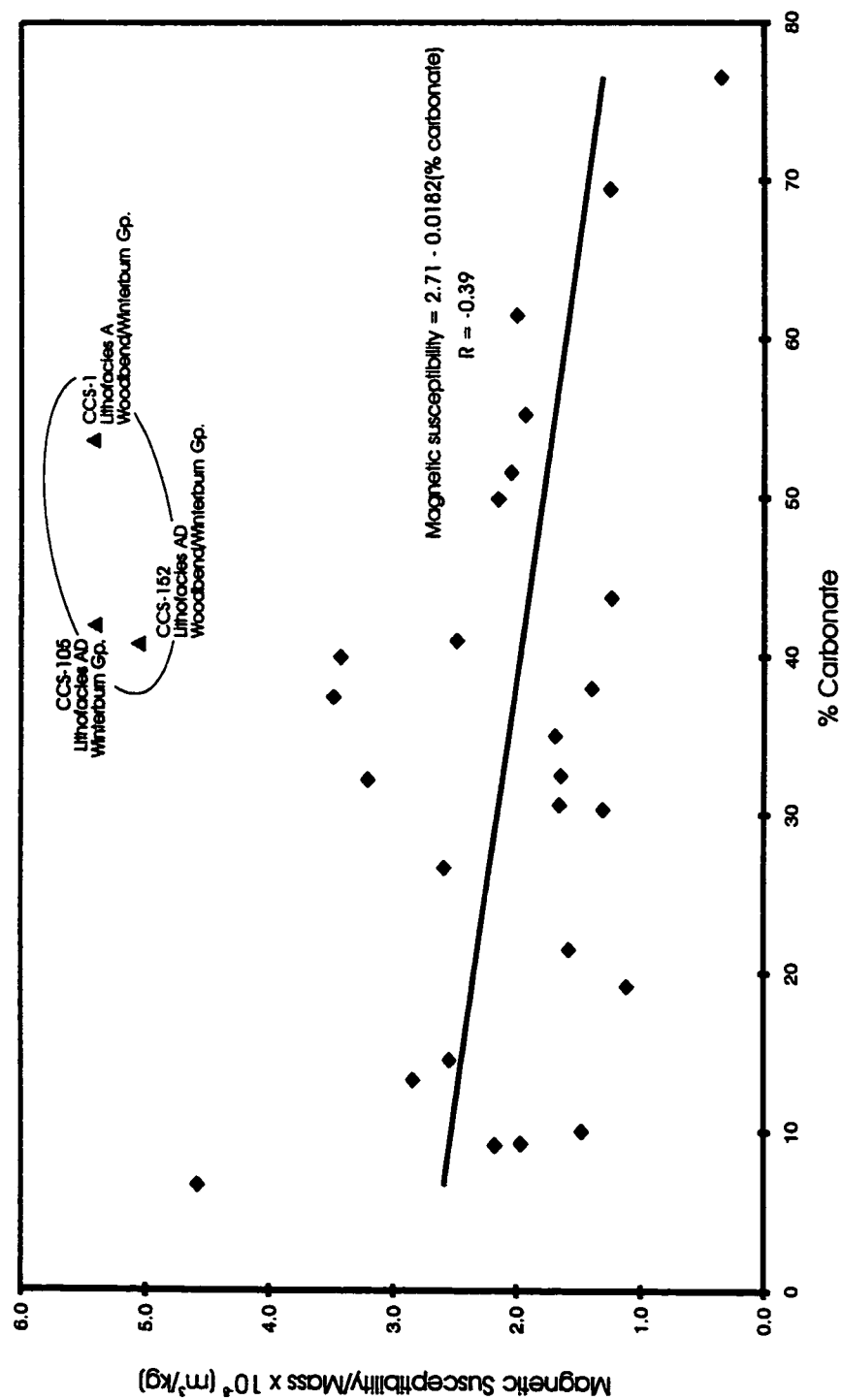


Figure 6.6: Profile of percent carbonate versus magnetic susceptibility/mass of samples. A slight negative correlation exists ($R = -0.39$) between the carbonate percentage and magnetic susceptibility for the majority of the samples. Three samples are anomalous in that they have greater magnetic susceptibilities than samples with similar carbonate percentages.

surface lag of such material, due to current winnowing at the sea floor, could account for the higher than background magnetic susceptibilities. It was also suggested that low magnetic susceptibilities record pulses of high carbonate sedimentation derived from glacial erosion of Paleozoic limestone and dolostone (Manley et al., 1993). The interpretations proposed by Hearn (1996) and Manley et al. (1993 and references therein) may account for the negative correlation between carbonate content and magnetic susceptibility present in this study. Thirdly, three anomalous values have been identified with magnetic susceptibilities over $5.00 \times 10^{-8} \text{ (m}^3\text{kg}^{-1}\text{)}$ (Figure 6.6). These anomalous values may be related to lithofacies or stratigraphy. Two of these samples are from lithofacies AD; while the third is from lithofacies A (Figure 6.5 and 6.6). Stratigraphically, one of the samples is from aquitard A in the Winterburn Group (CCS 105 in Figure 6.7), whereas the other two samples (CCS 1 in Figure 6.7 and CCS 152 in Figure 6.8) are from the undivided Woodbend/Winterburn Group. Further refinements in stratigraphic correlations are required to determine if the samples representing the undivided Woodbend/Winterburn Group, actually represent aquitard A of the Winterburn Group. If this can be confirmed, it is possible that magnetic susceptibilities over $5.00 \times 10^{-8} \text{ (m}^3\text{kg}^{-1}\text{)}$ may be useful in "fingerprinting" aquitard A. Thus, magnetic susceptibilities $>5.00 \times 10^{-8} \text{ (m}^3\text{kg}^{-1}\text{)}$ may have implications for locating the division between the Woodbend and Winterburn Group. In previous studies, magnetic susceptibilities have been successful in identifying stratigraphic correlations (e.g., Manley et al., 1993) and in this study, may be useful in identifying lithofacies AD and/or aquitard A.

6.4. Fluid Flow Migration Patterns

6.4.1. Introduction

The circumstantial geochemistry, MICPM data, and magnetic susceptibility tests presented and analyzed in Chapters 3, 4, 5, and 6 state that (paleo-) fluids, including both brines and hydrocarbons, are overall confined to the aquifers. Incorporating these results along with structural cross sections

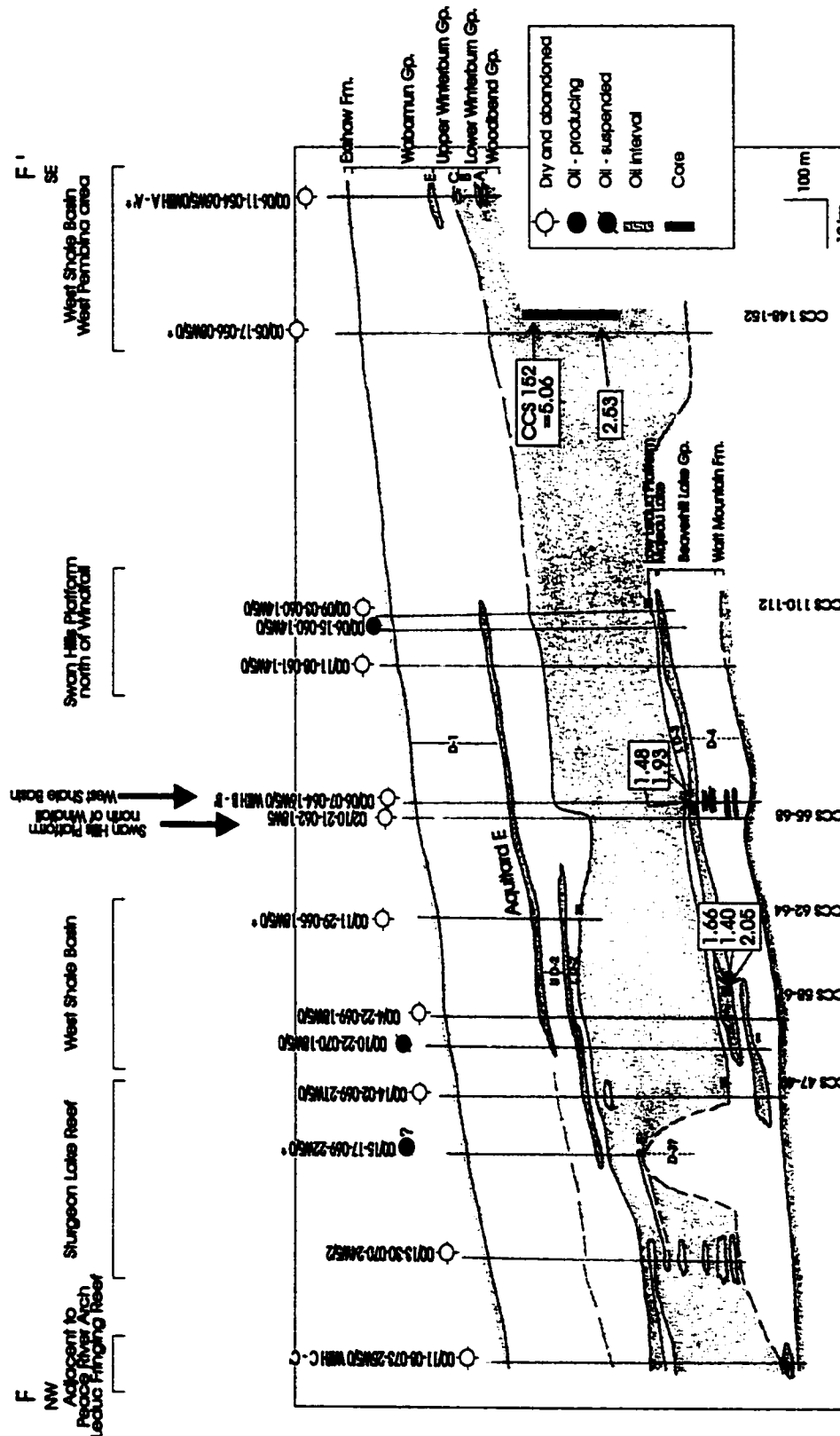


Figure 6.8: Cross section F-F' indicating the magnetic susceptibilities ($\times 10^{-6} \text{ m}^3/\text{kg}$) and locations of whole-rock samples tested. One of the three anomalous samples, CCS 152, identified in Figure 6.6 is included and is located in the undifferentiated Woodburn/Wintaburn Group in the West Pembina area. Smaller values (between 1 and $3 \times 10^{-6} \text{ m}^3/\text{kg}$) are located throughout the remainder of the cross section. The location of the cross section is indicated in Figure 3.1.

(A-A' to F-F') from Chapter 3 (geographic locations are shown in Figure 3.1), potential pathways of fluids travelling in a predominantly northeast direction (after Bachu, 1995) that may have been responsible for precipitating the ^{87}Sr enriched late-calcite cements in the Devonian system are presented. Localized evaporitic aquicludes within the D-1 to the D-4, which have not been separately mapped, could further impede migration patterns within these intervals.

6.4.2. Cross Section A-A'

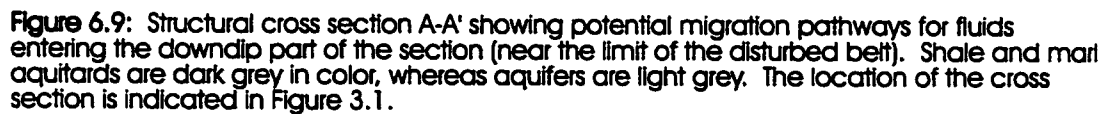
In this cross section (Figure 6.9), fluids originating downdip, near the limit of the disturbed belt, could enter several, thin D-2 aquifers as well as the D-1 aquifer, and migrate updip towards the northeast in the direction of the West Pembina area. In the central portion of the section where the Graminia Silt (aquitard E) is absent and thicker aquitards in the Lower Winterburn Group are present, fluids would most likely merge and travel along the D-1 aquifer. Fluids could easily migrate updip through the D-1 aquifer, beyond the limit of this cross section.

In the structural section, it is shown that a gas-producing pool is located downdip from the oil-producing well (Figures 3.3 and 6.9). If these productive intervals were interconnected, then the gas should be located updip from the oil. Thus, the oil-producing interval appears to be relatively "sealed" by shale and marl aquitards (for further discussion refer to Appendix 2).

6.4.3. Cross Section B-B'

In this cross section (Figure 6.10), fluids originating in the disturbed belt region could enter the D-4 aquifer. Interconnection of the D-1 to the D-4 aquifers, which are merged in the southwestern part of the cross section, could provide a pathway for significant vertical migration of fluids, followed by updip migration through separate D-4, D-2, and D-1 aquifers. In the central part of the section, in the Marlboro and Pine Creek Basin areas, the D-3 aquifer is possibly connected to the D-4 as the intervening aquitard is missing. In the stratigraphically upper part of the section, fluids within the U D-2 and the D-1 aquifers could migrate updip beyond the section, whereas the presence of

A'
NE



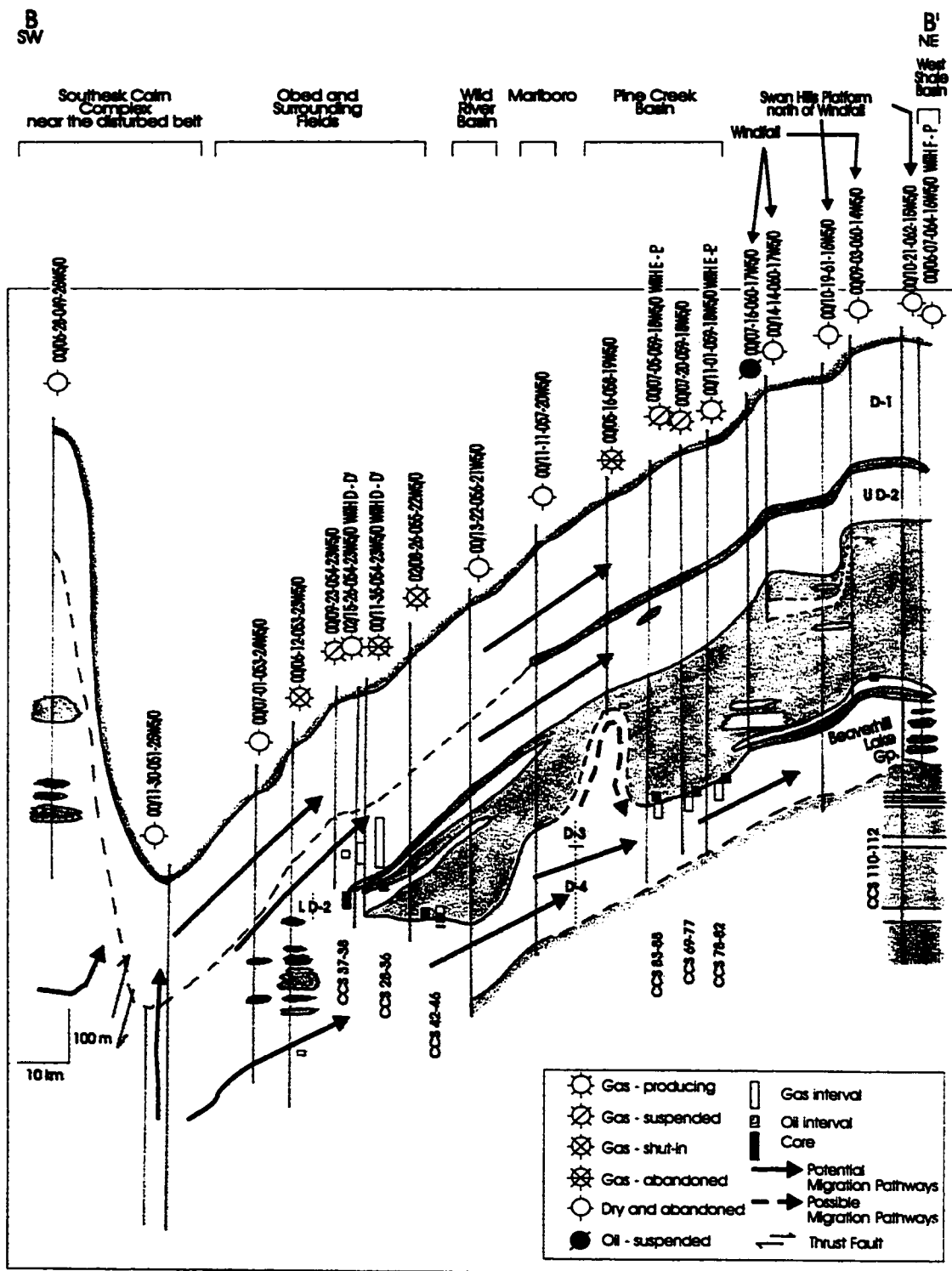


Figure 6.10: Structural cross section B-B' showing potential migration pathways for fluids entering the downdip part of the section in the Southesk Calm Complex near the limit of the disturbed belt. Shale and marl aquitards are dark grey in color, whereas the aquifers are light grey. The location of the cross section is indicated in Figure 3.1.

shales and marls in the Beaverhill Lake Group act as barriers to fluid preventing further updip migration. The closure in the Beaverhill Lake Group of the Pine Creek Basin is an updip stratigraphic trap, although it is not well illustrated at the small scale of this cross section. The closure in other significant gas plays in the Obed area are probably not related to shale and marl aquitards but to evaporitic aquicludes.

6.4.4. Cross Section C-C'

Fluid migration originating in the disturbed belt region may enter the Gold Creek Reef via the D-3 aquifer, and possibly the D-4, as these two aquifers appear to be connected (Figures 6.11). Fluids could also enter the interconnected D-2 and D-1 aquifers, and possibly the thin, L D-2 aquifer. In the stratigraphically lower part of the section, fluids would subsequently migrate updip through thin units of L D-3 and D-4, which in places appear interconnected. Longitudinal aquitard lenses separating these two aquifers may act as migration barriers, however, fluids may migrate around them. The absence of productive intervals in these lower aquifers suggests the latter. In the upper part of the section, fluids entering the interconnected D-1 and D-2 aquifer would continue to migrate updip, unimpeded by shale and marl aquitards. As thin carbonate aquifers exist in the lower part of the D-2, it is possible that fluids would preferentially migrate within the thick, upper intervals of the interconnected D-1 and D-2 aquifers. Fluids travelling within the D-1 through to the D-4 could easily migrate beyond the most updip well in the section.

6.4.5. Cross Section D-D'

This cross section (similar to cross sections E-E' and F-F', subsequently discussed) is oriented in a northwest-southeast direction parallel to the limit of the disturbed belt, extending from the Leduc Fringing Reef of the Peace River Arch to the West Pembina area (Figures 3.1 and 6.12). The gentle slope of the strata in cross section D-D' is significant, in that fluids could preferentially migrate updip from northwest to southeast, i.e., from the Leduc Fringing Reef to the West Pembina area. However, the present regional flow in the Devonian

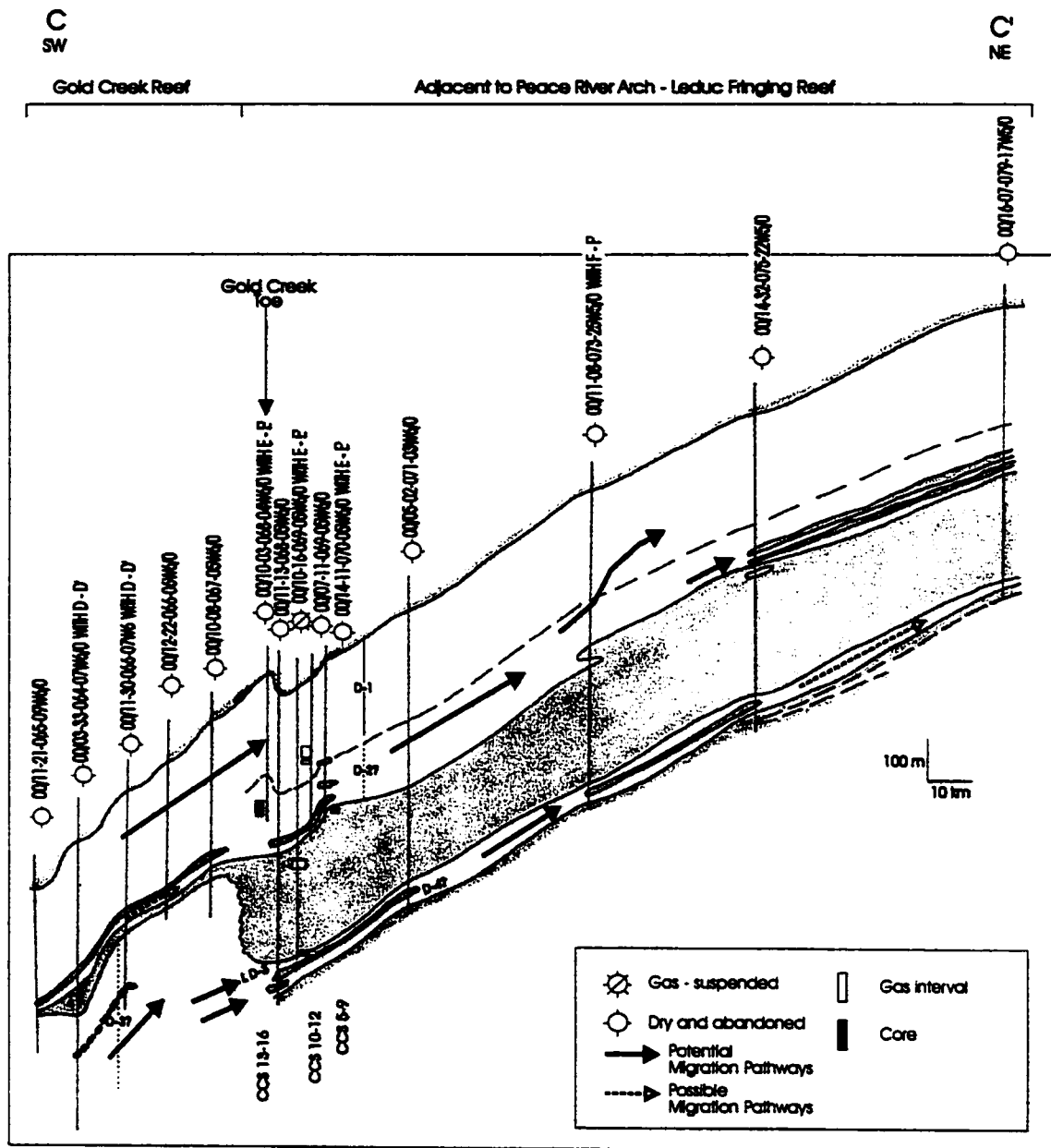


Figure 6.11: Structural cross section C-C' showing potential migration pathways for fluids entering the downdip part of the section, near the limit of the disturbed belt. Shale and marl aquitards are dark grey in color, whereas the aquifers are light grey. The location of the cross section is indicated in Figure 3.1.

aquifers is toward the northeast (e.g., Bachu, 1995), which is perpendicular to the plane of this cross section (and also cross section E-E' and F-F'). As such, the vectors shown in Figures 6.12 to 6.14 merely represent possible cross formational fluid flow and/or vectors to be added to those of Bachu (1995). With respect to fluid migration pathways in cross section D-D', there are three major components to discuss. Firstly, in the southeast part of cross section D-D', in the Swan Hills Platform and West Pembina areas, aquitard E is present. However, in a large part of the cross section, due to the absence of aquitard E, the D-1 and the U D-2 are hydrologically connected. Secondly, in the center of the section, i.e., in Simonette, Bigstone, and Wild River Basin areas, fluids entering the interconnected D-3 and D-4 aquifer could potentially migrate (sub)vertically where interconnection of the D-1 through to the D-4 is likely. This is similar to the interconnectedness of the D-1 through to the D-4 aquifers in the southwestern part of cross section B-B' (Figure 6.10). Thirdly, in the Windfall reef and Swan Hills Platform area, to the southeast, fluids entering the combined D-3 and D-4 aquifer could possibly exist through a thin, but laterally extensive L D-2 aquifer near the top of this merged D-3 and D-4 unit.

6.4.6. Cross Section E-E'

Similar to section D-D', section E-E' is oriented parallel to the disturbed belt. Again, gently dipping strata towards the northwest or towards the direction of the Leduc Fringing Reef of the Peace River Arch is present (Figure 6.13). Preferential fluid flow would be updip, towards the southeast in the direction of the West Pembina area. However, for reasons stated in the previous section, the vectors shown in Figure 6.13 merely represent possible cross formational fluid flow and/or vectors to be added to those of Bachu (1995).

In cross section E-E', similar to cross section D-D', an absence of aquitard E in the central to northwest part of the section causes interconnection of the D-1 and the undifferentiated D-2 aquifers. Secondly, fluids within the D-3(?) aquifer in the Windfall reef and Swan Hills Platform area could migrate to the southeast via a thin, but laterally continuous L D-2 aquifer. It is unlikely migration through

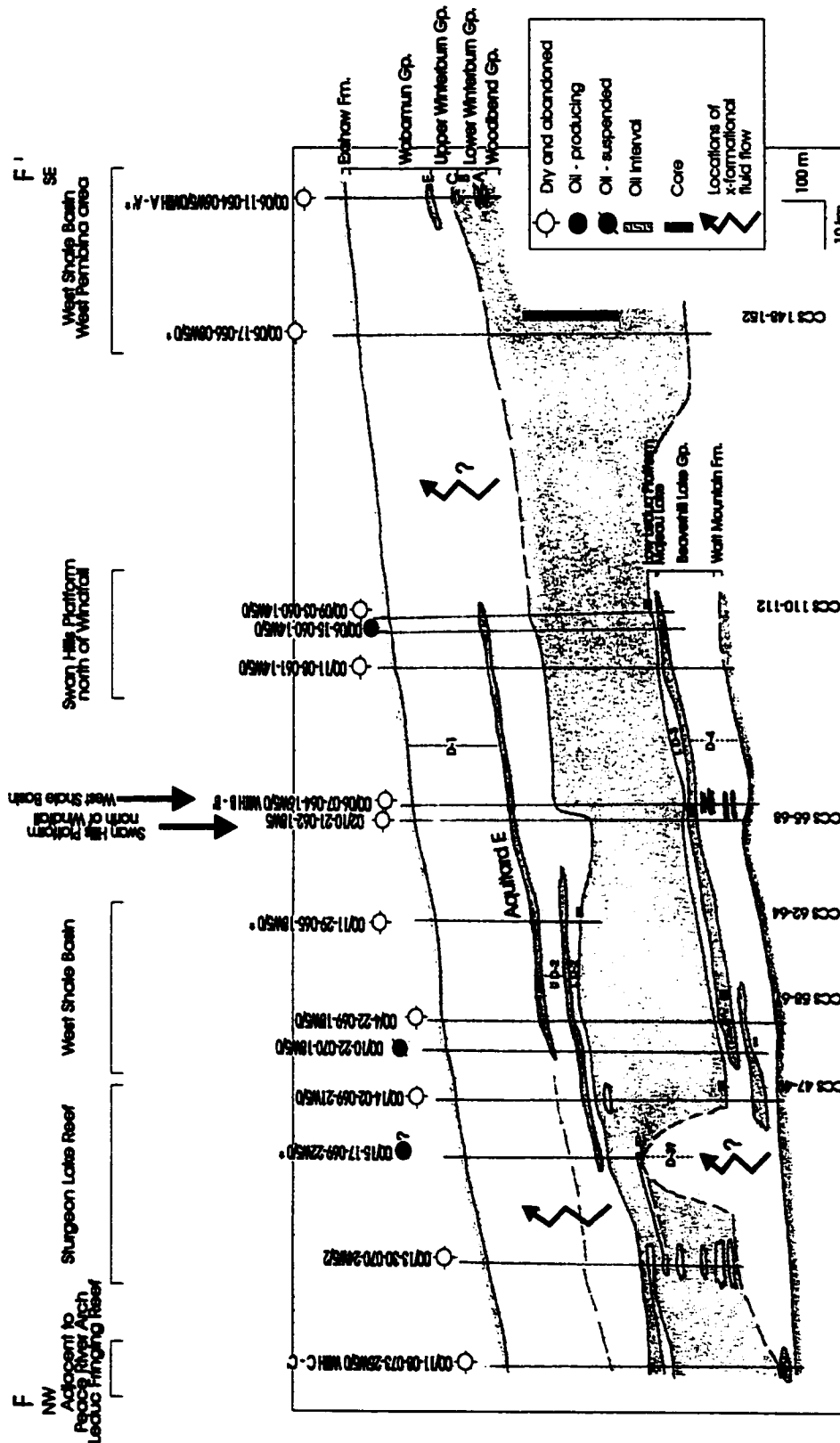


Figure 6.14: Structural cross section F-F' showing the locations of cross-formational fluid flow due to the absence of intervening aquitards. Shale and marl aquitards are dark grey in color, whereas the aquifers are light grey. The location of the cross section is indicated in Figure 3.1.

the thin L D-2 aquitards overlying this reef to the D-2 aquifer would occur.

6.4.7. Cross Section F-F'

A gentle slope from the Leduc Fringing reef of the Peace River Arch to the West Pembina area is present (Figure 6.14). Preferential fluid flow would be updip, towards the southeast in the direction of the West Pembina area. However, the vectors shown in Figure 6.14 merely represent possible cross formational fluid flow and/or vectors to be added to those of Bachu (1995).

The D-4 and the L D-3, although separated in some locations by the Majeau Lake Formation and also, by wedge-shaped, laterally-discontinuous, aquitards, appear to be hydrologically interconnected in parts of the cross section. In the Sturgeon Lake Reef area, fluids entering the combined D-4 and the L D-3 could migrate upwards to the D-3. Similar to both cross sections D-D' and E-E' (Figures 6.12 and 6.13), aquitard E appears to be absent throughout a large part of the section. This causes an interconnection of the L D-2, the U D-2 and the D-1 aquifers throughout the area.

6.5. Summary

MICPM data of several basinal facies indicate that the aquitards are relatively effective seals to hydrocarbons. Secondly, magnetic susceptibilities do not reveal possible hydrocarbon migration patterns, e.g., potential breaches through the aquitards. However, they do reveal a negative correlation between magnetic susceptibility and carbonate content, and that magnetic susceptibilities $>5.00 \text{ m}^3\text{kg}^{-1}$ may prove to "fingerprint" aquitard A in the Winterburn Group and/or lithofacies AD. This may be useful in finding a subdivision between the Woodbend and the Winterburn Group.

Evidence presented in Chapter 5 indicates that it is unlikely that extra-basinal fluids responsible for precipitating anomalously radiogenic strontium carbonate cements in the carbonate aquifers (Patey, 1995, and Machel et al., 1996) interacted with the aquitards, with the possible exception of localized interaction with aquitards within the Obed and Wild River Basin areas. These extra-basinal fluids are likely confined to aquifers D-1 through to the D-4; cross-

formational fluid flow is likely to occur in locations where shale and marl aquitards are absent.

A predominant southwest-northeast fluid flow migration pattern is evident within the Devonian system in the Alberta Basin (Bachu, 1995). Possible flow patterns of the fluids responsible for precipitating the late-stage calcite cements within the Devonian system are presented in cross sections A-A', B-B', and C-C'. Interconnection of the D-1 through to the D-4 aquifers occurs e.g., in regions towards the disturbed belt. Although not true fluid migration patterns, in cross sections D-D', E-E', and F-F', vectors merely represent locations within the cross sections where cross formational fluid flow is likely, due to the absence of intervening aquitards. In particular, interconnection of the D-1 through to the D-4 is noted in cross sections D-D' (and also in sections B-B'). It is also quite common for the D-1 and the D-2 to be interconnected, due to the absence of intervening aquitards, such as Graminia Silt (aquitard E).

Chapter 7 - Conclusions

1) Stratigraphically within west-central Alberta:

- a) Winterburn Group and Majeau Lake Formation aquitards are thin (generally less than 20 m in thickness), whereas Woodbend Group aquitards and stacked Winterburn/Woodbend aquitards can attain thicknesses of up to 315 m
- b) In areas such as the Obed field, Wild River Basin, Simonette and Bigstone reefs (i.e., in the general vicinity of the limit of the disturbed belt), the stacked Woodbend/Winterburn aquitard and aquitard E of the Winterburn Group thin or disappear. This permits interconnection between the Devonian carbonate aquifers (e.g., the D-1 to the D-4). Evaporites within these sequences have not been mapped and may significantly impede flow, however.

2) Structurally within west-central Alberta:

- a) Devonian strata dip steeply towards the limit of the disturbed belt; and,
- b) a gentle depositional/structural slope also exists towards the Leduc Fringing Reef of the Peace River Arch.

3) Lithologically, eight major lithofacies (A, B, AD, AE, C, G, GE, and F) have been identified in aquitards investigated from the Woodbend and Winterburn Groups. Within the Woodbend Group, lithofacies representative of basinal, slope, and near-reef environments have been identified; within the Winterburn Group, lithofacies representative of deep-ramp, shallow-ramp, and near-reef environments are present. The eight major lithofacies identified within these two Groups show correlations between lithofacies and stratigraphic intervals.

4) Mineralogically, four different facies have been identified within the aquitards using XRD; QCp, CQp, Qdp, and Cq. Facies QCp and CQp are widespread

throughout the study area, the others are more localized. Facies Qdp is found in only one core within the Obed area, while Cq is centered around the Obed and Wild River Basin areas.

- 5) Mercury injection capillary pressure measurements (MICPM) reveal that the aquitards are relatively effective seals to hydrocarbons.
- 6) Magnetic susceptibilities do not reveal any clues regarding hydrocarbon migration. They do reflect some other interesting trends, however. The most important finding is that anomalous magnetic susceptibilities (i.e., above 5.00×10^{-8} (m³/kg) may be diagnostic of lithofacies AD and/or aquitard A of the Winterburn Group.
- 7) Stable isotopic analyses ($\delta^{13}\text{C}$ and $\delta^{18}\text{O}$) of the carbonate whole-rock fraction, in addition to several individual carbonate components (e.g., carbonate nodules and lenses), within the aquitards strongly suggest that the aquitards have acted as effective barriers to aqueous fluid flow since the Late Devonian or Early Carboniferous.
- 8) Radiogenic isotopic data ($^{87}\text{Sr}/^{86}\text{Sr}$) of the carbonate whole-rock fraction, individual carbonate components, and a celestite sample within the aquitards, are not nearly as radiogenic as late-stage calcite cements in adjacent carbonate aquifers. This finding supports the notion that an external fluid source is involved in precipitating these late-stage carbonate cements in Devonian carbonate aquifers (e.g., in the Leduc Formation of the Obed field).
- 9) Extrabasinal fluids entering the Devonian system probably:
 - b) followed a general southwest-northeast fluid flow pattern, which is similar to the present flow within the Devonian system in the Alberta Basin (Bachu, 1995);

a) travelled within Devonian carbonate aquifers, and probably did not cross aquitards. Where these aquitards are absent, particularly in regions towards the disturbed belt (such as Obed field, Wild River Basin, and Simonette and Bigstone Reefs), the D-1 to the D-4 aquifers are hydrologically connected, and cross formational fluid flow was and is likely.

References

- Ahr, W.M., 1973, The carbonate ramp: an alternative to the shelf model. *In* Transactions, Gulf Coast Association of Geological Societies 23rd Annual Convention, p. 221-225.
- Allen, J. and Creaney, S., 1991, Oil families of the Western Canada Basin: *Bulletin of Canadian Petroleum Geology*, v.39, p. 107-122.
- Amthor, J.E., Mountjoy, E.W., and Machel, H.G., 1993, Subsurface dolomites in Upper Devonian Leduc formation buildups, central part of Rimbey-Meadowbrook reef trend, Alberta, Canada: *Bulletin of Canadian Petroleum Geology*, v.41, p. 164-185.
- Andrews, P.R.A. and Collings, R.K., 1991, Celestite in Canada: *CIM Bulletin*, v.84, No. 951, p. 36-39.
- Andrichuk, J.M., 1958, Cooking Lake and Duvernay (Late Devonian) sedimentation in Edmonton area of central Alberta, Canada: *American Association of Petroleum Geologists Bulletin*, v.42, p. 2189-2222.
- Bachu, S., 1995, Synthesis and model of formation-water flow, Alberta Basin, Canada: *American Association of Petroleum Geologists Bulletin*, v.79, p. 1159-1178.
- Bachu, S. and Burwash, R.A., 1994, Geothermal regime in the Western Canada Sedimentary Basin *In* Geological Atlas of the Western Canada Sedimentary Basin. G.D. Mossop and I. Shetsen (comps.). Calgary, Canadian Society of Petroleum Geologists and Alberta Research Council, p. 447-455.
- Baker, P.A. and Bloomer, S.H., 1988, The origin of celestite in deep-sea carbonate sediments: *Geochimica et Cosmochimica Acta*, v.52, p. 335-339.
- Banner, J.L., 1995, Application of the trace element and isotope geochemistry of strontium to studies of carbonate diagenesis: *Sedimentology*, v.42, p. 805-824.
- Burke, W.H., Denison, R.E., Hetherington, E.A., Koepnick, R.B., Nelson, H.F., and Otto, J.B., 1982, Variation of seawater $^{87}\text{Sr}/^{86}\text{Sr}$ throughout Phanerozoic time: *Geology*, v.10, p. 516-519.
- Burrowes, O.G. and Krause, F.F., 1987, Overview of the Devonian system: subsurface of Western Canada Basin. *In* Devonian Lithofacies and Reservoir Styles in Alberta, Second International Symposium on the Devonian System, 13th Canadian Society of Petroleum Geologists Core Conference and Display, p. 1-20.
- Burton, E.A., Machel, H.G., and Qi, J., 1993, Thermodynamic constraints on anomalous magnetization in shallow and deep hydrocarbon seepage environments. *In* Applications of Paleomagnetism to Sedimentary Geology, SEPM Special Publication No. 49. p. 193-207.
- Bush, P. 1973, Some aspects of the diagenetic history of the sabkha in Abu Dhabi, Persian Gulf. *In*: The Persian Gulf, Purser, B.H. (ed) p. 395-407. Springer-Verlag.
- Bustin, R.M., 1991, Organic maturity in the Western Canada Sedimentary Basin: *International Journal of Coal Geology*, v.19, p. 319-358.
- Campbell, F.A. and Oliver, T.A., 1968, Mineralogic and chemical composition of Ireton and Duvernay Formations, central Alberta: *Bulletin of Canadian Petroleum Geology*, v.16, p. 40-63.

- Carpenter, S.J., Lohmann, K.C., Holden, P., Walter, L.M., Huston, T.J., and Halliday, A.N., $\delta^{18}\text{O}$ values, $^{87}\text{Sr}/^{86}\text{Sr}$ and Sr/Mg ratios of Late Devonian abiotic marine calcite: Implications for the composition of ancient seawater. *Geochimica et Cosmochimica Acta*, v.55, p. 1991-2010.
- Cavell, P.A. and Machel, H.G., 1996. Tectonic expulsion of fluids into Devonian paleoaquifers in the Alberta Basin. *In* Ross, G.M. (compiler), 1996, Alberta Basement transects workshop, Lithoprobe Report #51, Lithoprobe Secretariat, University of British Columbia, p. 225-233.
- Cavell, P.A. and Machel, H.G., 1997, Tectonic expulsion of fluids into the Obed area of west-central Alberta: Sr isotope evidence for fluid pathway, extent and possible sources. *In* Ross, G.M. (compiler), 1997 Alberta Basement transects workshop, Lithoprobe Report #59, Lithoprobe Secretariat, University of British Columbia, p. 171-181.
- Chow, N., Wendte, J., and Stasiuk, L.D., 1995., Productivity versus preservation controls on two organic-rich carbonate facies in the Devonian of Alberta: sedimentological and organic petrological evidence: *Bulletin of Canadian Petroleum Geology*, v.43, p. 433-460.
- Correns, C.W., 1968, *Einführung in die Mineralogie*, 2. Aufl. Berlin, Springer-Verlag. p. 245-248.
- Craig, J.H., 1987, Depositional environments of the Slave Point Formation, Beaverhill Lake Group, Peace River Arch. *In* Devonian lithofacies and reservoir styles in Alberta, Second International symposium on the Devonian system, 13th Canadian Society of Petroleum Geologists Core Conference and Display, p.181-200.
- Creaney, S. and Allen, J., 1990, Hydrocarbon generation and migration in the Western Canada Sedimentary Basin. *In* Brooks, J. (ed), *Classic Petroleum Provinces*, Geological Society Special Publication No. 50, p. 189-202.
- Degens, E.T. and Epstein, S., 1964, Oxygen and carbon isotope ratios in coexisting calcites and dolomites from recent and ancient sediments: *Geochimica et Cosmochimica Acta*, v. 528, p. 23-44.
- Downey, M. W., 1994, Evaluating seals for hydrocarbon accumulations: *American Association of Petroleum Geologists Bulletin*, v.68, p. 1752-1763.
- Duggan, J.P., 1997, Sedimentology and diagenesis of Swan Hills Simonette oil field, west-central Alberta Basin: unpublished M.Sc. thesis, McGill University, Montreal, 177 p.
- Duggan, J.P., Green, D.G., and Mountjoy, E.W., 1998, Faulting and reservoir-scale diagenesis of Swan Hills Formation, Devonian Beaverhill Lake Group, deep west-central Alberta Basin. *In* CSPG-CSEG-CWLS Joint Convention, June 16-19, 1998, Calgary, AB, Geo-Triad '98 Abstracts, p. 526-529.
- Elmore, R.D., McCollum, R., and Engel, M.H., 1989, Evidence for a relationship between hydrocarbon migration and diagenetic magnetic minerals - Implications for petroleum exploration: *Bulletin of the Association of Petroleum Geochemical Explorationists*, v. 5, p. 1-17.
- Emery, D. and Robinson, A., 1993, *Inorganic geochemistry: applications to petroleum geology*. Blackwell Scientific Pub., Oxford., 254 p.
- Friedman, I. and O'Neil, J.R., 1977., Compilation of stable isotope fractionation factors of geochemical interest. *In* *Data of Geochemistry*, United States Geological Survey Professional Paper 440-KK, p. 1-12.

- Fritz, P. and Smith, D.G.W., 1970, The isotopic composition of secondary dolomites: *Geochimica et Cosmochimica Acta*, v.34, p. 1161-1173.
- Froehlich, P.N., Klinkhammer, G.P., Bender, M.L., Luedtke, N.A., Heath, G.R., Cullen, D., Dauphin, P., Hammond, D., Hartman, B., and Maynard, V., 1979, Early oxidation of organic matter in pelagic sediments of the eastern equatorial Atlantic: suboxic diagenesis: *Geochimica et Cosmochimica Acta*, v.43, p. 1075-1090.
- Green, D.G., 1999. Dolomitization and deep burial diagenesis of the Devonian of west-central Alberta deep basin: Kaybob South and Fox Creek (Swan Hills Formation) and Pine Creek fields (Leduc and Wabamun Formations): unpublished Ph.D. thesis, McGill University, Montreal, 267 p.
- Grzymala-Busse- Witold. J, 1995, Evaluation of magnetic susceptibility as a lithological indicator: unpublished B.Sc. thesis, Princeton University, Princeton, 68 p.
- Halbertsma, H.L., 1994, Devonian Wabamun Group of the Western Canada Sedimentary Basin. *In Geological Atlas of the Western Canada Sedimentary Basin*. G.D. Mossop and I. Shetsen (comps.). Calgary, Canadian Society of Petroleum Geologists and Alberta Research Council, p. 203-220.
- Hay, P.W., 1994, Oil and Gas Resources of the Western Canada Sedimentary Basin. *In Geological Atlas of the Western Canada Sedimentary Basin*. G.D. Mossop and I. Shetsen (comps.). Calgary, Canadian Society of Petroleum Geologists and Alberta Research Council, p. 469-470.
- Hearn, M.R., 1996, Stratigraphic and Diagenetic Controls on Aquitard Integrity and Hydrocarbon Entrapment, Bashaw Reef Complex, Alberta, Canada: unpublished M.Sc. Thesis, University of Alberta, Edmonton, 135 p.
- Horrigan, E.K., 1996. Extent of dolomite recrystallization along the Rimbey-Meadowbrook reef trend, Western Canada Sedimentary Basin, Alberta, Canada: unpublished M.Sc. thesis, University of Alberta, Edmonton, 137 p.
- Huebsher, H., 1996, Regional controls on the stratigraphic and diagenetic evolution of Woodbend Group carbonates, north-central Alberta, Canada: unpublished Ph.D. thesis, University of Alberta, Edmonton, 231 p.
- Jennings, J.B., 1987, Capillary pressure techniques: application to exploration and development geology. *American Association of Petroleum Geologists Bulletin* v.71, p. 1196-1209.
- Kalkreuth, W. and McMechan, M., 1988, Burial history and thermal maturity, Rocky Mountain Front Ranges, Foothills, and Foreland, east-central British Columbia and adjacent Alberta, Canada. *American Association of Petroleum Geologists Bulletin*, v.72, p. 1395-1410.
- Krushin, J.T., 1997, Seal capacity of nonsmectite shale., *In R.C. Surdam, ed., Seals, traps, and the petroleum system: American Association of Petroleum Geologists Memoir* 67, p. 31-47.
- Larson, L.H. (ed.), 1969, Gas fields of Alberta. Alberta Society of Petroleum Geologists (pub.). 407 p.
- Machel, H.G., 1983, Facies and diagenesis of some Nisku buildups and associated strata Upper Devonian, Alberta, Canada. *In Carbonate Buildups. SEPM Core Workshop No. 4*, p. 144-181.

- Machel, H.G., 1996, Magnetic contrasts as a result of hydrocarbon seepage and migration. *In* D. Schumacher and M.A. Abrams, eds., *Hydrocarbon migration and its near-surface expression: American Association of Petroleum Geologists Memoir 66*, p. 99-109.
- Machel, H.G., 1998, Indications for tectonically induced fluid flow into the Rocky Mountain Foreland Basin; with implications for petroleum exploration: *Canadian Society of Petroleum Geologists Reservoir*, v.25, p. 7.
- Machel, H.G. and Cavell, P.A., in press (1999), Low-flux, tectonically induced squeegee fluid flow ("hot flash") into the Rocky Mountain Foreland Basin: *Bulletin of Canadian Petroleum Geology*.
- Machel, H.G., Cavell, P.A., and Patey, K.S., 1996. Isotopic evidence for carbonate cementation and recrystallization and for tectonic expulsion of fluids into the WCSB. *Geological Society of America Bulletin*, v.108, p. 1108-1119.
- Machel, H.G. and Hunter, I.G., 1994, Facies models for Middle to Late Devonian shallow-marine carbonates, with comparisons to modern reefs: A guide for facies analysis: *Facies*, v.30, p. 155-176.
- Magara, K., 1976, Thickness of removed sedimentary rocks, paleopore pressure, and paleotemperature, southwestern part of Western Canada Basin: *American Association of Petroleum Geologists Bulletin*, v.60, p. 554-565.
- Manley, W.F., MacLean, B., Kerwin, M.W., and Andrews, J.T., 1993, Magnetic susceptibility as a Quaternary correlation tool: Examples for Hudson Strait sediment cores, eastern Canadian Arctic: *Current Research, Geological Survey of Canada Paper 93-1D*, p. 137-145.
- Manzano, B.K., 1995, Organic geochemistry of oil and sour gas reservoirs in the Upper Devonian Nisku Formation, Brazeau River area, central Alberta, Canada: unpublished M.Sc. thesis, University of Alberta, Edmonton, 101 p.
- Mason, B.H., 1966, *Principles of Geochemistry*. Third Edition. Wiley, New York. 329 p.
- McCrossan, R.G., 1957, Upper Devonian inter-reef calcareous shales of central Alberta, Canada: unpublished Ph.D. thesis, The University of Chicago, Chicago. 121 p.
- McCrossan, R.G., 1961, Resistivity mapping and petrophysical study of Upper Devonian inter-reef calcareous shales of central Alberta, Canada: *American Association of Petroleum Geologists Bulletin*, v.45, p.441-471.
- McKenzie, M.C., 1999, Carbonates of the Upper Devonian Leduc Formation, southwestern Peace River Arch, Alberta: Indications for tectonically-induced fluid flow: unpublished M.Sc. thesis, University of Alberta, Edmonton, 131 p.
- McLean, R. A. and Klapper, G., 1998, Biostratigraphy of Frasnian (Upper Devonian) strata in western Canada, based on conodonts and rugose corals. *Bulletin of Canadian Petroleum Geology*. v.46, p. 515-563.
- Meijer Drees, N.C., 1994, Devonian Elk Point Group of the Western Canada Sedimentary Basin. *In* *Geological Atlas of the Western Canada Sedimentary Basin*. G.D. Mossop and I. Shetsen (comps.). Calgary, Canadian Society of Petroleum Geologists and Alberta Research Council, p. 129-147.

- Moore, P.F., 1988, Devonian Geohistory of the Western interior of Canada. *In* Devonian of the World, McMillan, N.J., A.F. Embry, and D.J. Glass (eds.) Canadian Society of Petroleum Geologists Memoir No. 14, v.1, p. 67-83.
- Mountjoy, E.W., 1980, Some Questions about the development of Upper Devonian carbonate buildups (reefs) Western Canada. *Bulletin of Canadian Petroleum Geology*, v.28, p. 315-344.
- Mountjoy, E.W., Qing, H., and McNutt, R.H., 1992, Strontium isotopic composition of Devonian dolomites, WCSB: significance of sources of dolomitizing fluids: *Applied Geochemistry*, 7, p. 59-75.
- Oldale, H.S. and Munday, R.J., 1994, Devonian Beaverhill Lake Group of the Western Canada Sedimentary Basin. *In* Geological Atlas of the Western Canada Sedimentary Basin. G.D. Mossop and I. Shetsen (comps.). Calgary, Canadian Society of Petroleum Geologists and Alberta Research Council, p. 149-162.
- Oliver, T.A. and Cowper, N.W., 1963, Depositional environments of the Ireton Formation, central Alberta, *Bulletin of Canadian Petroleum Geology*, v.11, p. 183-202.
- Patey, K.S., 1995, Facies, Stratigraphy, and Diagenesis of the Upper Devonian carbonates in the Obed area, West-Central Alberta, Canada: unpublished M.Sc. thesis, University of Alberta, Edmonton, 147 p.
- Potter, P.E., Maynard, J.B., and Pryor, W.A., 1980, *Sedimentology of shale, study guide and reference*. Springer-Verlag, New York., 306 p.
- Purcell, W.R., 1949, Capillary pressures - their measurement using mercury and the calculation of permeability therefrom: *Transactions of the American Institute of Mining and Metallurgical Engineers (Petroleum Transactions, AIME)*, v. 186, p. 39-48.
- Rich, J.L., 1951, Three critical environments of deposition and criteria for recognition of rocks deposited in each of them: *Bulletin of the Geological Society of America*, v.62, p. 1-20.
- Ricketts, B.D., 1989. *Western Canada Sedimentary Basin - A Case History*. Canadian Society of Petroleum Geologists, 320 p.
- Rock, L., 1999, Sedimentology, diagenesis and reservoir characteristics of the Devonian Simonette (Leduc Formation) and Ante Creek (Swan Hills Formation) Fields: A Comparison between a Limestone and Dolomite Field, West-Central Alberta Basin: unpublished M.Sc. Thesis, McGill University, Montreal. 168 p.
- Rostron, B.J., 1995, Cross-formational flow in Upper Devonian to Lower Cretaceous strata, west-central Alberta: unpublished Ph.D. Thesis, University of Alberta, Edmonton, 201 p.
- Rostron, B.J. and Toth, J., 1996, Ascending fluid plumes above Devonian pinnacle reefs: numerical modeling and field example from west-central Alberta, Canada. *In* D.Schumacher and M.A. Abrams, eds., *Hydrocarbon migration and its near-surface expression: American Association of Petroleum Geologists Memoir 66*, p. 185-201.
- Rostron, B.J., Toth, J, and Machel, H.G., 1997, Fluid flow, hydrochemistry and petroleum entrapment in Devonian reef complexes, south-central Alberta, Canada., *In* Basin-Wide Diagenetic Patterns: Integrated Petrologic, Geochemical, and Hydrologic Considerations, SEPM Special Publication No. 57, p. 139-155.

- Rose, M.L. (ed.), 1990, Oil and gas pools of Canada series, The Canadian Society of Petroleum Geologists (pub.), Calgary, AB, v.1.
- Rudd, N. and Pandey, G.N., 1973, Threshold pressure profiling by continuous injection. AIME Special Paper #4597, 7 p.
- Schowalter, T.T., 1979, Mechanics of secondary hydrocarbon migration and entrapment: American Association of Petroleum Geologists Bulletin, v. 63, p. 723-760.
- Selley, R.C., 1985, Elements of petroleum geology. W.H. Freeman and Company, 449 p.
- Sharma, T. and Clayton, R. N., 1965, Measurement of O^{18}/O^{16} ratios of total oxygen of carbonates: *Geochimica et Cosmochimica Acta*, v.29, p. 1347-1353.
- Sneider, R.M., Sneider, J.S., Bolger, G.W., and Neasham, J.W., 1997, Comparison of seal capacity determinations: conventional cores vs. cuttings., *In* R.C. Surdam, (ed.), Seals, traps, and the petroleum system: American Association of Petroleum Geologists Memoir 67, p. 1-12.
- Stewart, F.H., 1949, The petrology of the evaporites of the Eskdale No. 2 boring, east Yorkshire; part 1, the lower evaporite bed. *Mineralogical Magazine*, v. 28, p. 621-675.
- Stoakes, F.A. and Creaney, S., 1984, Sedimentology of a carbonate source rock: the Duvernay Formation of central Alberta, *In* Carbonates in subsurface and outcrop: 1984 Canadian Society of Petroleum Geologists Core Conference, p. 132-147.
- Stoakes, F.A. and Creaney, S., 1985, Sedimentology of a carbonate source rock: the Duvernay Formation of Alberta Canada, SEPM Core Workshop No. 7, Golden, August 10-11, p. 343-375.
- Stoakes, F.A., 1979, Sea level control of carbonate-shale deposition during progradational basin-filling; the Upper Duvernay and Ireton Formations of Alberta, Canada: unpublished Ph.D. thesis, University of Calgary, 346 p.
- Stoakes, F.A., 1980, Nature and control of shale basin fill and its effect on reef growth and termination: Upper Devonian Duvernay and Ireton Formations of Alberta, Canada. *Bulletin of Canadian Petroleum Geology*, v.28, p. 345-410.
- Stoakes, F.A., 1992, Woodbend Megasequence., *In* Wendte, J.C., F.A. Stoakes, and C.V. Campbell (Eds.) Devonian-Early Mississippian carbonates of the WCSB: A sequence stratigraphic framework. SEPM Short Course No. 28, Calgary, AB, p.183-206.
- Switzer, S.B., Holland, W.G., Christie, D.S., Graf, G.C., Hedinger, A.S., McAuley, R.J., Wierzbicki, R.A., and Packard, J.J., 1994, Devonian Woodbend-Winterburn strata of the Western Canada Sedimentary Basin, *In* Geological Atlas of the Western Canada Sedimentary Basin. G.D. Mossop and I. Shetsen (comps.). Calgary, Canadian Society of Petroleum Geologists and Alberta Research Council, p.165-201.
- Tucker, M.E. and Wright, P., 1990. Sedimentary petrology - an introduction to the origin of sedimentary rocks. Blackwell Scientific Pub., Oxford, 482 p.
- Watts, N.R., 1987. Carbonate sedimentology and depositional history of the Nisku Formation (within the Western Canada Sedimentary Basin) in south central Alberta. *In* Devonian lithofacies and reservoir styles in Alberta, second international symposium on the Devonian system, 13th Canadian Society of Petroleum Geologists Core Conference and Display, p. 87-152.

- Weissenberger, J.A.W., 1988, Sedimentology and preliminary conodont biostratigraphy of the Upper Devonian Fairholme Group, Nordegg area, west-central Alberta, Canada. *In* Devonian of the world; proceedings of the second international symposium on the Devonian system; v.2, Sedimentation. McMillan, N.J., Embry, A.F., and Glass, D.J. (eds.) Canadian Society of Petroleum Geologists Memoir 14, p. 451-461.
- Weissenberger, J.A.W., 1994, Frasnian reef and basinal strata of west central Alberta: A combined sedimentological and biostratigraphic analysis: Bulletin of Canadian Petroleum Geology, v.42, p. 1-25.
- Wendte, J.C., 1992, Overview of the Devonian of the WCSB. *In* Wendte, J.C., F.A. Stoakes, and C.V. Campbell (Eds.) Devonian-Early Mississippian carbonates of the WCSB: A sequence stratigraphic framework. SEPM Short Course No. 28, Calgary, AB, p. 1-24.
- Wendte, J., 1998, Devonian summary cross-section, Wild River Basin, west-central Alberta. Open-file report, Geological Survey of Canada, Calgary, AB, Canada. 2 p.
- Wendte, J., Dravis, J.J., Stasiuk, L.D., Qing, H., Moore, S.L.O., and Ward, G., 1998, High-temperature saline (thermoflux) dolomitization of Devonian Swan Hills platform and bank carbonates, Wild River area, west-central Alberta. Bulletin of Canadian Petroleum Geology, v. 46, p. 210-265.
- Wendte, J., Stoakes, F., Bosman, M., Bernstein, L., 1995, Genetic and stratigraphic significance of the Upper Devonian Frasnian Z-Marker, west-central Alberta., Bulletin of Canadian Petroleum Geology, v.43, p. 393-406.
- White, R.J. (ed.), 1960, Oil fields of Alberta, Alberta Society of Petroleum Geologists (pub.), Calgary, AB, 272 p.
- Wright, G.N., McMechan, M.E., and Potter, D.E.G., 1994, Structure and architecture of the Western Canada Sedimentary Basin. *In* Geological Atlas of the Western Canada Sedimentary Basin. G.D. Mossop and I. Shetsen (comps.). Calgary, Canadian Society of Petroleum Geologists and Alberta Research Council, p. 25-40.

Appendix 1 - Details of core descriptions, and stable and radiogenic isotope analyses

Core ID	Location	Core Length (m)	Core Depth (m)	Core Diameter (cm)	Core Weight (kg)	Core Material
02/06-05-051-07W5/0 PCP et al. Pembina 6-5		2,334-2,352 m	59	18		WINTERBURN
00/02-22-051-07W5/0 Chevron et al. Moon 2-22		7,417-7,476 ft	59	18		WINTERBURN
00/09-17-050-10W5/0 Texaco et al. Pembina 9-17		2,710-2,729 m	62	19		WINTERBURN
00/07-04-049-12W5/0 Chevron NorcenPI Brazeau 7-4		10,060-10,300 ft	240	73		WINTERBURN
00/02-09-054-12W5/0 Amoco E- 1 Nilton 2-8		2,555-2,615 m	197	60		WINTERBURN
00/06-06-046-15W5/0 Encal et al. Columbia 6-6-46-15		4,112-4,130 m	59	18		WINTERBURN
00/11-29-065-18W5/0 Texaco Kaybob 11-29		2,553-2,563 m	33	10		WINTERBURN
02/15-26-054-23W5/0 Esso et al. Obed 15-26		3,985-4,001 m	52	16		WINTERBURN
00/11-35-054-23W5/3 IOE et al. Obed 11-35		13,652-13,685 ft	33	10		WINTERBURN
00/06-28-061-26W5/0 Sun Agol Deep Valley 6-28		12,810-12,840 ft	30	9		WINTERBURN
00/05-17-056-08W5/0 Imperial Paddle River No. 1		7,010-8,043 ft	1033	315		WOODBEND/WINTERBURN
00/14-11-070-05W6/0 Gulf Gold Creek 14-11		11,138-11,163 ft	25	8		WOODBEND/WINTERBURN
00/08-19-066-12W6/0 Amoco Cigol Shell Nose 8-19		17,214-17,274 ft	60	18		WOODBEND/WINTERBURN
00/15-23-053-21W5/2 MSR North Medicine Lodge 15-23-53-21		4,027-4,041 m	46	14		WOODBEND
02/08-26-055-22W5/0 CNRL Futurity B-1 Obed 8-26-55-22		12,515-12,570 ft	55	17		WOODBEND
00/04-13-056-23W5/0 Hees et al. CR EB Pinto 4-13-56-23		13,515-13,547 ft	32	10		WOODBEND
00/10-17-057-23W5/0 Bluemount Futurity Barir 10-17		13,117-13,147 ft	30	9		WOODBEND
00/09-35-048-12W5/0 Chevron Brazeau 9-35		10,303-10,363 ft	60	18		IRETON
00/01-26-058-18W5/0 Chevron BLGU 3 Kaybobs 2-26-58-18		11,140-11,169 ft	29	9		DUVERNAY
00/11-01-059-18W5/0 Chevron Clark 11-1		10,849-10,885 ft	36	11		DUVERNAY
00/07-05-059-18W5/0 SOBC Clark 7-5		11,254-11,340 ft	86	26		DUVERNAY
00/14-02-069-21W5/0 Enemex Panther Sturils 14-2		2,750-2,763 m	43	13		DUVERNAY
00-09-03-060-14W5/0 Gulf Windfall 9-3		2,677-2,692 m	16	5		DUVERNAY/LOWER LEDUC
00/10-16-069-05W6/0 Wascana et al. Gold Creek 10-16-69-5		12,314-12,324 ft	10	3		DUVERNAY/LOWER LEDUC
00/06-13-058-18W5/0 PCI et al. Kaybobs 6-13		11,175-11,218 ft	43	13		LOWER LEDUC/MAJEAU LAKE
02/10-21-062-18W5/0 Chevron Gulf et al. Foxck 10-21		9,891-9,942 ft	51	16		MAJEAU LAKE
00/04-22-069-18W5/0 B.A. Snipe Lake 4-22		8,990-9,035 ft	45	14		MAJEAU LAKE
00/07-20-059-18W5/0 Chevron Clark 7-20		10,475-10,535 ft	60	18		MAJEAU LAKE/SWAN HILLS

28 Cores in Total
Total of 788 m
of core

Details of core examined in this study.

Sample Number	Stratigraphic Interval	Carbonate or Sulphate Component	Geographic Location	Lithological Facies	Mineralogical Facies	$\delta^{18}\text{O}$	$\delta^{13}\text{C}$
CCS 35	WINT	Ankerite Whole-Rock	Obed	AD	QCp	-5.65	4.38
CCS 19	WINT	Ankerite Whole-Rock	Simonette Reef	A	QCp	-7.63	0.77
CCS 105	WINT	Ankerite Whole-Rock	West Pembina	AD	QCp	-6.28	1.31
CCS 129	WINT	Ankerite Whole-Rock	West Pembina	AD	QCp	-5.27	1.05
CCS 117	WINT	Ankerite Whole-Rock	West Pembina	A	QCp	-6.08	2.25
CCS 106B	WINT	Ankerite Whole-Rock	West Pembina	F	QCp	-5.65	1.62
CCS 355	WINT	Carbonate Layer	Obed	G & A	Cq	-6.55	3.48
CCS 132	WINT	Calcite Whole-Rock	West Pembina	AD	QCp	-6.92	4.08
CCS 36	WINT	Calcite Whole-Rock	Obed	AD	QCp	-7.85	3.27
CCS 133	WINT	Calcite Whole-Rock	West Pembina	B	QCp	-7.20	4.04
CCS 95	WINT	Calcite Whole-Rock	Obed	AD	QCp	-7.61	3.40
CCS 123	WINT	Calcite Whole-Rock	West Pembina	C	QCp	-6.25	3.09
CCS 18	WINT	Calcite Whole-Rock	Simonette Reef	A	QCp	-8.04	0.55
CCS 129	WINT	Calcite Whole-Rock	West Pembina	AD	QCp	-6.91	1.20
CCS 105	WINT	Calcite Whole-Rock	West Pembina	AD	QCp	-7.39	0.98
CCS 117	WINT	Calcite Whole-Rock	West Pembina	A	QCp	-7.84	2.71
CCS 119	WINT	Calcite Whole-Rock	West Pembina	B	QCp	-7.13	3.40
CCS 106A	WINT	Calcite Cement	West Pembina	F		-7.76	1.41
CCS 145	WINT	Calcite Rugose Coral	West Pembina	F		-6.87	4.24
CCS 1	WOOD/WINT	Ankerite Whole-Rock	Peace River Arch	A	QCp	-6.15	2.16
CCS 3B	WOOD/WINT	Ankerite Whole-Rock	Peace River Arch	A	QCp	-6.44	2.03
CCS 152	WOOD/WINT	Ankerite Whole-Rock	West Pembina	AD	QCp	-5.69	1.44
CCS 1	WOOD/WINT	Calcite Whole-Rock	Peace River Arch	A	QCp	-7.88	1.18
CCS 3B	WOOD/WINT	Calcite Whole-Rock	Peace River Arch	A	QCp	-7.55	1.22
CCS 152	WOOD/WINT	Calcite Whole-Rock	West Pembina	AD	QCp	-7.28	1.02
CCS 142A	IRET	Calcite Rugose Coral	West Pembina	F & G		-7.28	-0.66
CCS 141	IRET	Calcite Rugose Coral	West Pembina	F & G		-6.97	-0.50
CCS 22A	WOOD	Calcite Lens	Wild River Basin	A	Cq	-6.62	-8.03
CCS 25	WOOD	Calcite Whole-Rock	Wild River Basin	A	QCp	-9.05	0.33
CCS 22B	WOOD	Calcite Whole-Rock	Wild River Basin	A	QCp	-8.44	-1.08
CCS 20	WOOD	Calcite Whole-Rock	Wild River Basin	A	QCp	-8.28	0.58
CCS 46	WOOD	Calcite Whole-Rock	Obed	A	QCp	-9.34	0.22
CCS 43	WOOD	Dolomite Whole-Rock	Obed	A	Qdp	-7.90	2.04
CCS 51	WOOD	Ankerite Whole-Rock	Lambert/Windfall	A	QCp	-7.09	0.42
CCS 53	WOOD	Calcite Whole-Rock	Lambert/Windfall	A	QCp	-8.43	0.04
CCS 10	DUV	Ankerite Whole-Rock	Peace River Arch	AE	QCp	-8.85	0.65
CCS 87A	DUV	Carbonate Hardground	Pine Creek Basin	A	Cq	-6.22	-1.38
CCS 79	DUV	Calcite Whole-Rock	Pine Creek Basin	A	QCp	-8.15	0.97
CCS 81	DUV	Calcite Whole-Rock	Pine Creek Basin	A	QCp	-8.78	-0.13
CCS 89	DUV	Calcite Whole-Rock	Pine Creek Basin	A	QCp	-8.49	0.26
CCS 11	DUV	Calcite Whole-Rock	Peace River Arch	A	QCp	-9.25	-2.29
CCS 10	DUV	Calcite Whole-Rock	Peace River Arch	AE	QCp	-9.48	0.64
CCS 87B	DUV	Calcite Whole-Rock	Pine Creek Basin	A	QCp	-6.53	0.99
CCS 98	ML	Carbonate Nodule	Pine Creek Basin	A	Cq	-6.68	2.61
CCS 73	ML	Carbonate Nodule	Pine Creek Basin	AE	Cq	-6.07	2.78
CCS 66	ML	Calcite Whole-Rock	Swan Hills Platform	A	Cq	-7.10	2.66
CCS 59	ML	Calcite Whole-Rock	East of Surgeon Lk	A	QCp	-7.78	1.18
CCS 95	ML	Calcite Whole-Rock	Pine Creek Basin	A	QCp	-8.14	1.02
CCS 61	ML	Calcite Whole-Rock	East of Surgeon Lk	A	QCp	-7.72	-0.39
CCS 98B	ML	Calcite Whole-Rock	Pine Creek Basin	A	QCp	-7.72	1.84
CCS 68	ML	Calcite Whole-Rock	Swan Hills Platform	AE	QCp	-7.38	0.81

Stable isotopic ($\delta^{18}\text{O}$, $\delta^{13}\text{C}$) compositions of whole-rock calcite, ankerite, and dolomite fractions and individual carbonate components in the aquitards. Wint - Winterburn Gp., Wood/Wint - Woodbend/Winterburn Gp., Iret - Ireton Fm., Wood - Woodbend Gp., Duv - Duvernay Fm., ML - Majeau Lake Fm. The $\delta^{18}\text{O}$ for dolomites and ankerites have been corrected. This correction is explained in Appendix 3.

Sample Number	Stratigraphic Interval	Carbonate or Sulphate Component	Geographic Location	Lithological Facies	Mineralogical Facies	$\delta^{18}\text{O}$	$^{87}\text{Sr}/^{86}\text{Sr}$
CCS 35	WINT	Ankerite Whole-Rock	Obed	AD	CCp	-5.65	0.70848
CCS 36	WINT	Calcite Whole-Rock	Obed	AD	CCp	-7.85	0.70905
CCS 35B	WINT	Carbonate Layer	Obed	G-A	Cq	-8.55	0.70847
CCS 35'	WINT	Calcite Whole-Rock	Obed	AD	CCp	-7.61	0.70948
CCS 132	WINT	Calcite Whole-Rock	West Pembina	AD	CCp	-8.92	0.70803
CCS 123	WINT	Calcite Whole-Rock	West Pembina	C	CCp	-6.25	0.70842
CCS 152	WOOD/WINT	Ankerite Whole-Rock	West Pembina	AD	CCp	-5.68	0.71041
CCS 38	WOOD/WINT	Ankerite Whole-Rock	Peace River Arch	A	CCp	-6.44	0.70887
CCS 38	WOOD/WINT	Calcite Whole-Rock	Peace River Arch	A	CCp	-7.55	0.70887
CCS 152	WOOD/WINT	Calcite Whole-Rock	West Pembina	AD	CCp	-7.26	0.71041
CCS 3	WOOD/WINT	Celestite	Peace River Arch	A	CCp	* -1.00	0.70876
CCS 43	WOOD	Dolomite Whole-Rock	Obed	A	Qdp	-7.90	0.71403
CCS 22A	WOOD	Calcite Horizon	Wild River Basin	A	Cq	-8.62	0.70839
CCS 20	WOOD	Calcite Whole-Rock	Wild River Basin	A	CCp	-8.28	0.70915
CCS 51	WOOD	Ankerite Whole-Rock	Lambert/Windfall	A	CCp	-7.08	0.7125
CCS 87A	DUV	Carbonate Hardground	Pine Creek Basin	A	Cq	-6.22	0.70869
CCS 89	DUV	Calcite Whole-Rock	Pine Creek Basin	A	CCp	-8.49	0.70996
CCS 81'	DUV	Calcite Whole-Rock	Pine Creek Basin	A	CCp	-8.76	0.70905
CCS 11	DUV	Calcite Whole-Rock	Peace River Arch	A	CCp	-9.25	0.71085
CCS 87B	DUV	Calcite Whole-Rock	Pine Creek Basin	A	CCp	-8.53	0.70976
CCS 73	ME	Carbonate Nodule	Pine Creek Basin	AE	Cq	-6.07	0.70828
CCS 66	ML	Calcite Whole-Rock	Swan Hills Platform	A	Cq	-7.10	0.70874
CCS 61	ML	Calcite Whole-Rock	East of Sturgeon Lk.	A	CCp	-7.72	0.70966
CCS 98	ML	Carbonate Nodule	Pine Creek Basin	A	Cq	-6.68	0.70845

Radiogenic ($^{87}\text{Sr}/^{86}\text{Sr}$) and $\delta^{18}\text{O}$ isotopic compositions of whole-rock calcite, ankerite, and dolomite fractions and other individual carbonate components in the aquitards. *One sample of celestite was designated a $\delta^{18}\text{O}$ ratio of -1. refer to stable isotopic composition table on previous page for definitions of stratigraphic intervals. The $\delta^{18}\text{O}$ for dolomites and ankerites have been corrected. This correction is explained in Appendix 3.

Appendix 2 - Detailed Stratigraphic and Structural Descriptions of Cross Sections A-A' to F-F'

Introduction

The following cross sections are presented in four parts: (1) an extensive description of the distribution of the lateral and vertical extent of aquitards present; (2) a summary involving a general perspective regarding the distribution of aquitards; (3) a brief discussion with respect to the distribution of aquifers; and (4) a brief structural analysis of each cross section that includes a description of the roles that aquitards may play in hydrocarbon production.

Cross Sections A-A'

Cross sections A-A' traverse the West Pembina area of the West Shale Basin (Figures 3.2 and 3.3). The stratigraphy of the Winterburn Group is well defined in the West Pembina area (e.g., Machel, 1983; Stoakes, 1992; Wendte et al., 1995). In this area, it is also relatively straightforward to determine the boundary between the Woodbend and the Winterburn Groups, whereas in other parts of the study area, such as the Wild River Basin, the stratigraphy is not so well defined and is often difficult to correlate. Construction of a cross section in the West Pembina area is fundamental, not only because a significant amount of core was investigated from this area (Appendix 1), but also because stratigraphic correlations from this area can be extrapolated westwards towards the disturbed belt to correlate throughout the remainder of the study area.

Hydrostratigraphy

- ***Aquitards***

The lateral distribution of the aquitards within cross section A-A' can only be interpreted for the Winterburn Group as most wells penetrate only the top of the Woodbend Group (Figure 3.2). However, the type well for the Nisku Formation, 7-4-49-12W5, also penetrates the Watt Mountain Formation of the

Elk Point Group. The vertical distribution of aquitards is available from this type well.

Woodbend Group aquitard - From the type well, the thickness of the Woodbend Group aquitard is interpreted to be approximately 250 m. The lateral extent of this interval is uncertain throughout the remainder of the cross section.

Winterburn Group aquitards - The type well for the Wolf Lake, Cynthia, Bigoray, and Lobstick Members of the Nisku Formation, 7-4-49-12W5, in addition to stratigraphic pics from Wendte et al. (1995) is important in understanding the division of the Winterburn Group aquitards in this section.

Aquitard A - Thin (generally less than 20 m in thickness), and laterally discontinuous, aquitard A pinches in and out across the section. It most likely represents the basal Bigoray Member, but in places it appears to merge with the basal Lobstick Member.

Aquitard B - Generally ranging between 50 and 60 m in thickness, aquitard B is laterally discontinuous and generally appears to be equivalent to the Cynthia Member.

Aquitard C - Very similar in character and distribution to that of aquitard A, aquitard C is also thin (less than 20 m thick) and laterally discontinuous. This particular aquitard forms the Calmar Formation.

Aquitard E - Thin (less than 20 m in thickness), aquitard E is laterally discontinuous. It is present in the northeast and the southwestern-most parts of the section, but it is absent in most locations in the central portion of the cross section. This aquitard is equivalent to the Graminia Silt.

Exshaw Formation aquitard - This regionally extensive, laterally continuous aquitard is a reliable marker except in one location, well 6-20-48-13W5.

- *General perspective regarding thickness and lateral continuity of aquitards in cross section A-A'*

Interpretation of the lateral and vertical distribution of aquitards is restricted to the Winterburn Group, due to the absence of data for the Woodbend Group. Winterburn Group aquitards appear to be thin, less than 20 m in thickness, with the exception of the aquitard B, which is considerably thicker, approximately 50 m in thickness. The thin aquitards are commonly interlayered with carbonate aquifers of similar thickness. In the center of the section, around wells 16-15-50-11 W5 and 9-35-48-12 W5, it is evident that Upper and the Lower Winterburn Group aquitards are either absent or laterally discontinuous.

- *Aquifers*

Specifically within cross section A-A', the D-2 aquifers, when separated by aquitards, are relatively thin (usually less than 20 m in thickness), and generally laterally continuous. The D-1 aquifer is thick (approximately 200 m in thickness throughout the section) and laterally continuous. It is important to note that in the center of the section, the L D-2 and the U D-2, in addition to the D-1, are not separated by aquitards A to E, allowing for interconnection.

Structure

A significant feature of structural cross section A-A' (Figure 3.3) is the presence of a steeply southwestern dipping slope towards the disturbed belt. No major faults are evident in the section. There are four hydrocarbon producing wells in this section. Two wells in the updip part of the section produce oil from the Lower and the Upper Winterburn Group. Two wells in the downdip region produce gas from the Lower Winterburn Group. In updip well 8-8-51-19W5, aquitards surrounding the well most likely form a lateral, as well as a vertical seal to trap oil. Clearly a seal must separate the updip-oil producing interval and the downdip-gas producing intervals. If they were connected, then gas would be

found updip from the oil in the section. The role of aquitards in trapping gas in the downdip part of the section is uncertain.

Cross Sections B-B'

Cross sections B-B' trend in a northeast-southwest direction through the middle of the study area (Figures 3.4 and 3.5). The sections traverse the Southesk Caim complex near the limit of the disturbed belt, Obed and surrounding fields, the Wild River Basin, the edge of Marlboro, Pine Creek Basin, the edge of the Windfall complex, parts of the Swan Hills Platform surrounding the Windfall complex, terminating in the West Shale Basin just north of the Windfall complex (Figure 3.1).

Generally the wells penetrate deeper parts of the basin compared to those in cross sections A-A' of the West Pembina area. In sections B-B', most wells penetrate the Beaverhill Lake Group, whereas wells in the central to northeastern part of the section penetrate the Watt Mountain Formation of the Elk Point Group.

Hydrostratigraphy

- ***Aquitards***

Watt Mountain Formation aquitard- The Watt Mountain Formation aquitard is present northeast of well 8-26-55-22W5. It is approximately 50 m in thickness in the deepest well in the section. The lateral distribution of this interval is inconclusive throughout the remainder of the cross section due to the lack of well log data from this interval.

Beaverhill Lake Group aquitard - Within the northeastern-most and southwestern-most wells in the section, relatively thin wedges of Beaverhill Lake Group aquitards are present.

Majeau Lake Formation aquitard - Northeast of well location 11-1-59-18W5, the base of the Woodbend Group aquitard subdivides into the Majeau Lake Formation aquitard. It is less than 20 m thickness (Figure 2.2).

Woodbend/Winterburn aquitard - In the northeastern-most part of the section, Lower Winterburn Group and Woodbend Group aquitards have merged to become a single unit ranging in thickness between 320 m and 350 m. In the northeast, this merged unit, now referred to as the Woodbend/Winterburn aquitard, is relatively laterally continuous with the exception of a few lenses of Lower Winterburn Group aquifers, e.g., between wells 14-14-60-17W5 and 9-3-60-14W5 and Woodbend Group aquifers, e.g., in well 7-16-60-17W5. Whereas in section A-A', it was possible to identify aquitards A, B, and C, in this cross section they are difficult to distinguish because they have merged into one unit. The Z-marker is evident in wells 8-26-55-22W5 and 13-22-56-21W5 within the Wild River Basin. In these areas the Z-marker most likely corresponds with the boundary between the Woodbend and Winterburn Groups. However, to the northeast, in the more basinal part of the section, the Z-marker appears to stratigraphically move downwards into the Woodbend Group aquitard.

In the Wild River Basin, in particular in well 13-22-56-21W5, and directly to the southwest, the Woodbend/Winterburn aquitard alternates with layers of aquifers. In Obed and surrounding fields, laterally discontinuous wedges of aquitards are present and are most likely remnants of the thicker Woodbend/Winterburn aquitard to the northeast. Further to the southwest, in the northeast part of the Southesk Caim complex near the limit of the disturbed belt, it is evident that there is a general absence of Woodbend or Winterburn Group aquitards. However, a laterally discontinuous wedge of an aquitard is apparent in the southwestern-most well and is likely part of the Woodbend Group.

Upper Winterburn Group aquitards

Aquitard E - Aquitard E is less than 20 m in thickness in the northeast part of the section; however, it pinches out to the southwest. It follows a similar pattern as that in cross section A-A'. The effectiveness of the aquitard as a seal in the northeast part of the section is questionable. In one well in the Pine Creek Basin, a less than 10 m wedge of aquitard below aquitard E exists, but is not laterally continuous.

The Exshaw Formation aquitard - This is a laterally continuous aquitard that seals the underlying D-1 aquifer.

- ***General perspective regarding thickness and lateral continuity of aquitards in cross section B-B'***

A significant feature of this cross section, with respect to the aquitards, is that towards the direction of the disturbed belt (to the southwest), the 320 to 350 m thick Woodbend/Winterburn aquitard present in the northeastern to central part of the section pinches out, disappearing in the southwestern-most part of the Obed area. Similarly, Aquitard E disappears to the southwest in the Wild River Basin.

- ***Aquifers***

The D-4 aquifer is thick, ranging between 125 to 150 m, throughout the section. In the Pine Creek Basin and Marlboro areas it appears that the D-3 aquifer may be in direct contact with the D-4 aquifer, e.g., in well 5-16-58-19W5. An approximately 20 m layer of L D-3 is present in the northeastern part of the cross section, and relatively thin wedges of D-3 aquifers are present in well 7-16-60-17W5. In the northeast, laterally discontinuous Lower Winterburn Group aquifers exist between the thick Woodbend/Winterburn aquitard, and are also present in the Wild River Basin, Obed, and surrounding fields. The U D-2 is present in the central to northeastern part of the section and ranges from approximately 100 to 200 m in thickness. The D-1 is approximately 200 m in thickness throughout the section.

Significant with respect to the aquifers in the Obed and surrounding fields, and to the southwest, in the Southesk Cairn complex near the disturbed belt, is the interconnection between the D-1 through to the D-4. However, in the well closest to the disturbed belt, or in the southwestern-most part of the section, wedges of Beaverhill Lake and/or Woodbend Group aquitards, which range between 5 and 50 m in thickness reappear.

Structure

In structural cross section B-B' (Figure 3.5), as in structural section A-A' (Figure 3.3), a steeply southwestern-dipping slope towards the disturbed belt is apparent. The southwestern-most well of structural section B-B' was drilled in the Foreland Fold and Thrust Belt. In this region, the strata were thrust several hundred metres updip, which explains the offset from the otherwise general southward dipping slope in the remainder of the section. Other than this offset, no major faults are evident in this cross section. Several wells in this section are presently, or have been, gas producers. There are two gas-producing wells in this section: one in the Beaverhill Lake Group (Swan Hills Formation); and the other in the Upper Winterburn Group. Additionally, three wells within the section have zones of suspended gas production in the same intervals as the productive wells. It is possible that another well has suspended oil production in the Leduc Formation. Two wells have abandoned gas zones, one within the Lower Winterburn Group, and one within the Upper Winterburn Group. Two gas shut-in wells are present within the Ireton/Lower Leduc Platform and the Beaverhill Lake Group (Swan Hills Formation). The role of shale and marl aquitards in trapping gas in the cross section is uncertain. Although closure in the Beaverhill Lake Group in the Pine Creek Basin is caused by the presence of shale caps of the Woodbend Group (Larson, 1969), it is not apparent in this cross section at this scale. In the Obed area, there are no lateral or vertical shale or marl aquitards surrounding the productive interval in the U D-2 aquifer, so it is apparent that it must be sealed by some other means, perhaps an evaporitic aquiclude.

Cross Sections C-C'

Cross sections C-C' (Figures 3.6 and 3.7) traverse the northwestern-most part of the study area and are located approximately 150 km from cross sections B-B'. They traverse the Gold Creek Reef, the Gold Creek Reef toe, and follow a northeastern path adjacent to the Leduc Fringing Reef of the Peace River Arch.

Most wells penetrate the Beaverhill Lake Group and the Watt Mountain Formation. In the southwestern part of the sections, however, a few shallow wells exist, which only penetrate the Winterburn Group or the uppermost part of the Woodbend Group.

Hydrostratigraphy

- *Aquitards*

Watt Mountain Formation aquitard - In the central to northeastern part of the section, the Watt Mountain Formation aquitard is present. Since the aquitard is never completely penetrated, its thickness is unknown.

Beaverhill Lake Group aquitards - Thin, discontinuous, longitudinal wedges of Beaverhill Lake Group aquitards (less than 20 m in thickness) are present.

Majeau Lake Formation aquitard - A thin Majeau Lake Formation aquitard is present within the central to northeastern part of the section separating the D-4 aquifer from the thin (less than 20 m in thickness) L D-3 aquifer.

Woodbend/Winterburn aquitard - Similar to cross section B-B', the Woodbend Group aquitard and the majority of the Winterburn Group aquitards have merged in the central to northeastern part of this section to form a thick, merged aquitard (up to approximately 300 m in thickness). Two thin Lower Winterburn Group aquitards are present within two of the northeastern-most wells above the thick Woodbend/Winterburn aquitard. The lenses appear to pinch out towards the middle of the cross section. In the southwestern part of the section, near the areas of Gold Creek Reef and Gold Creek Reef toe, one of these reappears as a thin (less than 10 m thick), laterally discontinuous aquitard. Traversing the Gold Creek Reef area, the thick, merged Woodbend/Winterburn aquitard thins, and caps a thick D-3 aquifer. The two aquitards in the southwestern part of the cross section area are most likely Lower Winterburn

Group aquitards B and C. The most probable location of the Z-marker is indicated on both stratigraphic and structural sections (Figures 3.6 and 3.7).

Upper Winterburn Group aquitards - Although the Graminia Silt is correlative across most of the cross section, from kicks to the right in the gamma log signature, it forms an aquitard only in one well in the section.

Exshaw Formation aquitard - This aquitard is regionally extensive, laterally continuous, and caps the D-1 aquifer.

- *General perspective regarding thickness and lateral continuity of aquitards in cross section C-C'*

A significant feature with respect to the aquitards in this cross section is that the thick Woodbend/Winterburn aquitard thins towards the limit of the disturbed belt, similar to that in cross section B-B' (Figure 3.4). In contrast to cross section B-B', a thin remnant of the thicker aquitard continues towards the disturbed belt in the vicinity of the Gold Creek toe and Gold Creek Reef.

- *Aquifers*

The D-4 aquifer is thin (less than 20 m) in this area compared to its thickness of between 125 and 150 m within cross section B-B' (Figure 3.4). The L D-3 aquifer is thin (approximately 30 m in thickness) and laterally continuous throughout the central to northeastern part of the cross section. The D-3 appears to be present in the Gold Creek Reef attaining thicknesses of up to 250 m.

It is important to note that the D-1 and the U D-2 aquifers are nearly always interconnected due to the general absence of aquitard E throughout the section. In most places, the L D-2 and the U D-2 aquifers are interconnected (and are simply referred to as the D-2 in Figures 3.6 and 3.7) but occasionally an aquitard can be found separating them, such as in the northeastern part of the cross section. Where the D-3 and D-4 aquifers are present, they are both

vertically and laterally hydrologically connected. In the Gold Creek Reef area, only two, less than 20 m intervals of aquitards cap the D-3 aquifer.

Structure

Similar to cross section A-A' and B-B', a steeply southwestern dipping slope towards the disturbed belt is present in structural section C-C' (Figure 3.7). No major faults are evident. Only one well in this section, 10-16-69-5W6, was possibly productive. It is a suspended gas well which may have produced from the Wabamun Group.

Cross Section D-D'

Cross sections D-D', the most widespread sections constructed in this study, trend in a northwest-southeast direction and are also the sections nearest to the limit of the disturbed belt (Figures 3.8 and 3.9). The sections traverse the Peace River Arch, Gold Creek Reef, Simonette, Bigstone, Wild River Basin, the Obed area, Windfall, Swan Hills Platform southeast of Windfall, and terminate in the West Pembina area. Most wells penetrate the Beaverhill Lake Group while some within the center of the sections penetrate the Watt Mountain Formation.

Hydrostratigraphy

- *Aquitards*

Watt Mountain Formation aquitard - This aquitard is present in three wells in the central part of the section, however, the thickness of the aquitard is not possible to determine because only the top of it is penetrated.

Beaverhill Lake Group aquitard - In this cross section, the Beaverhill Lake Group aquitards are generally absent.

Majeau Lake Formation aquitard - On the edge of the Swan Hills Platform in the southeastern part of the section, wedges of aquitards possibly equivalent

to the Majeau Lake Formation aquitard, are present. They do not appear to extend to the northwest, and their extent to the southeast is unknown.

Woodbend Group aquitard and Woodbend/Winterburn aquitards- In the southeast part of the section, a thick (approximately 145 m) Woodbend Group aquitard is present on the Swan Hills Platform southeast of Windfall, and potentially in the West Pembina area. The thickness of this aquitard changes to the northwest. As the section crosses over the Windfall reef complex, between wells 3-12-51-19W5 and 6-23-52-20W5, the Woodbend Group aquitard pinches out. On the northwest edge of Windfall, the Woodbend Group aquitard and the majority of the Lower Winterburn Group aquitards merge into one unit, approximately 145 m in thickness. In well 6-12-53-23W5 in the Obed area, the aquitard thins and interfingers with aquifers. In the Bigstone and Simonette Reef areas, the aquitard completely pinches out. A remnant of this Woodbend/Winterburn aquitard is present as a stringer (less than 15 m in thickness) in the Gold Creek Reef and Peace River Arch areas. Below this stringer, a few laterally discontinuous aquitard wedges (between 10 and 50 m in thickness) are also present in the Peace River Arch area. They are possibly Woodbend Group and/or Majeau Lake Formation aquitards comparable to those in well 6-19-49-18W5 in the southeast.

Lower and Upper Winterburn Group aquitards - In the West Pembina area, Lower and Upper Winterburn Group aquitards (aquitards A, B, C and E) can be distinguished from the Woodbend Group aquitard (Figures 3.8 and 3.9).

Aquitard A - Thin, generally less than 30 m in thickness, Aquitard A confines aquifers of equal thickness. Towards the Obed area in the central part of the section, the aquitard tends to downlap onto the Woodbend Group aquitard.

Aquitard B - Very similar in character to aquitard A in the southeastern part of the section, aquitard B again appears to downlap onto the Woodbend Group aquitard in the Windfall area. In the Wild River Basin, Simonette Reef,

and on the southeast edge of Gold Creek Reef, an aquitard of approximately 60 m in thickness appears separate from the Woodbend Group aquitard. It is possible that this represents merged aquitards A, B, and C that separated from the thick Woodbend Group aquitard and merged to become one unit. In the Wild River Basin a thin Lower Winterburn Group aquifer separates the Woodbend Group aquitard from the merged A, B, and C aquitard package.

Aquitard C - This aquitard is thin (less than 10 m in thickness) and laterally discontinuous in the southeastern to central part of the section. In the Simonette Reef area, in the northwestern part of the section, aquitard C, although thin, becomes relatively laterally continuous and continues as such towards the Peace River Arch.

Aquitard E - The Graminia Silt, although correlative throughout most of the section from kicks to the right in the gamma log signature, it is only present as a thin aquitard in the West Pembina area and on the southeast edge of the Windfall complex.

The Exshaw Formation - This thin, laterally continuous aquitard caps the D-1 aquifer.

- *General perspective regarding thickness and lateral continuity of aquitards in cross section D-D'*

A significant feature with respect to aquitards in this cross section is that the Woodbend/Winterburn aquitard of approximately 145 m in thickness in and around the Obed area, gradually pinches out to the northwest so that near the Bigstone and Simonette Reefs it disappears. Southeast of Obed, the upper part of this merged aquitard splits into thin, generally numerous, laterally continuous aquitards, interbedded by aquifers.

- *Aquifers*

The D-4 is generally greater than 120 m in thickness. In some locations, it is capped by a thick Woodbend Group aquitard or Woodbend/Winterburn

aquitard package. In most locations, however, the D-3 aquifer is in direct contact or association with the D-4, such as in the Windfall Reef complex, the Obed area, and Bigstone and Simonette Reefs. In these locations, the combined aquifers can reach up to 300 m in thickness.

In the southeastern part of the cross section, several thin (approximately 30 to 50 m) intervals of L D-2 are interfingered with Lower Winterburn Group aquitards. In the Windfall area, a part of the L D-2, the D-3, and the D-4 appear to be hydrologically interconnected (refer to area between wells 3-12-51-19W5 and 6-30-51-20W5). It appears that this could potentially provide a lateral escape route for fluids in the updip direction, from the top of the D-3/D-4 aquifer package into the thin L D-2 aquifer. The L D-2 and the U D-2 are most likely in contact in the Obed area, and these aquifers are also in direct contact with the D-1 in some locations.

A significant feature with respect to the aquifers in this cross section is the interconnection of the D-1 through to the D-4 aquifers in the Bigstone and Simonette areas. Towards the northwestern edge of Simonette, in Gold Creek Reef, and in the Peace River Arch area, longitudinal and wedge-shaped aquitards can be found separating the D-4, D-3, and the L D-2 providing disconnection between the aquifers in these areas. In the Gold Creek Reef and Peace River Arch area, the U D-2 and D-1 appear to be connected, due to an absence of aquitard E in this area.

Structure

A significant structural feature in this section (Figure 3.9) is the presence of a shallow northwestern dipping slope towards in the direction of the Peace River Arch. No major faults are evident.

One gas-producing well exists in this cross section and is located within the Obed area and produces from the Upper Winterburn Group. One abandoned gas well exists in the section. It also occurs in the Obed area and produced from the Upper Winterburn Group. A suspended gas well occurs in the Simonette Reef and most likely produced from the Lower Winterburn Group.

Two gas shut-in wells occur in the section: one in the Wild River Basin within the Upper Winterburn Group; and the second in the Obed area within the Swan Hills Formation of the Beaverhill Lake Group. A suspended oil well also exists in the section, but the interval of past productivity is uncertain.

In the one productive well shown in the Obed region, shale and marl aquitards do not appear to play a major role in sealing gas. In this region, aquitards are scarce and if present, are laterally discontinuous. An evaporitic aquiclude is more likely responsible for closure of this gas play.

Cross Sections E-E'

These cross sections (Figures 3.10 and 3.11) traverse the center of the study area and trend parallel to cross section D-D' (Figure 3.1). They traverse the Peace River Arch, Gold Creek toe, the Karr Basin, the Swan Hills Platform north of Fir and Pine Creek fields, the Pine Creek Basin, Windfall, Swan Hills Platform southeast of the Windfall Complex, and terminate in the West Pembina Area.

Most of the wells penetrate the Beaverhill Lake Group in addition to the top of the Watt Mountain Formation. In the West Pembina area, however, wells only penetrate the top of the Woodbend Group.

Hydrostratigraphy

- ***Aquitards***

Watt Mountain Formation aquitard - The Watt Mountain Formation aquitard is present in five wells in this section. To the northwest, it moves stratigraphically updip towards the Peace River Arch area resulting in a restricted D-4 aquifer in this area. The entire Watt Mountain Formation aquitard is present in well 6-13-58-18W5, in the Pine Creek Basin, and is approximately 25 m in thickness. This aquitard, if laterally continuous, is potentially an effective barrier to fluid flow for the underlying aquifer.

Beaverhill Lake Group aquitards - In the Pine Creek Basin, 10 and 15 m thick, laterally discontinuous aquitard wedges are present.

Majeau Lake Formation aquitard - This aquitard is present throughout the majority of the cross section and varies between 15 and 20 m in thickness.

Woodbend Group aquitard - The boundary between the Woodbend Group in the extreme southeastern part of the cross section, in the West Pembina area, has been determined from correlations within the intersecting dip cross section A-A'. Thus, the thickness of the Woodbend Group aquitard in the Swan Hills Platform region southeast of the Windfall reef is approximately 125 m. This aquitard thins to approximately 50 to 75 m in the Windfall Reef area due to the presence of a D-3 and a thin (less than 5 m) L D-3 aquifer. In the Pine Creek Basin, the Woodbend and Winterburn Group aquitards merge.

Woodbend and Winterburn Group aquitards - In the extreme southeastern part of the cross section, the Woodbend Group aquitard forms the base of well 9-17-50-10W5. However, in the Pine Creek Basin and towards the limit of the disturbed belt, it is difficult to distinguish the Woodbend Group from the Winterburn Group; and therefore the aquitard in this area is referred to as the Woodbend/Winterburn aquitard. In these locations the Woodbend/Winterburn Group aquitard is 125 m in thickness. It remains relatively homogeneous and laterally continuous towards the Peace River Arch.

The Lower and Upper Winterburn Group aquitards - In the southeastern part of the section, aquitards A, B, and E are present and separated by intervening aquifers. Aquitards A and B merge in the northwest area of West Pembina, and aquitard C becomes present. In the Swan Hills Platform, aquitards A, B, and C split into several thin intervals of aquitards and aquifers. Interfingering of thin (less than 5 m) aquitards and aquifers is due to the presence of a D-3 aquifer in the Windfall Reef.

Located above the D-3 aquifer in the Windfall Reef area, an aquitard (most likely a combination of aquitards B and C) of approximately 90 m in thickness, could potentially provide an effective seal. However, the reef is not productive to hydrocarbons in this section.

In the central to northwestern part of the section, stratigraphically located between aquitards E and the merged Woodbend/Winterburn aquitard, minor, laterally discontinuous wedges of aquitards are present, and most likely represent aquitards B and C. In the Pine Creek Basin and Windfall Reef areas, minor Upper Winterburn Group aquitard wedges exist.

Aquitard E - In the southeastern part of the section in the West Pembina area and into the Pine Creek Basin, aquitard E is thin (less than 10 m in thickness). Although correlative between the Pine Creek Basin and the Peace River Arch, the Graminia Silt is no longer an aquitard. In the northwestern-most well in the section, however, it reappears as an aquitard

Exshaw Formation aquitard - Thin, but laterally continuous, the Exshaw Formation aquitard overlies the D-1 aquifer across the entire section.

- *General perspective regarding thickness and lateral continuity of aquitards in cross section E-E'*

Similar to cross section D-D' (Figures 3.8 and 3.9), Winterburn Group aquitards in the Windfall area downlap onto the Woodbend Group aquitard. In contrast to cross section D-D', the thick aquitard package (in this case it is a combined Woodbend/Winterburn aquitard rather than a Woodbend Group aquitard) does not pinch out to the northwest. This is due to the section crossing through a basinal area, the Karr Basin, and not intersecting reefs such as Bigstone or Simonette as in cross section D-D'.

- *Aquifers*

In the Swan Hills Platform region southeast of Windfall, the D-4 aquifer is approximately 120 m in thickness. It gradually thins as it moves stratigraphically

updip to the southwest to less than 15 m in the vicinity of the Peace River Arch area. The L D-3 aquifer is thin (less than 5 m in thickness) and laterally continuous from the Swan Hills Platform region to West Pembina and again from the northwest edge of the Pine Creek Basin to the Peace River Arch. It is absent in the central part of the Pine Creek Basin. Two laterally discontinuous, thin lenses of D-3? aquifers are present in the Windfall and Pine Creek Basin areas.

An octopus-shaped D-3 aquifer in the Windfall area that could potentially be overlain by an L D-2 aquifer, has extensions of associated aquifers in basinal deposits on either side of the reef. In the southeastern part of the section, aquitard E separates the D-2 aquifer from the D-1 aquifer. However, aquitard E pinches out on the northwestern edge of Pine Creek Basin allowing for interconnection between the D-2 and the D-1 aquifers. Northwest of Pine Creek Basin in the Swan Hills Platform region, Karr Basin, and Gold Creek Reef toe areas, a connection between the D-2 and the D-1 exists. The D-1 aquifer is approximately 150 m in thickness across the whole section.

A significant feature of this cross section is that in the central to northwestern part of the section, the D-1 and the D-2 aquifers are interconnected. The presence of an octopus-shaped D-3 aquifer in the Windfall complex with lenses of thin aquifers extending from it is intriguing.

Structure

Similar to cross section D-D' (Figure 3.9), a gentle southwestern dip towards the Peace River Arch exists in structural cross section E-E' (Figure 3.11). No major faults are evident in this cross section.

One gas-producing well is present in this section. It is located in the Pine Creek Basin and produces from the Beaverhill Lake Group (Swan Hills Formation). There are two suspended gas wells, one in the Peace River Arch area which could have possibly produced from the Wabamun Group, and the other in the Pine Creek Basin which produced from the Swan Hills Formation. One suspended oil well exists in the Karr Basin which produced from the Swan Hills Formation. Two abandoned gas wells exist within the section. One is in the

Swan Hills Platform to the southeast of Windfall Reef could have possibly produced from the Upper Winterburn Group. The other is in the Pine Creek Basin and produced from the Swan Hills Formation. One injected gas well exists in the section. It is located in the Pine Creek Basin where gas was injected into the Beaverhill Lake Group.

From this cross section it is uncertain what the role of aquitards are in presently trapping gas in D-4 in the Pine Creek Basin. As discussed in the description of cross section B-B', the Woodbend Group shales are known to act as a vertical seal (Larson, 1969).

Cross Sections F-F'

These cross sections (Figures 3.12 and 3.13) trend in a southeast-northwest direction and border the most northeastern part of the study area (Figure 3.1). They traverse an area adjacent to the Peace River Arch, the Sturgeon Lake Reef, the West Shale Basin northeast of Sturgeon Lake, the West Shale Basin and Swan Hills Platform north of the Windfall complex, and terminate in the West Pembina area. Wells generally penetrate the Woodbend Group; however, several also penetrate the top of the Watt Mountain Formation.

Hydrostratigraphy

- ***Aquitards***

Watt Mountain Formation aquitard - Although present in six wells, the thickness of this interval cannot be determined due to the fact that the wells do not penetrate it entirely. The aquitard moves updip towards the southwest in the direction of the Peace River Arch area, similar to that in cross section E-E' (Figure 3.10).

Beaverhill Lake Group aquitards - In the West Shale Basin, in well 6-7-64-16W5, thin, laterally discontinuous wedges of Beaverhill Lake Group aquitards are present. In three wells, on the edge of Sturgeon Lake and in the West Shale Basin immediately southeast of it, a wedge-shaped aquitard, ranging between

approximately 5 and 45 m in thickness, is present. It also appears to be present in the well adjacent to the Leduc Fringing Reef of the Peace River Arch.

Majeau Lake Formation aquitard - Throughout the central part of the section, the Majeau Lake Formation aquitard is thin and laterally continuous. It ranges in thickness from approximately 15 m in the Swan Hills Platform region, north of the Windfall Reef complex, to approximately 30 m in the West Shale Basin immediately southeast of Sturgeon Lake Reef. It may also be present adjacent to the Peace River Arch as an approximately 20 m thick aquitard. In the southeastern-most well in the Sturgeon Lake Reef, the Majeau Lake Formation aquitard appears to be absent.

Woodbend Group aquitard - From correlations with cross section A-A' and, also, from stratigraphic pics in a cross section by Wendte et al. (1995) proximal to this one, the Woodbend Group and the Winterburn Group are possible to distinguish in the southeastern part of the cross section in wells 6-11-54-6W5 and 9-3-60-14W5. In the majority of the section, the Winterburn Group aquitard directly overlies the Woodbend Group aquitard. In these areas, the merged aquitard is referred to as the Woodbend/Winterburn aquitard. The thickness of the Woodbend Group aquitard in the West Pembina area is unknown due to the fact that the well only penetrates the top of the aquitard.

The Z-marker can be correlated throughout most of the cross section and it is tempting to correlate it with the boundary between the Woodbend and Winterburn Groups. It is correlative with the boundary between these two Groups in the West Pembina, and Swan Hills Platform north of the Windfall reef but in the central to northwestern part of this section, the Z-marker descends and becomes part of the middle of the Woodbend Group aquitard (Figures 3.12 and 3.13).

Woodbend/Winterburn aquitard - In the Swan Hills Platform north of the Windfall Reef complex, Woodbend and Winterburn Group aquitards are distinguishable from each other. However, because they are in direct contact

with each other they will be combined and discussed as the Woodbend/Winterburn aquitard. This aquitard ranges in thickness from approximately 220 m to 315 m in the central to northwestern part of the section and is generally laterally continuous. The thinnest part of the aquitard (approximately 220 m) occurs in well 10-21-62-18W5 in the central part of the section. The presence of an L D-2 aquifer is possible and responsible for the thinning of the aquitard.

In the Sturgeon Lake Reef area, well 15-17-69-22W5 only penetrates the top of the Woodbend/Winterburn aquitard. It is inferred that a D-3 aquifer may be present just below the termination of the well log data in this location. Evidence for this includes: (1) a possibly productive zone just under the termination and possible remnants; and (2) stringers of the Leduc Reef (D-3) present in adjacent well 13-30-70-24W5.

Winterburn Group aquitards - In locations across the section, aquitards A, B, C, and E of the Lower and Upper Winterburn Group can be distinguished because they are separate from the thick, merged Woodbend/Winterburn aquitard. In the extreme southeastern part of the section, in the West Pembina area; aquitard A and aquitard C are present as thin (approximately 5 m thick) aquitards, and aquitard B is approximately 40 m in thickness. These three aquitards merge towards the northwest. From the Swan Hills Platform, surrounding the Windfall Reef complex, to the area north of the Pine Creek Basin, they form one thick Winterburn Group aquitard, directly overlying the Woodbend Group aquitard. In the Sturgeon Lake Reef area and the West Shale Basin region (immediately to the southeast), a thin, longitudinal lens (5 to 20 m) of aquitard C is present and separate from the thick, underlying Woodbend/Winterburn aquitard. It is laterally continuous in this area, but appears to merge with the Woodbend/Winterburn aquitard towards the southeast.

In the Sturgeon Lake Reef area and into the area adjacent to the Peace River Arch, a part of aquitard B is separated from the thick

Woodbend/Winterburn aquitard package by an intervening aquifer approximately 20 m in thickness.

Aquitard E - From the West Pembina area to the West Shale Basin, northeast of the Sturgeon Lake Reef, aquitard E is present. Although the Graminia Silt, is correlative in the Sturgeon Lake and the Peace River Arch areas, from kicks to the right in the gamma log signature, it does not form an aquitard.

Exshaw Formation aquitard - Thin (approximately 25 to 30 m thick) and laterally continuous, the Exshaw Formation aquitard overlies the D-1 aquifer. The location and thickness of this aquitard is uncertain in only one well, 5-17-56-8W5.

- *General perspective regarding thickness and lateral continuity of aquitards in cross section F-F'*

Stratigraphic cross section F-F' (Figure 3.12) is generally similar in appearance to that of E-E' (Figure 3.10). The major differences in cross section F-F' are that: (1) the Woodbend/Winterburn aquitard is overall much thicker, ranging between 220 to 315 m, in contrast to 150 to 165 m in cross section E-E'; and (2) the Majeau Lake Formation aquitard is separated from the Woodbend/Winterburn aquitard by a moderately thicker aquifer than in cross section E-E'; (3) the Woodbend/Winterburn aquitard appears to be more laterally extensive towards the southeast than in cross section E-E', although poor well data in this area leads to difficulties in correlations.

- **Aquifers**

The D-4 aquifer is regionally extensive and ranges from approximately 125 m in the Swan Hills Platform and gradually thins towards the Peace River Arch to approximately 20 m. The L D-3 aquifer is thin and ranges from approximately 10 to 20 m in thickness. It appears to be continuous throughout the section, and may thin towards the Peace River Arch area. In the Sturgeon

Lake Reef area the D-4 and the D-3 aquifers appear to be connected, which does not occur in cross section E-E'. The D-3 aquifer is present as thin stringers in the Sturgeon Lake Reef area. A large D-3 aquifer may also be present in the Sturgeon Lake area.

In the West Pembina area, L D-2 aquifers are thin and laterally discontinuous. In the Swan Hills Platform north of Windfall, in well 10-21-62-18W5, a thick (approximately 80 m) L D-2 aquifer, possibly a Nisku Reef, is present. Aquifer U D-2 is present throughout the section and varies in thickness from approximately 45 m to 90 m. Aquifers L D-2 and U D-2 are infrequently separated by an aquitard. If an aquitard does separate these aquifers, it is relatively thin and laterally discontinuous. Aquifer D-1 often directly overlies aquifer U D-2, for example in the Sturgeon Lake Reef and adjacent to the Peace River Arch areas. Direct communication between the L D-2, the U D-2, and the D-1 aquifers exists in these areas. This is very similar that in the Karr Basin and adjacent to the Peace River Arch in cross section E-E'.

Structure

In structural cross section F-F' (Figure 3.13), as in the two other structural strike cross sections D-D' (Figure 3.9) and E-E' (Figure 3.11), a gently northwestern dipping slope from the West Pembina area towards the direction of the Peace River Arch exists. No major faults are evident in this cross section.

There is one oil-producing well in this section located in the Swan Hills Platform north of the Windfall Reef complex. It produces from the Low Leduc Platform. A suspended oil well exists within the West Shale Basin northeast of the Sturgeon Lake Reef and it produced oil from the Beaverhill Lake Group. A questionable oil-producing well exists within the Sturgeon Lake Reef complex. It appears that there might be production occurring from the Leduc reef in that area. The role of aquitards in sealing oil and gas in this area is uncertain.

Appendix 3 - Methodology

Cleaning and Crushing

Prior to crushing or drilling, all core samples were thoroughly cleansed and washed in tap water, followed by several rinses in distilled and millipore (deionized) water. The core samples were then dried in a clean environment. Whole-rock samples were crushed in a thick polypropylene bag with a hammer to obtain pea-sized pieces. If necessary, the samples were further crushed using a steel mortar and pestle to obtain smaller pieces. These pieces were crushed to a fine powder (generally less than 400 μm) for approximately 1 minute, in a stainless steel container of a swingmill (shatterbox). Between each sample, the stainless steel container was thoroughly cleansed with silica sand for approximately 1 minute, followed by a cleansing in tap water and rinsing in millipore water.

Individual components of the aquitards e.g., cements, fossils, and nodules, were drilled using a modified dentists' drill. Diamond-tipped drill bits were required in several cases to extract individual components of the aquitards, such as those containing a significant amount of quartz.

X-Ray Diffraction (XRD)

Analyses were conducted on a Rigaku Geigerflex powder diffraction system attached to an on-line computer capable of analog and digital processing and routine search-and-match procedures of diffraction patterns using the JCPDS database. The unit measured from 10-90° 2 θ in a single scan.

Most samples were analyzed using a backpacking technique. However, when samples were not large enough, such as with individually drilled components of the aquitards, a quartz mount plate/ethanol slurry technique was used instead.

Carbonate Dissolution

The weight percent carbonate of whole-rock powders was determined using a simple chemical dissolution procedure as follows (modified after Cavell and Machel, 1997). A 1 g sample of whole-rock powder was reacted with up to 15 mL of 1 N HCl for approximately 5 days or until the reaction was complete. Over the duration of the reaction the slurry was repeatedly mixed and placed in an ultrasonic bath for several minutes at a time.

After complete acid digestion, the samples were centrifuged for 2 minutes, and the supernatant was removed with a pipette and discarded. Millipore water was added to the residue. The solution was slurried, centrifuged for another 2 minutes, the supernatant was removed and discarded again. The residue was dried overnight in an oven at 100°C, subsequently desiccated for approximately an hour, and finally weighed. The weight loss from the acid digestion is attributed to the total dissolution of carbonate.

Stable Isotopes ($\delta^{13}\text{C}$ and $\delta^{18}\text{O}$)

Depending on the percent carbonate content of the whole-rock samples and individual components of the aquitards, obtained from either carbonate dissolution or estimated from XRD peak-height counts, the amount of sample used in stable isotopic analyses varied between 30 and 260 mg. Samples were not treated with bleach or chloroform to remove any organic residue, nor were they roasted to remove organic matter. This follows a previous study (Hearn, 1996), in which an organic-rich sample was tested to assess whether phosphoric acid also digests organic matter, which could alter the carbon isotope ratios. Hearn (1996) found that, within reproducible error, the isotopic ratios of treated and untreated samples were comparable. Isotope ratios were thus assumed to be the sole product of carbonate digestion, and all other samples were analyzed untreated.

Coexisting carbonate phases within whole-rock samples, i.e., calcite and ankerite, ideally should have been physically separated from the host rock prior to stable isotopic analysis, rather than chemically through acid leaching.

However, the carbonate phases were not mechanically separable. Each of these whole-rock samples was reacted with 4 mL of 100% phosphoric acid for approximately 1 to 2 hours in a 25°C water bath. The resulting CO₂, representative of the reaction with the calcite fraction, was analyzed with a Finnigan-MAT 252 mass spectrometer. If the coexisting whole-rock ankerite fraction amounted to greater than approximately 10 weight percent, estimated from XRD patterns, the remaining residue consisting of whole-rock powder and phosphoric acid was left to react for a further 5 days in a 25°C water bath (following Degens and Epstein, 1964). A second CO₂ sample, representative of the reaction with ankerite was extracted.

Whole-rock samples or individual components within the aquitards containing only one carbonate phase, i.e., calcite, ankerite, or dolomite, were extracted once, following the procedure above for the respective mineral. Analysis of dolomite follows the same procedure as ankerite.

The ¹³C/¹²C and the ¹⁸O/¹⁶O isotopic ratios of all specimens are expressed relative to the PDB standard. Analytical error is estimated to be generally less than ±0.1 ‰ for both δ¹³C and δ¹⁸O. The δ¹⁸O values of ankerite and dolomite were corrected by -0.82 for phosphoric acid fractionation (Sharma and Clayton, 1965).

Radiogenic Isotopes (⁸⁷Sr / ⁸⁶Sr)

Using standard cation exchange techniques described below, strontium was extracted from the carbonate fraction of the whole-rock powders and individual components within the aquitards. Isotope ratios were determined on a VG (Micromass) 354 mass spectrometer. The samples were loaded as a phospho-tantalate gel on a single rhenium ribbon bead assembly. Precision of individual runs was better than ±0.00003 (2σ). Results were standardized to NBS-SRM-987. Repeated measurements of Sr isotopic standard NBS-SRM-987 during the study gave a value of 0.71018 ± 0.00002 (2σ).

Dissolution/Extraction Techniques

A. Whole-rock samples containing siliciclastics

Step 1: *Removing the most soluble, non-carbonate portion of radiogenic Sr*

Between 75 and 100 mg of dry powder was weighed into a labelled, 15 mL centrifuge tube, and dissolved in 3 mL 0.01 N HCl. This solution was repeatedly mixed and placed in an ultrasonic bath for approximately 1 hour. The sample was centrifuged, the supernatant was removed by pipette and discarded.

Step 2: *Carbonate Dissolution*

One milliliter of 1 N HCl, was added dropwise to the residue from Step 1. To contain sputtering, the mixture was immediately capped. When effervescence subsided, a further 1.25 mL of 1 N HCl was added (totalling 2.25 mL). The solution was repeatedly mixed and placed in an ultrasonic bath over the duration of the reaction of between 2 and 5 days. The mixture was centrifuged for 10 minutes, and the supernatant was removed by pipette and saved for use in Step 3.

Step 3: *Filtering*

Prior to loading into the first cation columns, all samples were again centrifuged at 10,000 RPM for 10 minutes and then filtered to remove any particles, using a 0.2 μm PTFE filter on a 5 mL syringe. The filter and syringe were then rinsed using a total of 0.75 mL of H_2O (a 0.5 mL + 0.25 mL rinse), making a total of 3 mL of 0.75 N HCl for loading.

B. Individual carbonate components (e.g., pure calcite fossils)

Between 10 to 15 mg of dry powder sample was weighed into a labelled, 15 mL centrifuge tube. One milliliter of 1 N HCl was added dropwise to the residue from Step 1. To contain sputtering, the mixture was immediately capped. When effervescence subsided, a further 2 mL of 1 N HCl was added (totalling 3 mL). The solution was repeatedly mixed and reacted

overnight. Prior to loading into the first cation columns, samples were centrifuged at 10,000 RPM for 10 minutes.

C. Celestite

Three milliliters of 1 N HCl were added to a trace amount of powdered celestite. It was capped tightly and placed on a hot plate at low temperature (approximately 70°) to dissolve for 2 days. The solution was centrifuged for 10 minutes at 10,000 RPM and the supernatant was removed by pipette, placed in a separate container, and left to evaporate in a clean environment. The dry sample was then loaded directly onto a rhenium assembly to be analyzed in the mass spectrometer.

Unspiked Sr Separation from Cation Columns

Resin: Bio-Rad AG50W-X8 cation resin, 200-400 mesh, H⁺ form.

Columns: Bio-Rad Econo-Columns (borosilicate glass and polypropylene); 15 x 0.7 cm containing 4.4 mL of wet cation resin.

Chromatography

STEP	Solvent	Quantity	Purpose	Comments
1.	0.75N HCl	3 mL	Load sample	Dropwise Load
2.	0.75N HCl	3 mL	Rinse column walls	3 x 1 careful rinses
3.	2.5 N HCl	3 mL	Remove 0.75 N HCl	3 x 1 careful rinses
4.	2.5 N HCl	20 mL	Waste	Rinse off Ca, Rb, etc.
5.	2.5 N HCl	7 mL	Collect Sr	in a clean 8 ml, labelled teflon container

Table 1: Summary of Cation Column Chromatography

Following elution of Sr (Step 5, Table 1) the solution was dried on a hot plate in a clean hood ready for the cleanup column procedure. The dried residue was dissolved in 0.25 ml oxalic acid/HCl acid mixture (1:1 0.25 M oxalic: 1 N HCl), and the steps in Table 2 were then performed.

Sr Cleanup Columns

Resin: Bio-Rad AG50W-X8 cation resin, 200-400 mesh, H⁺ form.

Columns: Hot-Shrink TFE 4:1 (Zeus # 164553, 7/8") containing 1.7 mL of wet cation resin.

Chromatography

STEP	Solvent	Quantity	Purpose	Comments
1.	oxalic:HCl	0.25 mL	Load sample	Dropwise Load
2.	oxalic:HCl	0.75 mL	Make sample load 1 mL and rinse	3 x 0.25 careful rinses
3.	2.5 N HCl	1 mL	Rinse and remove oxalic	2 x 0.5 careful rinses
4.	2.5 N HCl	7 mL	Waste	
5.	2.5 N HCl	5 mL	Collect Sr	

Table 2: Summary of Sr Cleanup Column Chromatography

The strontium solution from Step 5 dried on a hotplate in a clean hood, leaving a residue ready for loading on a mass spec filament assembly as outlined above.

Mercury Injection Capillary Pressure Measurements (MICPM)

The majority of core plugs for MICPM, one inch in length by one inch in diameter, were drilled horizontally through drill core as opposed to the conventional vertical plugs used on shale seals (e.g., Sneider et al., 1997; Krushin, 1997). Mercury intrusion prior to initial entry, as determined from examination of the plots of pressure versus mercury volume injected (Figures 6.2 a, b, and c), were subtracted prior to the calculation of capillary pressure versus percent of pore space (pore volume) occupied (Figures 6.3 a, b, and c). These calculations were made for all of the MICPM curves measured in this study (after Sneider et al., 1997), which compensates forunjacketed core plugs, i.e., they were not covered in epoxy prior to mercury injection.

Under the direction of B. Schulmeister and S. Reddy at PRI (Petroleum Recovery Institute) in Calgary, MICPM tests were conducted on eight samples. Three of the eleven samples originally selected could not be tested for MICPM

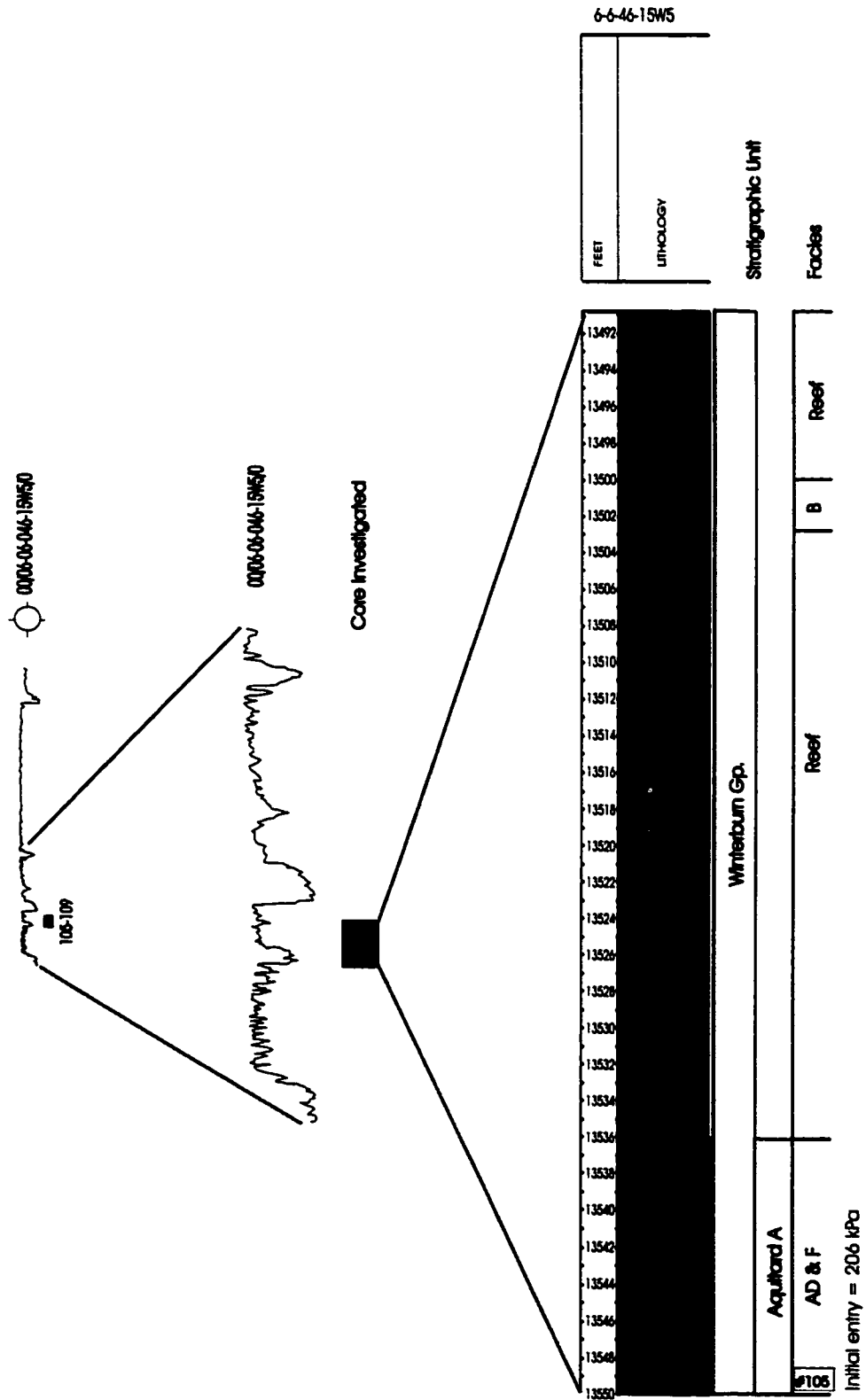
because of their low porosity and small pore sizes. All measurements were performed on an Automated Micromeritics Autopore 9220 instrument with a maximum working pressure of 60,000 psi (or approximately 414,000 kPa). The samples were first evacuated under vacuum, and then mercury was incrementally injected at predetermined equilibrium pressures up to the maximum working pressure. The volume of mercury injected into the pores at each pressure was recorded digitally after the reading stabilized.

Magnetic Susceptibility Tests

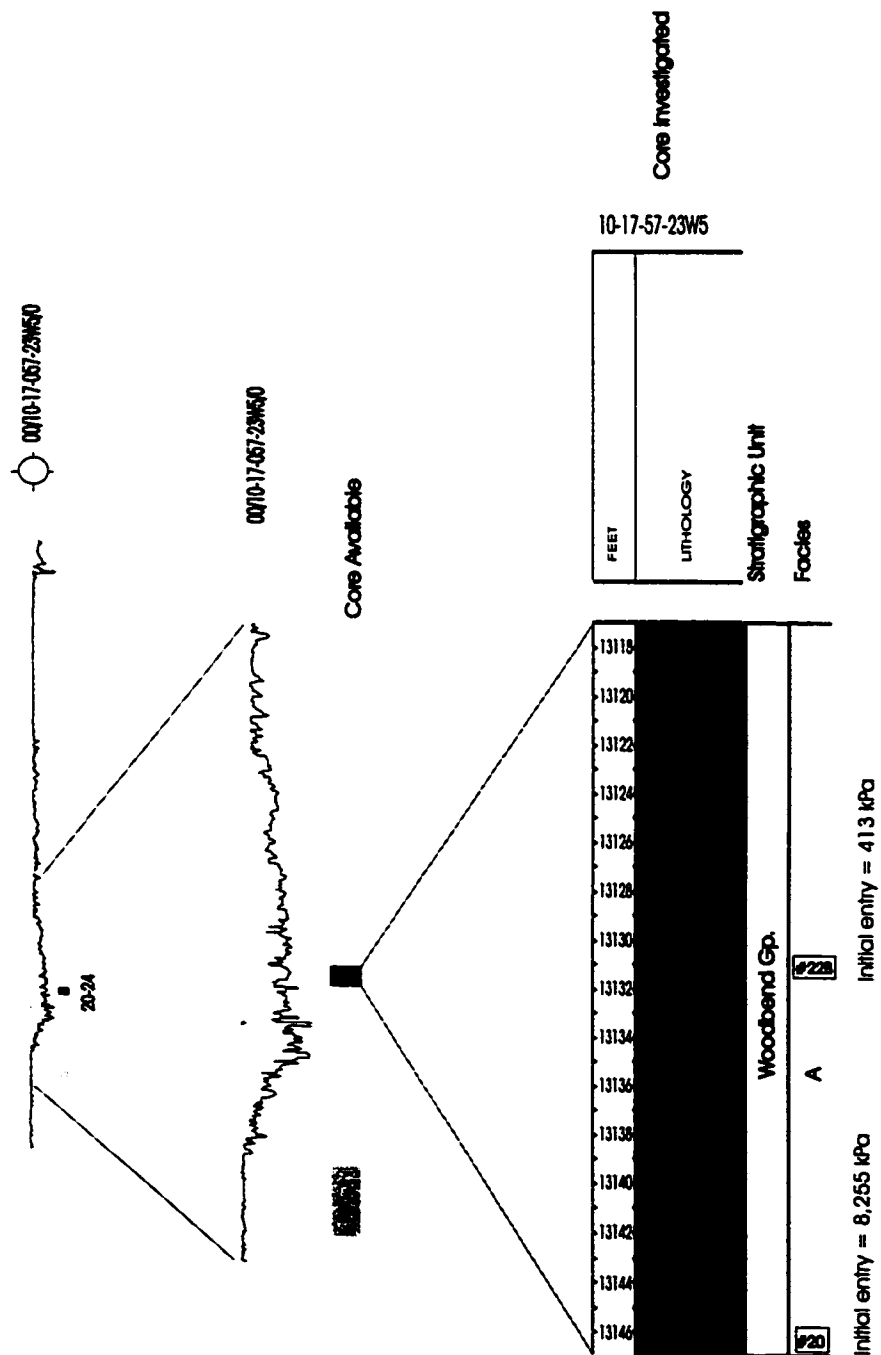
Between approximately 400 and 785 mg of crushed, whole-rock powder was used to conduct low-frequency magnetic susceptibility tests on individual samples. Magnetic susceptibility (X) was measured at low frequency (0.465 kHz) on a Bartington MS2 meter. Each sample was analyzed 3 times with two of these measurements conducted with the sample container upright at different orientations, and the third measurement conducted with the sample container turned on its side, which repeatedly produced higher readings. The readings used in the study represent an average of the three readings in SI units of 10^{-5} . To account for the difference in mass of each sample, the low-frequency susceptibility readings (converted to susceptibility readings of 10^{-8}) were divided by the samples' mass (in kg) to produce measurements in m^3/kg .

Appendix 4 - MICPM data

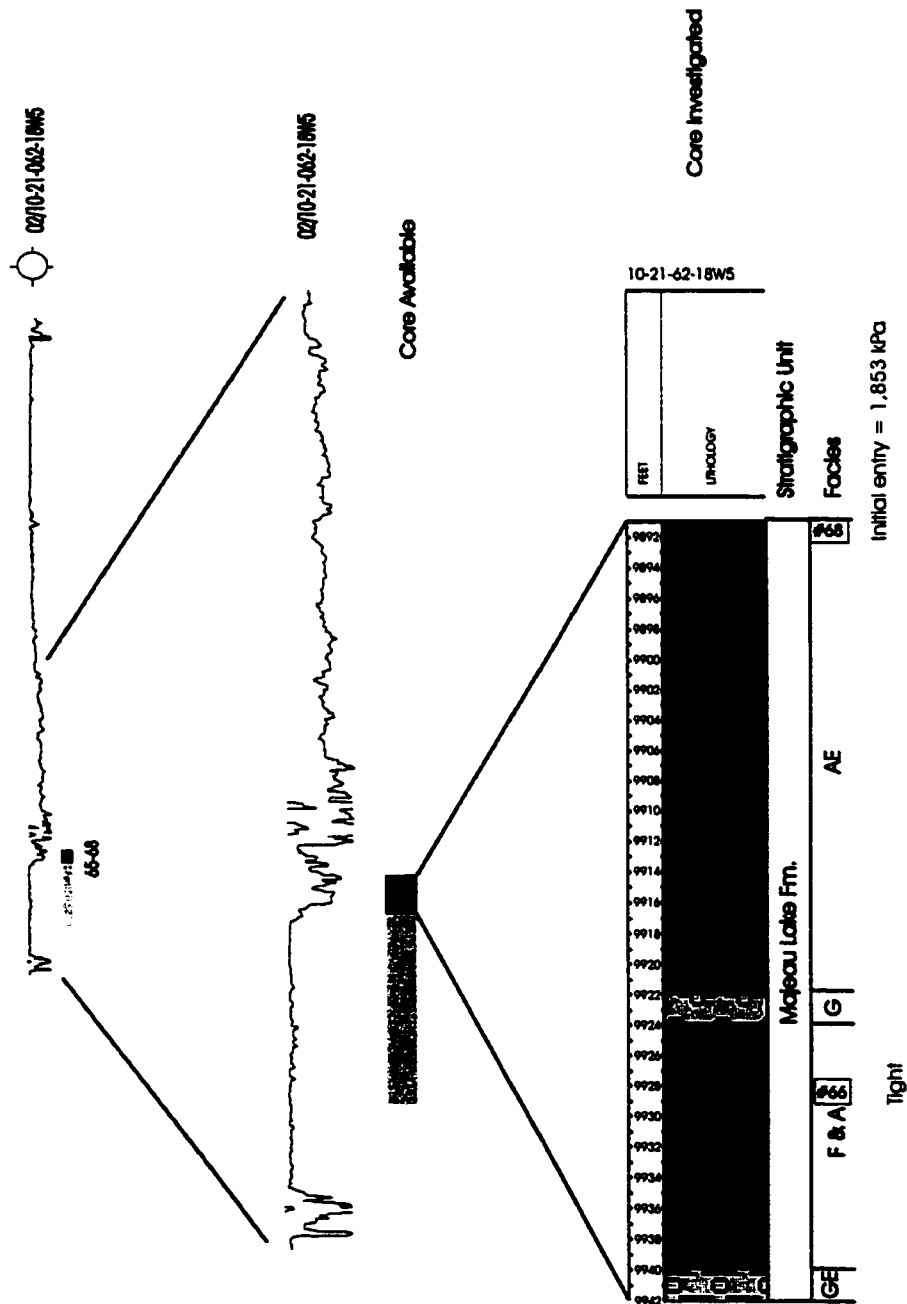
The following cored well logs, overleaf, include the initial entry pressures of the samples selected for MICPM.



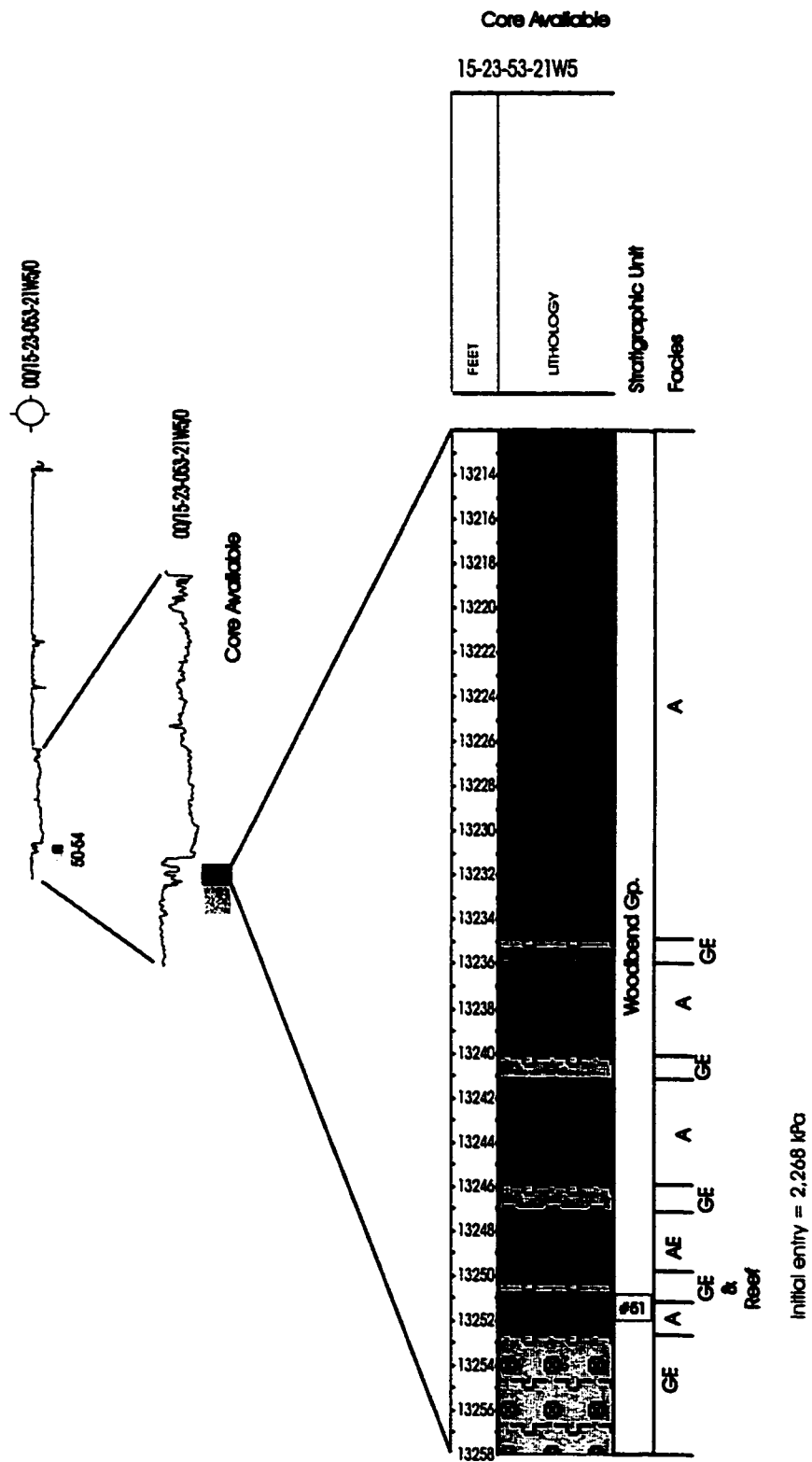
Interval of core investigated and associated gamma log of the Winterburn Group, including aquitard A. The initial entry pressure derived from MICPM is included for sample #105.



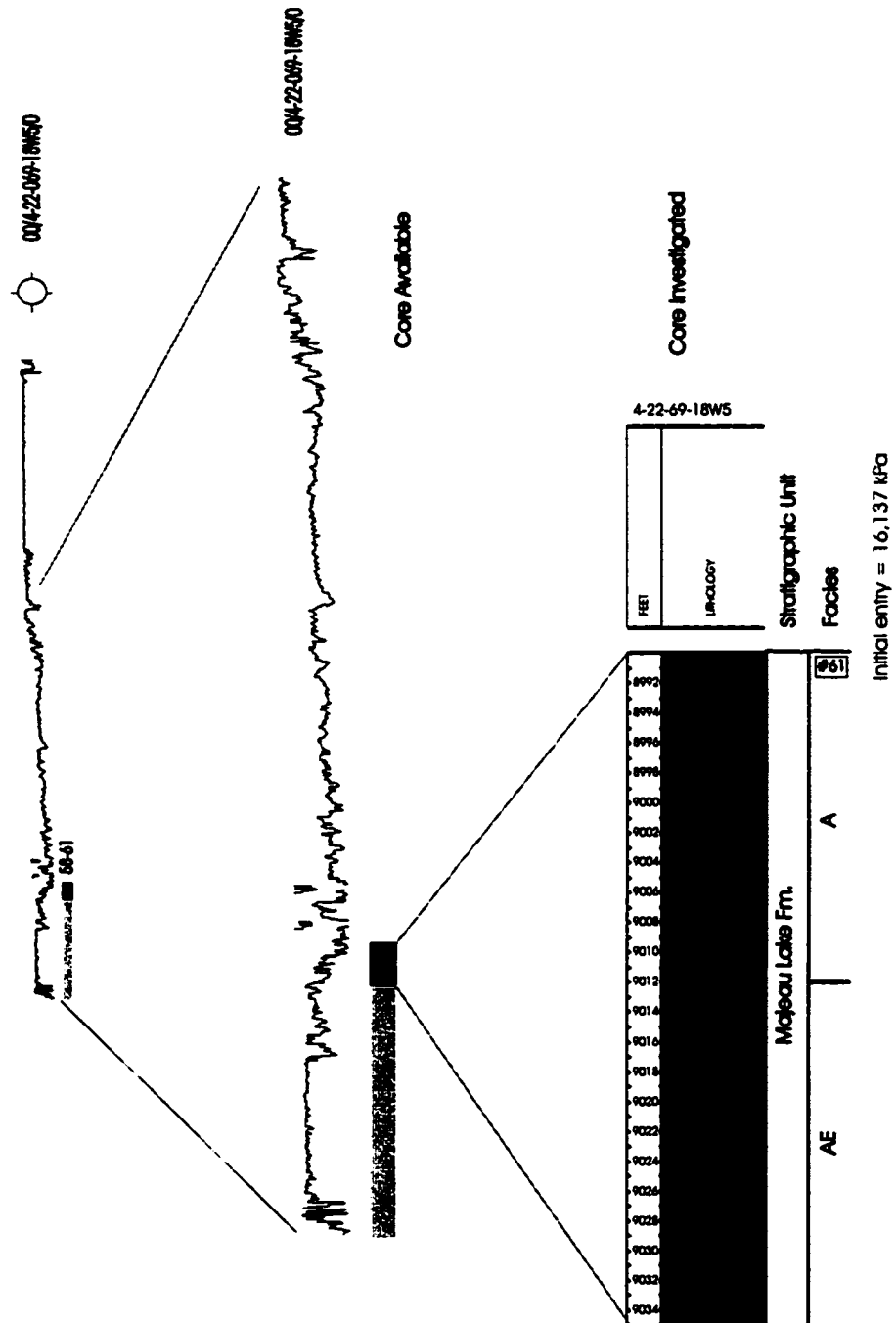
Interval of core investigated (in black) and associated gamma log of the undivided Woodbend Group aquitard. The initial entry pressures derived from MICPM are included for samples #20 and #22B.



Interval of core investigated shown in black, and associated gamma log of the Majeau Lake Formation. The initial entry pressure derived from MICPM is included for sample #68, whereas sample #66 could not be analyzed for MICPM due to low porosity and small pore size, and is therefore assumed to be tight.

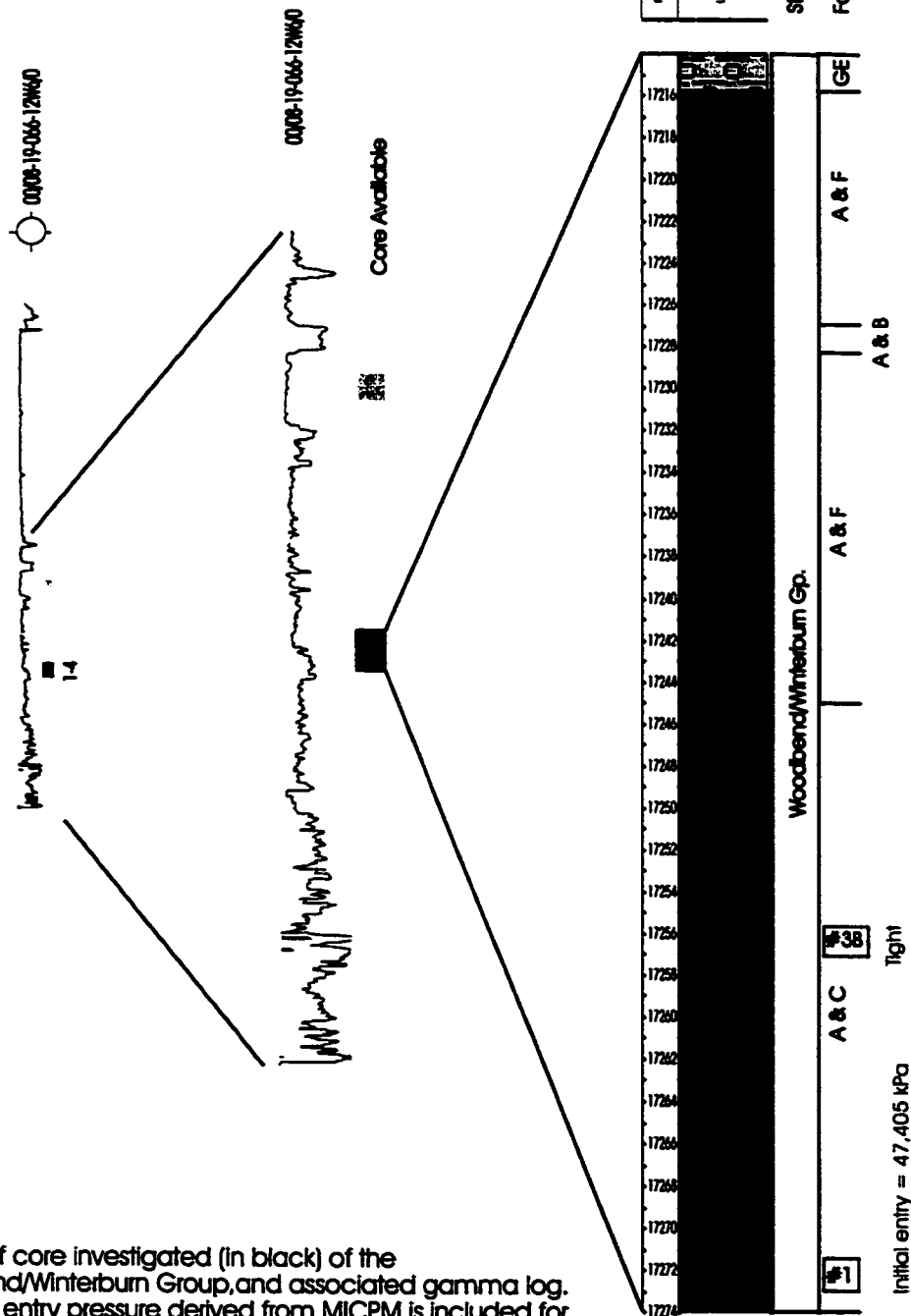


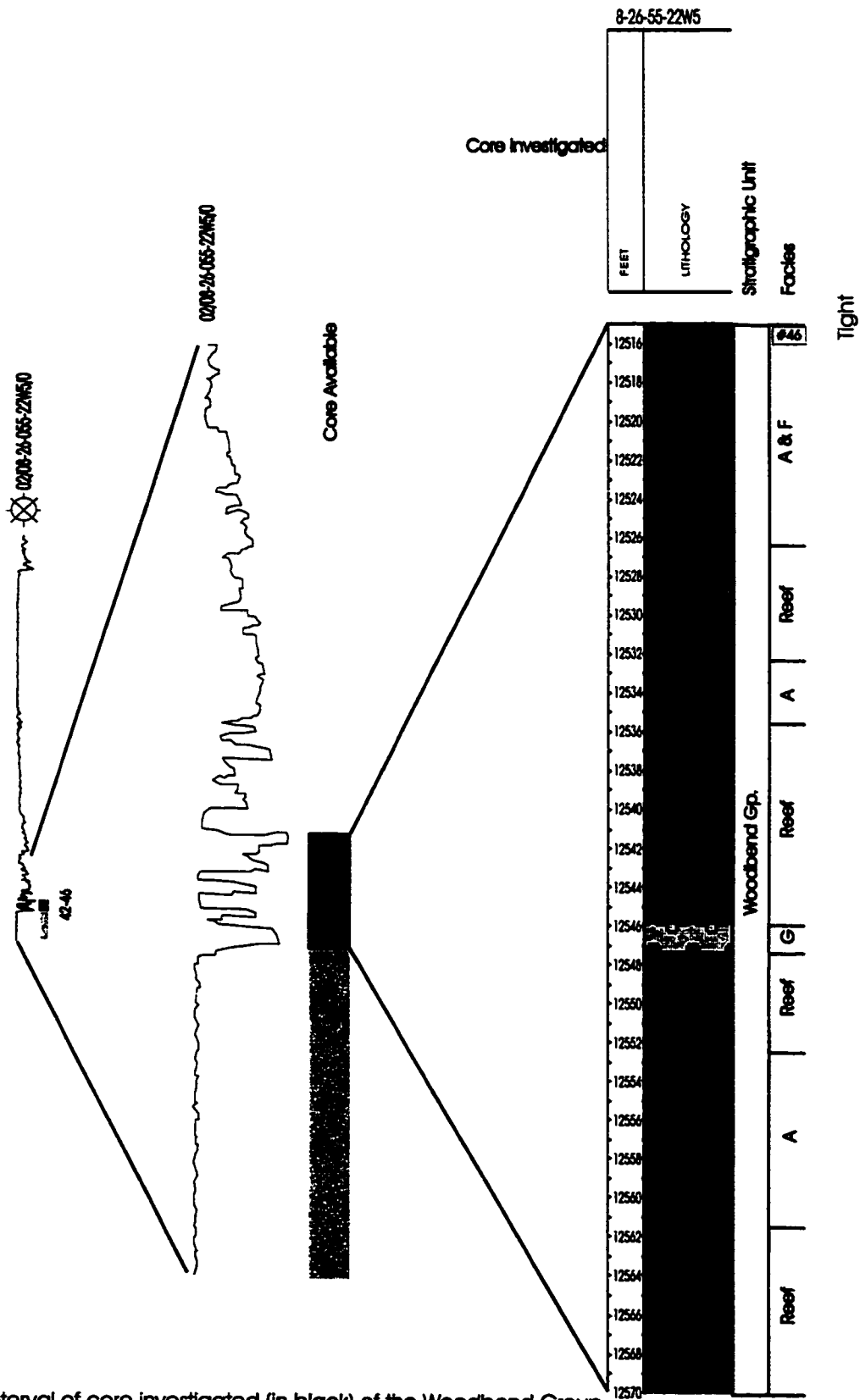
Interval of core investigated (in black) of the Woodbend Group, and associated gamma log. The initial entry pressure derived from MICPM is included for sample #51.



Interval of core investigated (in black) of the Majeau Lake Formation aquitard, and associated gamma log. The initial entry pressure derived from MICPM is included for sample #61.

Interval of core investigated (in black) of the Woodbend/Winterburn Group, and associated gamma log. The initial entry pressure derived from MICPM is included for sample #1, whereas sample #38 could not be tested because of its low porosity and small pore size, and is therefore assumed to be tight.





Interval of core investigated (in black) of the Woodbend Group, and associated gamma log. Sample #46 could not be analyzed for MICPM due to its low porosity and small pore size, and is therefore assumed to be tight